2012

Towards More Reliable MAC and PHY Layer Designs for High QoS Achievements for Safety Messaging in DSRC Systems

Nabih Jaber

Towards More Reliable MAC and PHY Layer Designs for High QoS Achievements for Safety Messaging in DSRC Systems

By

Nabih Jaber

A Dissertation
Submitted to the Faculty of Graduate Studies
through the Department of Electrical Engineering
in Partial Fulfillment of the Requirements for
the Degree of Doctor of Philosophy at the
University of Windsor

Windsor, Ontario, Canada

2012

Towards More Reliable MAC and PHY Layer Designs for High QoS Achievements for Safety Messaging in DSRC Systems

by

Nabih Jaber

APPROVED BY:

_____

A. Yongacoglu, External Examiner
University of Ottawa

_____

A. Azab
Department of Industrial & Manufacturing Systems Engineering

_____

H. Wu
Department of Electrical and Computer Engineering

_____

M. Mirhassani
Department of Electrical and Computer Engineering

_____

E. Abdel-Raheem, Co-Advisor
Department of Electrical and Computer Engineering

_____

K. Tepe, Advisor
Department of Electrical and Computer Engineering

_____

V. Mogyorody, Chair of Defense
Faculty of Graduate Studies and Research

27 January 2012

Declaration of Co-Authorship / Previous Publication

I. Co-Authorship Declaration

I hereby declare that this thesis incorporates material that is result of joint research, as follows: This thesis also incorporates the outcome of a joint research undertaken in collaboration with William Cassidy and Kazi Rahman under the supervision of Professor Kemal Tepe. The collaboration is covered in parts of Chapters 2 and 4 of the thesis. In all cases, the key ideas, primary contributions, experimental designs, data analysis and interpretation, were performed by the author, and the contribution of co-authors were primarily through the provision of discussing the simulation results in Chapter 2, and discussing the generation of the vehicles' traffic model in a highway using the SUMO software in Chapter 4.

I am aware of the University of Windsor Senate Policy on Authorship and I certify that I have properly acknowledged the contribution of other researchers to my thesis, and have obtained written permission from each of the co-author(s) to include the above material(s) in my thesis.

I certify that, with the above qualification, this thesis, and the research to which it refers, is the product of my own work.

II. Declaration of Previous Publication

This thesis includes 6 original papers that have been previously published/submitted for publication in peer reviewed conferences/journals, as follows:

Thesis Chapter	Publication title/full citation	Publication status
In Parts of Chapter 2	Nabih Jaber, Kazi Rahman, Esam Abdel-Raheem, Kemal Tepe, "A Quantitative Analysis of Improved DSRC System using Repetition Based Broadcast Safety Messaging with Hidden Terminals," *In the Proceedings of IEEE IWCMC - Wireless Communications and Mobile Computing Conference 7th International Symposium on Vehicular Communications, pp. 1772 - 1777, August 2011.*	Published
In Parts of Chapters 3 and 4	Nabih Jaber, William Cassidy, Kemal Tepe, Esam Abdel-Raheem, "New Passive Cooperative Collision Warning (PCCW) MAC Protocol Designs for Reliability Enhancement of Vehicular Safety Messaging," *Submitted to IEEE Journal on Selected Areas in Communications (JSAC on Emerging Technologies in Communications).*	In Press
In Parts of Chapters 3 and 4	Nabih Jaber, William Cassidy, Esam Abdel-Raheem, Kemal Tepe, "New Vehicular Broadcast Messaging Reliability Enhancement Protocol for Emergency Vehicle Communication," *Submitted to the 5th International Conference on New Technologies, Mobility and Security (NTMS), IFIP/IEEE.*	In Press
In Parts of Chapter 5	Nabih Jaber, Kemal Tepe, Esam Abdel-Raheem, "Improved Performance at High Code Rates of DSRC PHY Systems using a Linear Demapper," *In the Proceedings of the 24th IEEE CCECE International Symposium on Vehicular Communications, pp.000370-000374, September 2011.*	Published
In Parts of Chapter 5	Nabih Jaber, Kemal Tepe, Esam Abdel-Raheem, "Performance Enhancement of the DSRC System Using Frequency-Domain MAP Equalization," *AEÜ International Journal of Electronics and Communications, Elsevier, vol. 19, no. 5, pp. 1294-1317, 2011.*	Published
Chapter 6	Nabih Jaber, Kemal Tepe, Esam Abdel-Raheem, "Reconfigurable simulator using graphical user interface (GUI) and object-oriented design for OFDM systems," *International Journal of Simulation Modelling Practice and Theory (SIMPAT), Elsevier, 2011. doi: 10.1016/j.aeue.2011.03.001.*	Published

I certify that I have obtained a written permission from the copyright owner(s) to include the above published material(s) in my thesis. I certify that the above material describes work completed during my registration as graduate student at the University of Windsor.

I declare that, to the best of my knowledge, my thesis does not infringe upon anyone's copyright nor violate any proprietary rights and that any ideas, techniques, quotations, or any other material from the work of other people included in my thesis, published or otherwise, are fully acknowledged in accordance with the standard referencing practices. Furthermore, to the extent that I have included copyrighted material that surpasses the bounds of fair dealing within the meaning of the Canada Copyright Act, I certify that I have obtained a written permission from the copyright owner(s) to include such material(s) in my thesis.

I declare that this is a true copy of my thesis, including any final revisions, as approved by my thesis committee and the Graduate Studies office, and that this thesis has not been submitted for a higher degree to any other University or Institution.

Abstract

Broadcast communications are widely proposed for safety messaging. In the case of highway vehicular networks and constantly communicating safety messages inevitably cause the well-known hidden terminal problem. Three existing leading repetition-based broadcasting protocols have shown to meet the reliability and delay requirements for Dedicated Short Range Communications (DSRC) safety systems. We propose a quantitative model to evaluate the quality of service (QoS) of DSRC systems using these three leading repetition-based protocols under hidden terminals and highway scenarios. The performance of our model is analyzed by means of probability of success and delay performances.

We also present three new Medium Access Control (MAC) layer design protocols for safety messaging applications. The main protocol we introduce is known as Passive Cooperative Collision Warning (PCCW) protocol for repetition based vehicular safety message reception reliability improvement in DSRC. The PCCW protocol and jointly proposed Enhanced-PCCW (EPCCW) and emergency-PCCW (ePCCW) protocols variants can work on top of existing repetition protocols for serving as a passive collision warning mechanism in the MAC Layer. A full analytical derivation of the relative reliability and delay performances for all three PCCW, EPCCW and ePCCW protocols are provided, serving as intuitive performance evaluators. EPCCW employs the physical (PHY) layer to create sub-slots for the purpose of further increasing reliability by both avoiding and minimizing probability of collision at slots that would nominally fail. Analytical and simulation results of PCCW and EPCCW agree, and show a significant reduction in message failure rate versus the leading repetition protocols, especially under high collision scenarios up to 40% at optimal, and 80% at higher repetitions. Additionally, an improvement in average timeslots delay is observed, which facilitates improved vehicular safety messaging. ePCCW is particularly useful for emergency vehicle (EV) communications. This enhancement makes meeting stringent quality of service (QoS) requirements particularly prevalent in safety applications of DSRC systems. ePCCW show up to 77% reliability improvement relative to a leading alternative is realized. Additionally, the proposed system is shown to have a decreased average timeslots delay that is well within acceptable delay threshold, and provides the best reliability in its class, which is key to safety messaging.

In all our simulation results, we use our accurate Orthogonal Frequency Division (OFDM) MAC and physical (PHY) layer designs. The PHY layer simulator is a new object-oriented simulation environment, and is achieved using high-level design, parallelism and usability for the simulation environment. A high-level design and GUI layouts of the proposed simulator is shown in details. This can serve as a learning/research tool for students or practiced professionals to investigate particular designs. In addition, we provide a simple technique to implement simulation partitioning for increased parallel performance of

reconfigurable object-oriented OFDM simulators. This simple technique applies to scenarios where there is disproportionate simulation duration between different OFDM configurations. It is shown to decrease total simulation time considerably.

Additionally, we present a study on different demapping schemes at the PHY level. We propose the use of a linear demapper over a recently proposed non-linear demapper. The study is also presented under different decoding schemes of DSRC receivers. We also propose the use of equalization concepts in frequency domain that exploit the frequency domain channel matrix to combat inter-carrier interference (ICI) instead of inter-symbol interference (ISI) in DSRC systems. It is shown that the DSRC system with the frequency-domain equalization scheme achieves a considerable performance enhancement compared to both the conventional and the Viterbi-aided channel estimation schemes that try to combat ISI in terms of both Packet Error Rate (PER) and Bit Error Rate (BER) at relatively high and low velocities.

Dedication

In the name of God, most gracious, most merciful.

In memory of my respectful father, Riad Ali Jaber.
For my mother Hannah Jaber, my wife Mahbegum Azimy, her parents and her family, and our two beloved children Riad and Iman. Also, for my supportive siblings Ghinwa and Fouad Jaber.

Acknowledgements

There are several people who deserve my sincere gratitude and appreciation for their invaluable contribution for this project.

I would first like to express my sincere appreciation to my supervisors, Dr. Kemal E. Tepe and Dr. Esam Abdel-Raheem for providing me with constant support, generosity and guidance throughout the entire project. They had a tremendous impact on me both academically and personally. I am honoured to have worked with them. I would also like to thank my committee members Dr. Huapeng Wu, Dr. Ahmed Azab, and Dr. Mitra Mirhassani for their support, guidance and time spent observing my project, and providing me with invaluable comments and suggestions. Also, I would like to thank my forever friend and brother Bill Cassidy for his support throughout both my undergrad and graduate studies. He has always been there for me and my family whenever we needed a helping hand. Truly, a friend in need is a friend indeed. Also, I would like to thank the WiCIP lab team members (Kazi, Khaja, Bill, Izhar, Ahmed, Shawn, Sami and Sarab), whom I have had a huge share of laughs and fun, and enjoyed every meal we shared together. The general discussions we shared with respect to WiCIP will always remain in my mind. It was a great pleasure to have met them all.

Many thanks go to my parents Riad Ali Jaber, and Hannah Jaber, whom have sacrificed so much for our well being and protection. Although my father is no longer with us, he was one of the main motivators for my pursuing graduate studies. Thank you dad and you will always be on our minds. I love you so much and may God bless your soul.

My mom's ongoing support and advice will never grow old. She has been there for me before I was born and till this day; truly a mother's love is priceless. I would like to also thank my very supportive and caring siblings Ghinwa and Fouad Jaber. I am very grateful and thankful to God for giving me such wonderful parents and siblings. I pray that God provides them with great health, happiness and prosperity.

Additionally, I would like to thank my most beautiful, respectful and intelligent wife Mahbegum Azimy, whom I fell in love with the moment I saw her, and this love only grows as we grow. My two most beloved children Riad's and Iman's funny and relaxing gestures with their cute expressions keep me going in life. Thank you all for your support, patience and your confidence in my ability. I truly am blessed to have them in my life. I pray that God provides them with great health, happiness and prosperity. My wife's talent and amazing character will always be an inspiration to me. Last but not least, I would like to thank my in-laws for their warm support and faith in me.

Table of Contents

Declaration of Co-Authorship / Previous Publication ..... **iv**

Abstract ..... **vi**

Dedication ..... **viii**

Acknowledgements ..... **ix**

List of Tables ..... **xiii**

List of Figures ..... **xiv**

List of Acronyms and Abbreviations ..... **xviii**

List of Symbols ..... **xx**

Chapter 1 Introduction **1**

1.1 Problem Statement 2

1.2 Main Contribution 3

1.2.1 MAC Layer Designs 4

1.2.2 MAC Layer Simulator Design 4

1.2.3 PHY Layer Receivers Comparison 5

1.2.4 PHY Layer Simulator Design 5

1.3 Organization of the thesis 5

Chapter 2 A Quantitative Analysis of DSRC Repetition Based Broadcast Safety Messaging with Hidden Terminals **8**

2.1 Safety Related Considerations and Traffic Model Formulation and Analysis 9

2.1.1 DSRC safety related considerations 9

2.1.2 Probability of having $\boldsymbol{m}$ interferers 10

2.1.3 Interferers for binomial transmission model 10

2.1.4 Interferers for Poisson transmission model 11

2.1.5 Validation of traffic model using Poisson under no-hidden nodes 11

2.2 Repetition Based Broadcast Models with Hidden Terminals 12

2.2.1 Probability of Success for Repetition Based Protocols with Hidden Terminals 12

2.2.2 Probability of Success for SPR with Hidden Terminals 13
2.2.3 Probability of Success for SFR with Hidden Terminals 14
2.2.4 Probability of Success for POC with Hidden Terminals 15
2.2.5 Delay Considerations for Repetition Protocols 15
2.3 Performance Results and Discussions 15

Chapter 3 New PCCW, EPCCW and ePCCW MAC Designs for Enhanced Vehicular Reliability Safety Messaging 20

3.1 Introduction 20
3.2 Related Work 21
3.3 Safety Related Consideration and Emergency Vehicle Communications 22
3.4 Repetition Protocols for Safety Messages 23
3.4.1 SFR, SPR, POC Repetition Protocols 23
3.5 Proposed New PCCW Design for Safety Messaging 24
3.5.1 State Entry Conditions 26
3.5.2 PCCW Analytical Analysis 29
3.6 PCCW over SPR, SFR and POC Analytical Analysis 35
3.7 Enhanced-PCCW (EPCCW) Design 36
3.7.1 EPCCW Analytical Analysis 38
3.8 Delay Considerations for PCCW and EPCCW 39
3.8.1 PCCW Average Delay 39
3.9 Simulation and Analytical Results 41
3.10 Emergency Vehicular Safety Messaging Reliability Enhancement using emergency-PCCW (ePCCW) MAC Protocol Design 52
3.10.1 Safety Consideration and EV Communications 52
3.10.2 ePCCW for Emergency Communications 53
3.11 Simulation and Analytic Results of ePCCW 56

Chapter 4 MAC/PHY Simulator Design for PCCW 60

4.1 Architecture 60
4.2 Mobility Model 61
4.3 PCCW Implementation 65
4.4 Channel Simulation 68
4.4.1 Model Broadcast 72
4.5 Model verification 72
4.5.1 Averaging of users 74

Chapter 5 Performance Enhancement of DSRC PHY Using Improved Equalization and Demapping Schemes 75

5.1 OFDM-Based DSRC System 75

5.2 Channel Modelling 78

5.3 Performance Enhancement of DSRC PHY Using Improved Demapper 81

5.3.1 Demapping and Decoding Schemes for the DSRC PHY Systems 81

5.3.2 Simulation Results 84

5.4 Performance Enhancement of DSRC PHY Using Improved Equalization 87

5.4.1 Frequency-domain equalizer 88

5.5 Performance Simulations 91

Chapter 6 Reconfigurable Simulator Using Graphical User Interface and Object Oriented Design for DSRC PHY 95

6.1 Introduction 95

6.2 Modelling 97

6.3 GUI Considerations 100

6.3.1 Simulation control 100

6.4 Simulation Design 105

6.4.1 Simulation Environment Overview 105

6.4.2 Simulation Configuration Considerations 107

6.5 Distributed and Parallel Computing 113

6.5.1 Simulation Partitioning 115

6.6 Distinctiveness of Proposed Design 121

Chapter 7 Conclusions 123

References 127

Appendix A Elsevier and IEEE Reprint Permissions 132

From AEÜ International Journal of Electronics and Communications, and Int. Journal of Simulation Modelling Practice and Theory (SIMPAT), Elsevier, 2011. doi: 10.1016/j.aeue.2011.03.001. 132

IEEE Reprint Permission 138

Appendix B List of Publications 140

Appendix C Pseudo Codes for PCCW, EPCCW and ePCCW Analytical Equations... 142

For Passive Cooperative Collision Warning (PCCW) and Enhanced-PCCW (EPCCW) 142

For emergency-PCCW (ePCCW) 148

Vita Auctoris 150

List of Tables

Table 3-1: Data traffic parameter ranges 23
Table 3-2: PCCW states 25
Table 3-3: PCCW state table 28
Table 3-4: Users transmission probability under CW0 state 33
Table 3-5: DSRC (IEEE802.11p) data rates 36
Table 3-6: Simulation parameters 42
Table 3-7: Data traffic parameter ranges 42
Table 3-8: Nominal parameter values 42
Table 3-9: Nominal parameter values 43
Table 3-10: Data rate success rate performance in descending order for PCCW and EPCCW 49
Table 3-11: Parameter values for larger communication range 49
Table 3-12: Users' transmission probability under CW0 state 55
Table 4-1: Class diagram attributes and methods descriptions 63
Table 4-2: Descriptions of the attributes and methods used in the MAC simulator class 66
Table 4-3: SNR thresholds and 802.11p data rates 68
Table 4-4: In range matrix 71
Table 4-5: Hidden node matrix 71
Table 4-6: Interference matrix 71
Table 5-1: Main IEEE 802.11p OFDM PHY system configuration parameters 76
Table 5-2: Main IEEE 802.11p DSRC PHY system timing related parameters 76
Table 5-3: Modulation relationship according to DSRC standard 82
Table 6-1: General IEEE 802.11p OFDM PHY parameter value combinations used in simulated examples. 98
Table 6-2: Main user configurable GUI platform parameters 102
Table 6-3: Attributes used in the classes defining the parameters used by the GUI and simulation levels 111

List of Figures

Figure 2.1 Hidden and in-range vehicle regions relative to center transmitter 10
Figure 2.2 Poisson and binomial traffic models with no hidden nodes 12
Figure 2.3 Probability of success for SPR protocol at load l = 0.3 16
Figure 2.4 Probability of success for SFR protocol at load l = 0.3 16
Figure 2.5 Probability of success for POC protocol at load l = 0.3 17
Figure 2.6 Delay plots for SPR, SFR, and POC under load $l = 0.3$ 18
Figure 2.7 Probability of success for POC at load $l = 1$ 18
Figure 2.8 Delay plot for POC at load $l = 1$ 19
Figure 3.1 PCCW state machine 25
Figure 3.2 PCCW activity drawing 27
Figure 3.3 Single node PCCW transmission control state machine 28
Figure 3.4 User relationship 29
Figure 3.5 BER plot showing different data rates for conventional DSRC PHY 37
Figure 3.6 PER plot showing different data rates for conventional DSRC PHY 38
Figure 3.7 Probability of success showing simulation and analytical results for 18 Mbps SFR vs. PCCW and EPCCW 43
Figure 3.8 Average delay showing simulation and analytical results for 18 Mbps SFR vs. PCCW and EPCCW 44
Figure 3.9 Probability of success showing simulation and analytical results for lower data rates SFR vs. PCCW and EPCCW 45
Figure 3.10 Average delay showing simulation and analytical results for lower data rates SFR vs. PCCW and EPCCW 46
Figure 3.11 Probability of success showing simulation and analytical results for 6 Mbps SPR, SFR, POC vs. PCCW 46
Figure 3.12 Average delay showing simulation and analytical results for 6Mbps SPR, SFR, POC vs. PCCW 47
Figure 3.13 Probability of success showing simulation and analytical results for 6 Mbps SPR, SFR, POC vs. EPCCW 47
Figure 3.14 Average delay showing simulation and analytical results for 6Mbps SPR, SFR, POC vs. EPCCW 48

Figure 3.15 Probability of success showing simulation results for proposed design's optimum data rate ... 48
Figure 3.16 Probability of success showing simulation results with150m communication range and with low vs. high traffic loads for SFR vs. PCCW vs. EPCCW ... 49
Figure 3.17 Average delay showing simulation results with150m communication range and with low vs. high traffic loads for SFR vs. PCCW vs. EPCCW. ... 50
Figure 3.18 Probability of success showing simulation results with medium size communication range for SFR vs. PCCW vs. EPCCW ... 50
Figure 3.19 Probability of success showing simulation results for higher data rate comparison between repetition-based SFR protocol, PCCW and EPCCW ... 51
Figure 3.20 Probability of success showing simulation results for higher data rate comparison between repetition-based SPR protocol, PCCW and EPCCW ... 51
Figure 3.21 CW0 behaviour for ePCCW ... 53
Figure 3.22 Pr(S) simulation and analytical results at N = 33, 150 slots/frame ... 57
Figure 3.23 Delay simulation and analytical results at N = 33, 150 slots/frame ... 57
Figure 3.24 Pr(S) plot simulation under high vehicle density at 441 slots/frame ... 58
Figure 3.25 Delay simulation under high vehicle density at 441 slots/frame ... 58
Figure 4.1 MAC simulation processing flow (include channel) including Hidden and warning matrices, for PCCW simulation. ... 61
Figure 4.2 Marked emergency and non-EVs in SUMO ... 62
Figure 4.3 Class diagram for mobility model, OFDM PHY and channel model ... 62
Figure 4.4 MAC simulator deployment diagram ... 64
Figure 4.5 UML class diagram of PCCW ... 65
Figure 4.6 Simulator change state activity diagram ... 67
Figure 4.7 Flow between MAC, PHY, and channel simulation ... 69
Figure 4.8 Mobility model: varying interference ranges ... 69
Figure 4.9 Interfering and hidden nodes ... 70
Figure 4.10 Broadcast simulation sequence diagram ... 73
Figure 4.11 Sequence diagram for computing success ratio for user broadcasts ... 73
Figure 4.12 Averaging users Sequence Diagram ... 74
Figure 5.1 Layout of the OFDM PHY model: (a) transmitter, (b) receiver. ... 76
Figure 5.2 Channel model with multipath scattering, specular (LOS), and Rayleigh (no-LOS) portions and AWGN ... 78
Figure 5.3. Scatter plots showing distortions caused by Doppler shift. ... 80
Figure 5.4. Scatter plots showing distortions caused by AWGN shift. ... 80
Figure 5.5 QAM modulation with associated linear decision mapping. ... 82
Figure 5.6 BER comparison for QAM16 DSRC with varying SNR at v = 238 km/h, R_c =1⁄2, at 12Mb/s in Rayleigh channel. ... 84

Figure 5.7 BER comparison for QAM64 DSRC with varying SNR at v = 238 km/h, R_c =3⁄4, at 27 Mb/s in Rayleigh channel. 85
Figure 5.8 BER comparison for QAM16 DSRC with varying SNR at v = 100 km/h, R_c =1⁄2, at 12 Mb/s in Ricean channel. 86
Figure 5.9 BER comparison for QAM64 DSRC with varying velocity at SNR = 30 dB, R_c =1⁄2, at 18Mb/s Rayleigh channel. 86
Figure 5.10 BER comparison for QAM16 DSRC with varying packet length at SNR = 10 dB, v = 238 km/h, at 12Mb/s Rayleigh channel. 87
Figure 5.11 BER vs. SNR at 238 km/hr for different demappers and decoders. 88
Figure 5.12 Rayleigh fading envelope examples for DSRC (a) over one packet with duration of 1.0 ms with 125 DSRC/OFDM symbols, and (b) over one DSRC symbol with duration of 8.0 μs. 89
Figure 5.13 DSRC Receiver Designs with: (a) Viterbi-aided channel tracking, (b) Frequency-domain equalization. 89
Figure 5.14 DSRC receiver design with frequency-domain equalization. 90
Figure 5.15 Subcarrier to subcarrier ICI contributions. 90
Figure 5.16 BER and PER vs. SNR at 238 km/hr and 60 OFDM symbols under Rayleigh fading. 92
Figure 5.17 BER and PER vs. SNR at 74 km/hr and 60 OFDM symbols under Rayleigh fading. 93
Figure 6.1 BER vs. signal to noise ratio for different channel, transmitter and receiver scenarios. 98
Figure 6.2 PER vs. Doppler shift for different channel, transmitter and receiver with different symbol durations. 99
Figure 6.3 BER vs. packet length for different channel, transmitter and receiver scenarios. 99
Figure 6.4 Example GUI parameter setup for the OFDM PHY model. 101
Figure 6.5 Example of GUI level state loading method. 104
Figure 6.6 Simulation environment overview. 106
Figure 6.7 Illustration of information exchange between GUI and simulator levels. 106
Figure 6.8 Tiered simulation with each path resulting in dataset for output. 107
Figure 6.9 Sequence diagram showing information exchange between the GUI and simulation levels. 108
Figure 6.10 The GUI level main simulation model control classes (*Model_Settings*). 109
Figure 6.11 Overview of main classes for simulation level showing relationship between its classes. 109
Figure 6.12 OFDM PHY and its transmitter and channel subclasses. 112
Figure 6.13 OFDM PHY and its receiver subclasses. 112
Figure 6.14 Modified tiered simulation to include iteration. 113
Figure 6.15 Processing units with inter-process communication showing the high level simulator layout. 114
Figure 6.16 General and uniformly distributed packet and scenario partitioning for four OFDM PHY design simulations. 115
Figure 6.17 Timing diagram showing both packet and scenario partitioning methods used for parallel processing. 116

Figure 6.18 Flow chart showing steps for scheduling the objects in the simulation. 117
Figure 6.19 Sequence diagram showing an example packet partitioning setup with four scenarios being processed by 2 main processing units and a controller unit. 117
Figure 6.20 Timing diagram for the example case study showing disproportionate simulation time favouring packet partitioning. 119
Figure 6.21 Bar plot showing the relative time for simulating different scenarios for the case study with both scenario and packet partitioning (top half scaled differently from bottom to fit). 120
Figure 6.22 Bar plot showing the overall time duration for simulating both scenario and packet partitioning. 120

List of Acronyms and Abbreviations

Acronym/Abbreviation	Definition
ACS	Add-compare-select
AWGN	Additive white Gaussian noise
BCJR	Bahl Cocke Jelinek Raviv (algorithm)
BER	Bit error rate
BPSK	Binary phase-shift keying
CDMA	Code division multiple access
CIR	Channel impulse response
CP	Collision potential
CP0	Collision at current slot
CS	Carrier sensing
CSMA/CA	carrier sense multiple access with collision avoidance
CTS	Clear to send
CW	Collision Warned
CW0	Collision warned about current slot
DAB	Digital audio broadcasting
DSRC	Dedicated short range communications
DVB	Digital video broadcasting
ePCCW	emergency PCCW
EPCCW	enhanced PCCW
EV	Emergency vehicle
FEC	Forward error correction
FFT	Fast Fourier transform
FPGA	Field programmable gate array
GI	Guard interval
GPS	Global positioning system
GUI	Graphical user interface

Acronym/Abbreviation	Definition
HDL	Hardware description language
ICI	Inter-carrier interference
iHW	I heard a warning
iW	I warned
iCS	Is current slot (collision occurring)
IFFT	Inverse fast Fourier transform
ISI	Inter-symbol interference
ITS	Intelligent transportation system
LAN	local area network
LoS	Line-of-sight
LUT	Lookup table
MAC	Medium access control
MAP	Maximum a posteriori
NS2	Network Simulator 2
OFDM	Orthogonal frequency division multiplexing
OOC	Optical orthogonal codes
OSI	Open systems interconnection
PCCW	Passive cooperative collision warning
PER	Packet error rate
PHY	Physical layer
PM	Path metric
POC	Positive orthogonal codes
QAM	Quadrature amplitude modulation
QoS	Quality of service
QPSK	Quadrature phase-shift keying
RMS	Root-mean-square
RTS	Request to send
SFR	Synchronous Fixed Repetition
SNR	Signal-to-noise ratio
SPR	Synchronous p-Persistent Repetition

List of Symbols

Symbols	Definition
τ	Message lifetime
l	Probability of transmission or load
r	Average number of repetitions
S_r	Probability of r^{th} slot success
λ	Rate of message generation
n	Number of messages generated
R	Communication range
R'	Primary interferers
R''	Final (primary and secondary) interferers
p_λ	POC transmission probability with maximum of λ overlapping transmissions
Pra_R and Prb_R	Probability of having a_R and b_R out of *a* and *b* users in the same sub slots
$\Pr_{r,\alpha,\beta,\gamma}(S_{D,j})_{Frame}$	Probability of the desired user (*D*), which could be any of the *j* users (α, β or γ), successfully transmitting in a slot of that frame having all possible combinations of the "other" remaining users competing for the same slot
$Pr\ (S)$	Probability of success in a frame
$Pr\ (\hat{S})$	Probability of having the i^{th} slot as the first successful slot
D_S	Average delay of a transmission being successfully received
E_m	Expected value of number of interferers
E_h	Expected value of number of hidden terminals or nodes
$leng$	Length in meters
ρ	Vehicle density in vehicles/meter
α	Alpha users
β	Beta users
γ	Gamma users
N	Number of total users
M	Number of interfering users

Symbols	Definition
H	Number of hidden nodes or terminals
$Pr(m)$	Probability of having m interfering users
$Pr\ (h)$	Probability of having h interfering users
S_W	Probability of window frame success
R_c	Code rate
N_{sc}	Number of subcarriers
T_s	Symbol period
$\boldsymbol{h}_{n,k}$	Complex channel frequency response for the n^{th} OFDM symbol and the k^{th} subcarrier
$\boldsymbol{w}_{n,k}$	AWGN for the n^{th} OFDM symbol and the k^{th} subcarrier
B_c	Coherence bandwidth
σ_τ	RMS spread
T_c	Coherence time
f_D	Doppler shift
f_c	Carrier frequency
V	Relative velocity
$LLR(.)$	Log-likelihood ratio

Chapter 1

Introduction

Vehicular safety communications is a developing technology meant to aid in making everyday travel safer by facilitating information exchange between vehicles in use of vehicular safety applications. Vehicles using this technology could be made aware of surrounding vehicle's position and status without relying on the use of radar, vision processing or sensor systems. Additionally, vehicular safety communications can be used in conjunction with other safety systems for improved vehicle safety. Its development started with the introduction of Dedicated Short Range Communications (DSRC), which was proposed with the main goal of reducing the number of motor vehicle accidents. In 1999 the Federal Communication Commission (FCC) in the United States approved spectrum licence of 75 MHz at the 5.9 GHz frequency band [1]. Communication between vehicles can be as simple as notification of presence, to including detailed positional and status information that can be used by safety applications in driving assistance, or even vehicle driving automation. Although the full range of applications vehicle communications have not been defined completely at this stage of development, and when it comes to safety messaging for prospective collision avoidance applications, there is a clear need for low latency, high reliability communications between vehicles. This 75 MHz capacity was subdivided into seven 10 MHz wide channels, with five 1 MHz spacing in between each channel. Of these 7 channels, two have been allocated specifically for safety messaging, one control channel, and the other four for other applications including potential multimedia and user defined applications. Due to multipath fading channel in vehicular environments, inter-symbol interference (ISI) problem is present, hence an Orthogonal Frequency Division Multiplexing (OFDM) PHY was chosen as a base for the DSRC PHY development to mitigate the effect of ISI. However, the Doppler shift experienced by vehicles traveling at non-zero relative velocities are compensated by using a frequency domain equalizer as shown in [2][3]. Recently, DSRC's physical layer (PHY) and lower medium access control layer (MAC), collectively known as IEEE 802.11p, has been approved.

For emerging designs for safety messaging, messages would be transmitted from vehicle-to-vehicle over one or more of the 10 MHz safety channels. These messages are of broadcast nature in the relationship of one transmitter to many receivers. The messages contain information such as position, speed and heading, braking indication, or even deployed airbag indication. The payload size of DSRC safety messages are relatively small, and have a variable transmission frequency. Additionally, because the

information is used for ensuring safety, the messages should arrive with low delay and with a high reliability in order to meet Quality of Service (QoS) requirements for the safety applications. Two important metrics for measuring quality of the safety message transmissions are reception reliability (also known as the probability of success), and average delay between transmission and successful reception of a broadcasted safety message.

1.1 Problem Statement

A problem with the MAC layer for safety messaging is controlling access to the channel in an efficient manner with minimal delay and high reliability. The problem exists in reducing the number of collisions between broadcasts from simultaneously broadcasting interfering users. The range of interference is dependent on three major factors namely: the intended range at which the safety message is intended to reach, the convolution coding rate (i.e. puncturing level of the convolution code), and modulation scheme [4] of the DSRC PHY. Additionally, recall that the DSRC's PHY must operate under multipath fading channel with Doppler shift being compensated by the PHY. Hence the system depends on the velocities involved, the surrounding environment, the number of vehicles, distance between vehicles, modulation scheme, coding rate, and intended message distance. These metrics affect the system's performance significantly, hence are fully considered in this work. These potential failures motivate the use of repetition codes that can increase reliability of safety messages through redundant repetitions (re-transmissions). Also average delay can be lowered if relatively few broadcast collisions occur, with sufficient number of repetitions. The basic design of a repetition code involves defining a useful lifetime in which a safety message will be made available for re-transmission. We'll refer to the safety message itself as the packet, and the useful lifetime as τ, measured in milliseconds. We define the frame of the message as τ milliseconds long, and we subdivide the frame into slots in which packets can transmit into, where the duration of a slot is the same duration of one packet transmission. The length of the safety message frame is said to be L slots long. At a minimum the repetition protocol must define the number of repetitions (r), and represent which slots of the frame are being used for these repetitions.

There are a number of protocols intended to increase reliability of broadcast messages by increasing redundancy in the transmission. One of the possible breakdown points of repetition based broadcasting is as repetitions increase the reliability only increases while the number of incurred collisions remains relatively low. During high load and with a small frame size, rapid reduction in reliability can happen with relatively few repetitions, due to high collision rates. Repetition protocols behave optimally when reliability is at a maximum given specific conditions and certain number of repetitions. Hence, the number of repetitions and corresponding collisions probability of those repetitions contribute to the probability of success of the respective repetition protocols. Synchronous p-persistent repetition (SPR) is a protocol that has a mean number of repetitions $\bar{r}$ chosen by random selection on a per slot basis as in [5]. Synchronous fixed repetition (SFR) is another repetition protocol that randomly chooses exactly r number of repetitions in random slot positions [5]. Positive orthogonal code (POC) [6] uses a CDMA inspired allocation scheme

that attempts to limit collisions by allocating sets of codes on a geographic region segmentation basis that reduces collisions between codes in the same region. In addition, POC can use a system known as adaptive elimination for voluntary omission of code selection. The performance of SFR is generally superior to that of SPR, and POC performance is generally superior to SFR.

As mentioned previously, IEEE 802.11p standard [7] also known as DSRC has recently been released. It is important to note that this release improves broadcast efficiency by enabling of the wildcard basic service set identification (BSSID) for broadcast communications. This enhancement directly impacts the performance on safety related communications because the nature of most safety communication systems is of broadcast type [8]. Broadcast type messages enable communication without setup handshaking. In 802.11-2007 standard, request-to-send (RTS) and clear-to-send (CTS) control messages are used for carrier sense multiple access with collision avoidance (CSMA/CA) to reduce frame collisions. The use of RTS and CTS control messages is not feasible in broadcast scenario due to flooding of CTS packets [8]. Also for safety messaging, the RTS and CTS packets approach the size of the actual safety messages themselves [9]. Hence broadcast safety communications cannot rely on RTS/CTS transmissions for reducing collisions. Additionally, the DSRC channel structure includes two channels intended for safety communications [5]. These channels can be separated into long-range and short range communications, or emergency vs. non-emergency communication depending on the application.

Additionally, we previously mentioned that OFDM systems are able to mitigate inter-symbol interference (ISI). However, the presence of vehicular mobility renders the orthogonality principle found in OFDM invalid causing ICI. ICI factor increases with increased vehicular speed. ISI and ICI exist due to two physical phenomena known as the multipath fading and the Doppler shift, respectively. Therefore, the research is ongoing and requires new and improved designs to mitigate the effect of these two physical phenomena.

1.2 Main Contribution

Authors in [6], proposed a quantitative approach to evaluate the broadcast performance of the conventional IEEE 802.11 MAC DSRC system in a highway scenario. The authors conclude that the designers of DSRC broadcast-based highway safety systems can shift their main focus to improving the probability of success performance as opposed to being too concerned with the delay study. This is one of the main key motivations of our study, which is improving the probability of success within acceptable delay threshold for safety messaging. Since we are also working on the PHY layer of DSRC, this dissertation also studies different PHY layer receiver designs and compare their relative bit error rate (BER) and packet error rate (PER) performance. This allows us to propose which receiver is best suited for its environment. In this context, the environment means the channel behaviour.

1.2.1 MAC Layer Designs

We first start by analysing the effect of the well-known hidden terminal problem in safety messaging applications. The three existing repetition-based broadcasting protocols mentioned earlier have shown to meet the reliability and delay requirements for DSRC safety systems. However, when compared with one another, all of these protocols have not been tested under hidden terminals scenario. Hence, this dissertation proposes a quantitative model to evaluate the quality of service (QoS) of DSRC systems using these three leading repetition-based protocols under hidden terminals and highway scenarios.

More precisely and when it comes to MAC layer designs and improving the probability of success performance, this dissertation introduces the design background and concepts of a new MAC layer protocol we called Passive Cooperative Collision Warning (PCCW). We have shown that PCCW considerably improves repetition based vehicular broadcast safety MAC reliability performance. The PCCW protocol's purpose is to inform other user nodes of potential collisions of repetitions. The protocol is passive as it does not incur additional transmissions to send this information, and instead appends a small header payload to packets that have been pre-determined by an underlying repetition protocol. This header payload incurs a slightly increased latency per slot, but as we will show, is not detrimental. In addition an improved form of PCCW is also proposed and analysed for further improvement, named enhanced PCCW (EPCCW), which uses the ability of the DSRC PHY in reducing the chance of collision in certain scenarios. It is important for the protocols not to incur additional data packet transmission to achieve an overall reduction of collisions. Importantly, we chose to design PCCW to make most of its decisions in each node, with error tolerance allowed so that node decisions will not adversely affect the other users. For this work, we consider only one channel usage, but can be expanded to be used over both channels by using PCCW on two separate MACs.

A third MAC protocol is also designed in this work to further increase reliability performance required by the emergency vehicles. This new emergency-PCCW (ePCCW) protocol makes meeting stringent quality of service (QoS) requirements particularly prevalent in safety applications of DSRC. ePCCW has shown to achieve a near 100% success performance.

In order to reduce collisions due to overlapping time slots it is recommended that global time synchronization be employed. The precise time synchronization can be achieved practically using a number of techniques including Global Positioning System (GPS), or through city wide time pulse [10]. Both analytical and simulation results that follow in this dissertation assume synchronized time slots between users in the same region.

1.2.2 MAC Layer Simulator Design

It is well known that the effect of mobility of vehicles cannot be ignored in DSRC, and a lot of work has been done to mitigate the effect of the channel, such as in [2]. Hence this is the reason why we have to use a precise physical layer (PHY) simulator, such as our PHY simulator proposed in [11], in our analysis and our simulator design in this proposal. Other network simulators commonly omit PHY simulation, and or

include less precise PHY implementation, and focus more on the upper layers. For instance in Network Simulator 2 (NS2), Nakagami fading simulator was just recently included, but the actual PHY implementation is limited in modulation schemes. Our OFDM Simulator models standard 802.11p DSRC PHY which includes channel equalization, modulation schemes as implemented according to [2]. The PHY broadcasts and receives through a Rayleigh fading channel model with each fading path's Doppler shift being modelled according to relative vehicle velocity from mobility model. Specifically, the Rayleigh paths from a transmitting vehicle's broadcast are generated at a different SNR and Doppler shift because each receiving vehicle is at a different distance and relative velocity to each other.

1.2.3 PHY Layer Receivers Comparison

This dissertation also proposes applying a receiver design for the 5.9 GHz DSRC system that can make use of ICI information caused by the time-varying channels. Hence, we compare our proposed receiver design against another receiver design that uses adaptive filtering scheme in its design. The proposed receiver uses a maximum a posteriori (MAP)-based equalization concept in frequency-domain to combat ICI instead of ISI in DSRC systems without the need of feedback loops. The receiver designs are tested for QPSK and BPSK modulation schemes, and are compared to the conventional DSRC system. The improvements are achieved through a worst-case scenario at relatively high and low speed limit studies, that is, by using Rayleigh fading channel at high and low legal limits of relative vehicular velocity.

1.2.4 PHY Layer Simulator Design

Finally, it is evident that OFDM systems intended to be used in dynamic environments must be tested under various conditions in order to be designed for optimality. Hence, a new simulation design is proposed coupling the GUI, parallelism, and high-level object-oriented design techniques to be beneficial to the researcher. GUI interface can serve as a learning/research tool for students or practicing professionals to investigate particular designs. A high-level design and GUI layouts of the proposed simulator is shown in detail. Important OFDM parameters needed for reconfiguration of transmitter components, channel condition parameters, and receiver components are discussed. In addition, we provide a simple technique to implement simulation partitioning for increased parallel performance of reconfigurable object-oriented OFDM simulators. This simple technique applies to scenarios where there is disproportionate simulation duration between different OFDM configurations. It is shown to decrease total simulation time considerably.

1.3 Organization of the thesis

The rest of this dissertation is organized as follows:

In Chapter 2 safety related considerations and traffic model formulation and analysis are discussed. Probabilities of success for the leading three repetition-based broadcast MAC protocols under hidden

terminal conditions are derived. We also present in this chapter the performance results and discussions on safety broadcast messaging under the effect of hidden terminals compared to the non-hidden scenarios.

Chapter 3 introduces the three new MAC layer designs, namely PCCW, EPCCW and ePCCW. The chapter starts with a brief literature review on repetition codes that are useful for working with and comparing to PCCW. The design process of PCCW for the scope of vehicle safety messaging, implementation and behaviour of the PCCW protocol including behaviour description, and interoperation considerations are then covered. We derive PCCW's analytical equations and present the modified versions of PCCW to include the underlying repetition protocols. EPCCW and ePCCW's are then introduced and their analytical equations are derived. Delay equations for all proposed protocol designs are also derived. Also, an illustration of the important technical aspects related to emergency scenario protocol is presented, which is crucial when it comes to our ePCCW protocol for emergency vehicles. Simulation and analytical performance results of PCCW, EPCCW and ePCCW protocols reliability enhancements under different scenarios using the simulation model and analytical models are also presented. Analytical and simulation results agree.

Chapter 4 presents our MAC simulation design which also uses a precise PHY model that we also present in a later chapter of this dissertation. Chapter 4 covers the simulation environment for PCCW, MAC, PHY, channel fading, channel interference, and mobility model assumptions, and details the respective interactions between each other with assistance of UML diagrams, essentially giving an explanation of our framework for testing vehicular safety messaging protocols.

In Chapter 5 we start with a description of the baseband model of the conventional DSRC PHY design, and then we discuss the enhanced different PHY receiver designs for DSRC, after which they are compared with each other. Specifically, a linear-decision demapper is compared with non-linear demapper with different decoders. It is shown that the linear demapper generally outperforms the non-linear demapper. Also, the channel mobility model is described in this chapter to better shed light on the reasons why different receiver designs for DSRC are required. The receiver design that uses frequency domain equalization to combat ICI is shown to outperform all the other designs, namely the conventional, Viterbi-aided receiver designs.

Chapter 6 describes important aspects of modelling the OFDM PHY. Also, the proposed GUI and object oriented simulator environment for OFDM PHY communication system is presented. More precisely, the chapter starts with a highlight of the simulation design overview. Then the simulation environment overview is presented, which is followed by the descriptive Unified Modelling Language (UML) class diagrams for the simulator design. Then, the relationship between the high level design and GUI is illustrated. Finally, we propose using simulation partitioning for distributed and parallel simulation with an example case study to show the resulting improvement in simulation run-time for different OFDM PHY designs. Sequence diagrams are used to highlight the flow between simulation processing units. A thorough explanation of the distinctiveness of our proposed design is also discussed.

Chapter 7 covers the conclusion and future works. Appendices A, B, and C contain the Elsevier and IEEE reprint permissions, list of publications, and the pseudo codes for the probability of success analytical equations for the 3 new MAC layer protocol designs, respectively.

Chapter 2

A Quantitative Analysis of DSRC Repetition Based Broadcast Safety Messaging with Hidden Terminals

Dedicated short range communications (DSRC) systems are currently being developed by the IEEE 802.11p workgroup, for vehicle-to-vehicle and vehicle-to-roadside communications [1]. The IEEE 802.11p amendment to the IEEE 802.11 standard has recently been released [2]. DSRC are an important part of Intelligent Transportation Systems (ITS). Although, their main reason for deployment is to provide significant road safety, they are also being considered for commercial purposes. DSRC system's medium access control (MAC) layer is based on IEEE 802.11 MAC, which uses carrier sensing medium access/collision avoidance (CSMA/CA) protocol [2]. Broadcast is widely used for safety messaging because it provides low latency, and is also proposed for highway safety communications [3]. Since, safety applications are very crucial, highway broadcast-based inter-vehicular safety applications are considered in this study.

Some MAC protocols use RTS and CTS schemes in their design to lower the chance of packet collisions such as in [2] and [4]. Safety messages are short and comparable in length to that of RTS, creating a similar chance of RTS/CTS packets causing a collision as the safety message. Additionally, safety messages such as environment hazards, position, direction and speed of the vehicles are usually broadcasted with frequency of 10-20 times per second [5]. Hence, if RTS are sent by a vehicle, the resulting flood of CTS packets in broadcast mode causes a flood of high collision probability. Therefore, these kinds of protocols are inefficient for short safety messaging. A quantitative approach to evaluate the broadcast performance of the conventional IEEE 802.11 MAC DSRC system in a highway scenario was presented in [6]. The authors conclude that the designers of DSRC broadcast-based highway safety systems can shift their main focus on improving the probability of success performance as opposed to being too concerned with the delay study.

Repetition-based protocols [6], [16] and [17] show an increase in probability of success relative to the conventional system, and meet the DSRC system requirements when tested under no hidden terminals scenarios. The protocols in [16] and [17], are random-based repetition protocols. These protocols are called Asynchronous p-Persistent Repetition or APR, Asynchronous Fixed Repetition or AFR,

Synchronous p-Persistent Repetition or SPR, and Synchronous Fixed Repetition or SFR. Generally, the synchronous protocols were shown to outperform asynchronous protocols, with the SFR systems performing better than SPR systems. Furthermore, they proposed a protocol that improved the performance of the AFR by adding a carrier sensing (CS) mechanism, which they call AFR-CS. The authors in [6] proposed a repetition protocol that is based on Optical Orthogonal Codes (OOC), which they called Positive Orthogonal Codes (POC). They have shown that POC outperforms SFR and SPR protocols.

The hidden nodes problem is well known in vehicular ad-hoc networks. Although, the hidden node area in broadcast is dramatically larger than that in unicast [15], in all the aforementioned repetition protocols, the authors do not take hidden nodes into account. This is the key motivation of our study. We examine the safety performance of repetition-based broadcast DSRC in a highway scenario when hidden nodes are taken into account. In our work, we construct detailed mathematical models of the probability of success under hidden terminals condition, and quantitatively compare against non-hidden terminals condition. Furthermore, we show how different traffic models compare under repetition protocols.

2.1 Safety Related Considerations and Traffic Model Formulation and Analysis

In this section, a description of relevant DSRC safety related information is presented, and then the probability of having m interfering in-range terminals and h interfering out of range hidden terminals is defined with respect to a transmitting user. For calculating the probability of having m interfering terminals, and h interfering hidden terminals, both binomial and Poisson traffic models are considered. In this section, the probability of success of one of the repetition protocols in both binomial and Poisson traffic models are also compared.

2.1.1 DSRC safety related considerations

At 5.9 GHz licensed band, the DSRC system is divided into seven 10MHz channels. One of these channels is restricted for communications of safety messages only [1]. A main purpose of DSRC is ensuring a high probability of delivery of critical safety of life broadcast safety messages. Broadcast mode was improved by the 802.11p workgroup as an important part of the amendment to 802.11 protocol [1] and [7], as is evident by the introduction of faster connection setup for broadcast mode over that of 802.11. Besides having faster connection time, RTS and CTS packets could be dropped in broadcast mode in order to minimize congestion that would be caused by one-to-many and many-to-one broadcast responses.

In regards to the DSRC safety message, its payload size is relatively small yet variable, and also has a range in QoS requirements ranging from routine to critical safety of life [14]. Routine messages could include small changes in position, velocity or acceleration, while critical safety of life message could include event information such as emergency braking or airbag activation messages. For these messages to be relevant and effective, they need to be received by other vehicles at low latency, and with high reliability, even under scenarios of high channel usage. For a safety message to be effective, it makes sense

that it should be received and interpreted in less time than human reaction time. Therefore, in order to greatly improve vehicular safety, the communication delay has been reported as not exceeding approximately 200 milliseconds (ms) [6]. If there are a large number of users transmitting at the same time, reliability of the message will decrease as a result of packet collisions. It has been shown that the amount of degradation in reliability can be mitigated through repetition based broadcasting methods [6], [16] and [17].

2.1.2 Probability of having m interferers

We define a maximum number of interferers named $m_{\max}$, which is used in determining the total probability of success in Section 2.2. Commonly utilized traffic models and assumptions as validated in [15] and [18] are used. Hence, we assume a highway environment with vehicles placed exponentially along a one dimensional ad-hoc network, as seen in Figure 2.1, using a Poisson process with density of ρ (vehicles per unit length).

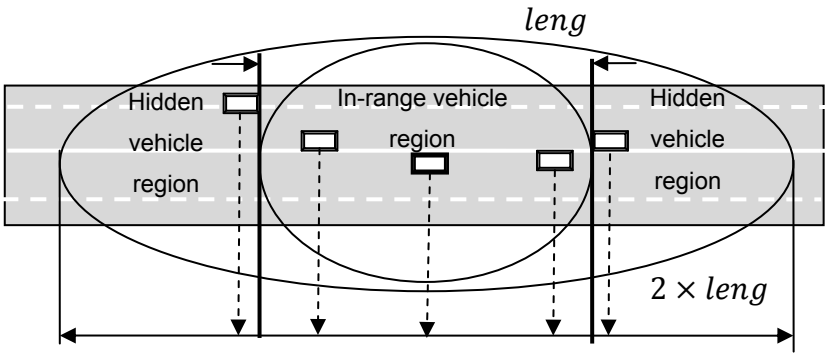

Figure 2.1 Hidden and in-range vehicle regions relative to center transmitter

Average number of vehicles within transmission range of the transmitting vehicle (center transmitter in Figure 2.1) including itself is $N = \rho \times leng$, where $leng$ is twice the transmission radius of a terminal. Hidden terminals are located outside the transmission range of the transmitting vehicle, but not exceeding $leng$ distance from the transmitting vehicle, as in Figure 2.1. When hidden terminals are included, H of them that could potentially interfere with the N users, where $H = 2 \times \rho \times leng - N$. Furthermore, to focus on performance degradation due to packet collisions, in this study an ideal channel is assumed.

2.1.3 Interferers for binomial transmission model

For binomial distributed interferers, we have the user load l (packets/user/frame) which can be interpreted as the probability of a user transmitting during the frame. For example, if l is 1, then the probability of each user sending is 100%, that is, each user is sending 1 packet per frame. Hence, it can be seen that the probability of having m interferers is given by:

$$\Pr_{\text{binomial}}(m \text{ interferers}) = \Pr_{\text{B}}(m) = \binom{m_{\max}}{m} l^{\text{m}}(1-l)^{m_{\max}-m}, \text{for } m = 0 \; to \; m_{\max}, \tag{2-1}$$

where $m_{\max}$ goes to $N-1$ trials because there are $N-1$ maximum amount of interfering users under binomial model.

Similarly, for h interfering hidden terminals we have:

$$\Pr_{\text{binomial}}(h \text{ hidden terminals}) = \Pr_{\text{B}}(h) = \binom{h_{\max}}{h} l^h (1-l)^{h_{\max}-h}, \text{for } h = 0 \; to \; h_{\max}, \quad (2\text{-}2)$$

where $h_{\max}$ goes to H trials because there are a maximum of H hidden terminals in the hidden terminal region under binomial model.

2.1.4 Interferers for Poisson transmission model

For Poisson distributed interferers, the probability of finding m interferers depends on the mean number of interferers. Hence, the probability of a user transmitting during a frame l to affect the expected value of number of interferers E_m is used. Therefore, the expected number of in-range interferers with respect to the transmitting user is the frame load l times the terminal density times the length of the in-range region less the transmitting user, and can be written as:

$$E_m = l \times \rho \times leng - 1 = lN - 1. \quad (2\text{-}3)$$

The probability of having m interferers in range of the transmitting user under Poisson distribution is:

$$\Pr_{\text{Poisson}}(m \text{ interferers}) = \Pr_{l}(m) = \frac{E_m^m}{m!} e^{-\alpha_m} = \frac{(lN-1)^m}{m!} e^{-(lN-1)}, \text{for } m = 0 \text{ to } m_{\max}. \quad (2\text{-}4)$$

Note that for Poisson, $m_{\max}$ goes to ∞ because Poisson probability models assume an infinite number of trials. It can be seen that as $m \gg E_m$, the probability added is negligible.

Similarly, for hidden nodes, there is a mean number of E_h hidden terminals which is $E_h = l(2 \times \rho \times leng - N) = lH$. The probability of having h hidden terminals in range of the transmitting user under Poisson distribution is:

$$\Pr_{\text{Poisson}}(h \text{ hidden terminals}) = \Pr_{l}(h) = \frac{E_h^h}{h!} e^{-\alpha_h} = \frac{(lH)^h}{h!} e^{-(lH)}, \text{for } h = 0 \text{ to } h_{\max}. \quad (2\text{-}5)$$

Similarly, $h_{\max}$ goes to ∞ because Poisson probability models assume an infinite number of trials, and it can be seen that as $h \gg E_h$, the probability added is negligible.

2.1.5 Validation of traffic model using Poisson under no-hidden nodes

In this section, a comparison of binomial and Poisson traffic models under the assumption of no-hidden nodes is presented. Let l be the probability that a vehicle will have packets to transmit. Figure 2 shows the probability of success for the SPR protocol under both binomial and Poisson traffic models and under various loads. Although, the probability of success equations are not presented until the next section, the purpose of this plot is to show that under non-hidden node scenario our model is comparable to other papers that use binomial traffic model as well. For this test, the vehicle density is fixed at $\rho = 0.1$ vehicles

per meter (i.e., 1 vehicle per 10 meters). The difference between binomial and Poisson in Figure 2.2 is negligible which validates that the Poisson and binomial cases can be compared directly.

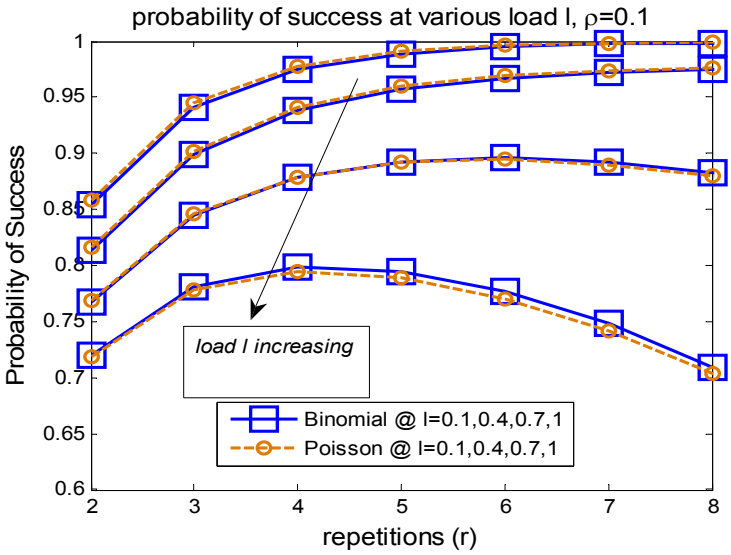

Figure 2.2 Poisson and binomial traffic models with no hidden nodes

2.2 Repetition Based Broadcast Models with Hidden Terminals

As mentioned earlier, repetition-based protocols introduced in [6], [16] and [17] assumed that vehicles were clustering within the transmission range together, and hence it ignored the effect of hidden terminals on the probability of success. This assumption is not made in our model and instead it takes collision of hidden node transmission into account. We choose SPR, SFR and POC for our study, due to the reasons mentioned in Chapter 1.

2.2.1 Probability of Success for Repetition Based Protocols with Hidden Terminals

Probability of success is defined as the probability of having at least one transmission in a frame that does not collide. A frame is divided into L time-slots. The decision on whether a user (or terminal) can transmit a safety message packet during a specific time slot depends on the repetition protocol. When taking into account hidden nodes, both the interference from non-hidden terminals and the effect of interfering hidden terminals must be included. Hence, the probability of success in a frame with N in-range terminals and H hidden terminals as $\Pr_{N,H}(S)$ is denoted as:

$$\Pr_{N,H}(S) = \Pr_{N}(S) \times \Pr_{H}(S). \tag{2-6}$$

When the vehicle's transmission success is not affected by hidden vehicles, the probability of success of the transmitting user is given by:

$$\Pr_{N}(S) = \sum_{m=0}^{\mathrm{m}} \Pr_{m,L}(S) \times \Pr(m), \tag{2-7}$$

where $\Pr_{m,L}(S)$ is the probability of success of the transmitting user given m interferers for a frame length of L time slots, $\Pr(m)$ is the probability of having m interferers which is dependent on the traffic model as shown in Section 2.1, and $m_{\max}$ is the maximum number of interferers for the interference model.
Likewise, for hidden terminals we have:

$$\Pr_{H}(S) = \sum_{h=0}^{h_{\max}} \Pr_{h,L}(S) \times \Pr(h), \tag{2-8}$$

where $\Pr_{h,L}(S)$ is the probability of success of the transmitting user given h hidden terminals for a frame length of L time slots. Whereas, $\Pr(h)$ is the probability of having h hidden terminals, shown in Section 2.1; and $h_{\max}$ is the maximum number of hidden terminals. Hence, the expanded equation of the probability of success for the transmitting terminal in Equation (2-6) becomes:

$$\Pr_{N,H}(S) = \sum_{m=0}^{m_{\max}} \Pr_{m,L}(S) \Pr(m) \times \sum_{h=0}^{h_{\max}} \Pr_{h,L}(S) \Pr(h). \tag{2-9}$$

2.2.2 Probability of Success for SPR with Hidden Terminals

SPR [16] works by repeating a packet within a frame a mean of r number of times. This is accomplished over a frame of length L time slots by choosing to transmit in a slot or not via a random slot transmission determination with mean of r/L.

Let s be the event of slot success, where for a slot, the transmitting user must transmit, and i terminals must not transmit for the transmitting user to be successful. For the entire frame success consisting of L independent time slots and m independent users, we need the probability of having one or more successful slot transmissions, which is equal to the inverse of L failures [6].

$$\begin{aligned} \Pr_{i,L,\mathrm{SPR}}(S) &= \Pr(s_1 \cup s_2 \cup \ldots \cup s_L) \\ &= \overline{(\bar{s})^L} = 1 - (1-s)^L = 1 - \left(1 - \frac{r}{L}\left(1 - \frac{r}{L}\right)^m\right)^L, \end{aligned} \tag{2-10}$$

where S is the frame success, and s_L is the L^{th} slot success.

Similarly, the equation for the probability of frame success for SPR due to h hidden terminals interfering is obtained as:

$$\Pr_{h,L,\mathrm{SPR}}(S) = 1 - \left(1 - \frac{r}{L}\left(1 - \frac{r}{L}\right)^h\right)^L. \tag{2-11}$$

Substituting Equations (2-4), (2-5), (2-10) and (2-11) into Equation (2-9), we derive the total probability of success for SPR with hidden terminals, and under Poisson distributed terminals we have:

$$\Pr_{N,H,\mathrm{SPR}}(S) = \sum_{\mathrm{m}=0}^{m_{\max}} \left[1-\left(1-\frac{r}{L}\left(1-\frac{r}{L}\right)^{m}\right)^{L}\right]\left[\frac{(leng\times N-1)^{m}}{m!}e^{-(lN-1)}\right] \times \sum_{h=0}^{h_{\max}} \left[1-\left(1-\frac{r}{L}\left(1-\frac{r}{L}\right)^{h}\right)^{L}\right]\left[\frac{(lH)^{h}}{h!}e^{-(lH)}\right]. \tag{2-12}$$

2.2.3 Probability of Success for SFR with Hidden Terminals

SFR [16] works by repeating a packet in random time slot positions exactly r times out of L total time slots in a frame. The probability of frame success is different from SPR because of the dependency between time slots that exist in SFR.

The probability of an interfering terminal transmitting zero times in the transmitting user's x successes is determined by the hyper geometric equation for dependent slots and independent m interfering users as follows:

$$\left(\frac{\binom{L-x}{r}\binom{x}{0}}{\binom{L}{r}}\right)^{m} = \left(\frac{\binom{L-x}{r}}{\binom{L}{r}}\right)^{m}. \tag{2-13}$$

Therefore, as shown in [6], the probability of having one or more successes out of r repetitions without hidden nodes taken into account is:

$$\Pr_{m,L,\mathrm{SFR}}(S) = \Pr(s_1 \cup s_2 \cup \ldots \cup s_r) = \sum_{x=1}^{r}(-1)^{x+1}\binom{r}{x}\left(\frac{\binom{L-x}{r}}{\binom{L}{r}}\right)^{m}, \tag{2-14}$$

where s_r is the r^{th} slot success.

Similarly, the equation for the probability of frame success for SFR with h hidden terminal interferers can be obtained as:

$$\Pr_{h,L,\mathrm{SFR}}(S) = \sum_{x=1}^{r}(-1)^{x+1}\binom{r}{x}\left(\frac{\binom{L-x}{r}}{\binom{L}{r}}\right)^{h}. \tag{2-15}$$

Once again, substituting Equations (2-4), (2-5), (2-14), and (2-15) into Equation (2-9), we obtain the total probability of success for SFR due to hidden terminals, and under Poisson distributed terminals we have:

$$\Pr_{N,H,\mathrm{SFR}}(S) = \sum_{m=0}^{m_{\max}}\left[\sum_{x=1}^{r}(-1)^{x+1}\binom{r}{x}\left(\frac{\binom{L-x}{r}}{\binom{L}{r}}\right)^{m}\right]\left[\frac{(lN-1)^{m}}{m!}e^{-(lN-1)}\right] \times \sum_{h=0}^{h_{\max}}\left[\sum_{x=1}^{r}(-1)^{x+1}\binom{r}{x}\left(\frac{\binom{L-x}{r}}{\binom{L}{r}}\right)^{h}\right]\left[\frac{(lH)^{h}}{h!}e^{-(lH)}\right]. \tag{2-16}$$

2.2.4 Probability of Success for POC with Hidden Terminals

POC works by using r repetitions that are arranged in a predetermined set of orthogonal code patterns [6]. These patterns are derived from code division multiple access (CDMA) based optical orthogonal codes (OOC), which provide a minimum overlap between sets of code words. The non-hidden terminal version of the probability of transmitting user success for POC as defined in [6] is:

$$\Pr_{m,L,\mathrm{POC}}(S) = \sum_{x=1}^{r} (-1)^{x+1} \binom{r}{x} (1 - x p_\lambda)^m, \tag{2-17}$$

where p_λ is the transmission probability for the POC repetition protocol with maximum of λ overlapping transmissions between the transmitting user's code and any other users' code pattern. As defined in [6], p_λ is $p_\lambda = a/\|C\|$, where $a = \frac{L-r}{r-\lambda}$, and $\|C\| = \left\lfloor \frac{L}{r} \left\lfloor \frac{L-1}{r-1} \cdots \left\lfloor \frac{L-r}{1} \right\rfloor \right\rfloor \right\rfloor$ is the total number of codewords ($\lfloor \cdot \rfloor$ represent the floor operation).

Similarly, the equation of the probability of frame success for POC protocol taking only hidden terminals into account is obtained as:

$$\Pr_{h,L,\mathrm{POC}}(S) = \sum_{x=1}^{r} (-1)^{x+1} \binom{r}{x} (1 - x p_\lambda)^h. \tag{2-18}$$

Therefore, substituting Equations (2-4), (2-5), (2-17), and (2-18) into Equation (2-9) gives the total probability of success for SFR with hidden terminals, and under Poisson distributed terminals as follows:

$$\begin{aligned} \Pr_{N,H,\mathrm{POC}}(S) = \sum_{m=0}^{m_{\max}} \left[\sum_{x=1}^{r} (-1)^{x+1} \binom{r}{x} (1 - x p_1)^m \right] \left[\frac{(lN-1)^m}{m!} e^{-(lN-1)} \right] \\ \times \sum_{h=0}^{h_{\max}} \left[\sum_{x=1}^{r} (-1)^{x+1} \binom{r}{x} (1 - x p_1)^h \right] \left[\frac{(lH)^h}{h!} e^{-(lH)} \right]. \end{aligned} \tag{2-19}$$

2.2.5 Delay Considerations for Repetition Protocols

Average delay is defined as the expected time slot count at which the transmitting user's packet is first received successfully, and is defined as $D_s = \sum_{m=0}^{m_{\max}} D_s(m) \Pr(m)$, where $D_s(m)$ is the average delay of a transmission being successfully received having m interfering users. This depends on the probability of success of a given repetition protocol. The delay without hidden terminals is derived in [6]. For this study, the delay is modeled the same as in [6], except the probability of success is replaced with the one with hidden terminals derived in this study.

2.3 Performance Results and Discussions

The protocols of SPR, SFR, and POC are tested in an idealized channel with Poisson traffic model with no hidden nodes versus the same channel with hidden nodes included. L − time slots is chosen to be 128. The

safety communication range is set to 300 meters. We choose three common traffic density scenarios to test the protocols, namely $\rho = 0.1$ (vehicles/meter) to represent highly congested amount of vehicles, $\rho = 0.06$ for medium, and $\rho = 0.03$ for low vehicle density scenarios. In order to show the trend of average load, we show condition of $l = 0.3$, which translates to a 30% transmission probability, and also compare to load at $l = 1$.

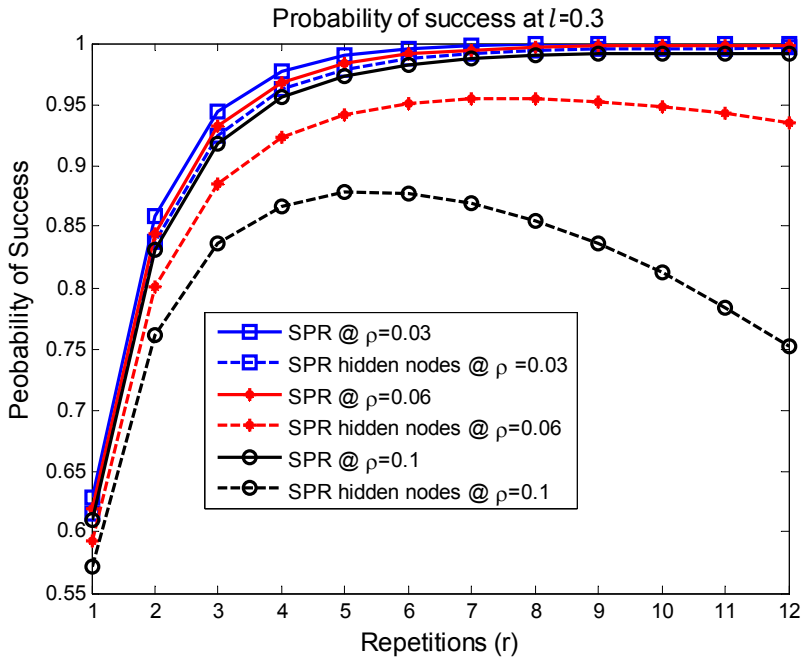

Figure 2.3 Probability of success for SPR protocol at load l = 0.3

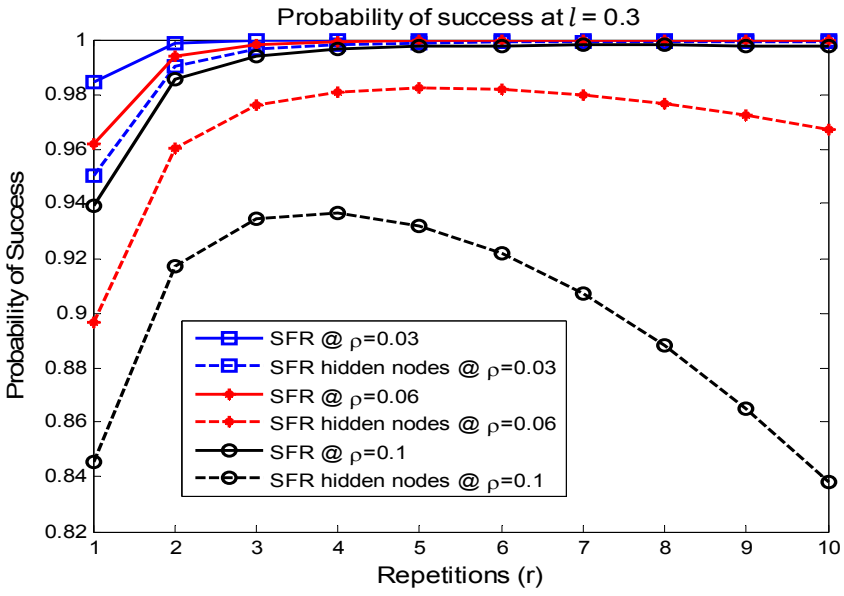

Figure 2.4 Probability of success for SFR protocol at load l = 0.3

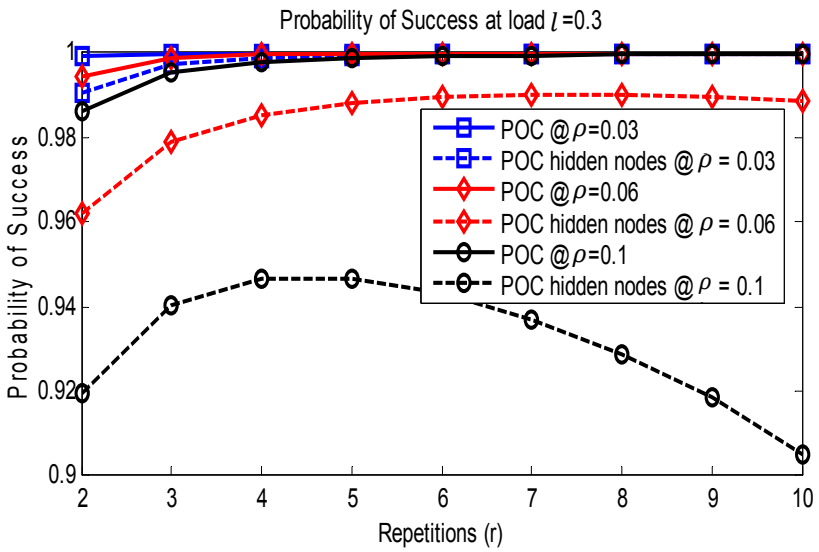

Figure 2.5 Probability of success for POC protocol at load l = 0.3

From Figures 2.3-2.5, we can see that for all three repetition protocols, and for hidden node scenarios, the optimum probability of success occurs at around 4 or 5 repetitions for high load $\rho = 0.1$, and between 5 and 7 repetitions for medium load conditions. The effect of hidden nodes on the performance of this repetition broadcast is significant at high vehicle density. Also, at the lower densities ($\rho = 0.03$), the performance is effected marginally. However, it can be seen that more repetitions are required under hidden terminal conditions to obtain the same reliability obtained with less amount of repetitions with no hidden terminals.

Critical safety of life transmissions rely on a 0.99 probability of success QoS [19]. Therefore, the probability of success reduction due to hidden nodes makes the critical safety QoS requirement unattainable except at very low vehicle densities. Other more routine safety applications also exist, which are not as stringent as 99%, each with their own set of maximum allowances for delay and reliability. Hence, using our model and these results, designers and researchers can evaluate their applications and make comparisons.

In Figure 2.6, it can be seen that the delays of the users in timeslots are not affected significantly by hidden terminals at load $l = 0.3$. In order to check delay requirement satisfaction, translation of slot durations to actual DSRC time is needed. Assuming that safety related applications require a delay less than that of human reaction time (not including decision time), and as defined earlier, the latency is constrained to be less than ~200ms. According to the standard [7] depending on modulation scheme and code rate, the data rate ranges from 3 Mbps to 27 Mbps. To tax the system we assume a relatively large average payload of 400 bytes for a safety message, and use the 3Mbps data rate for calculating maximum delay. It is found that the 50 timeslot maximum seen in Figure 2.6 translates to $\frac{400\times8\ (\text{bits/slot})}{3\times10^6(\text{bits/s})} \times 50(\text{slots}) = 0.053\text{s} < 0.200\text{s}$. Therefore, the delay requirement is satisfied at low load of $l = 0.3$

regardless of the vehicle density. This latency will obviously be less if the data rate is increased and the average payload is reduced to less extreme values.

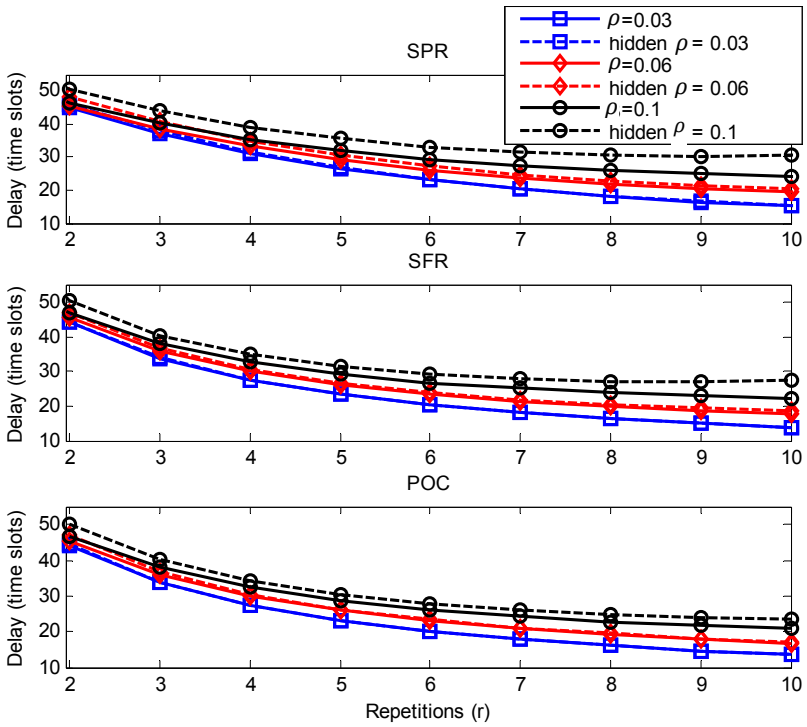

Figure 2.6 Delay plots for SPR, SFR, and POC under load $l = 0.3$

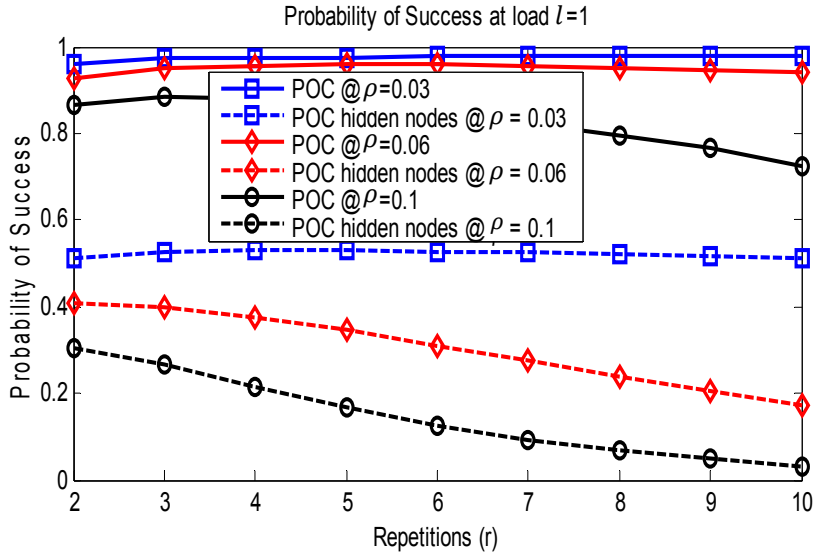

Figure 2.7 Probability of success for POC at load $l = 1$

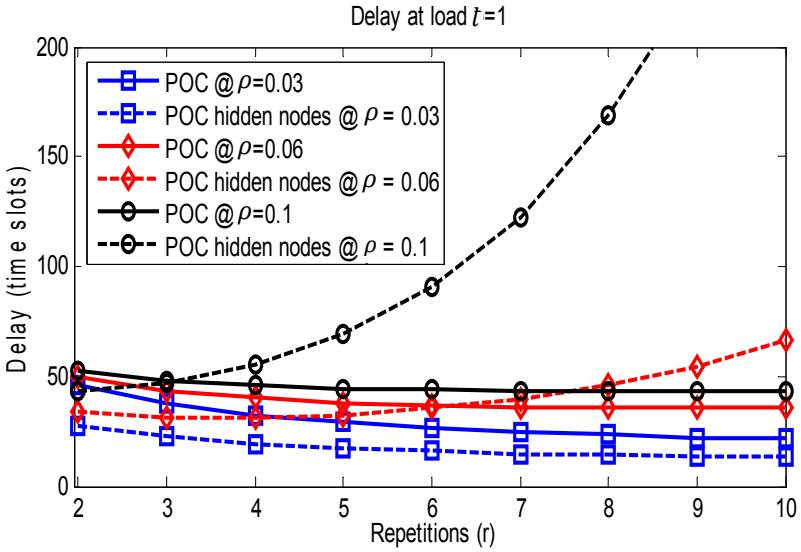

Figure 2.8 Delay plot for POC at load $l = 1$

Maximum load condition is shown in Figures 2.7 and 2.8 for probability of success and delay, respectively. POC is used for these plots because it performed the best in terms of probability of success. Figure 2.7 shows a very detrimental outcome due to hidden terminals, an approximately 50-70% reduction in probability of success. Figure 2.8 shows that delay becomes unbounded at high load and high vehicle density under hidden terminal conditions. From Figure 2.7, the optimum probability of success is shown to be at $r = 2$ or 3. From Figure 2.8, and at these optimum repetition values, the delay corresponds to a similar conclusion as from Figure 2.6. Hence the delay requirements are met. However, as the repetitions increase, the unbounded delay leads to unacceptable latency.

Chapter 3

New PCCW, EPCCW and ePCCW MAC Designs for Enhanced Vehicular Reliability Safety Messaging

3.1 Introduction

This chapter introduces the design background and concepts of passive cooperative collision warning (PCCW) for improving repetition based vehicular broadcast safety MAC reliability performance. The PCCW protocol's purpose is to inform other user nodes of potential collisions of repetitions. The protocol is passive as it does not incur additional transmissions to send this information, and instead appends a small header payload to packets that have been pre-determined by an underlying repetition protocol. This header payload incurs a slightly increased latency per slot, but as we will show, is not detrimental. In addition an improved form of PCCW is also proposed and analysed for further improvement, named enhanced PCCW (EPCCW), which uses the ability of the DSRC PHY in reducing the chance of collision in certain scenarios. It is important for the protocols not to incur additional data packet transmission to achieve an overall reduction of collisions. Importantly, we chose to design PCCW to make most of its decisions in each node, with error tolerance allowed so that node decisions will not adversely affect the other users.

PCCW works on top of an existing repetition protocol to pass warning information to surrounding users of potential collisions. By having users warn each other of transmissions and collisions, collectively packet collisions can be reduced by selective intentional transmission back-off during warned transmission slots. As previously mentioned, it is a passive warning system because it does not incur additional packet transmissions in order to warn in range users of impending transmission, but instead uses existing transmissions themselves to carry the warning information as a header payload. Distinctively, the PCCW header payload is processed in a distributed fashion at each node without requiring transmission of results to one another (the protocol tolerates some differences between node information, as the protocol is imperfectly distributed as in [20]).

The amount of vehicles in a region affects the reliability of a protocol because increasing the number of users in range of each other correspondingly increases the chance of collision from competing safety broadcasts. The interference range of messages magnifies the vehicle density's effect on the number of

collisions and is modelled in this dissertation according to [4] as described in the next chapter. Interference also depends on power of transmission, which we assume is set to achieve the message range at the SNR at set data rate. The amount of packet collisions, or potential collisions for the case of PCCW also depend on other factors including the message lifetime, PHY modulation scheme, and coding rate used.

Message security is required to prevent malicious activity and ensure anonymity and privacy. This security can be applied before the MAC layer as PCCW does not add any per vehicle identifiable information that might be of concern, and hence is not discussed in this dissertation.

Delay of a safety message is a critical issue that must be taken into consideration when designing a vehicular safety message protocol. If the delay of a safety message is too long, some applications interpreting the messages may not operate properly and lose effectiveness. This happens if the delay exceeds the minimum reaction time of a human [21], because it renders any vehicle safety system too slow to be of assistance to the driver. The human reaction time has been listed as being between 500-1200 ms [21], and hence for our analysis, we invalidate implementations if they go above this limit. In repetition protocols specifically, as the packet size increases, so too does the average successful reception delay on the repetition system used because the frame slots increase. Also, a factor in delay for repetition protocols is the probability of success, that is, the average delay is inversely proportional to the probability of success. That means increasing the probability of success of a protocol effectively lowers its average delay. This additionally validates PCCW's goal of increasing probability of success.

PCCW utilizes the benefit of being a distributed protocol in that each node has its own view of the surrounding environment, and hence does not need to continuously pass this information around. Hence, the choice for the name passive in PCCW, and it does not have a completely accurate view of all nodes accessing the medium. PCCW does not incur additional packet transmissions, and instead piggy backs on pre-determined packet transmissions.

3.2 Related Work

From the literature related to QoS for safety communications, protocols such as HIPERLAN/1 [22] have been designed to reduce reception delay in communications by categorizing messages according to QoS for priority messaging. The proposal [23] extended Distributed Coordination Function (EDCF) was also presented to reduce frame size for packets that are of high quality of service as a way to increase relative probability of success through a smaller potential collision period. Yin et. al [24] performed accurate modelling of the DSRC PHY, and showed that the 802.11 DCF required improvement to achieve satisfactory performance on both latency and throughput. Our proposed design of PCCW offers improved latency indirectly by increasing probability of reception success, directly reducing average delay. Additionally the literature, [5] presents a repetition based medium access control protocol based on 802.11 DCF, incorporating variations of SFR and SPR protocols. Here Qing et. al presents the idea of using a Cooperative Active Safety System (CASS) as a theoretical safety application architecture for the purpose of modelling constrains when designing MAC protocols for vehicular safety messaging. We also adopt a

similar strategy for our design in order to stay within design criteria specified as part of our assumptions. For their repetition based safety messaging protocol design, a dependency on number of rebroadcasts, transmission power, modulation scheme, coding scheme, and vehicular traffic volumes is identified. However we choose to model the PHY layer accurately according to our OFDM PHY model simulator design in [11], to precisely represent effects of coding, modulation, and vehicular power for each repetition, as described in the next chapter (Chapter 4). Also, in the literature related to repetition protocols is that of Positive Orthogonal Codes (POC) [6], which presents the idea of assigning repetition slots to users based on geographic location from a subset of topology-transparent orthogonal codes. This contrasts from Slotted Aloha, SPR, and SFR repetition protocols because it uses a pseudo random slot assignment scheme instead of the random-based transmission protocols. This design has been shown to outperform the SPR and SFR protocols in many scenarios, hence we chose to test PCCW running on top of POC, SPR, and SFR protocols in our analytical and simulation performance testing. We will show in this dissertation how the proposed PCCW protocol can work on top of other repetition protocols such as the ones mentioned above for potential improvement in reliability and delay performance.

3.3 Safety Related Consideration and Emergency Vehicle Communications

DSRC safety message has a relatively small but variable payload size, with a QoS range from routine to critical safety of life [17]. Routine messages may include small changes in velocity or acceleration and position. Critical safety of life messages may include information that conveys for example emergency braking messages, airbag deployment messages, or other imminent danger warnings. All of these messages need to be received by other vehicles at low latency for it to be effective, and with high reliability, even under scenarios of high channel usage. It is reported that in order to greatly improve vehicular safety, the end-to-end communication delay should not exceed approximately 200 milliseconds (ms). This is because if the delay is more than this, it would be slower than human reaction time. Repetition-based broadcasting protocols, has shown to considerably mitigate the amount of degradation caused during a large number of users transmitting at the same time. It is prudent to attempt to gain more reliability out of repetition protocols by further avoiding transmission collisions of repetitions as our PCCW protocol does.

Packet synchronization of the repetition protocol is helpful because it reduces the chance of having overlapping packet collisions. In order for multiple vehicles to be synchronized, they have to maintain an accurate clock that is identical, or near identical to each other clock. This can be achieved using GPS which provides time measurement accurate within 10 and 20ns [25]. Alternatively, a time pulse system could be implemented to allow for regional based synchronization using an FM radio pulse [10].

For safety messaging transport requirements, we have an idea of what kind of information will be useful for vehicle-to-vehicle (v2v) transmissions. Although messages can occur from roadside units as well, in this dissertation we focus on v2v communications only, but PCCW could be used for infrastructure to vehicle communications as well if the applications required high reliability, low delay or under high load.

Table 3-1 provides important parameters we assume for constructing the analytical and simulation models for evaluating performance of the proposed PCCW protocol vs. other protocols.

Table 3-1: Data traffic parameter ranges

Parameter	Value
Message rate (messages/msec)	1/50 – 1/500
Packet Payload (Bytes)	100 to 400
Communication Range (meters)	50 to 300
Average Inter-Vehicular density (meters)	10 (jammed) to 30
Lane number per road	2 to 8
Maximum Latency	0.2 s

3.4 Repetition Protocols for Safety Messages

For the safety messages to be received by users with increased reliability, repetition schemes have been suggested. Since our protocol's main aim is to improve the probability of success for repetition schemes, the following descriptions will aid in the understanding of how our protocol is unique with respect to other designs. Repetition-based MAC layer protocols' goal is to decide which packets to repeat, which timeslots, and how frequently in order to achieve QoS goals of the applications.

3.4.1 SFR, SPR, POC Repetition Protocols

Synchronous p-Persistent Repetition (SPR) [5], Synchronous Fixed Repetition (SFR) [5] and Positive Orthogonal Codes (POC) [6] are three leading repetition protocols for safety communication. SPR works by choosing which slots to transmit based on a random likelihood equal to the average desired repetitions over the number of slots in the frame, while SFR chooses a fixed number of repetitions at which to re-transmit a packet in each MAC frame. Essentially, SFR will have exactly r repetitions, while SPR will not necessarily have r average repetitions. POC repetition codes use the concept of having partially orthogonal codes used to specify slot positions of the repetitions. Each node chooses a different code from a look up table (LUT) so as to try and reduce repetitions of other users. In our experience of implementing POC, it is difficult to find a very large subset of LUTs necessary for optimum POC performance. This is because of the complexity of the search function for finding optimum codes. It was shown that POC is generally superior to both SPR and SFR, while SFR is superior to that of SPR. The detailed analytical equations and simulation results for these protocols can be found in [5] [6] and [8]. However, we include in this dissertation the final probabilities of success equations, given in [6], for all three protocols as they will be used in our initial "window" success in our proposed protocol design, as will be explained later.

The probability with at least one successful transmission for SPR [6] is:

$$\underset{L,r,mSPR}{Pr}(S) = 1 - \left(1 - \frac{r}{L}\left(1 - \frac{r}{L}\right)^{m}\right)^{L}, \tag{3-1}$$

where m is the number of interfering users, and L Is the amount of slots in a frame.

The probability with at least one successful transmission for SFR [6] is:

$$\underset{L,r,m,SFR}{Pr}(S) = \sum_{r=1}^{r_{max}} (-1)^{r+1} \binom{r_{max}}{r} \left(\frac{\binom{L-r}{r_{max}}}{\binom{L}{r_{max}}} \right)^m , \tag{3-2}$$

Finally, the probability with at least one successful transmission for POC [6] is:

$$\underset{i,L,POC}{Pr}(S) = \sum_{r=1}^{r_{max}} (-1)^{r+1} \binom{r_{max}}{r} (1 - rp_t)^m, \tag{3-3}$$

where p_t is the transmission probability for the POC repetition protocol with maximum of t overlapping transmissions between the transmitting user's code and any other users' code pattern. As defined in [6], p_t is $p_t = a/\|C\|$, where $a = \frac{L-r}{r-t}$, and $\|C\| = \left\lfloor \frac{L}{r} \left\lfloor \frac{L-1}{r-1} \cdots \left\lfloor \frac{L-t}{r-t} \right\rfloor \right\rfloor \right\rfloor$ is the total number of codewords ($\lfloor \cdot \rfloor$ represent the floor operation).

3.5 Proposed New PCCW Design for Safety Messaging

Passive Cooperative Collision Warning (PCCW) protocol can work on top of existing repetition-based protocols for serving as a passive collision warning mechanism in the MAC layer for reducing the number of node collisions. It is important to note that PCCW can also be adapted for other protocols. The protocol cooperatively uses distributed storage of potential future collisions, where each node imperfectly decides when to transmit or omit packet repetitions, without adding additional warning packets into the channel (hence, passive), and appends specialized header payloads to predetermined safety message transmissions. PCCW benefits from the message repetitions found in the underlying repetition-based protocols, and have shown to considerably improve reliability for all repetition-based protocols, especially at high loads. Additionally, it is shown to have a decreased average timeslots delay that is well within acceptable delay threshold. Its inherent increased success is due to the fact that it does not increase packet repetitions and includes warning messages in pre-planned packet repetitions.

In its basic form, PCCW works by expanding the header by adding warning message containing the location of future packet repetitions, which result in nodes either omitting repetitions, or deciding to transmit, based on a random function deterministically. Specifically, repetitions will be omitted if warnings have been detected, bringing the node's state for that slot into CW state, and the result of a randomized probability function with probability inversely proportional to the number of received warnings returns false. Table 3-2 provides a description of the PCCW states shown in Figure 3.1.

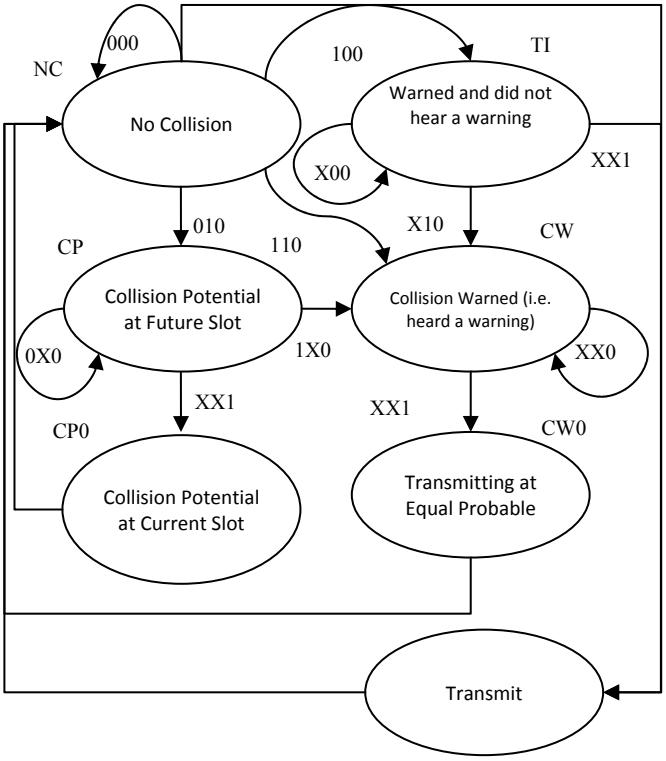

Figure 3.1 PCCW state machine

Table 3-2: PCCW states

State	State Name	Description
NC	No Collision	Default state that has no collision information available for the node.
TI	Transmission Informed	Slots are set to this state when no warnings have been heard from other users, but a warning has been attempted by the slot's host.
CP	Collision potential	Slots are set to this state when warnings have been heard from other users, but the host user has not attempted a warning.
CW	Collision Warned	Slots are set to this state when warnings have been heard from other users, and the host user has warned about this slot.
CP0	Collision potential of current slot	Slots are set to this state only when they are the current state next for transmission into the PHY, and the previous state was CP. This will result in CP0 back-off.
CW0	Collision warning for current slot	Slots are set to this state only when they are the current state next for transmission into the PHY, and the previous state was CW. This will result in CW0 operation.

The uniqueness of our protocol is how the warning messages are generated and processed by PCCW as a whole. PCCW is a non-greedy protocol that acts passively to correct some errors, instead of attempting to fix all errors. This is facilitated by nodes being aware of other nodes' transmission intentions. The warnings are interpreted by the PCCW protocol to change state according to Figure 3.1, for use in inferring an optimal decision on how to transmit based on the available information. Every node has a state machine for each timeslot in the frame in which it is intending to have a repetition. The states operate and change based on comparing incoming warnings from all nodes, interpreting the number of warning users per slot, taking into account the node's intended action for each slot, as well as the warning status of the node's past transmissions. We will illustrate a simple scenario between two users. If user A broadcasts a transmission

that is received by user B, warning of user A's future transmissions at a slot that is 10 slots in the future, the receiving user B marks that slot as a CP slot. User A marks that same slot as being in the TI state because it has informed of a transmission. If user B has its own transmission in that slot, but has not warned for that slot, it will remain in CP state for that slot until that slot becomes the current slot set for transmission, where CP0 back-off then occurs. Contrastingly, if user B was able to warn of its transmission before user A transmitted its warning, user B would have already had that state set to TI mode, for which user B's slot would transition to CW state on receiving a warning from user A. Likely user A's slot would also transition from CP state to the CW state. Both users' states for that slot will become the CW0 state when that slot becomes the current slot set for transmission. The CW0 state activates deterministic transmission based on the number of users that have successfully warned, and attempts to distribute success probability fairly between the users that are in that state. This state's behaviour is described in detail later in this chapter, and its mathematical model will also be derived and presented.

Of course the above scenario is simplified as it assumes that packets were successfully received by the users. For example, in the second scenario where both users warned each other, user B's first transmission could have been blocked from user A by another user C that is hidden to user B. Here again, user B sets the state for the slot it is warning about from NC to TI, because it sent out a warning. In this case, when user A warns of its intention to transmit at the future slot (i.e. the 10th slot from time of user A's warning, that user B now failed to warn for), user A will transition that slot from state NC to TI state, while user B will transition from TI to CW state. Hence, when that slot occurs, user A will transmit normally, while user B will transmit according to CW0. This still results in a potential success for user A, due to the nature of CW0 state operation.

We categorize the users' behaviour based on the situations they may encounter as being either an alpha (α), beta (β), and gamma (γ) users, for use in PCCW analytical modelling. Where α users are interpreted as users that successfully warned of transmission, β users attempted to warn of their transmission but failed unknowingly, and γ users for users that have not warned previously, and will only transmit in a slot if they do not hear a warning. Both α and β users will either transmit from TI state, or enter CW0 state from CW, while γ users will either transmit from TI or enter CP0 backoff from CP state.

3.5.1 State Entry Conditions

In Figure 3.2, a UML activity diagram is used to illustrate basic functionality of a slot processing. The main decision branches are based on whether the user is transmitting in the slot, broadcasted a warning payload in the past for the slot, and also is based on whether a user has been warned by other users of potential collisions in the slot. Each slot will enter the states of TI, CP, CW, or NC states, and from there will be able to either transmit directly, or enter CP0 or CW0 states for further processing based on available information. The CW0 state uses a transmission determination function that is calibrated according to equations derived in this chapter, from the number of users that have warned about the slot in question. The function allows transmissions at a probability that optimizes the probability of success for all users that

have succeeded warnings. Part of the transmission determination function must use a random seed that is unique to the particular node. This is required so that each user's determination function does not operate identically, as this would result in identical outcomes. So instead each user that enters CW0 has a fair chance of success in the slot. One of the beneficial results that this function allows is that even if a user failed in their actual warning, they still have a chance of succeeding in that slot transmission with at least 2 other simultaneous users, but their chance of transmitting is less than that of the users that succeeded in warning for the slot. The CP0 back-off allows for users that were able to warn in the slot transmission to succeed where normally a collision would occur.

The state entry decisions can be represented according to three control signals for deciding the state flow, namely iWarned (*iW*), iHeardWarning (*iHW*), and isCurrentSlot (*iCS*). The signal *iW* is triggered for a slot when its upcoming transmission has been warned about through a sent packet at a different slot.

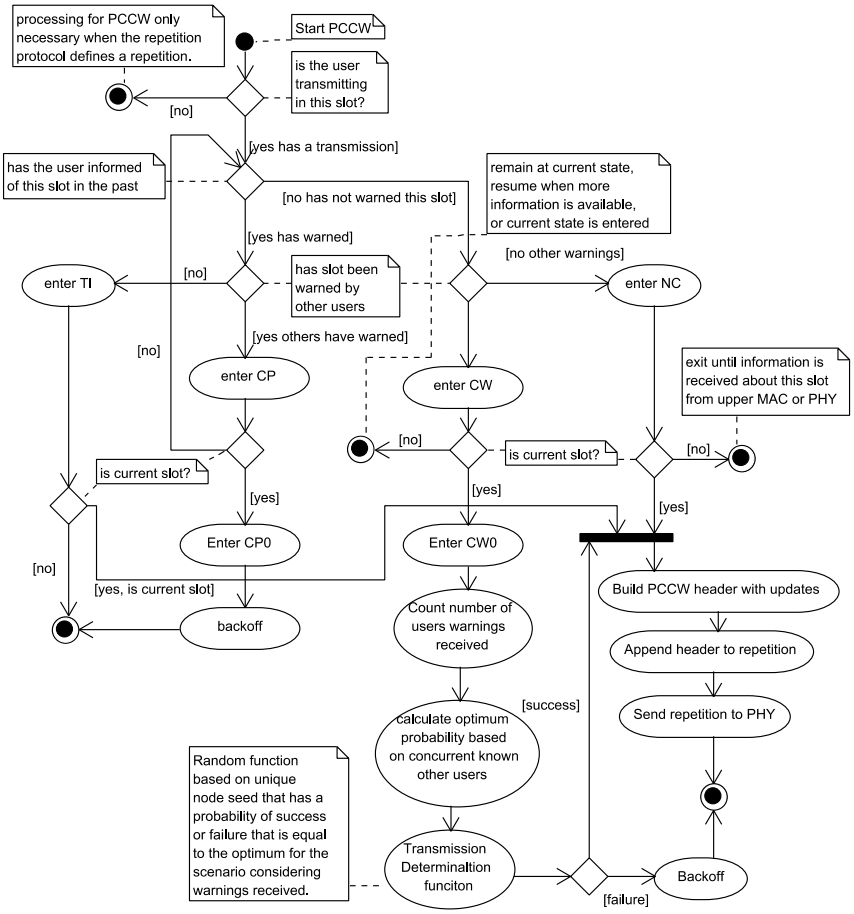

Figure 3.2 PCCW activity drawing

The signal *iHW* is triggered for a slot when the MAC receiver receives a PCCW payload attached to a packet that indicates that another user intends to transmit in that slot. Finally, the *iCS* signal is triggered when a slot is ready for transmission, as triggered by the repetition protocol detected by PCCW. These signals are directly related to state changes as represented in Table 3-3. Also important to observe is the

control of sending and receiving of a user/node's MAC transmissions using the PCCW transmission control state machine as shown in Figure 3.3. Here the sending of packets only occur when *iCS* is 1, and during a transmission triggers *iW* as 1 for upcoming slots that have been warned. Also, from the MAC Receiver connected to the DSRC PHY, successful reception of warnings from other users can be processed triggering *iHW* for applicable slots, before sending the packet to the upper MAC.

We interpret these state machine actions analytically in the next section.

Table 3-3: PCCW state table

Input1 iWarned (iW)	Input2 iHeard-Warning (iHW)	IsCurrentSlot (ICS)	Present	Next
0	0	0	NC	NC
0	1	0	NC	CP
1	0	0	NC	TI
1	1	0	NC	CW
X (0)	X (0)	1	NC	TX
0	X (1)	0	CP	CP
1	X (1)	0	CP	CW
X (0)	X (1)	1	CP	CP0
X (1)	0	0	TI	TI
X (1)	1	0	TI	CW
X (1)	X (0)	1	TI	TX
1	1	0	CW	CW
1	1	1	CW	CW0
X	X	X	TX	NC
X	X	X	CW0	NC
X	X	X	CP0	NC

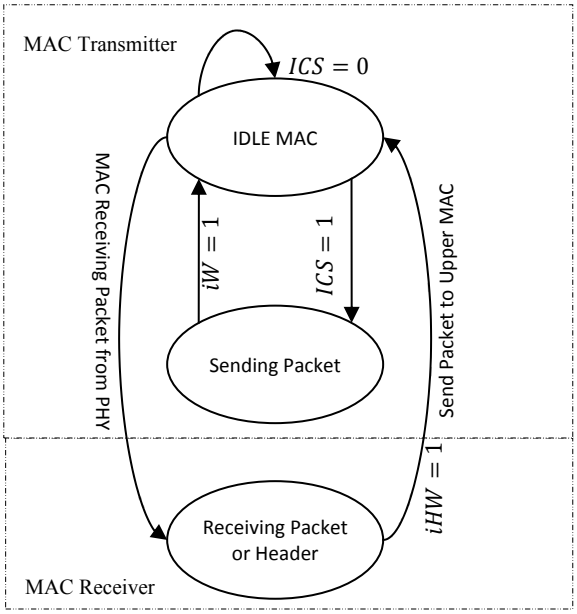

Figure 3.3 Single node PCCW transmission control state machine

3.5.2 PCCW Analytical Analysis

In order to calculate the probability of success for PCCW, we need its probability of entering each CP0 or CW0 states (shown in Figure 3.3), because these states contributes to success that would not normally occur in the regular underlying repetition protocol. In other words, we need to take these states into account because they offer corrections and preventions of collisions that would otherwise result in broadcast failures.

Previously, we introduced the three different types of users that a vehicular system may encounter. We will further discuss it in this section in order to clarify their roles mathematically. The probability of success in a given slot is determined by the ratio of alpha, beta and gamma users, and is composed of transmission load (l) and probability of success with event S ($\Pr(S)$). Alpha (α) users are the users that have successfully warned about their future transmission during their "present" transmission. Beta (β) users are the users that "thought" that they have successfully warned, however their transmission resulted in a collision and failed to warn about their future transmission. Finally the gamma (γ) users are the remaining users who "know" that they haven't warned, and that occurs when users don't transmit during a frame. Figure 3.4 shows the relationship of the probability of each node being categorized as a particular user type, either α, β or γ.

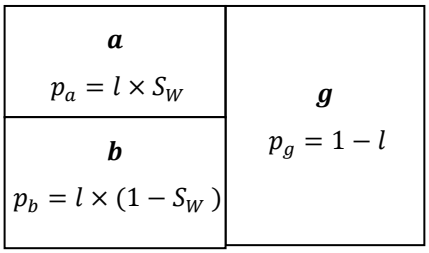

Figure 3.4 User relationship

In Figure 3.4, l is the transmission load or probability of transmission and s is slot success probability assuming normal operation. The probability of having α, β and γ users can be written as $p_\alpha = l \times S_W$, $p_\beta = l \times (1 - S_W)$, and $p_\gamma = 1 - l$, respectively. Whereas, S_W is the probability of "window" frame success and is used as "window" frame warning in PCCW protocol. PCCW's initial "window" frame warning comes from the underlying repetition protocol, hence the initial probability of "window" frame success, S_W is one of the repetition-based probability of success of Equations (3-1), (3-2) and (3-3). However, after that initial frame, the subsequent success is based on the PCCW protocol.

In analytical analysis of PCCW, it is necessary to obtain S_W as R recursive subsequent window successes, as follows:

$$\forall\, 1 < R < R_{max}: S_W = \Pr\big(S_{PCCW}(R)\big) = \Pr\big(S_{PCCW}(R-1)\big), \tag{3-4}$$

where ∀ means "for all", hence Equation (3-4) is for all R greater than 1 and less than the maximum number of recursions (R_{max}), the probability of success for PCCW is recursively related to itself. This can also be seen in pseudo code in the Appendix.

Assuming the desired user is transmitting a message, the probability of the overall PCCW with at least one successful transmission with a defined traffic model for safety vehicles can be written as:

$$Pr(S_{PCCW}) = \sum_{r=1}^{r_{max}} \sum_{m}^{N-1} \underset{m}{Pr}(S_{PCCW})\, P(M = m), \tag{3-5}$$

where, m is the random variable denoting the number of interfering users, $\Pr_m(S_{PCCW})$ is the probability of PCCW's success of the event S given that there are m interfering users, and N is the total amount of users. For a given transmitter/receiver pair, and according to [5], a good approximation for m when the interference range is much larger than the lane is calculated as:

$$m = \frac{2 \times R''}{Meters\ per\ Vehicle} \times Number\ of\ Lanes, \tag{3-6}$$

where meters per vehicle is the reciprocal of vehicle traffic density, and R'' is the interference range. In this dissertation, the interference range is slightly different in that it is calculated to accurately model the physical layer taking into account not only hidden nodes, but also secondary interferer used for the passive feedback system.

Whereas, $P(M = m)$ in Equation (3-5) is the probability of having m interfering users and it depends on the traffic model. For Binomially distributed traffic, we define it as:

$$\underset{l,m,N}{Pr}(M = m) = \binom{N-1}{m} l^m (1-l)^{N-m-1}, \tag{3-7}$$

where l is the probability of transmission, and m is the number of mobile interferers. For Poisson distributed traffic, we define it as:

$$\underset{l,m,N}{Pr}(M = m) = e^{-m\lambda\tau} \frac{(m\lambda\tau)^n}{n!}, \tag{3-8}$$

where λ and τ are the rate of message generation and lifetime of a message, or the time duration of a frame, respectively; while n is the number of messages generated. Each MAC frame is defined by a useful life (τ), and that useful life is separated into timeslots (L), where the amount of slots depends on the packet size, useful life, and data rate, as:

$$L = \frac{\tau \times Data\ Rate}{Packet\ Size}, \tag{3-9}$$

As previously mentioned, we need the PCCW's probability of entering each CP0 or CW0 states to determine its success. Hence, the probability of PCCW's success given that there are m interfering users is defined as:

$$Pr_m(S_{PCCW}) = \sum_{\gamma=0}^{m} Pr_{m,\gamma}(S_{state=CP0}) \times \sum_{\alpha=0}^{m-\gamma} Pr_{r,m,\alpha,\gamma}(S_{state=CW0}). \tag{3-10}$$

The term $\sum_{\gamma=0}^{m} \Pr_{m,\gamma}(S_{state=CP0})$ is the probability of the desired user due to other user's success being in CP0 state, and is mainly due to γ users, as they are the only users that "know" that they have not transmitted during a frame, which I turn mean that they have not warned other users. It is defined as:

$$\sum_{\gamma=0}^{m} \underset{m,\gamma}{Pr}(S_{state=CP0}) = \sum_{\gamma=0}^{m} \binom{m}{\gamma} \times (p_g)^{\gamma} \times (1-p_g)^{m-\gamma}, \tag{3-11}$$

where $\mathrm{p_g}$ is the probability of having gamma users as in Figure 3.4 ($\mathrm{p_g} = 1 - l$).

We now derive the desired user's success being in the CW0 state, namely $\sum_{\alpha=0}^{m-\gamma} \Pr_{m,\alpha,\gamma}(S_{state=CW0})$ seen in Equation (3-10). As noted earlier, the γ users either transmit or they do not, however the remaining α and β users have to "fairly compete" for a slot. The α users go up to $m-\gamma$, while the remaining users, the β users, which are users that were not heard by others, while they "think" that they have been heard is fixed to $\beta = m - \gamma - \alpha$, which obviously depend on the values of the γ and α users during the all combination calculations. Therefore, we define the probability of having α users, $\Pr_{m,\alpha,\gamma}(A=\alpha)$, having $m, \alpha,$ and γ users in the system as follows:

$$\underset{m,\alpha,\gamma}{Pr}(A=\alpha) = \binom{m-\gamma}{\alpha} (p_\alpha)^{\alpha} (1-p_\alpha)^{m-\gamma-\alpha}, \tag{3-12}$$

where, p_α is the probability of having alpha users in a particular frame, which depends on the probability of previous window frame success (S_W), derived in Equation (3-4), and the probability of packet transmission (l) in that previous frame, that is $p_\alpha = l \times S_W$.

Again, assuming the desired user is transmitting a message, their success probability when in CW0 state requires the calculations of having alpha users in a frame, and the probabilities of the desired user's slot success being an $\alpha, \beta \; or \; \gamma$ users, while having all the "other" users compete for those same slots in the frame. It is defined as follows:

$$\begin{aligned}\sum_{\alpha=0}^{m-\gamma} \underset{r,m,\alpha,\gamma}{Pr}(S_{state=CW0}) &= \sum_{\alpha=0}^{m-\gamma} \left\{ \underset{m,\alpha,\gamma}{Pr}(A=\alpha) \right. \\ &\times \left[\left(p_{D=\alpha} \times \underset{\alpha,\beta,\gamma}{Pr}(S_{D=\alpha})_{\text{Frame}} \right) + \left(p_{D=\beta} \times \underset{\alpha,\beta,\gamma}{Pr}(S_{D=\beta})_{\text{Frame}} \right) \right. \\ &\left. \left. + \left(p_{D=\gamma} \times \underset{\alpha,\beta,\gamma}{Pr}(S_{D=\gamma})_{\text{Frame}} \right) \right] \right\},\end{aligned} \tag{3-13}$$

where $\Pr_{m,\alpha,\gamma}(A=\alpha)$ is given in Equation (3-12), and $p_{D=\alpha}$ is the probability of having α users in the frame with respect to their transmissions. In this case, the desired user can either be an α, β or γ user, that is, $p_{D=\alpha} = p_\alpha = l \times S_W, p_{D=\beta} = p_\beta = l \times (1 - S_W)$ and $p_{D=\gamma} = p_\gamma = (1-l)$, as seen in Figure 3.4.

The terms $\Pr_{\alpha,\beta,\gamma}(S_{D=\alpha})_{\text{Frame}}$, $\Pr_{\alpha,\beta,\gamma}(S_{D=\beta})_{\text{Frame}}$, and $\Pr_{\alpha,\beta,\gamma}(S_{D=\gamma})_{\text{Frame}}$ are the probabilities of the desired user's success in a transmission slot of that frame having all possible combinations of the "other" remaining users competing for the same slot alongside with the desired user D being an α, β or γ user respectively. In its general form, it is derived as:

$$\Pr_{r,\alpha,\beta,\gamma}(S_{D,j})_{Frame} = 1 - \left(1 - \Pr_{\alpha,\beta,\gamma}(S_{D,j})\right)^{r}. \tag{3-14}$$

Note that the variable j is used as an index to differentiate between the different users. We define $j = 0, j = 1, \text{and } j = 2$ to represent α, β and γ users respectively. Additionally, the individual slot successes are defined, also in general form as:

$$\Pr_{\alpha,\beta,\gamma}(S_{D,j}) = \sum_{g=0}^{\gamma} Prg \times \sum_{a=0}^{\alpha} Pra \times \sum_{b=0}^{\beta} Prb \times s_{D,j} \times (1 - s_{a,j})^{a} \times (1 - s_{b,j})^{b} \times (1 - s_{g,j})^{g}, \tag{3-15}$$

where Prg, Pra and Prb are the probabilities of having specific amounts of γ, α and β users, respectively, transmitting in a slot.

$$\begin{aligned} Prg &= \binom{\gamma}{g} p^{g}(1-p)^{\gamma-g} \\ Pra &= \binom{\alpha}{a} p^{a}(1-p)^{\alpha-a} \\ Prb &= \binom{\beta}{b} p^{b}(1-p)^{\beta-b}. \end{aligned} \tag{3-16}$$

where the variable p is the probability of a slot transmission, which depends on the underlined repetition protocol. As discussed previously, it is $\frac{r}{L}, \frac{r}{L}$ and $\frac{L-r}{r-t} \Big/ \left\lfloor \frac{L}{r} \left\lfloor \frac{L-1}{r-1} \cdots \left\lfloor \frac{L-t}{r-t} \right\rfloor \right\rfloor \right\rfloor$ [6] for SFR, SPR and POC respectively. In addition if D is used as the first index, the second index, j, represents the "other" α, β and γ users. However, if the first index is the "other" α, β and γ users, then the second index, j, represents the desired user. For the desired user to succeed it is necessary that all the "other" users fail, hence we have $(1 - s_{\mathrm{a},j})^{\mathrm{a}}, (1 - s_{\mathrm{b},j})^{\mathrm{b}}$ and $(1 - s_{\mathrm{g},j})^{\mathrm{g}}$, where $s_{\mathrm{a},j}$, $s_{\mathrm{b},j}$ and $s_{\mathrm{g},j}$ are the probabilities of success of the "other" users, for all combinations of namely α, β and γ users competing with the desired user D in the same slot of the frame.

In order to derive $s_{\mathrm{a},j}$, $s_{\mathrm{b},j}$ and $s_{\mathrm{g},j}$, we first present the probabilities of transmission of all the different users in Table 3-4 shows all the users' (α, β or γ) transmission probabilities when under CW0 state. The first row shows the desired user's transmission probability having the "other" users in the system (shown as the columns in the table). As an example to illustrate its meaning, having alpha (α) users ($j = 0$) that transmitted successfully in a warning frame (these users are in CW0 state or cause the user to enter CW0 state), the probability that the desired user will transmit (S_D) is $\left(\frac{1}{\alpha+1}\right)$. Note that the desired user in this case has also warned about their transmissions. We call this the transmission determination process for CW0. This ensures that a fair transmission process is taking place among all the warned vehicles. When looked at the "other" users having the desired user to "compete" with during a slot, the columns represent

the desired user, and the rows the "other" users. For example, for alpha users' $s_{a,j}$, their probability of transmissions are $1/(\alpha+1)$ or $1/\alpha$ depending on which kind of a user is the desired user. If $j=0$ then the desired user is an alpha user, hence the "other" alpha users will transmit at a probability that accounts for that desired alpha user (hence the +1 in the denominator). As for the other 2 cases, the transmission probability only relies on other alpha users being in the system, that is, the fact that the desired user is a beta user ($j=1$), the alpha users could not have heard the desired user, which in turn reduces the desired user's success. If the desired user is a gamma user ($j=2$), the desired user will not transmit as they will go into the CP0 state as defined in Equation (3-11), meanwhile the alpha users will all go through the transmission determination procedure with other alpha users in the system.

Table 3-4: Users transmission probability under CW0 state

Users	J=0 for alpha	J=1 for beta	J=2 for gamma
SD (desired)	$\frac{1}{\alpha+1}$	$\frac{1}{\alpha+1}$	$\begin{cases}1, & \alpha=0\\ 0, & \alpha>0\end{cases}$
Sa (alpha)	$\frac{1}{\alpha+1}$	$\frac{1}{\alpha}$	$\frac{1}{\alpha}$
Sb (beta)	$\frac{1}{\alpha+2}$	$\frac{1}{\alpha+1}$	$\frac{1}{\alpha+1}$
Sg (gamma)	0	$\begin{cases}0, & \alpha\geq 1\cup g=0\\ 1, & otherwise\end{cases}$	$\begin{cases}0, & \alpha\geq 1\cup g=0\\ 1, & otherwise\end{cases}$

Based on Table 3-4, and the logic behind the different users' behaviours in a vehicular communications system, we provide all the users' (α, β or γ) transmission probabilities equations under CW0 state at the slot level. The control variable j represents the desired user D's behavior as being an α, β or γ user. For the desired user, having other users "competing" with them, we obtain the desired user's (D) transmission probability $s_{D,j}$ given α, β or γ competing users in a slot as:

$$s_{D,j}=\begin{cases}\frac{1}{\alpha+1}, & when\ j<2\\ 1, & when\ j\ is\ 2\ and\ \alpha=0\\ 0, & when\ j\ is\ 2\ and\ \alpha\geq 1\end{cases}. \tag{3-17}$$

As for the transmission probability for the alpha users (α), $s_{a,j}$, is simplified in respect to the desired user competing in the same slot is derived as:

$$s_{a,j}=\frac{1}{\alpha+\frac{1}{2}j^2-\frac{3}{2}j+1}. \tag{3-18}$$

The transmission probability for the beta users (β), $s_{b,j}$, having j representing the behavior of the desired user D being an α, β or γ user, compete with probability of transmission as:

$$s_{b,j}=\frac{1}{\alpha+\frac{1}{2}j^2-\frac{3}{2}j+2}. \tag{3-19}$$

As for the transmission probability for the gamma users (γ), $s_{g,j}$, we similarly have:

$$s_{g,j} = \begin{cases} 0, & \text{when } j = 0, or\ \alpha \geq 1, or\ g = 0 \\ 1, & \text{otherwise} \end{cases}. \tag{3-20}$$

Therefore, the desired user's PCCW's success probability when in CW0 state can now be derived by first substituting Equations (3-16), (3-17), (3-18) , (3-19) and (3-20) into Equation (3-15), and then the result into Equation (3-14). Finally, combine Equation (3-14) result with Equation (3-12) into Equation (3-13).

$$\begin{aligned} &\sum_{\alpha=0}^{m-\gamma} \Pr_{r,m,\alpha,\gamma}(S_{state=CW0}) \\ &\quad = \sum_{\alpha=0}^{m-\gamma} \left\{ \binom{m-\gamma}{\alpha} (p_\alpha)^\alpha (1-p_\alpha)^{m-\gamma-\alpha} \right. \\ &\quad \times \left((l \times S_W) \times \Pr_{\alpha,\beta,\gamma}(S_{D=\alpha})_{\text{Frame}} \right) + \left(p_{D=\beta} \times \Pr_{\alpha,\beta,\gamma}(S_{D=\beta})_{\text{Frame}} \right) \\ &\quad \left. + \left(p_{D=\gamma} \times \Pr_{\alpha,\beta,\gamma}(S_{D=\gamma})_{\text{Frame}} \right) \right\}, \end{aligned} \tag{3-21}$$

From Equation (3-10), the probability of PCCW's success given that there are m interfering users, can now be fully defined by substituting Equations (3-11) and (3-21) into Equation (3-10).

For the final probability of success for PCCW taking into account the traffic model, we substitute the final result obtained in Equation (3-21) together with (3-11) into (3-10) for PCCW success, finally combining that with Equations (3-7) or (3-8) into Equation (3-5).

$$\begin{aligned} \sum_{\alpha=0}^{m-\gamma} \Pr_{r,m,\alpha,\gamma}(S_{state=CW0}) &= \sum_{\alpha=0}^{m-\gamma} \left\{ \binom{m-\gamma}{\alpha} (p_\alpha)^\alpha (1-p_\alpha)^{m-\gamma-\alpha} \right. \\ &\times \left((l \times S_W) \times \sum_{g=0}^{\gamma} \binom{\gamma}{g} p^g (1-p)^{\gamma-g} \right. \\ &\left. \times \sum_{a=0}^{\alpha} \binom{\alpha}{a} p^a (1-p)^{\alpha-a} \times \sum_{b=0}^{\beta} \binom{\beta}{b} p^b (1-p)^{\beta-b} \times s_{D,0} \times (1-s_{\mathrm{a},0})^{\mathrm{a}} \times (1-s_{\mathrm{b},0})^{\mathrm{b}} \times (1-s_{\mathrm{g},0})^{\mathrm{g}} \right) \\ &+ \left((l \times S_W) \times \sum_{g=0}^{\gamma} \binom{\gamma}{g} p^g (1-p)^{\gamma-g} \right. \\ &\left. \times \sum_{a=0}^{\alpha} \binom{\alpha}{a} p^a (1-p)^{\alpha-a} \times \sum_{b=0}^{\beta} \binom{\beta}{b} p^b (1-p)^{\beta-b} \times s_{D,1} \times (1-s_{\mathrm{a},1})^{\mathrm{a}} \times (1-s_{\mathrm{b},1})^{\mathrm{b}} \times (1-s_{\mathrm{g},1})^{\mathrm{g}} \right) \\ &+ \left((l \times S_W) \times \sum_{g=0}^{\gamma} \binom{\gamma}{g} p^g (1-p)^{\gamma-g} \right. \\ &\left. \left. \times \sum_{a=0}^{\alpha} \binom{\alpha}{a} p^a (1-p)^{\alpha-a} \times \sum_{b=0}^{\beta} \binom{\beta}{b} p^b (1-p)^{\beta-b} \times s_{D,2} \times (1-s_{\mathrm{a},2})^{\mathrm{a}} \times (1-s_{\mathrm{b},2})^{\mathrm{b}} \times (1-s_{\mathrm{g},2})^{\mathrm{g}} \right) \right\}, \end{aligned} \tag{3-22}$$

Equation (3-22) can also be understood through inspection of the included detailed pseudo code for CW0 state for PCCW provided in Appendix C.

3.6 PCCW over SPR, SFR and POC Analytical Analysis

As previously mentioned, we selected repetition-based protocols to implement into our PCCW because we want to improve on the reliability of these protocols for improved vehicular safety messaging.

We take the equations derived earlier and discuss the different modifications required for PCCW to accommodate these changes for the different repetition-based protocols, namely, SFR, SPR and POC, noting that PCCW is not limited to these protocols.

For both SPR and SFR it is $\frac{r}{L}$, while for POC it is $\frac{L-r}{r-t}\Big/\left\lfloor\frac{L}{r}\left\lfloor\frac{L-1}{r-1}\cdots\left\lfloor\frac{L-t}{r-t}\right\rfloor\right\rfloor\right\rfloor$ [6]. These changes are reflected in the equations where there is the transmission probability p, such as in Equations (3-16) and (3-21).

The main difference between SPR and the other two protocols is that SPR doesn't have a fixed amount of repetitions in its frame. We derive the mathematical difference of SPR in this section.

We show only where the modification takes place. Note that the change occurs at the slot level, since it is not known how many repetitions there are in a frame for SPR, hence we start by modifying the CW0 state as it is inside that set of equations that we start going into the slot level. The difference starts in Equation (3-13), where we have to start with repetition ($\hat{r} = 0$) for all possible repetitions all the way up to repetition ($\hat{r} = L$ slots) given r average repetitions, hence Equation (3-13) becomes:

$$\begin{aligned}\sum_{\alpha=0}^{m-\gamma}\sum_{\hat{r}=0}^{L}\Pr_{r,m,\alpha,\gamma}(S_{state=CW0}) &= \sum_{\alpha=0}^{m-\gamma}\sum_{\hat{r}=0}^{\mathrm{L}}\Big\{\Pr_{\mathrm{m},\alpha,\gamma}(\mathrm{A}=\alpha)\\ &\times\Big[\Big(p_{D=\alpha}\times\Pr_{\alpha,\beta,\gamma}(S_{D=\alpha})_{\text{ Frame}}\Big)+\Big(p_{D=\beta}\times\Pr_{\alpha,\beta,\gamma}(S_{D=\beta})_{\text{ Frame}}\Big)\\ &+\Big(p_{D=\gamma}\times\Pr_{\alpha,\beta,\gamma}(S_{D=\gamma})_{\text{ Frame}}\Big)\Big]\Big\}.\end{aligned} \tag{3-23}$$

Since it could be any amounts of repetitions, we also need to know the probability of having $\hat{r}$ repetitions out of L total slots given the average repetition r, PrL_r as follows:

$$PrL_{\hat{r}} = \binom{\mathrm{L}}{\hat{r}}\times\left(\frac{r}{L}\right)^{\hat{r}}\times\left(1-\frac{r}{L}\right)^{\mathrm{L}-\hat{r}}. \tag{3-24}$$

Equation (3-24) will be multiplied to the CW0 state, hence Equation (3-10) for SPR becomes:

$$\Pr_{m}(S_{PCCW})_{SPR} = \sum_{\gamma=0}^{m}\Pr_{m,\gamma}(S_{state=CP0})\times\sum_{\alpha=0}^{m-\gamma}\sum_{r=0}^{L}\Pr_{r,m,\alpha,\gamma}(S_{state=CW0})\times PrL_{\hat{r}}. \tag{3-25}$$

Finally, since we are looping or summing through $\hat{r}$, the probability of the desired user's success in a transmission frame derived in Equation (3-14) goes to $\hat{r}$ instead of r, hence Equation (3-14) for SPR becomes:

$$\Pr_{\hat{r},\alpha,\beta,\gamma}(S_{D,j})_{Frame} = 1 - \left(1 - \Pr_{\alpha,\beta,\gamma}(S_{D,j})\right)^{\hat{r}}. \quad (3\text{-}26)$$

As presented, the equations for probability of frame success are the same for each repetition type SFR, SPR and POC with the exception that the probabilities of slot transmissions are different for each type.

3.7 Enhanced-PCCW (EPCCW) Design

Enhanced-PCCW (EPCCW) combines the capability of the OFDM PHY layer to change data rates with the PCCW warning scheme. In essence EPCCW increases the transmission data rates of selected packet slots, effectively creating sub slots, which simultaneously reduce transmission time and collision potential of selected slots for multiple users. An example will be where users are aware of a collision potential at a certain slot via PCCW protocol, and in EPCCW these users will randomly select a sub slot within that slot. Table 3-5 shows the different data rates of the current DSRC system with its relative modulation and code rate schemes.

Table 3-5: DSRC (IEEE802.11p) data rates

Modulation Scheme	Code Rate	Data Rate (Mbps)
BPSK	1/2	3
BPSK	3/4	4.5
QPSK	1/2	6
QPSK	3/4	9
16QAM	1/2	12
16QAM	3/4	18
64QAM	2/3	24
64QAM	3/4	27

However, increasing to higher data rates is well known to increase the bit error rate (BER) and packet error rate (PER) at the PHY layer level. In literature [26], including our experience working with the PHY [4], [11], [27], [28], [29], [30], and [31], it has been observed that this significant increase in BER and PER occurs at the highest modulation schemes (QAM16 and QAM64). Hence, regardless of the decoding schemes used, increasing the 3Mbps BPSK-modulated DSRC to a 9Mbps QPSK-modulated DSRC data rates the BER and PER difference is relatively insignificant. In addition, EPCCW design increases the data rate only at slots that were detected as being warned of collision, hence the increased chance of BER and PER is negligible. This is interesting because with EPCCW, the collisions at the MAC layer will have a higher chance to be avoided without increasing the chance of a packet drop due to corruption caused by the channel at the PHY layer. Examples are shown in the Figures 3.5 and 3.6. We, therefore, only use two variations to the EPCCW in our proposed design, namely, we will consider both the doubling and tripling of the 3Mbps data rate. We refer to these modifications as EPCCW_{R2} and EPCCW_{R3} with the increased 3Mbps data rate to 6Mbps and 9Mbps respectively.

Figures 3.5 and 3.6 are simulated using our OFDM simulator in [28], and the parameters are carefully considered to ensure that the situations are tested in wireless access vehicular environment (WAVE) [1]. Additionally, in order to justify the use of EPCCW_{R2} and EPCCW_{R3}, these simulations are carried out under the worst case scenario, namely no line of sight (NLOS) Rayleigh fading channel, and with varying signal

to noise ratios (SNR) for DSRC systems. Since the parallel OFDM PHY subcarriers are always fixed in DSRC to 48 subcarriers, only choosing different modulation schemes and forward error correction (FEC) code rates for convolution coding will provide the desired data rates. That is, 3Mbps BPSK-modulated DSRC, 6Mbps QPSK-modulated DSRC, and 9Mbps QPSK-modulated DSRC. The 12Mbps 16QAM-modulated DSRC is also shown in the figures for highlighting that this data rate begins to show a significant increase in BER and PER. Puncturing is used to achieve the higher code rates ($2/3$ and $3/4$ convolutional encoding) as per the IEEE802.11p standard [7]. The legal maximum relative speed in highways is assumed to be 238 km/h, hence is used as worst case Doppler shift Rayleigh fading channel. We use 5000 OFDM packets with 2880 data bits for each of the modulation schemes. The figures show a significant increase in both BER and PER at the higher data rates, i.e. at 12 Mbps and higher. Both 12 Mbps and 27 Mbps respond with error floor. As for the higher than the 12Mbps modulation scheme, it can only get worse, especially that puncturing is used to achieve these higher data rates. However, the BER and PER between 3, 6, and 9 Mbps are comparable, and none of them result in error floor.

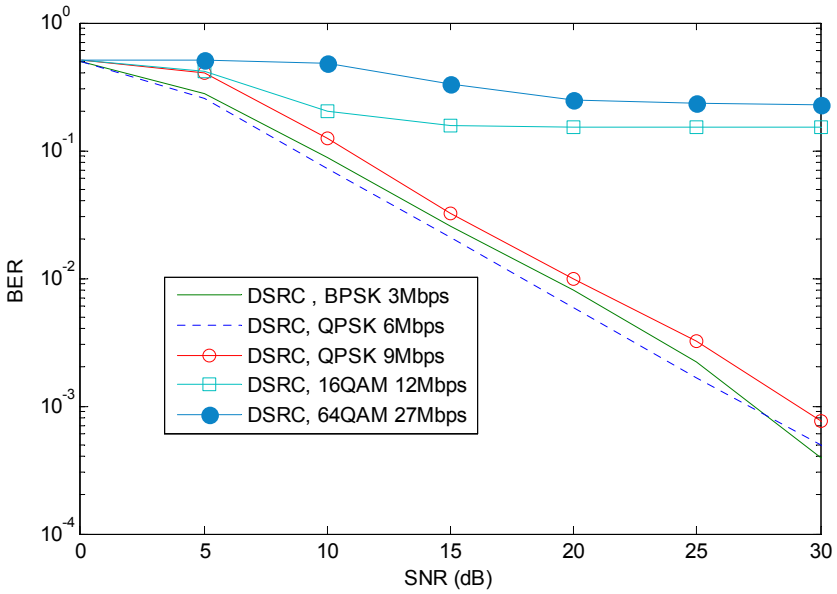

Figure 3.5 BER plot showing different data rates for conventional DSRC PHY

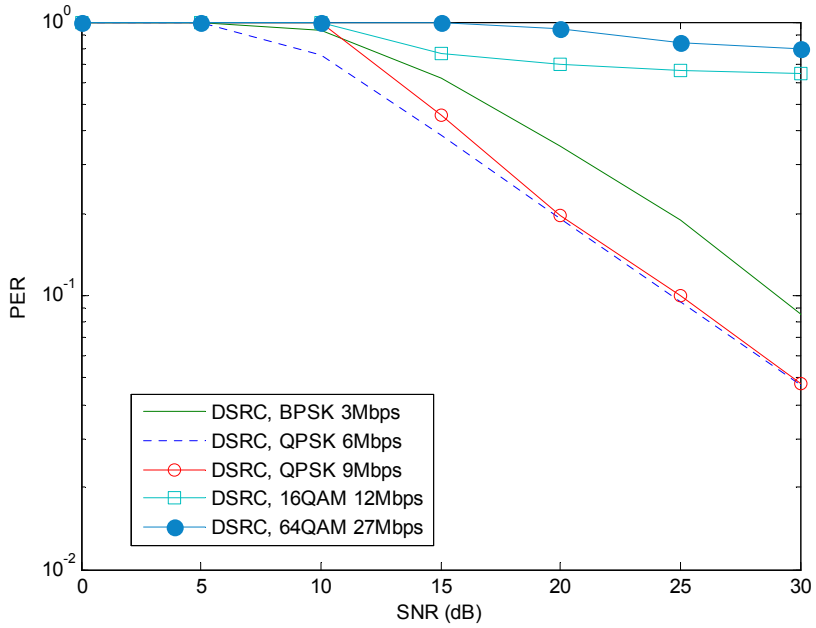

Figure 3.6 PER plot showing different data rates for conventional DSRC PHY

3.7.1 EPCCW Analytical Analysis

EPCCW has the same logic and design as the PCCW except for when the colliding users will split into sub slots 1, 2 or 3. Hence, the change or difference between PCCW and EPCCW occurs at these sub slots. This change occurs at the CW0 state in Equation (3-13), specifically in the $Pr_{\alpha,\beta,\gamma}(S_{D,j})$ probability of Equation (3-15), which becomes the probability of the desired user's success in a transmission slot of that frame having all possible combinations of the "other" remaining users competing for the same sub slot alongside with the desired user D being an α, β or γ user respectively, $Pr_{\alpha,\beta,\gamma,a,b}(S_{D,j})$. Note the addition of the extra input variables a and b in that probability are necessary to obtain the probabilities of having a_R and b_R users of the a and b of the α and β users "competing" in that sub slots, respectively. These extra variables represent all combinations of different user types interacting in the environment so that the probability of success given each user type is represented. In addition, it is worth noting that since γ users do not participate in sub slots for the same reason that they did not warn of their transmissions, hence we do not add g_R users in the equation. We now derive the equation as follows:

$$\begin{aligned} \underset{\alpha,\beta,\gamma,a,b}{Pr}(S_{D,j}) = & \sum_{g=0}^{\gamma} Prg \\ & \times \sum_{a=0}^{\alpha} Pra \\ & \times \sum_{b=0}^{\beta} Prb \sum_{a_R=0}^{a} Pra_R \sum_{b_R=0}^{b} Prb_R \times s_{D,j} \times (1-s_{a,j})^{a} \times (1-s_{b,j})^{b} \\ & \times (1-s_{g,j})^{g}. \end{aligned} \tag{3-27}$$

As previously mentioned, Pra_R and Prb_R are the probabilities of having a_R and b_R out of a and b "competing" users in the same sub slots, given α and β frame transmitting users, respectively, and are defined as:

$$Pra_R = \binom{a}{a_E} {p_R}^{a_R}(1-p_R)^{a-a_R} \tag{3-28}$$

and,

$$Prb_R = \binom{b}{b_E} {p_R}^{b_R}(1-p_R)^{b-b_R}. \tag{3-29}$$

where $\mathrm{p_R} = 1/\mathrm{R_{factor}}$ and is the probability of a user success in a sub slot with $\mathrm{R_{factor}} = 1$ or 2 or 3 depending on the amount of sub slots, and hence data rate increase.

Everything else stays the same for EPCCW as compared to PCCW, and the final desired user's EPCCW's success probability is derived in a similar fashion as we did for PCCW.

3.8 Delay Considerations for PCCW and EPCCW

Similarly defined in [6], average delay is defined as the expected timeslot count at which the transmitting user's packet is first received successfully:

$$D_{PCCW} = \sum_{m=0}^{m_{max}} D_{PCCW}(m)\, Pr(m), \tag{3-30}$$

where $D_{PCCW}(m)$ is the average delay of a transmission being successfully received having m interfering users; while $\Pr(m)$ is the probability of having m interfering users as in Equations (3-7) or (3-8) . The translation from timeslot to real time accounting for number of bits in header and the message is explained in the simulations chapter, Chapter 4.

3.8.1 PCCW Average Delay

1) *For PCCW over either SFR or POC:* where a fixed amount of repetitions is used is defined similarly in [6]:

$$D_{PCCW}(m)|_{\mathrm{SFR\ or\ POC}} = \sum_{i=0}^{r} \frac{Pr_i(\hat{S}_{PCCW})}{\underset{m}{Pr}(S_{PCCW})} \times \sum_{d=i}^{L-r+i} d \times P_m(D = d|\hat{S}_i), \tag{3-31}$$

The variables $Pr_i(\hat{S}_{PCCW})$ and$Pr_m(S_{PCCW})$ are the probabilities of having the i^{th} slot as the first successful timeslot and the PCCW's probability of success, respectively. These two obviously defer from SFR and POC protocols, whereas the variable $P_m(D = d|\hat{S}_i)$ is the probability that the delay is equal to "d" when the i^{th} transmission is the first successful transmission and is the same for all three protocols (PCCW, SFR and POC). It is defined using the hypergeometric function, and is used due to the fact that in both

SFR and POC repetition protocols, hence also for PCCW over those protocols, the slots are depended with one another whereas the interfering users are not. This is given by:

$$\frac{\binom{d-1}{i-1}\binom{L-d}{r-i}}{\binom{L}{r}}. \tag{3-32}$$

The probability of PCCW with at least one successful transmission $Pr_m(S_{PCCW})$ is derived earlier in this chapter. In order to derive $Pr_i(\hat{S}_{PCCW})$, we first need to find the probability of PCCW with at least one successful transmission up to $i-1$ transmissions, $Pr(\hat{S}_{i-1})$, and subtract that from the probability of PCCW with at least one successful transmission up to i^{th} transmissions, $Pr(\hat{S}_i)$, hence it can be written as:

$$Pr_i(\hat{S}_{PCCW}) = Pr(\hat{S}_i) - Pr(\hat{S}_{i-1}), \tag{3-33}$$

where both $Pr(\hat{S}_i)$ and $Pr(\hat{S}_{i-1})$ are same as the probability of PCCW,$Pr_m(S_{PCCW})$, except that the probability of frame success goes up to i and $i-1$ respectively, instead of r repetitions. This is accomplished by modifying Equation (3-14) to loop up to i and $i-1$ respectively, instead of r, that is:

$$\underset{\hat{r},\alpha,\beta,\gamma}{\Pr}(S_{D,j})_{Frame} = 1 - \left(1 - \underset{\alpha,\beta,\gamma}{\Pr}(S_{D,j})\right)^{i}, \tag{3-34}$$

and,

$$\underset{\hat{r},\alpha,\beta,\gamma}{\Pr}(S_{D,j})_{Frame} = 1 - \left(1 - \underset{\alpha,\beta,\gamma}{\Pr}(S_{D,j})\right)^{i-1}, \tag{3-35}$$

respectively.

The only difference between SFR and POC representation is that the probability of frame success has different transmission probabilities due to SFR having fixed transmissions, while POC's transmission are related to LUT codeword generation.

2) *For PCCW over SPR:* the slots are independent as well as the interfering users. Similarly defined in [6], the average delay of a transmission being successfully received having m interfering users is defined as:

$$D_{PCCW}(m)|_{\text{SPR}} = \sum_{i=0}^{L} \frac{i \times Pr_i(\hat{S}_{PCCW})}{\underset{m}{Pr}(S_{PCCW})}. \tag{3-36}$$

Note that in the SPR case, there could be up to L repetitions. Both $Pr_i(\hat{S}_{PCCW})$ and$Pr_m(S_{PCCW})$ have the same meaning as the ones used in PCCW over SFR and POC, the main difference is their derivations. The PCCW over SPR's probability of having at least one successful transmission is $Pr_m(S_{PCCW})$, and is derived previously earlier. To obtain the probability of having the i^{th} slot as the first successful timeslot $Pr_i(\hat{S}_{PCCW})$ over SPR, and since the slots are independent, first find the probability of success of any of the slots in the frame by modifying Equation (3-14) to not include all possible r repetitions but rather one slot success as follows:

$$Pr(\hat{S}) = \sum_{\gamma=0}^{m} \Pr_{m,\gamma}(S_{state=CP0}) \times \sum_{\alpha=0}^{m-\gamma} \Pr_{r,m,\alpha,\gamma}(S_{state=CW0}) \times \frac{r}{L}. \quad (3\text{-}37)$$

Note how the probability of having r repetition in L slots ($PrL_{\hat{r}}$) is being replaced with the transmission probability of an SPR slot $\left(\frac{r}{L}\right)$ in the Equation (3-37). Using Bernoulli distribution, we then multiply Equation (3-37) by the $i-1$ slots failures to obtain the first i^{th} slot success. Hence, the probability of having the i^{th} slot as the first successful timeslot $Pr_i(\hat{S}_{PCCW})$ over SPR can be written as:

$$Pr_i(\hat{S}_{PCCW}) = Pr(\hat{S}) \times \left(1 - Pr(\hat{S})\right)^{i-1}. \quad (3\text{-}38)$$

Substituting Equation (3-38) into Equation (3-36), we obtain the average delay of the entire frame having i^{th} slot being any slot up to L slots with m interfering users as:

$$D_{PCCW}(m)|_{\text{SPR}} = \sum_{i=0}^{L} \frac{i \times Pr(\hat{S}) \times \left(1 - Pr(\hat{S})\right)^{i-1}}{\underset{m}{Pr}(S_{PCCW})}, \quad (3\text{-}39)$$

The average delay for EPCCW protocol is same as for the PCCW, except we replace the probability of PCCW's success, $Pr_m(S_{PCCW})$, with the probability of EPCCW's success, $Pr_m(S_{EPCCW})$, derived earlier in this chapter. Additionally, the probability of having the i^{th} slot as the first successful timeslot, $Pr_i(\hat{S}_{EPCCW})$, can easily be derived similarly to $Pr_i(\hat{S}_{PCCW})$, with EPCCW's probability of success instead of PCCW's probability of success in its calculations.

3.9 Simulation and Analytical Results

As previously mentioned, we simulate the system in a highway environment from SUMO to generate a mobility model which influences our accurate PHY layer environment. Based on the DSRC standard [7] and simulator design, Tables 3-6 to 3-8 provides the parameter values used for simulations and they are according to the IEEE 802.11p standard on the PHY and MAC layers [7].

As mentioned earlier, we are assuming a highway traffic environment under two, four, and eight lane scenarios. DSRC safety systems would actually influence the movement of vehicles for the purpose of providing a safe driving experience. The movement of vehicles could include braking times, acceleration, and turning. Because we are simulating on a frame by frame basis, and the length of a frame (τ) is not fixed, this vehicle movement within that period of time is not significant to frame performance. Hence, this information is not used to influence our mobility model of our simulator, and the movement is determined entirely by the SUMO [32] validated mobility simulation [32].

Although our simulator design is capable of measuring success for both unicast and broadcast traffic, we focus on the description of broadcast success because PCCW is intended for broadcast safety messaging. Regarding accurate measurement of delay and success performance, it is important to note that the users at the ends of the highway (due to limited highway simulations in SUMO) have much less interference due to having no vehicles present beyond either end of the road. These vehicles are not

included in calculating the probability of reception failure (PRF) because it is not fair relative to the users not at the edges of the simulation. However we include all vehicles as interferers regardless if they are at the edge or not.

Table 3-6: Simulation parameters

Parameter	Value
MAC Header	24 Bytes + additional Bytes for PCCW
Preamble Duration	32 μs
Antenna Gain	4 dB
Channel Frequency	5.9 GHz
Channel Width	10 MHz
Thermal Noise	- 96 dBm
PHY Subcarriers	48
PHY Pilot Subcarriers	4
PHY Training Symbols	2

The simulated communication takes place in a 5.9-GHz 802.11p DSRC channel and not in a 2.4 GHz 802.11a channel. The reception signal-to-interference-plus-noise ratio (SINR) thresholds for all the data rates supported by the radio are listed in Table 3-3, and were thoroughly studied in [4]. It can also be noted that these SINR thresholds are not that different from the ones used in [5] to simulate the IEEE802.11a DSRC standard. The transmission power is calculated based on these SINR thresholds for the different DSRC data rates, and intended communication range. Similar to the literature, such as [32] and [5], in our model, the Friis freespace channel model is used for short transmitter/receiver (TX/RX) distances and the two-ray model should be used for long distances. In addition to those channel models, we use Rayleigh fading channel caused by Doppler shift.

Table 3-7: Data traffic parameter ranges

Coding Rate	Modulation	Data Rate (Mbps)	SINR Thresholds (dB)
1/2	BPSK	3	7
3/4	BPSK	4.5	10
1/2	QPSK	6	8
3/4	QPSK	9	11
1/2	16QAM	12	11
3/4	16QAM	18	15
2/3	64QAM	24	18
3/4	64QAM	27	20

Table 3-8: Nominal parameter values

Parameter	Value
Message rate (messages/msec)	1/50- 1/500
Packet Payload (Bytes)	170, 250
Communication Range (meters)	50, 75, 150
Average Inter-Vehicular Density (meters)	10 (jammed), 30
Lane number per road	2, 4, 8
Maximum Latency	0.2 s

Each highway segment is of length 2 km, as per maximum and DSRC possible communication range; however for safety messaging the communication range is less as per Table 3-1. The highway is straight that includes entrances and exits to allow the vehicles to enter and leave the highway for a more accurate highway representation. The number in of vehicles in each lane varied according to SUMO, such that vehicles in the centre lane tended to travel fastest, and were furthest apart from each other. We measured and averaged the number of vehicles per lane between the density ranges given in Table 3-8. Based on the vehicle densities and interference ranges, the average number of total repetitions per second are $(RoadLength \times numberLanes\ /AvgDensityPerLane) \times RepetitionsPerSecond$. Additionally, we simulated for 300 seconds, leading to a large number of messages. For example if the maximum number of repetitions is 12 messages per second, with an average vehicle density of 0.2 per lane, we have (2000*4/0.2)*12*300 = 144 million messages maximum (not including repetitions systematically reduced by PCCW).

Table 3-9: Nominal parameter values

Parameter	Value
Packet Payload (Bytes)	170
Communication Range (meters)	50
Average Inter-Vehicular density (meters)	30
Lane number per road	2, 4

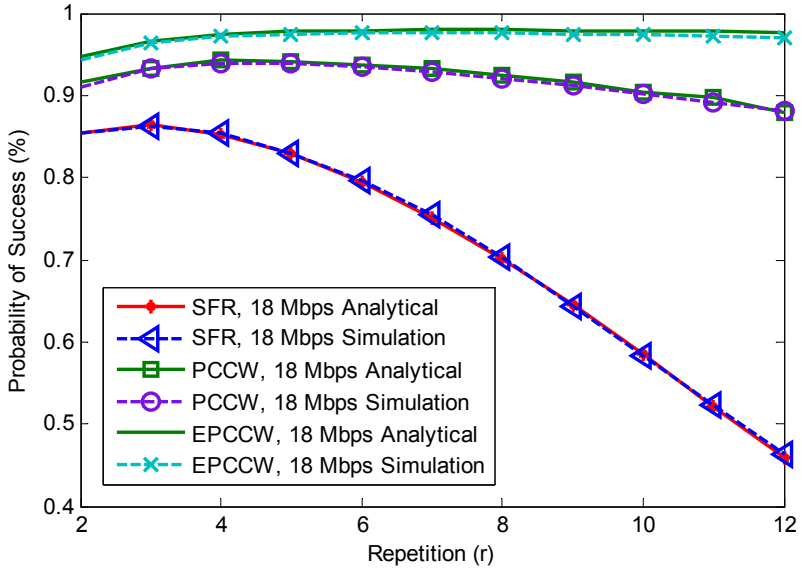

Figure 3.7 Probability of success showing simulation and analytical results for 18 Mbps SFR vs. PCCW and EPCCW

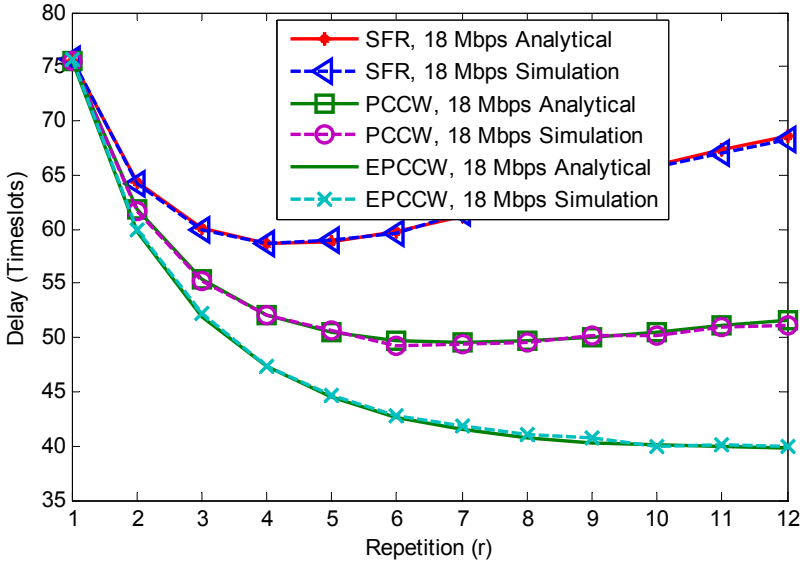

Figure 3.8 Average delay showing simulation and analytical results for 18 Mbps SFR vs. PCCW and EPCCW

Figures 3.7-3.20 show the results of all our proposed protocol designs presented in this chapter of the dissertation, and the leading repetition-based protocols discussed earlier under varying scenarios at the parameters shown in Tables 3-6 to 3-8. Whenever simulation is compared to analytical results, the Rayleigh fading channel is turned off in our PHY layer simulator. However all the different types of interfering users present in SUMO are taken into account. That is, interferers within or outside the communication range, and primary and secondary hidden nodes are also present. The plots with only simulation results have the Rayleigh fading channel turned on in our PHY layer simulator. Table 3-9 summarizes the parameters used to simulate Figures 3.7-3.14.

Figures 3.7 and 3.8 show both simulation and analytical performances in terms of probability of success and average delay in timeslots of our proposed designs compared to SFR repetition-based protocol. For fair comparison, both PCCW and EPCCW protocols had SFR as their underlying repetition protocol.

We show the behaviour for 18 Mbps data rate, which is neither too low nor the highest data rate used in DSRC. Compared to SFR, and when safety is concerned, Figure 3.7 show a significant increase in success probability of around 12% and 16% for PCCW and EPCCW respectively. This increase in success results to a near 100% performance, especially for EPCCW protocol where 98% probability of success is observed. Relative to that of SFR, it is interesting to note that the proposed designs have a constant performance improvement as the number of repetitions is increased. This indicates that our designs are very well suited to be used over repetition-based protocols. The optimal repetition values for SFR, PCCW and EPCCW are 3, 4 and 7 repetitions respectively. As for the average delay, our proposed designs show a significant decrease in timeslots as opposed to SFR protocol. This timeslots can easily be translated to real time as a check whether these protocols meet the maximum latency requirement as follows:

$$\left(\frac{Packet\ size + MAC\ Header + address\ Header\ bits\ for\ PCCW}{Data\ Rate}\right) \times Timeslots\ delay \quad (3\text{-}40)$$

Packet size in this scenario is 170 Bytes. The extra address header bits are required for PCCW and EPCCW to add information about future transmissions, and it depends on the number of repetitions and the number of average slots in a frame derived in Equation (3-9). That is, the address Header bits for PCCW/EPCCW is:

$$\begin{aligned} &address\ Header\ bits\ for\ PCCW or\ EPCCW \\ &= number of\ repetions\ in\ a\ frame \\ &\times min.\#\ of\ bits\ required\ to\ address\ the\ L\ slots\ in\ a\ frame \end{aligned} \quad (3\text{-}41)$$

The frames in our simulations are not fixed, however the average number of slots in the frame for Figures 3.7 and 3.8 is 150 slots. Hence from Equations (3-42) and (3-43), and at the optimal success repetitions, the average delay for PCCW and EPCCW are 4.5 ms and 3.7 ms respectively. Hence, they both easily meet the maximum latency requirement of 0.2 s. Although we used the optimal repetitions for the delay calculations as it is fair to do so, it can easily be noted that at all the repetitions the delay requirement is met. Additionally, both simulation and analytical results match.

Figures 3.9 and 3.10 show both simulation and analytical performances in terms of probability of success and average delay of our proposed designs compared to SFR repetition-based protocol. For these plots, we show the behaviour for 2 of the lower DSRC data rates, 4.5 Mbps and 6 Mbps. At these data rates, all protocols responded in an above 90% success rate. However, only our proposed protocols converge to a 100% success rate, while SFR success rate declines after repetition 4. The optimal repetition values for SFR, PCCW and EPCCW are around 4 and 7 repetitions respectively. Similarly, our proposed designs show a decrease in timeslots delay.

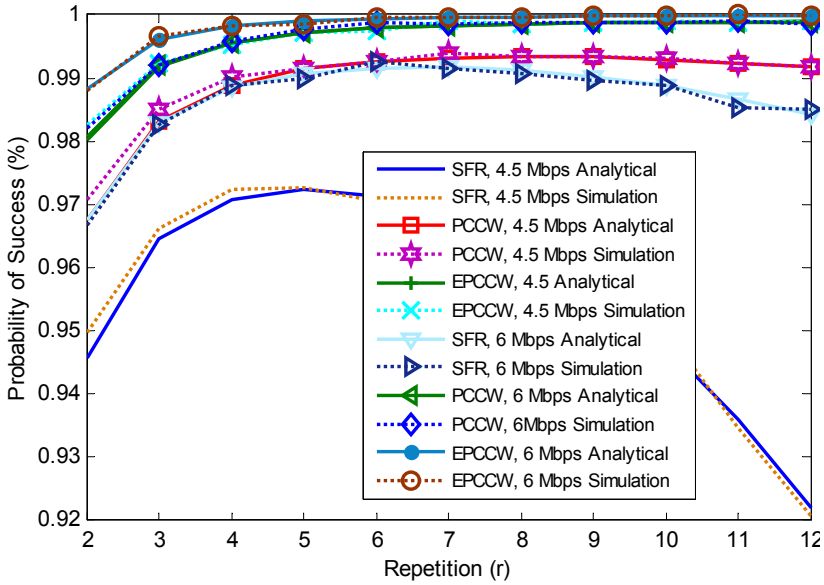

Figure 3.9 Probability of success showing simulation and analytical results for lower data rates SFR vs. PCCW and EPCCW

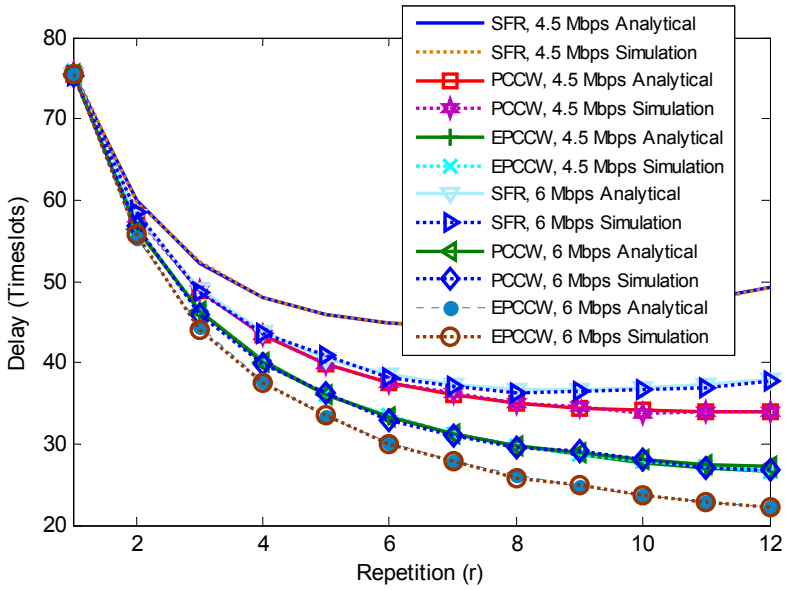

Figure 3.10 Average delay showing simulation and analytical results for lower data rates SFR vs. PCCW and EPCCW

At its worst, i.e. with the smaller data rate, the average delay for PCCW and EPCCW are 0.013 *s* and 0.011 *s* respectively. Hence, they both meet the maximum latency requirement. Both simulation and analytical results agree.

Figures 3.11-3.14 show the probability of success and average delay of our proposed designs compared to the different types of repetition protocols, SPR, SFR and POC. Figures 3.11 and 3.12 show simulation and analytical performances of PCCW compared to SPR, SFR and POC, while Figures 3.13 and 3.14 compares EPCCW with SPR, SFR and POC.

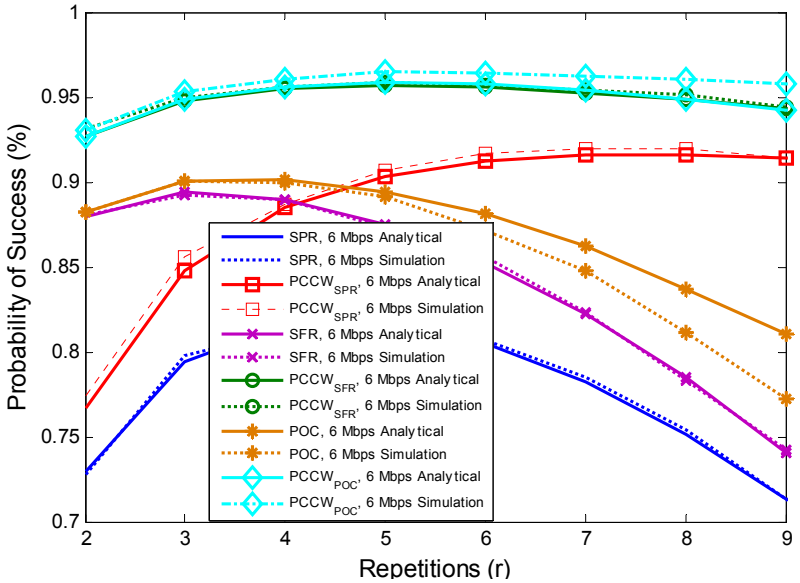

Figure 3.11 Probability of success showing simulation and analytical results for 6 Mbps SPR, SFR, POC vs. PCCW

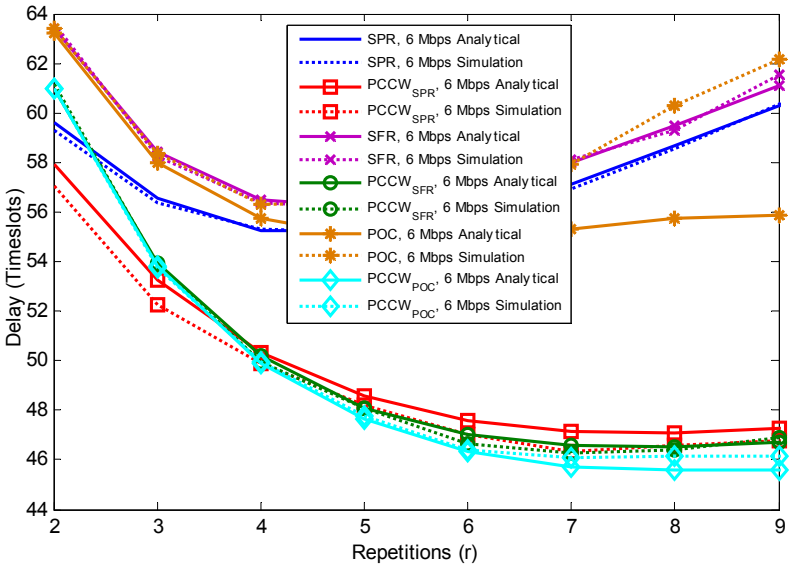

Figure 3.12 Average delay showing simulation and analytical results for 6Mbps SPR, SFR, POC vs. PCCW

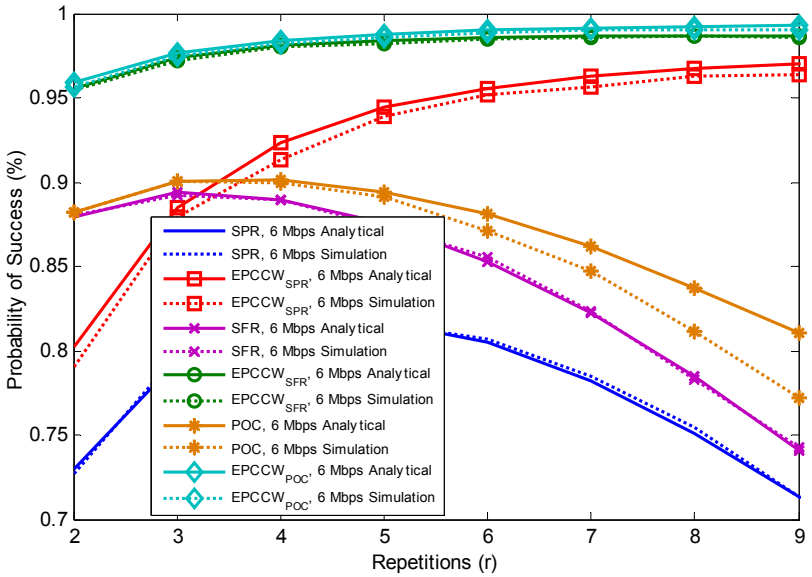

Figure 3.13 Probability of success showing simulation and analytical results for 6 Mbps SPR, SFR, POC vs. EPCCW

All of the simulation and analytical results match except with POC protocol where a slight difference is observed. The reason why the POC simulation have a slight disagreement from the POC analytical results is due to the fact that "the all combination" of POC codes are not possible to generate in simulation, and hence the POC codes we use in our simulation is from a set smaller than the theoretical maximum. It is interesting to note that although we used a subset of the maximum number of codes, our proposed protocols PCCW and EPCCW (built over POC protocol) simulations are still able to approach very closely the theoretical POC with PCCW. This is because collisions are reduced using PCCW or EPCCW. Hence, when PCCW and EPCCW are used instead of POC, it is not a requirement to have all the possible codes in

the system for an almost 100% success performance. From these figures, it can be seen that PCCW and EPCCW outperform all of their underlying repetition protocols (SPR, SFR and POC). Significant improvement is observed with our proposed designs, with EPCCW again converging to close to a 100% success rate. Similarly, the average delay can be calculated, and all of which meet the latency requirement.

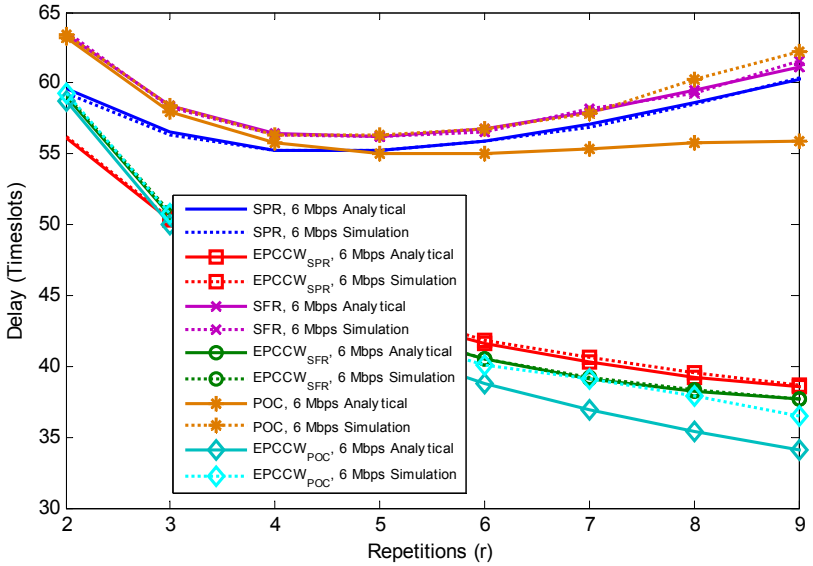

Figure 3.14 Average delay showing simulation and analytical results for 6Mbps SPR, SFR, POC vs. EPCCW

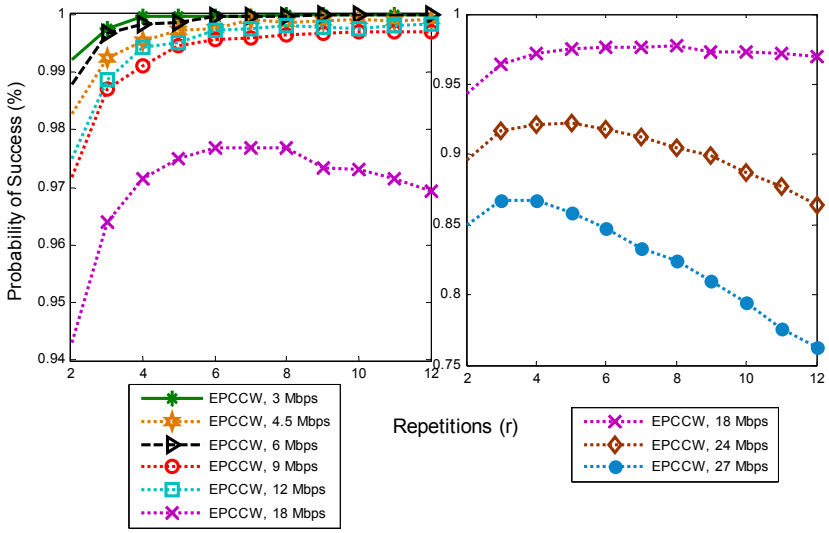

Figure 3.15 Probability of success showing simulation results for proposed design's optimum data rate

Figure 3.15 shows the simulation result for optimal study between all data rates found in DSRC. The plot is divided into two for improving visual clarity. Communication range used is 50m with 4 lanes, and average inter-vehicular density of 30 meters/vehicle. We only show EPCCW protocol because both PCCW and EPCCW responded the same for this study. Table 3-10 provides the success rate performance in descending order for PCCW or EPCCW.

Table 3-10: Data rate success rate performance in descending order for PCCW and EPCCW

Coding Rate	Modulation	Data Rate (Mbps)
1/2	BPSK	3
1/2	QPSK	6
3/4	BPSK	4.5
1/2	16QAM	12
3/4	QPSK	9
3/4	16QAM	18
2/3	64QAM	24
3/4	64QAM	27

Table 3-11 summarizes the parameters used to simulate Figures 3.16-3.18.

Table 3-11: Parameter values for larger communication range

Parameter	Value
Packet Payload (Bytes)	170, 250
Communication Range (meters)	150
Average Inter-Vehicular density (meters)	10, 30
Lane number per road	4, 8

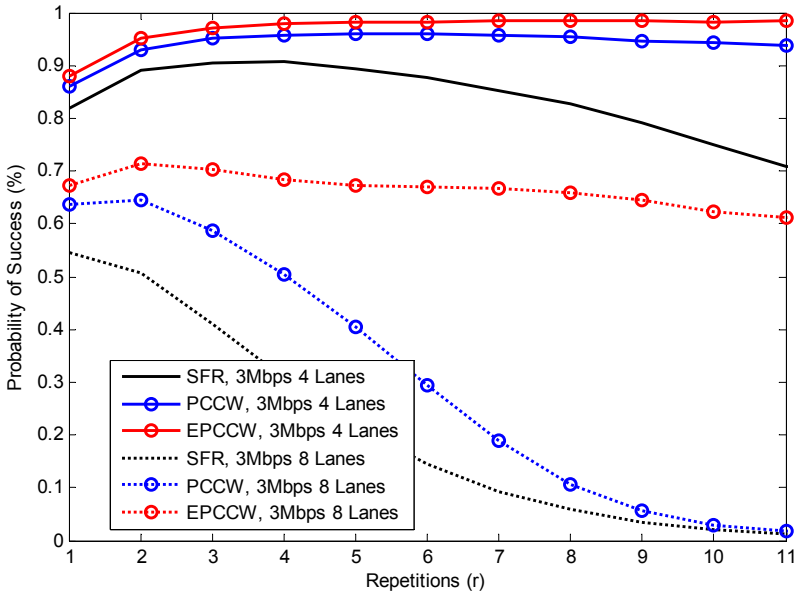

Figure 3.16 Probability of success showing simulation results with150m communication range and with low vs. high traffic loads for SFR vs. PCCW vs. EPCCW

Figure 3.16 shows the difference between having an 8-lane and 4-lane scenario at relatively high communication range of 150m. At the 8-lane scenario, the figure shows that at the very high load, PCCW outperforms the repetition protocol; however unlike EPCCW both do not perform well at higher repetitions. Although this scenario is rare, we use it to show that EPCCW is the protocol to choose under high interference load.

Figure 3.17 shows that EPCCW reduces the average delay by around 50 timeslots. It is interesting to note at its worst with the 8-lane scenario and average 375 frames; both PCCW and EPCCW meet the latency requirement of approximately 0.148 s and 0.145 s respectively.

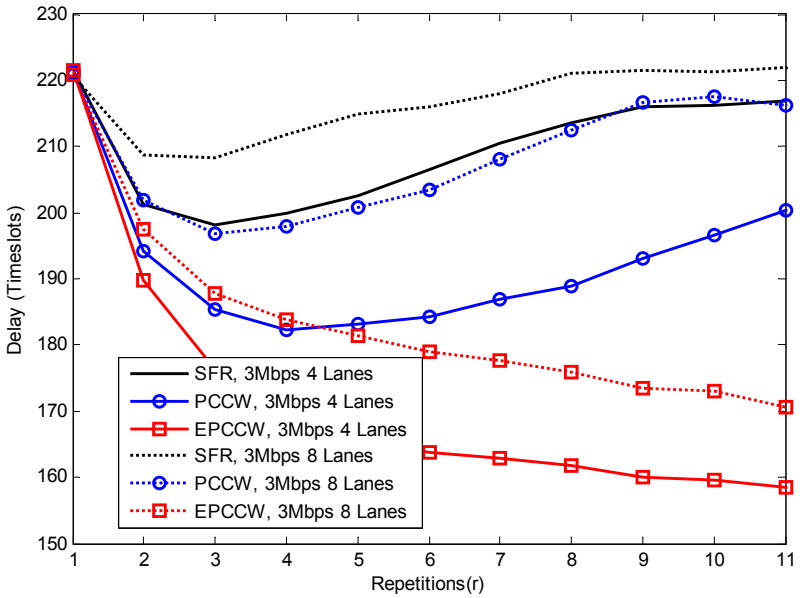

Figure 3.17 Average delay showing simulation results with150m communication range and with low vs. high traffic loads for SFR vs. PCCW vs. EPCCW.

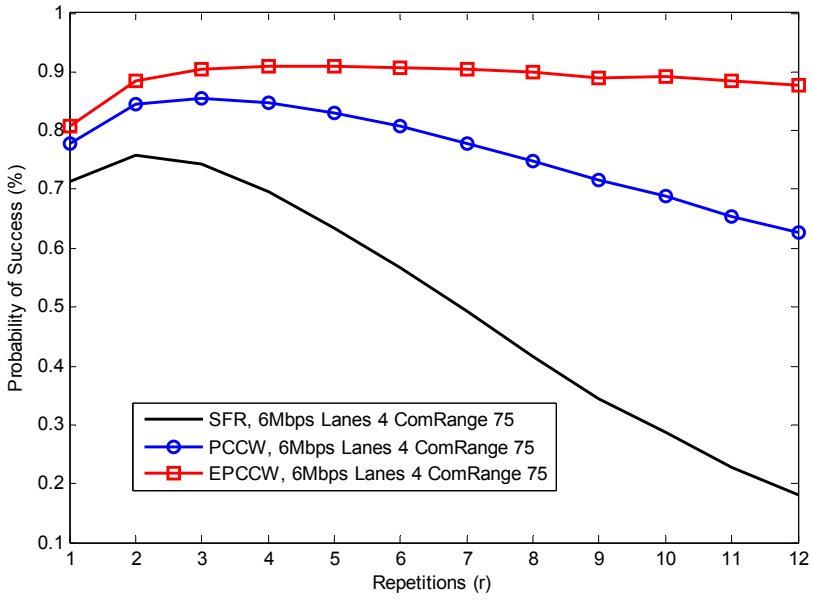

Figure 3.18 Probability of success showing simulation results with medium size communication range for SFR vs. PCCW vs. EPCCW.

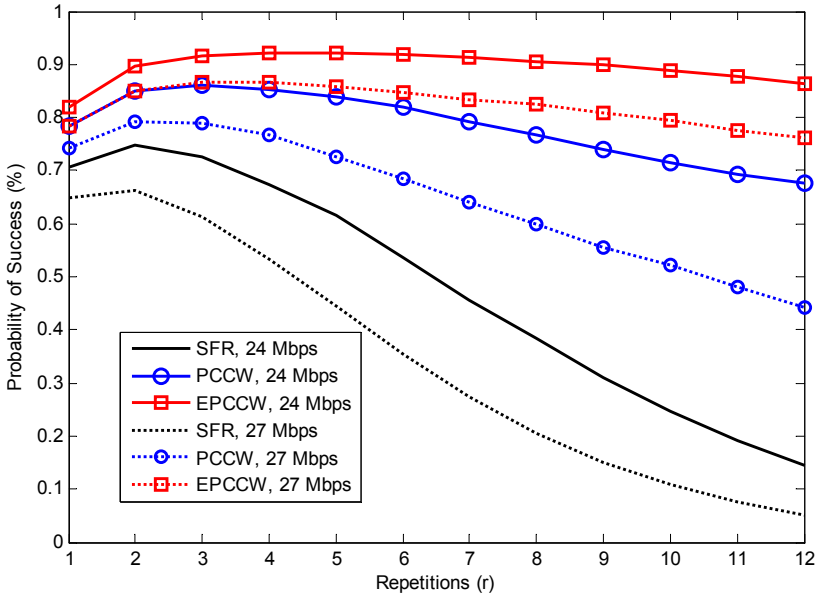

Figure 3.19 Probability of success showing simulation results for higher data rate comparison between repetition-based SFR protocol, PCCW and EPCCW.

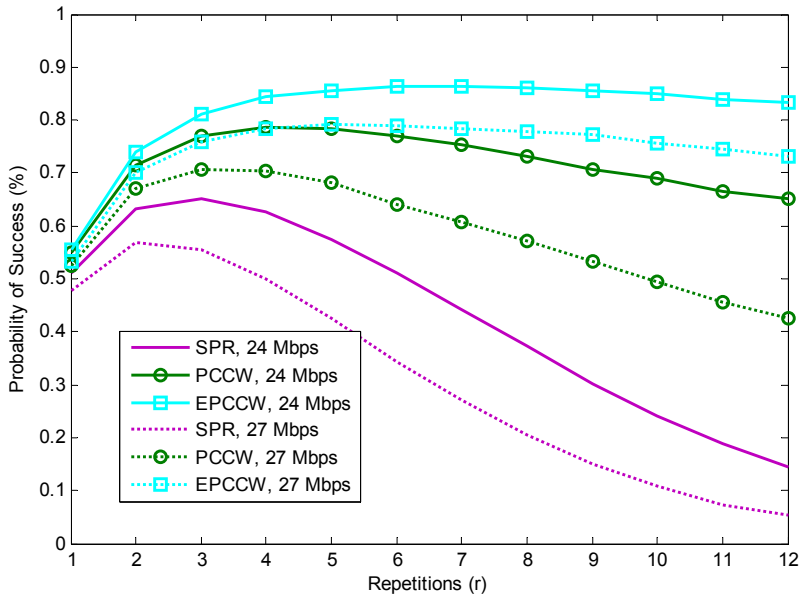

Figure 3.20 Probability of success showing simulation results for higher data rate comparison between repetition-based SPR protocol, PCCW and EPCCW.

Figure 3.18 shows the performance improvement achieved by both PCCW and EPCCW as compared to SFR at 75m communications range and inter-vehicular spacing of 10m. It shows that our proposed protocol designs significantly improve success rate performance, where EPCCW protocol's success rate goes beyond 90%.

Figures 3.19 and 3.20 show the performance of PCCW and EPCCW in the highest data rates used in DSRC. Significant improvement is shown in both PCCW and EPCCW when compared to both SFR and SPR. Again, it can be seen that only the repetition protocols reduce to near percent success rate, while PCCW and EPCCW stay almost constant throughout repetitions.

3.10 Emergency Vehicular Safety Messaging Reliability Enhancement using emergency-PCCW (ePCCW) MAC Protocol Design

In this dissertation we derive and demonstrate the Medium Access Control (MAC) layer enhancement of V2V safety messaging specifically benefiting transmission from emergency vehicles (EVs) using DSRC. In [4], we presented a Passive Cooperative Collision Warning (PCCW) MAC protocol for enhancing reliability of safety messages in DSRC. While in this work EVs are considered as requiring higher priority than that of other vehicles for conveying safety information to surrounding vehicles. Our design allows for the sharing of channel between EVs and non-EVs, while maintaining high Quality of Service (QoS) for both user types. We call this new emergency-based PCCW (ePCCW). In order to work effectively, the protocol requires synchronized time slots in the MAC layer in order to prevent collisions in the DSRC Physical layer (PHY). The precise time synchronization can be achieved practically using a number of techniques including Global Positioning Satellite System (GPS), or alternatively city wide pulse [5]. For this dissertation, communication access is limited to one DSRC channel that is shared by both EVs and non-EVs, this is the worst case.

3.10.1 Safety Consideration and EV Communications

Ranging in QoS requirements, DSRC safety message has a relatively small but variable payload size. It ranges from routine to critical safety of life [9]. Routine messages may include small changes in velocity or acceleration and position. Critical safety of life message may include event information such as emergency braking or airbag activation messages. All of these messages need to be received by other vehicles at low latency for it to be effective, and with high reliability, even under scenarios of high channel usage. It is reported that in order to greatly improve vehicular safety, the communication delay should not exceed approximately 200ms [8].

As mentioned earlier, one of the primary roles of DSRC is to improve vehicle safety through effective communications. Hence, higher safety standards can be achieved if EVs can provide information about the immediate surroundings to other vehicles. This is a key motivation of our study. Each EV is given priority over regular vehicles such that the EVs achieve the highest reliability communications which are broadcast to all surrounding nodes. Our ePCCW protocol presented allows non-EVs to share the same channel for conveying safety information as the EVs, but in a way that lets EVs achieve higher reliability without increasing the number of repetitions. Full functionality and analysis of performance in relation with other repetition based protocol in also presented.

3.10.2 ePCCW for Emergency Communications

ePCCW follows the PCCW state machine with a redesigned conditional transmission CW0 state. It is different in that unlike the PCCW protocol, the ePCCW protocol differentiates between EV and non-EV decision making. EVs have a higher priority mode for sending safety messages. This improved reliability requires non-EVs to intentionally operate in non-greedy mode. When a non-EV detects the presence of an EV, it will only operate in CP0 mode and never enter CW mode.

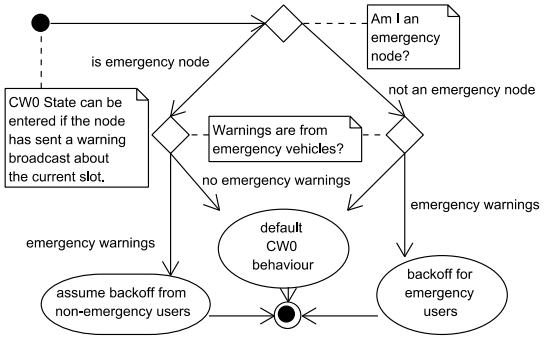

Figure 3.21 CW0 behaviour for ePCCW

In essence, when a non-EV hears the EV, they will not transmit into the same slots as the EV. Figure 3.21 illustrates the decision making behavior of the ePCCW CW0 state. In order to enter CW0 state, the node must have warned, and have sent a warning message via a previous recent broadcast, informing of the node's intentions. If a node is an EV node, it will also transmit into the slot either directly, or if other EVs are present, will randomly decide to transmit based on the number of EVs it heard warning. If the node is a non-EV, then it will back off for EVs that have warned to use the slot, or otherwise behave as PCCW standard algorithm if no EVs warning are received.

Based on this description we will now model the performance of this state analytically. We define the length of the warning window used in ePCCW as X. Probability of the EV success, $\Pr_X(S_{\mathrm{EV}})$ for a given warning window of length X, we require the probability of past frame success for a given repetition protocol. Recall, for SFR the probability of success (S) is given by the equation relating to repetitions and interferers [7]:

$$\Pr_{m,r}(S_{SFR}) = \sum_{k=1}^{r} (-1)^{k+1} \binom{r}{k} \left(\frac{\binom{\frac{L-k}{r}}{\binom{X}{r}}}{} \right)^{m}, \tag{3-42}$$

where k is the number of successful repetitions out of r total, L is the frame length, and m is the number of interferers. All slots collide in the frame for EV at a probability of $1 - Pr(S)$, at which point the ePCCW equation uses the window X to predict non-EV back-off. This warning gives success improvement over other protocols.

In order to calculate the probability of success for ePCCW, we need its probability of entering each CP0 or CW0 states, because these states contribute to success that would not normally occur in the regular

underlying repetition protocol. In other words, we need to take these states into account because they offer corrections and preventions of collisions that would otherwise result in broadcast failures. The ePCCW version of CW0 gives preference to EVs by sending non-EVs to CP0 state instead of conditionally transmitting state, CW0. Hence as long as the EV is heard by other non-EVs, the EV will take all the benefits of the CW0 state, while the non-EVs will result in success benefits assuming CP0 state.

To summarize the relationship of ePCCW to its parent PCCW, we recall the probability of success in a given slot is determined by the ratio of alpha, beta and gamma users, and is composed of transmission load l and probability of success with event S, $\Pr(S)$. Alpha (α) users are the users that has successfully warned about their future transmission during their "present" transmission. Beta (β) users are the users that thought that they successfully warned, however their "present" transmission resulted in a collision and failed to warn about their future transmission. Finally the gamma (γ) users are the users who know that they haven't warned for the "present" frame, and that occurs when users don't transmit within the window of the "present" frame.

Assuming the desired user is transmitting a message, the probability of the overall ePCCW success with a defined traffic model for EVs can be written as:

$$\Pr(S_{\text{ePCCW}}) = \sum_{m}^{N-1} \Pr_{m}(S_{ePCCW})\, P(M = m), \tag{3-43}$$

where, m is the random variable denoting the number of interfering users, $\Pr_m(S_{ePCCW})$ is the probability of ePCCW success of the event S given that there are m interfering users, and N is the total amount of users. $P(m = m)$ is the probability of having m interfering users according to the traffic model. For Binomially and Poisson distributed traffic, we respectively have:

$$\Pr_{l,m,N}(M = m) = \binom{N-1}{m} l^m (1-l)^{N-m-1}, \tag{3-44}$$

and,

$$\text{and for Poisson } \Pr_{l,m,N}(M = m) = e^{-m\lambda\tau}\frac{(m\lambda\tau)^n}{n!}, \tag{3-45}$$

where l is the probability of transmission, λ is the message rate, τ is message lifetime; and n the number of messages.

To calculate success we need the probability of ePCCW entering each CP0 or CW0 states, dependent on m interferers:

$$\Pr_{m}(S_{ePCCW}) = \sum_{\gamma=0}^{m} \Pr_{m,\gamma}(S_{state=CP0}) \times \sum_{\alpha=0}^{m-\gamma} \Pr_{r,m,\alpha,\gamma}(S_{state=CW0}). \tag{3-46}$$

The term $\sum_{\gamma=0}^{m} \Pr_{m,\gamma}(S_{state=CP0})$ is the probability of the desired user due to other user's success being in CP0 state, and is mainly due to γ users, as they are the only users that "know" that they have not warned other users, where we have:

$$\sum_{\gamma=0}^{m} \Pr_{m,\gamma}(S_{state=CP0}) = \sum_{\gamma=0}^{m} \binom{\mathrm{m}}{\gamma} \times \left(p_g^{\gamma}\right) \times \left(1-\mathrm{p_g}\right)^{\mathrm{m}-\gamma}, \tag{3-47}$$

where $\mathrm{p_g}$ is the probability of having gamma users. The difference between ePCCW and PCCW lies in the probability of the desired user's success with other users being in the CW0 state, namely $\sum_{\alpha=0}^{m-\gamma} \Pr_{m,\alpha,\gamma}(S_{state=CW0})$. The success of the desired user relies on all the users bahaviour in the system from Table 3-12 which shows all the users' (α, β or γ) transmission probability under CW0 state.

Table 3-12: Users' transmission probability under CW0 state

Users	J=0 for alpha	J=1 for beta	J=2 for gamma
SD (desired)	$\frac{\mathbf{1}}{\boldsymbol{e+1}}$	1	$\begin{cases}\mathbf{1}, & \alpha = 0 \\ \mathbf{0}, & \alpha > 0\end{cases}$
Sa (alpha)	0	$\frac{\mathbf{1}}{\boldsymbol{\alpha}}$	$\frac{\mathbf{1}}{\boldsymbol{\alpha}}$
Sb (beta)	0	$\frac{\mathbf{1}}{\boldsymbol{a+1}}$	$\frac{\mathbf{1}}{\boldsymbol{a+1}}$
Sg (gamma)	0	$\begin{cases}\mathbf{0}, & \boldsymbol{a \geq 1 \cup g = 0} \\ \mathbf{1}, & \boldsymbol{otherwise}\end{cases}$	$\begin{cases}\mathbf{0}, & \boldsymbol{a \geq 1 \cup g = 0} \\ \mathbf{1}, & \boldsymbol{otherwise}\end{cases}$

The probability that the desired user will transmit is $1/(e+1)$, where e stands for the number of EVs, who are actually the number of alpha (α) users that transmitted successfully in a warning frame as EVs. This ensures that a fair transmission takes place among the EVs. The variable j is used as an index to differentiate between the different users.

Alternatively, for the desired user (D) we obtain:

$$s_{D,j} = \begin{cases} \dfrac{1}{e+1}, & when\ j < 2 \\ 1, & when\ j \text{ is } 2 \text{ and } \alpha = 0 \\ 0, & when\ j \text{ is } 2 \text{ and } \alpha \geq 1 \end{cases}. \tag{3-48}$$

As for the α, β and γ users, we respectively obtain:

$$s_{\mathrm{a},j} = \frac{1}{\alpha}\left(\frac{3}{2}j - \frac{1}{2}j^2\right). \tag{3-49}$$

and,

$$s_{\mathrm{b},j} = \tfrac{1}{\alpha+1}\left(\tfrac{3}{2}j - \tfrac{1}{2}j^2\right). \tag{3-50}$$

and,

$$s_{\mathrm{g},j} = \begin{cases} 0, & when\ j = 0, \text{or } \alpha \geq 1, \text{or } \mathrm{g} = 0 \\ 1, & otherwise \end{cases}. \tag{3-51}$$

Next we calculate the probability of success of transmission for the desired user D given the remaining other user types. The probability of success for D given a, b, and g users is:

$$\Pr_{\mathrm{a,b,g}}(S_D) = s_{D,j} \times \left(1-s_{\mathrm{a},j}\right)^{\mathrm{a}} \times \left(1-s_{\mathrm{b},j}\right)^{\mathrm{b}} \times \left(1-s_{\mathrm{g},j}\right)^{\mathrm{g}}, \tag{3-52}$$

and the probability of success for D given all α, β or γ users is:

$$\Pr_{\alpha,\beta,\gamma}(S_D) = \sum_{g=0}^{\gamma} \mathrm{Prg} \sum_{a=0}^{\alpha} \mathrm{Pra} \sum_{b=0}^{\beta} \mathrm{Prb} \times s_{D,j} \times \left(1 - s_{\mathrm{a},j}\right)^{\mathrm{a}} \times \left(1 - s_{\mathrm{b},j}\right)^{\mathrm{b}} \times \left(1 - s_{\mathrm{g},j}\right)^{\mathrm{g}}, \tag{3-53}$$

where $\mathrm{Prg} = \binom{\gamma}{g} p^g (1-p)^{\gamma-g}$, and $\mathrm{Pra} = \binom{\alpha}{a} p^a (1-p)^{\alpha-a}$, and $\mathrm{Prb} = \binom{\beta}{b} p^b (1-p)^{\beta-b}$. Finally, the desired user's frame success given all α, β or γ users at CW0 state is:

$$\Pr_{r,\alpha,\beta,\gamma}(S_{state=CW0}) = 1 - \left(1 - \Pr_{\alpha,\beta,\gamma}(S_D)\right)^r . \tag{3-54}$$

Looking back at Equation (3-46), the probability of ePCCW's success given that there are m interfering users, can now be derived by substituting Equations (3-47) and (3-54) into Equation (3-46). Substituting that result with Equation (3-44) or (3-45) into Equation (3-43) will in turn obtain the final probability of success for ePCCW with the traffic model taken into account.

Also modeled is a user's average delay, when the first success occurs, giving $D_s = \sum_{m=0}^{m_{\max}} D_s(m)\, Pr(m)$ where $D_s(m)$ is the average delay of a transmission being successfully received having m interfering users; while $Pr(m)$ is the probability of having m interfering users.

3.11 Simulation and Analytic Results of ePCCW

The simulation environment we use for ePCCW is the same one we developed in the next chapter, and validated against analytics results from [33]. It uses a realistic mobility model based on the Simulation of Urban MObility (SUMO) [34] for vehicle movement simulation. We also employ our accurate PHY DSRC simulator [11], which we have shown to provide a more accurate representation of PHY relative to other simulators, such as Network Simulator 2 (NS2). The SUMO highway environment mobility model supports different vehicle types in the simulation, such that we could define a new vehicle type for EVs that behaves different from the standard vehicles. The properties of the EV included higher priority when entering and exiting on ramps, higher average velocity, and higher priority entering of intersections with increased likelihood of lane changes.

The SUMO simulation has 2, 4, and 8 lanes and we consider a road length of 1000m. Additionally, because the simulation model has a boundary at which no communications are heard from beyond the simulation, we do not include nodes that are close to the edge boundary in the success calculations. Specifically, our simulator still processes these nodes, but does not take their transmission success into account for the final results, while allowing them to interfere with other users in the mobility model. Channel model depends on the mobility model's relative velocities and relative positions to model Doppler shift and signal to noise ratio (SNR) respectively.

The performance of the EV is shown in the Figures 3.22-3.25. We choose SFR as the repetition protocol and compare directly with PCCW and the proposed ePCCW. The data is averaged over 1000 frames of transmission to get a relatively accurate statistical performance trend. The results found in Figures 3.22 and 3.23, is where the number of vehicles is relatively low representing a rural scenario, and it can be seen that ePCCW outperforms both SFR and PCCW protocols. What is more important is that the

reliability is close to a 100%. Both simulation results and analytical results agree. The analytical plots are generated using the equations derived in this dissertation, and the traffic generation is based on the Poisson model.

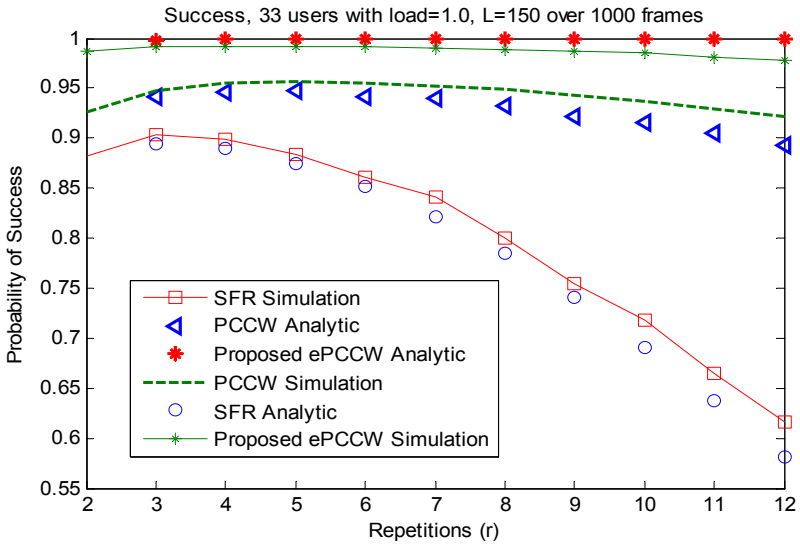

Figure 3.22 Pr(*S*) simulation and analytical results at N = 33, 150 slots/frame

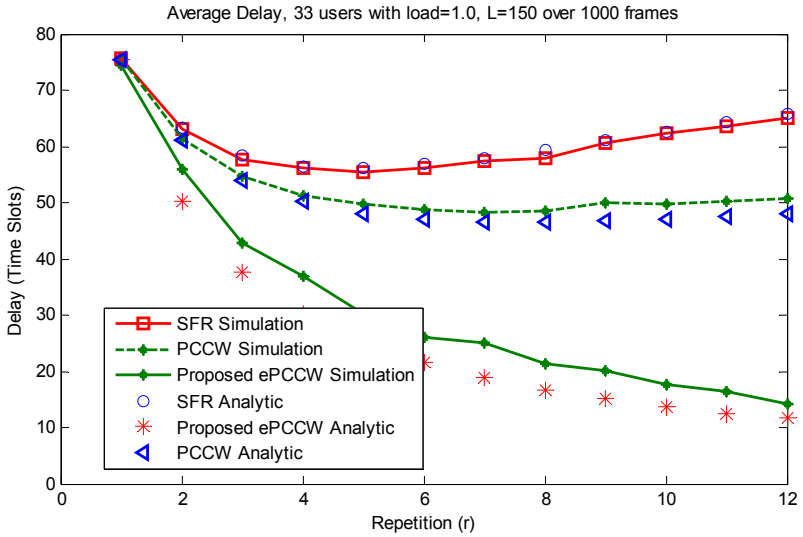

Figure 3.23 Delay simulation and analytical results at N = 33, 150 slots/frame

Figure 3.23 shows the average delay of that same scenario, and it can be seen that ePCCW has a much lower average delay than the other two protocols in terms of time slots. The data rate in DSRC ranges from 3 Mbps to 27 Mbps. To tax the system, we assume a relatively large average payload of 400 bytes used for safety messages, under 3Mbps rate for maximum delay. In ePCCW, it is necessary to have extra header bits to add information about future transmission, and it depends on the number of repetitions and the number of slots in a frame. The additional header bits used in the above example is equal to 96 bits (8 bits

to represent 150 slots in the frame per repetition, and in this example we choose 12 repetitions for a timeslot delay of approximately 12 slots). It is found that the 12 timeslots delay at 12 repetitions translates to $12 \text{ timeslots} \times \left((400 \times 8) \frac{\text{bits}}{\text{slot}} + (9 \times 12) \frac{\text{header bits}}{\text{packet}} \right) / 3e^6 = 0.013s \ll 0.200s.$ Therefore, the latency or delay requirement is met.

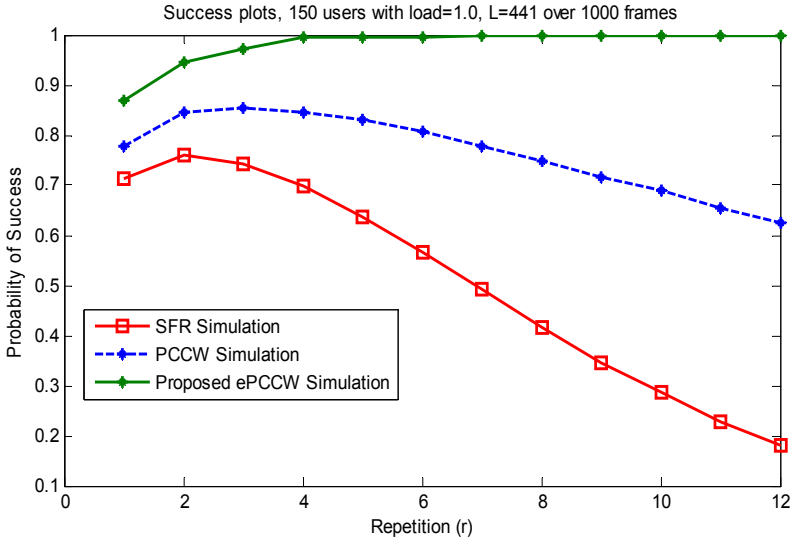

Figure 3.24 Pr(*S*) plot simulation under high vehicle density at 441 slots/frame

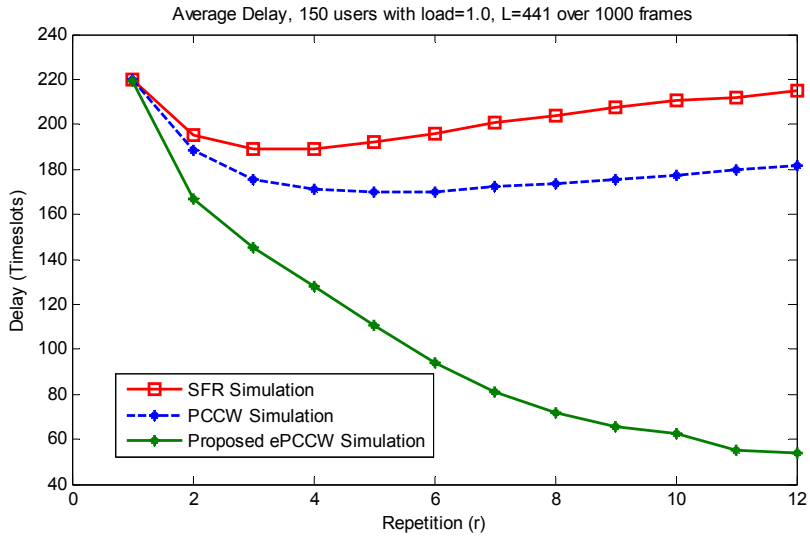

Figure 3.25 Delay simulation under high vehicle density at 441 slots/frame

The second important scenario, shown in Figures 3.24 and 3.25 is with a high number of vehicles representing a dense traffic scenario. In the second scenario overall success goes down, but with sufficient repetitions ePCCW maintains a very high reliability above 95%. Hence ePCCW is the protocol of choice especially at very high load or high vehicular densities.

Similarly, it can be shown that the delay requirements are met for this scenario as well. We use the worst case scenario with 400 bytes safety messages at 3Mbps rate. It is found that the approximately 54 timeslots delay at 12 repetitions for the example in Figure 3.25, gives $0.06s \ll 0.200s$. Again, the delay requirement is met easily. In addition, this latency is less if data rate is increased and payload reduced.

Chapter 4

MAC/PHY Simulator Design for PCCW

4.1 Architecture

The following illustrates our proposed architecture for simulation of the MAC layer in a vehicular safety environment. This is done over a realistic mobility model, with vehicle positions, and relative velocities used to influence channel conditions. Additionally, the OFDM PHY is fully simulated across the channel conditions with multiple PHY simulations performed per transmission to determine appropriate success for each intended reception, as is discussed later in this chapter.

We now present some important aspects of the MAC portion of the simulator, importantly describing how MAC transmissions are processed under the assumption of message feedback that is present in such a protocol as PCCW. First a transmission matrix is generated for each node which represents the intended next frame of transmission, with appropriate repetition patterns included. This matrix will be modified by the PCCW protocol based on information from the previous frame, where applicable, including which nodes were heard by other nodes. This information comes from the MAC upstream of each node that the PCCW node has access to, which has influenced its state according to its design as mentioned in the last chapter. Combining the hidden node matrix with the warning matrix gives a very accurate representation of which nodes actually hear the PCCW warnings. Figure 4.1 clearly illustrates the relationship of the simulator behaviours to one another. The warning matrix represents the view of each node's transmissions according to PCCW protocol. The influencing mobility and channel models are used for generating the Hidden node matrix, which obscures information exchange between users. The warning and hidden node matrices are used to form a view of which nodes successfully warned each other, which is used in making decisions for future slots and frames.

Essentially, to simulate PCCW, the protocol's functionality is duplicated in the simulator so that a warning matrix can be generated for each node, basically indicating which nodes are known potential problems. This accurately emulates the distributed memory that PCCW has in regards to warning knowledge, where not every node has that same warning information due to position, channel, or circumstantial reasons (such as if they were transmitting in the same slot as another node, hence not hearing a warning during that slot). In order to simulate the effects of vehicle movement on the MAC performance,

the mobility model is used to get the precise locations for the purpose of simulating interference and communication range effects on the communications. The mobility model is used to calculate relative success of broadcast data. Now that we have a full node view based on in range nodes and received intentions from other nodes, the PCCW protocol can then be used to broadcast into the channel. The PCCW state changes after receiving new information from the PHY. This process repeats for each slot of every frame being processed as long as at least one user is transmitting during that slot.

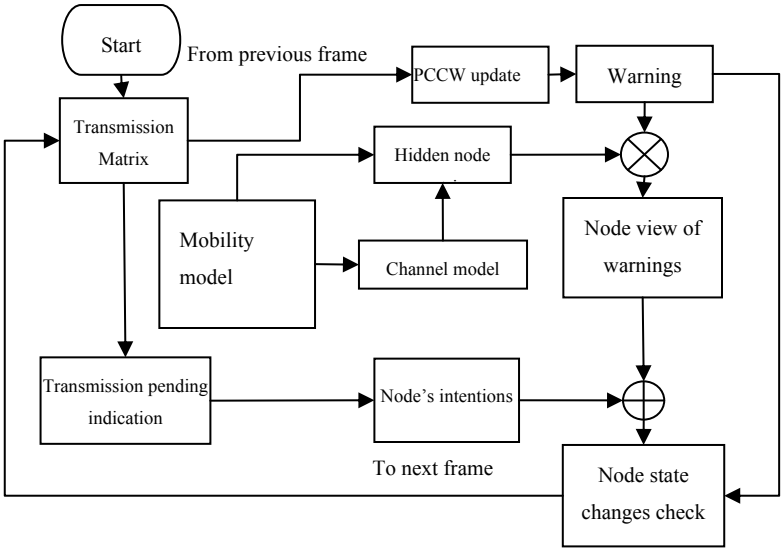

Figure 4.1 MAC simulation processing flow (include channel) including Hidden and warning matrices, for PCCW simulation.

Also in Figure 4.1 the transmission matrix exists to represent expected transmissions as generated by the chosen repetition protocol. This information will directly affect PCCW performance because of the passive nature of our design, where both pending possible transmissions are derived as well as potential transmission slots in which to include warning information. As mentioned, the warning matrix contains a list of future time slots that are marked for potential collisions, where each collision determination calculation is performed according to PCCW warnings that each node successfully received. The success of the warnings is partially correlated with the mobility model discussed later on in this chapter, which is used to generate the hidden node matrix for the simulator. Node view of warnings is where the view of each warning message is interpreted by the PCCW state machine from the previous chapter.

4.2 Mobility Model

The mobility model is used to model positions, densities, number of vehicle lanes, and velocities of vehicles being simulated. It is used to modify channel conditions due to distance, affecting SNR between users as well as Doppler shift due to relative velocities of each vehicle to each other. The mobility model is a federated mobility model defined in Simulation of Urban MObility (SUMO) [32], which is a validated vehicle traffic simulator used for traffic management.

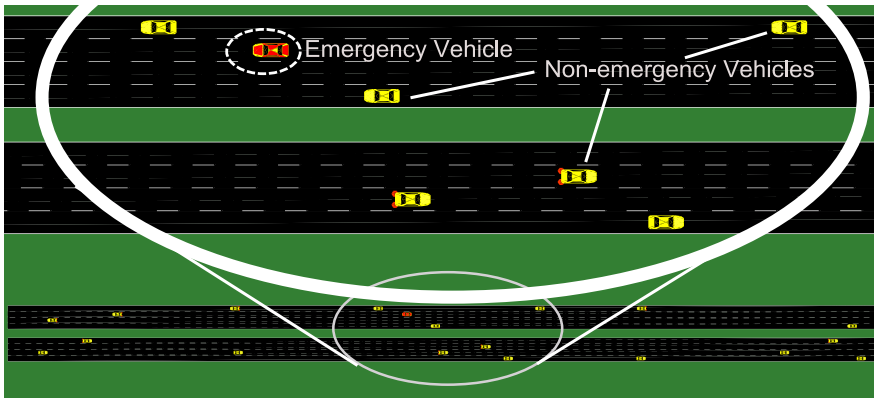

Figure 4.2 Marked emergency and non-EVs in SUMO

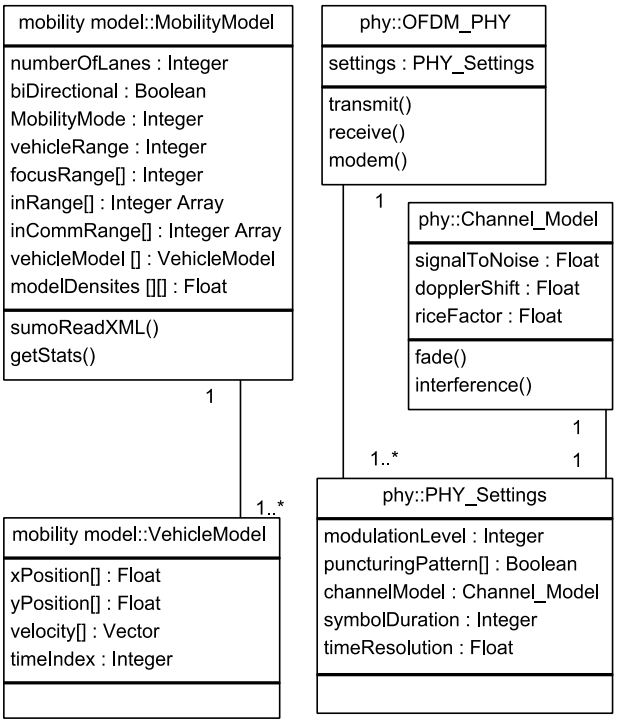

Figure 4.3 Class diagram for mobility model, OFDM PHY and channel model

Figure 4.2 shows a visual representation of the vehicles for both emergency and non-EVs obtained in SUMO. The EVs were marked in simulation by name so that their success can be measured differently from non-EV nodes. SUMO uses eXtensible Markup Language (XML) for its configuration and output, which we were able to interface with using Matlab. Hence, while the simulations of the movements were done using the Java based simulator SUMO, the configuration settings were mirrored in Matlab for federating SUMO into our simulator. The important variables used in Matlab for defining the mobility model are show in Figure 4.2, and described briefly in Table 4-1. Although not all parameters were easily controlled through Matlab, (for example to achieve a particular density of vehicles, the density was an average calculated post simulation after adjusting starting number of vehicles in the SUMO simulator.

Figure 4.3 shows the class diagram for the mobility model, OFDM PHY, and channel models. For the mobility model, the x and y coordinates are stored as well as the velocity for each node. The number of lanes, mobility model, range of users in the mobility model, and focus range are the parameters that are important for the mobility model. The OFDM PHY and channel models are used to send and receive broadcast data on a per node basis.

Table 4-1: Class diagram attributes and methods descriptions

Variable	Purpose
MobilityModel	
numberOf-Lanes	Defines the number of lanes to use in SUMO highways.
bidirectional	Boolean variable configuring SUMO to run under either uni or bi-directional highways.
Mobility-Mode	Used for Matlab to select from predefined SUMO mobility model settings
Mmodel	Mobility model defines SUMO specific settings and connection details used to federate with Matlab.
vehicleRange	Used to limit model analysis to a group of users in a specific geographic region.
inComm-Range	Flag each node as being within theoretical communication range of each other, or not (uses PHY in conjunction with mobility model).
inRange	Flag each node as being within interference range of each other, or not (uses PHY in conjunction with mobility model).
vehicleModel	Stores vehicles positions and velocities for time range interval.
model-Densities	Stores position and time of various vehicle densities for calculating average model density, and for testing performance at particular vehicular densities.
sumoRead-XML()	Function for reading SUMO model files to get the vehicle information.
getStats()	Function for generating mobility model statistics such as vehicle densities.
VehicleModel	
xPosition, yPosition	X and Y coordinates at particular times for individual vehicles, for calculating interference of different vehicles.
velocity	Velocity of vehicles for use by PHY to calculate relative velocities between vehicles for returning Doppler shift.
timeIndex	Used for knowing which time the x and y coordinates are for each vehicle at specific time.
OFDM_PHY	
settings	Stores the OFDM PHY settings for particular vehicles, and is used to simulate the PHY.
transmit()	Simulates transmission of a packet into the channel from the MAC.
receive()	Simulates reception of a packet from the channel for processing by the MAC.
modem()	Performs various PHY processing such as modulate, demodulate, equalize etc.
PHY_Settings	
modulation-Level	Is used for part of choosing data rate, selects the number of modulation bits per OFDM symbol.
puncturing-Pattern	Contains a matrix of 0s and 1s for indicating which symbols will be punctured after convolution.
channel-Model	Stores the channel model simulator for the broadcast.
symbol-Duration	Defines the length of time that an OFDM symbol takes to transmit, for DSRC this is 8us.
timeResolution	Used for synchronizing the Mobility, MAC and PHY simulators to use the same time units.
Channel_Model	
signalTo-Noise	Used for modeling signal to noise ratio of each broadcast.
dopplerShift	Used to model Doppler shift of each broadcast.
riceFactor	Used for line of sight transmissions.
fade()	Used to simulate fading of a broadcast.
Interference()	Simulates interference between multiple broadcasts.

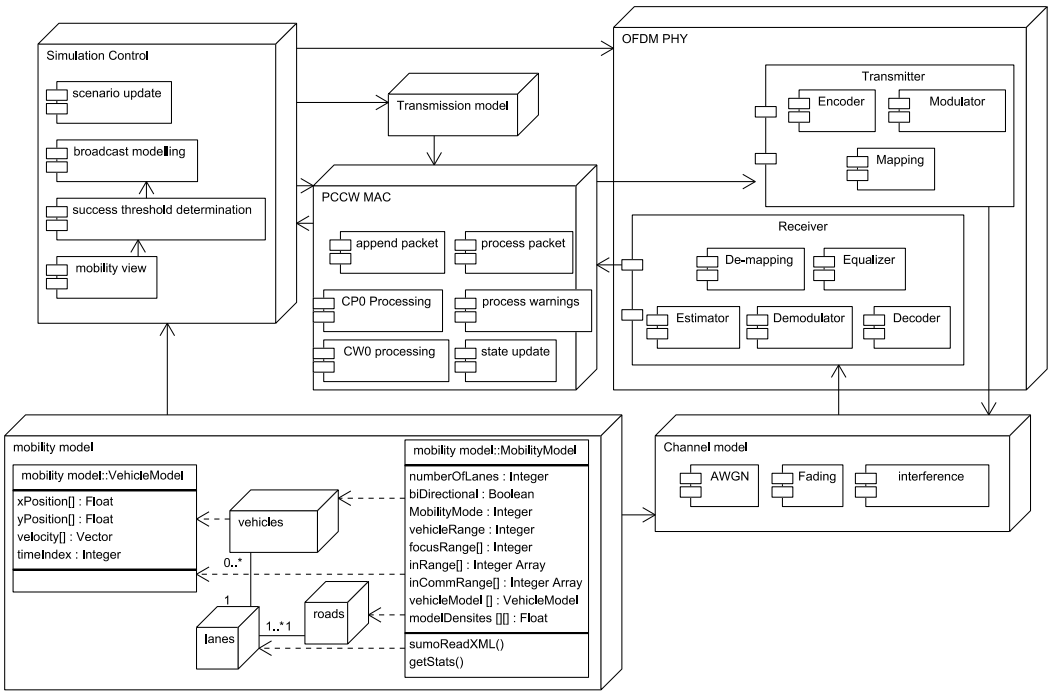

Figure 4.4 MAC simulator deployment diagram

The full description of the Physical layer (PHY) class can be found in our OFDM PHY simulator design [11] and presented in Chapter 6 of this dissertation. We use a deployment diagram in Figure 4.4 to represent the inner components within each module of the simulator to improve understanding of how the components are related. The deployment diagram shows the relationship between the simulation control, transmission model, PCCW MAC protocol simulation, mobility model, OFDM PHY simulation, and channel model. The simulation control performs the operations of scenario update which includes maintaining the time of the simulation by setting global timer, broadcast modeling (described later in this chapter), maintaining a mobility view for determining success of each broadcast, as well as performing other statistics such as delay and throughput of the protocol. The mobility model has many parameters derived from the SUMO XML files such as lane number, and position and velocity of moving vehicles. As can be seen in Figure 4.4, the mobility model has multiple vehicles per lane and multiple lanes per road, but we need to process the communication as a whole and hence we combine all the data together in our simulator as the mobility model class. The OFDM PHY simulator module shown in Figure 4.4 is the same as from [11], and is used to prevent and correct errors when broadcasting over the simulated DSRC channel environment. It is important to model each broadcast message properly with respect to each receiver because each node that is broadcast to has a different distance and relative velocity, meaning that the Doppler shift and SNR will be different as well. We achieve this by running multiple versions of the OFDM PHY in parallel for each broadcast with the parameters set based on the mobility model relative velocities and distances. The channel simulation used for the DSRC simulator requires SNR, Doppler and fading. As mentioned earlier, similar to the CASS environment specified in [5] and our study done in [4]

we use Friis free space model and two-ray model for calculating the SNR for short and long communication distances respectively [4].

4.3 PCCW Implementation

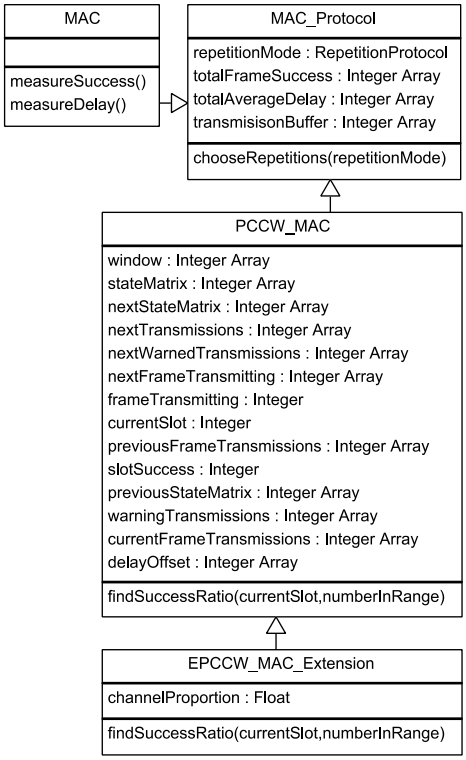

Figure 4.5 UML class diagram of PCCW

The initial state of a node using PCCW is that of its inherited repetition protocol, and proceeds based on the state table from Figure 3.1. For the simulation, the PCCW state machine is implemented on a per node basis by creating loops that process each node. In the class diagrams, an arrow is used to represent the relationship between a descendent class and its parent class. Figure 4.5 shows the relationship between the MAC layer protocols' simulator's representations of class diagrams. Class inheritance is represented by an arrow that points to the class that another class inherits attributes and methods from.

For the base MAC protocol class we assume the capability of repetition in each frame, where repetition mode is one of the leading repetition protocols [5] and [6], totalFrameSuccess represents the total frame success of each user, totalAverageDelay represents the total average delay measurements for each user. PCCW extends the basic MAC protocols by adding state condition variables, predictive window memory, and other attributes and methods for accomplishing the PCCW MAC protocol directives. PCCW specific variables will now be discussed. The stateMatrix attribute stores the current PCCW state of each node, while nextStateMatrix stores the next state for PCCW processing. The nextTransmissions variable is used to store the next transmission pattern that comes from the transmission model, while

nextWarnedTransmissions is used to store each node's view of warned transmissions. The descriptions of the attributes and methods used in the MAC simulator class diagrams from Figure 4.5 are in Table 4-2. Setting the states of PCCW in the simulator is done by taking each user's individual perspective based on the received data through the OFDM PHY and Channel model. The OFDM PHY and channel model are described later in this chapter, and the states are the same as described in the protocol description section. It is important to note that each slot has its own state based on warning information received and processed by the PCCW protocol. In the simulation of the protocol, for each node we check for state changes on a per slot basis. After each time slot for a node the simulator loops through and changes the node's state based on a stored view of received messages from other nodes in the immediate region.

If a node transmitted in the previous frame and heard no other node's transmit warnings, the states for its upcoming time slots would be updated to match that assumption, namely as a "transmission informed" (TI) state. Similarly, if a node transmitted, but other users were also heard with some overlaps of future, the affected slots would be updated to CW state. The simulator must deal with all scenarios of state changes that a real node will experience. For example if the node transmitted but other nodes transmitted at the same time, that node must still update its states under the assumption that it thinks that it warned.

Table 4-2: Descriptions of the attributes and methods used in the MAC simulator class

Attribute	Description
MAC	
MeasureSuccess()	Abstract method for measuring success of a particular MAC implementation.
MeasureDelay()	Abstract method for measuring average delay of a particular MAC implementation.
MAC_Protocol	
totalFrameSuccess	Total frame success.
totalAverageDelay	Total frame delay.
transmissionBuffer	Transmission buffer for measuring performance
chooseRepetitions()	Function that uses a repetition protocol to decide which slots to transmit in.
PCCW_MAC	
window	Memory for each user for storing warnings to use in predictions of potential future collisions.
stateMatrix	Stores the states of each users in the PCCW simulator (i.e. default, CP, CW, CW0, CP0 etc. slot states).
nextStateMatrix	Stores the next states of the PCCW simulator.
nextTransmissions	Next transmission patterns for the users.
nextWarned-Transmissions	Next frame warnings.
nextFrame-Transmitting	Next frame transmitting users.
frameTransmitting	Current frame transmitting users.
previousFrame-Transmissions	Previous frame transmissions.
slotSuccess	Slot success.
previousState-Matrix	Previous state matrix for verification and validation testing purposes.
warning-Transmissions	Successful warning transmissions for each slot for all users.
currentFrame-Transmissions	Current frame slot transmissions for all users.
delayOffset	Stores time offset when first successful repetition in the frame occurs.
findSuccessRatio()	Function that uses the current slot, users transmitting in that slot and number of users in range to determine success ratio of the broadcast.
EPCCW_MAC_Extension	
channelProportion	Defines the proportion of channel usage for EPCCW during warned slots.

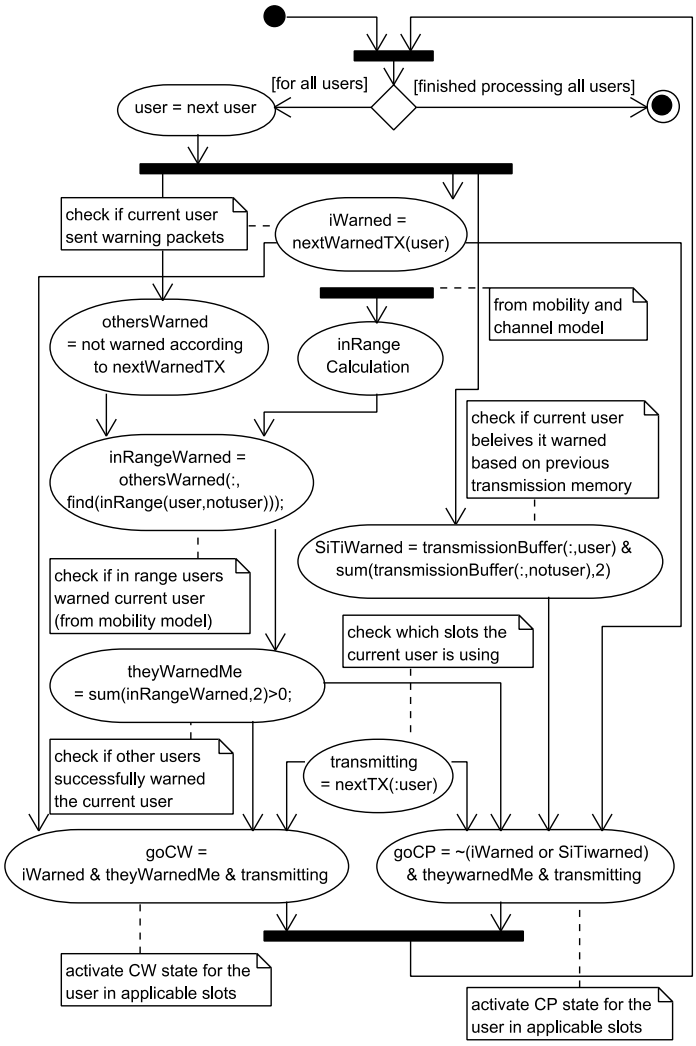

Figure 4.6 Simulator change state activity diagram

In Figure 4.6, the behaviour of PCCW for all users in the system is computed based on interference depending on mobility model and channel, and warning messages that have been successfully or unsuccessfully received, for every slot that the users are transmitting into. The activity diagram starts at the end of a time slot in a frame, where decisions can be made about future slot states. It is assumed that each node has access to its past frame transmissions, as required by the PCCW protocol. Also some warning messages from each user may have been transmitted successfully to other users.

We make this determination by cross referencing the users that successfully communicated with a selected user, where in Figure 4.6, we refer to these as "inRange" users. If they are in range, and successfully transmitted warnings to the selected user at least one time, we say that those users have warned the selected user successfully. Also a factor is the concept that the selected user may think it warned successfully, when it actually did not, this is computed by comparing the received previous frame packets (transmissionBuffer) by all other users, where we can then isolate warning messages that were not received and which users didn't receive them. This is used only to ensure that the decision of whether to

enter a CW, CP state, or no information state is done accurately. From here each user can make a determination about future time slots it is transmitting at from the information on its thinking it warned, and other users warning for the same slots. That is, if the user warned about a slot, and other users warned about that same slot then the user will enter CW state for that slot, and otherwise will enter CP for not warning, or remain in the default no-information state.

The mobility model influencing the in range criteria used above in Figure 4.6 comes from the federated Simulation of Urban MObility (SUMO) vehicle traffic simulator. At the time of this writing, SUMO supports export of simulation trace data to simulators such as NS2, but has no built in support for Matlab interactions, and hence we present a way to facilitate this interaction.

4.4 Channel Simulation

The channel model is composed of AWGN portion and a Rayleigh Fading simulator that has parameters defined by the PHY class settings and the mobility model. The mobility model is very important because it affects the signal to noise ratio based on the distance between receiver and transmitter, and also affects the relative velocity, in turn affecting Doppler shift. Authors in [5] use minimum required SNR values to achieve effective communication for IEEE802.11a. We modelled in [4] the SNR thresholds for IEEE802.11p used in current DSRC system. These SNR thresholds for achieving effective communication at different DSRC PHY data rates are given in [4]. These thresholds affect the power level at which the OFDM PHY must transmit at, affecting the signal to noise ratio heard by nodes at different locations. The channel simulation requires SNR for the AWGN and Doppler shift for the Rayleigh fading simulation, where SNR and Doppler shift are derived from the mobility model for each node that is broadcasting.

Table 4-3: SNR thresholds and 802.11p data rates

Data Rate (Mbps)	SNR Thresholds (dB)
3	7
4.5	10
6	8
9	11
12	11
18	15
24	18
27	20

The deployment diagram in Figure 4.4 contains the data path, showing information exchange between mobility model and channel simulator. After the MAC layer has determined to transmit into the channel or not based on PCCW on top of the repetition protocol, the message is sent to our federated OFDM simulator [11]. For faster simulation, only transmissions within interference range [4] of the broadcast were sent through the PHY simulation. We model the vehicular channel under the same channel simulation used in OFDM PHY, and since we are broadcasting each packet into the channel with multiple potential receivers, and multiple potential interferers, interference occurs with multiple channel conditions. It is very important to consider the effects of not just a single channel condition per broadcast, but multiple conditions relative to each in-range node. Figure 4.7 shows the simplest case where a single node is communicating with one

other node. Our model generates multiple channel models depending on the distance and relative velocities of each node, and also considers interfering nodes as they affect the broadcast.

A packet that receives at least 1 bit error after OFDM PHY processing is considered to have failed, and is passed to the MAC for checksum processing which drops the packet. Many simulators do not take into account the transmissions with the accuracy of having a full OFDM PHY such as NS2, and other simulators [35], [36], [37]. Although NS2 has recently been extended to support a more accurate PHY, it is still limited in implementation and at the time of this writing, only supports limited data rates of BPSK.

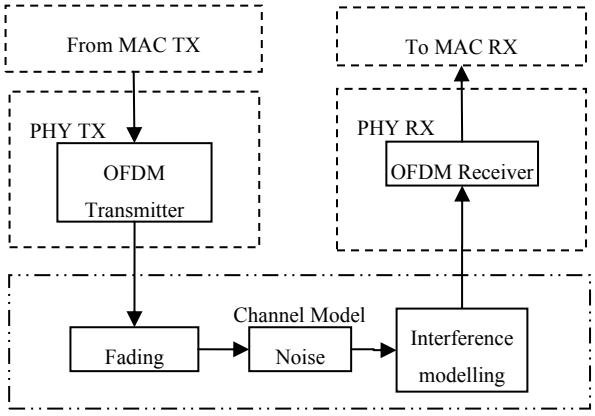

Figure 4.7 Flow between MAC, PHY, and channel simulation

In order to calculate the interference of each user to another user we need to take into account the data rate of each user, and the intended range of each broadcast. For our interference modelling, we use the distance between vehicles, and transmission power as calculated from the minimum SNR required for path loss the same as in [4].

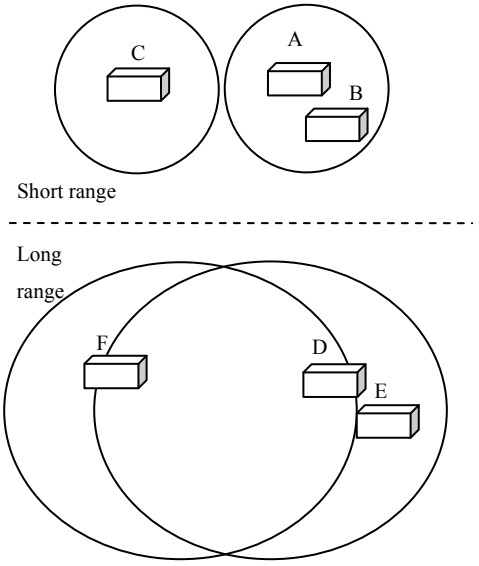

Figure 4.8 Mobility model: varying interference ranges

Figure 4.8 shows a simplified example of the vehicle model with respect to interference range. We do not assume that we know the communication range of each vehicle positions and hence we assume a transmission power related to the desired range we want the messages to be heard. We call this range the minimum safety message range (MSMR). This is important for incoming vehicles to be able to receive broadcasts from oncoming vehicles, but this is only possible if the transmission power can reach at least the safety message, for example in Figure 4.8, if the power of user A, is set to minimum required to transmit with user B, then user C will not be able to properly receive messages from A. Conversely while D maintains communication with E, user F can detect and understand communications from D. This increased message range increases safety communications at the expense of a much larger interference range.

Interfering users must be taken into account to accurately simulate the communication system we are testing. We accurately model the physical layer taking into account not only hidden nodes, but also secondary interferers. This is necessary because of the passive feedback system can only be accurately modeled by taking into account these extra interfering users.

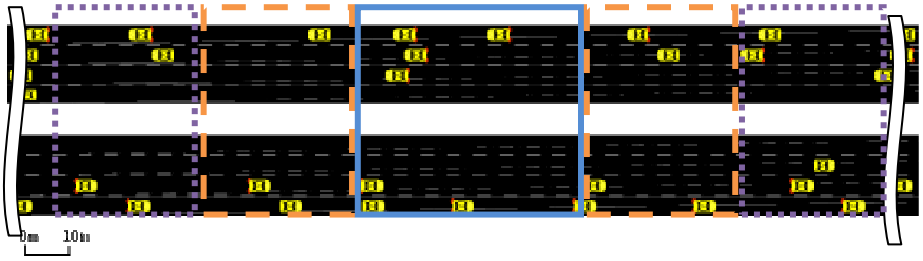

Figure 4.9 Interfering and hidden nodes

In Figure 4.9, the nodes that are out of range of the marked user but still causing communication failures due to their transmission power. The transmission power is related to the intended range of the transmitter, and the code rate and modulation schemes. Here the solid line rectangle surrounds the region of communication range; the dashed rectangle shows the Hidden nodes from the desired user, while the dotted lined rectangle represents the regions where interfering nodes can cause secondary interference to users within the communication range. The primary interference range R' is found to be:

$$R' = 10^{SNR/20} \times R \tag{4-1}$$

where R is the communication range, and resultantly the secondary and final interference range R'' is therefore:

$$R'' = R' + R = \left(10^{SNR/20} + 1\right) \times R \tag{4-2}$$

In order to properly measure PCCW success from the simulation we need to take into account hidden terminals, defined as nodes hidden from the user who's performance we are measuring, but detectible nodes within one hop (i.e. detectible by users within the marked node's communication range by other users). Also, we must take into account interfering hidden terminals that are out of communication range of

each other. Hence in the simulator, we construct both a hidden node matrix and an interference node matrix for relating the users visibility to each other in terms of communication and interference range. Tables 4-4, 4-5, and 4-6 illustrate the contents of the inRange, hidden, and interfering matrices respectively using a simple example with 9 users. Here for the hidden node matrix a 1 indicates that a node is hidden from the adjacent node, while a 0 represents not hidden.

Table 4-4: In range matrix

N	1	2	3	4	5	6	7	8	9
1	-	1	1	1	0	0	0	0	0
2	1	-	1	1	1	0	0	0	0
3	1	1	-	1	1	1	0	0	0
4	1	1	1	-	1	1	0	0	0
5	0	1	1	1	-	1	0	0	0
6	0	0	0	1	1	-	1	1	0
7	0	0	0	0	0	1	-	1	1
8	0	0	0	0	0	1	1	-	1
9	0	0	0	0	0	0	1	1	-

Table 4-5: Hidden node matrix

N	1	2	3	4	5	6	7	8	9
1	-	0	0	0	1	1	0	0	0
2	0	-	0	0	0	1	1	0	0
3	0	0	-	0	0	0	1	0	0
4	1	1	0	-	0	0	1	1	0
5	1	1	0	0	-	0	0	1	1
6	1	1	1	0	0	-	0	0	1
7	0	1	0	1	0	0	-	0	0
8	0	0	0	0	1	0	0	-	1
9	0	0	0	0	0	1	0	0	-

Table 4-6: Interference matrix

N	1	2	3	4	5	6	7	8	9
1	-	0	0	0	0	0	1	1	0
2	0	-	0	0	0	0	0	1	1
3	0	0	-	0	0	0	0	1	1
4	0	0	0	-	0	0	0	0	1
5	0	0	0	0	-	0	0	0	0
6	0	0	0	0	0	-	0	0	0
7	1	0	1	0	0	0	-	0	0
8	1	1	1	1	0	0	0	-	0
9	0	1	1	1	1	0	0	0	-

We can use these matrices in the success calculations by multiplying the successes a user achieves relative to all nodes, so as to block out hidden and interfering users from the calculation. Additionally, when measuring success of a broadcast message, we assume a success threshold $\aleph$ for which we count a broadcast as being successful if the ratio between the actual number of receivers χ' and possible receivers

χ is greater than the success threshold. That is if $\frac{\chi'}{\chi} \geq$ א, then success for the broadcast is considered successful, for example if א is 0.9 (90% success threshold). If there are 10 in range users, and 9 out of 10 receive the broadcast, then the broadcast is considered successful even though there was a failure. An algorithm for determining success was used and operates as follows: for each transmitting user, compare against all possible interferers.

4.4.1 Model Broadcast

In order to appropriately model and measure broadcast success of a MAC protocol, we need to know the quality of service requirements, the range at which a message is intended to reach. The sequence diagram in Figure 4.10 is used to describe the operations of our MAC simulator while performing accurate broadcast simulation. The broadcast simulator module requires access to the channel, transmission, and vehicle mobility models in order to setup and keep track of the simulated broadcasts for measuring statistics from each broadcast and correlated receptions.

For the first step of simulating the broadcast, the PHY parameters are set based on the current node's transmission parameters. Vehicle positions are updated to match the time of the current node's transmission based on the mobility model. Next the transmission matrix is accessed to determine other transmissions currently taking place for users within the interference range of the current node. The broadcast simulator activates the transmission to the various vehicles present in the model. Success and delay statistics are measured and stored for comparison of each broadcast.

4.5 Model verification

Another important aspect of simulating besides accurately measuring the result is that of simulating the systems under more realistic scenarios that may not be as accessible from a purely analytical approach. Our simulation is first verified to behave correctly under all the same assumptions as analytic, and related to the analytical results in later in this chapter. Afterwards, more realistic conditions are applied to the simulation for more accurately representing real world results. For example, we can assume more users in simulation because the analytical probability functions rely on combinatorics and factorials that have a limited amount of precision when working with large numbers.

For improving understanding of our simulation, we have separated the simulator into important elements that can make up the entire process of simulating DSRC in a vehicular environment.

As seen in Figure 4.11, these elements include: the simulator as a whole representing the starting point at which user makes interaction; the broadcast simulator which controls the broadcasts of the users based on the transmission model defined by the MAC protocols used; vehicle model for representing the positions and velocities of all the vehicles; mobility model which define the movements and possible routes in which vehicles may travel; and the channel model which defines the BER and PER due to conditions present in the mobility model and transmission models together.

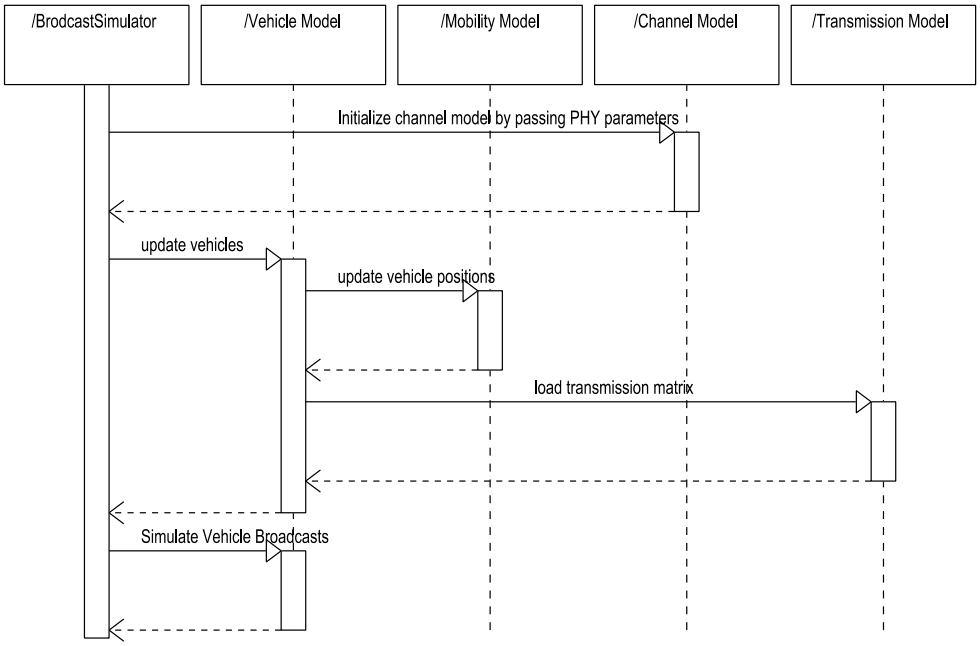

Figure 4.10 Broadcast simulation sequence diagram

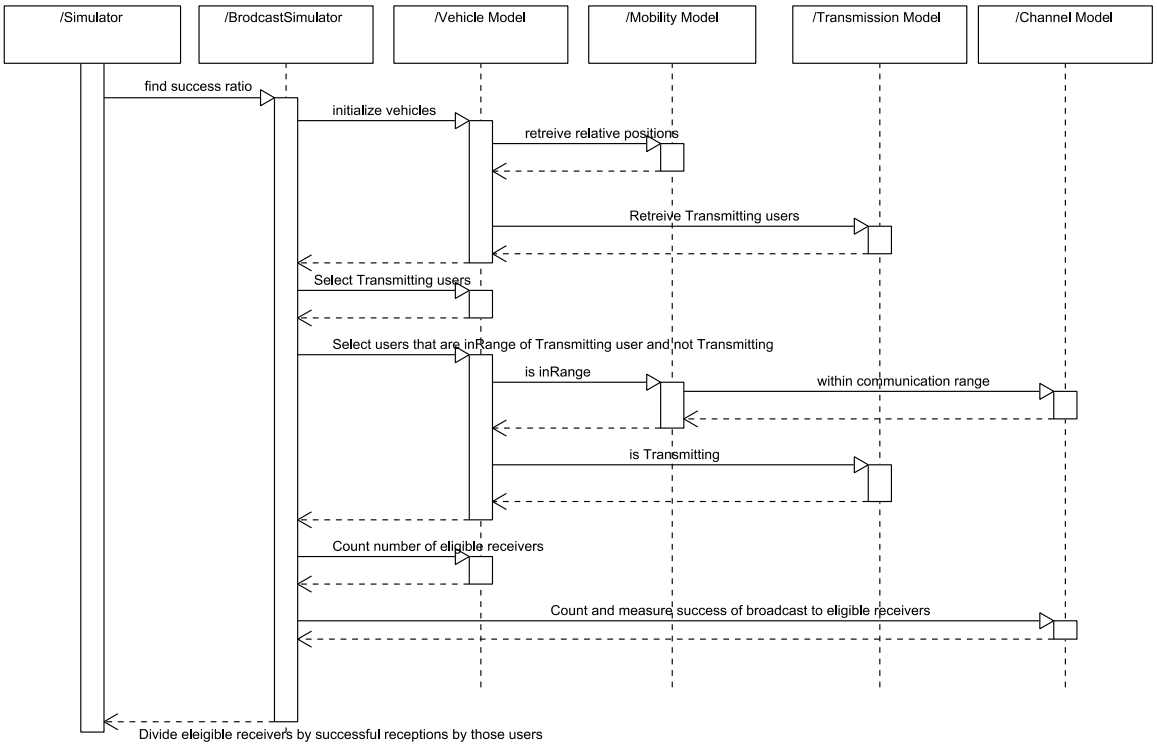

Figure 4.11 Sequence diagram for computing success ratio for user broadcasts

Also in Figure 4.11 we present an algorithm for calculating the ratio of success for each broadcast. We measure this success according to the transmission model, mobility model, and channel model. A node is eligible to be included as a potential receiver in this calculation if it is within the range of the broadcast

message's intended scope according to mobility and channel models, and the node is not attempting to transmit itself in that particular time. A node is designated as an eligible receiver if its PHY is in the state of reception, i.e. the node is not transmitting during the time slot at which the broadcast is being transmitted. We do not count nodes that are in range of a broadcasting node, but not in a state that is capable of reception as part of the users that determine overall broadcaster's success. A broadcasted transmission is determined to be successful for a particular receiver if the received message is sufficiently stronger than any interfering transmissions, as determined by mobility model, transmission model, and channel model.

4.5.1 Averaging of users

For displaying the results, obtained from the simulation, averaging of users over a time is performed. This is a common practice that generally produces results that are more applicable to the average case. We measure the frame success of the protocol by measuring the success of a group of users averaged together to get an averaged response for both delay and frame success performance.

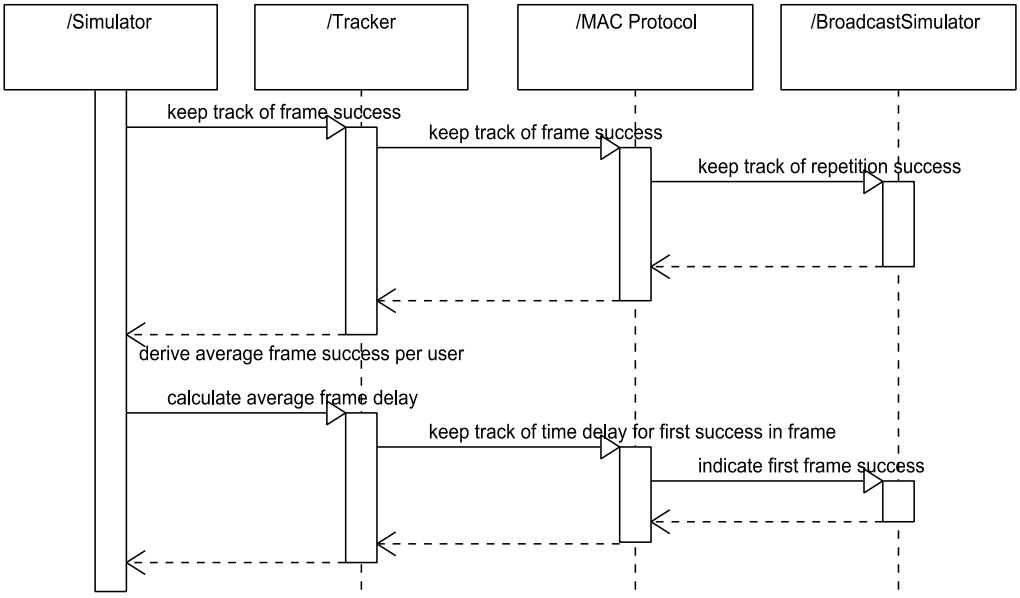

Figure 4.12 Averaging users Sequence Diagram

Figure 4.12 indicates the simulator systems responsible for keeping track of the protocol slot successes. The broadcast simulator component passes broadcast success ratio on a per time slot basis to the MAC Frame protocol tracker. The MAC frame protocol tracker passes total frame success to the Simulation tracker one frame at a time for all users. The main simulator component can then use the total frame success to perform statistical analysis including averaging for the performance metrics of success and delay for a group of users.

Chapter 5

Performance Enhancement of DSRC PHY Using Improved Equalization and Demapping Schemes

Before we discuss the enhanced receiver designs for DSRC, we first describe the conventional DSRC PHY layer design, so that a better understanding of the DSRC PHY systems is achieved when they are all compared with each other. Also, the channel mobility model is described to better shade light on the reasons why different receiver designs for DSRC are required.

5.1 OFDM-Based DSRC System

OFDM systems function by partitioning a signal across many low symbol rate orthogonal subcarriers. The main challenge presented to an OFDM system designer is to optimize the coherent detections and processing of these subcarriers for a given application maintaining quality of service requirements and usually minimizing hardware complexity. Through the use of sufficient guard intervals inserted in front of each OFDM symbol, the OFDM systems are able to mitigate inter-symbol interference (ISI), which naturally exists in multipath scatter environments [38]. The orthogonal subcarriers carry the modulated data symbols that compromise the OFDM symbols.

IEEE 802.11p specifications [7] are extensively exploited by researchers to understand or test a wireless link, and are built using OFDM systems. For a more detailed look at the individual elements in an OFDM system, the readers may refer to [39]. The major 802.11p configuration and timing related parameters are listed in Table 5-1 and Table 5-2 respectively [7], which can be reconfigured for representing other OFDM systems. As shown in Tables 5-1 and 5-2, the IEEE 802.11p standard has a total of 64 subcarriers, with only 52 subcarriers used for transmission, 4 subcarriers of which are pilots and the remaining 48 subcarriers carry the actual data. The symbol duration is 8.0 μs with 1.6 μs guard interval and signal bandwidth of 10 MHz. The subcarrier bandwidth is 0.15625 MHz (10 MHz/64).

Figure 5.1 shows the DSRC PHY layout. From that figure, the bold faced letters are used to denote a variable in frequency-domain, *FFT/IFFT* denote the Fast Fourier Transform and Inverse Fast Fourier Transform, respectively. The symbols $\boldsymbol{x}_{n,k}$ and $\boldsymbol{y}_{n,k}$ denote the transmitted and the received OFDM data symbols, respectively. The thin line arrows and the thick block arrows represent the transmission of serial

data and parallel data, respectively. The figure illustrates the transmitter and receiver configuration and their internal components, which need to be modeled as objects in the simulator. From Figure 5.11(a), the binary message goes through a series of components before transmission. First the message is encoded for forward error correction coding (FEC) with a convolution encoder whose generator is $[133_8, 177_8]$ in octal, and constraint length of 7.

Table 5-1: Main IEEE 802.11p OFDM PHY system configuration parameters

System Parameter	Parameter Range
Modulation	BPSK, QPSK, QAM16, QAM64
Coding Type	Convolution
Coding generation Polynomial	[133 171]
Decoding Type	Viterbi
Interleaver	Block
Bandwidth	10 MHz
Number of non-zero subcarriers	52
Number of data subcarriers	48
Number of pilot subcarriers	4

Table 5-2: Main IEEE 802.11p DSRC PHY system timing related parameters

System Parameter	Parameter Range
Subcarrier frequency spacing	0.15625 MHz
FFT/IFFT period	6.4 $\boldsymbol{\mu s}$
Preamble duration	32 $\boldsymbol{\mu s}$
Guard interval duration	64 $\boldsymbol{\mu s}$
Symbol interval	8 $\boldsymbol{\mu s}$

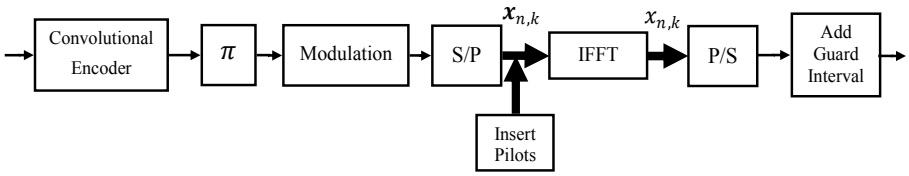

(a) Transmitter

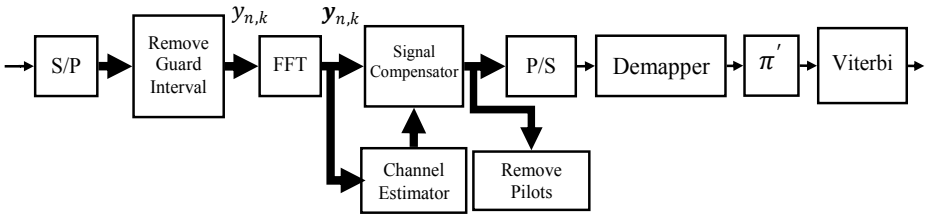

(b) Receiver

Figure 5.1 Layout of the OFDM PHY model: (a) transmitter, (b) receiver.

The encoded message is then interleaved (π) to avoid long burst errors due to fading. The interleaved message is then digitally modulated using one of the Gray-Coded constellations binary phase shift keying (BPSK), quadrature phase shift keying (QPSK), quadrature amplitude modulation (16 QAM), and 64 QAM [7]. The resulting modulated message is then divided into 64 shorter and parallel data symbols $\boldsymbol{x}_{n,k}$ (includes the 4 pilot symbols, and 12 zero-padding), for the n^{th} OFDM symbol and the k^{th} subcarrier. The pilot symbols are inserted in the 6th, 20th, 34th, and 48th subcarriers for each OFDM symbol, in order to estimate the frequency and track the phase of the received message [7]. These symbols are then multiplexed into a 64-point (*IFFT*) using the OFDM modulation scheme, denoted by $x_{n,k}$. This resulting symbol ($x_{n,k}$) is transformed into an 80-point length vector after the addition of the guard interval, and then serially transmitted over the channel. The data rate is calculated as follows [7]:

$$R_d = \frac{R_c \log_2(m) N_{sc}}{T_s}, \tag{5-1}$$

where R_c is the code rate, m is the number of modulation points in the mapping constellation, and N_{sc} is the number of data subcarriers in an OFDM symbol. At the receiver end, shown in Figure 5.1(b), and after the removal of the *GI*, and converting the received signal to parallel signals ($y_{n,k}$), the signal is transformed into a frequency-domain signal $\boldsymbol{y}_{n,k}$ as follows:

$$FFT(y_{n,k}) = \boldsymbol{y}_{n,k} = \boldsymbol{h}_{n,k} \cdot \boldsymbol{x}_{n,k} + \boldsymbol{w}_{n,k}, \tag{5-2}$$

for $0 \leq n \leq N_s, 0 \leq n \leq N_s$, where $\boldsymbol{h}_{n,k}$ and $\boldsymbol{w}_{n,k}$ are the complex channel frequency response and the additive white Gaussian noise (AWGN) for the n^{th} OFDM symbol and the k^{th} subcarrier, respectively. In the channel estimator, the two training symbols are used to obtain the estimated channel response for the first OFDM symbol over the first two received symbols as follows,

$$\widetilde{\boldsymbol{h}}_{0,k} = \frac{\boldsymbol{h}_{\boldsymbol{y_1},k} + \boldsymbol{h}_{\boldsymbol{y_2},k}}{2.\boldsymbol{X}_{ce,k}}, \tag{5-3}$$

Defined earlier, the $\boldsymbol{X}_{ce}$ is one of the two identical training symbols. The subscripts $\boldsymbol{y_1}$ and $\boldsymbol{y_2}$ represent the first two received OFDM symbols. The conventional IEEE 802.11p system uses the same channel response estimated for the first OFDM symbol throughout the entire packet, in other words the channels were assumed time-invariant and do not change throughout the packet (i.e., $\widetilde{\boldsymbol{h}}_{0,k} \cong \widetilde{\boldsymbol{h}}_{n,k}$). Therefore, different channel estimation and/or equalization schemes need to be implemented in a simulator design for time-variant channels. Examples of such designs include [40], [38], and [37]. After channel estimation, the signal compensator compensates the received data symbols of the packet by the estimated channel response, as follows:

$$\widetilde{\boldsymbol{y}}_{n,k} = \frac{\boldsymbol{y}_{n,k}}{\widetilde{\boldsymbol{h}}_{0,k}}, \tag{5-4}$$

The components of Figure 5.1 are modeled dynamically in our simulator using object-oriented techniques presented in Chapter 6 to allow for the data rate, the amount of subcarriers, and the bit interleaver type (modeled as either block or symbol) to be variable. Additionally, this allows for the

modulation level to change symmetrically across the transmitter and receiver, and the channel to be dynamic. As well, the entire receiver module of the simulator is modeled assuming adaptive feedback architecture to cover a wide array of implementations.

5.2 Channel Modelling

Modelling of the communication channel can be done in many different ways, which includes AWGN, interference, fading, time-varying channels with Doppler shift, and time-invariant channel models. The OFDM PHY is designed to cope with many of these different channel scenarios that it may encounter in urban, non-urban, mobile or static channel environments. What follows is a more detailed description of the channel models that can be selected in our reconfigurable simulator for a wireless OFDM PHY system. Details of different channel modelling in OFDM systems can be found in [41], [39], and [42].

The wireless access vehicular environment (WAVE) channel model can be modeled using statistical methods presented in [41] and [42]. Figure 5.2 illustrates the WAVE channel model, showing both specular and scattering ray components. The WAVE channel model can be used in simulating the effects of an L path Rayleigh/Rician multipath scattering channel with K factor affecting specular to scatter component fading path ratio and AWGN.

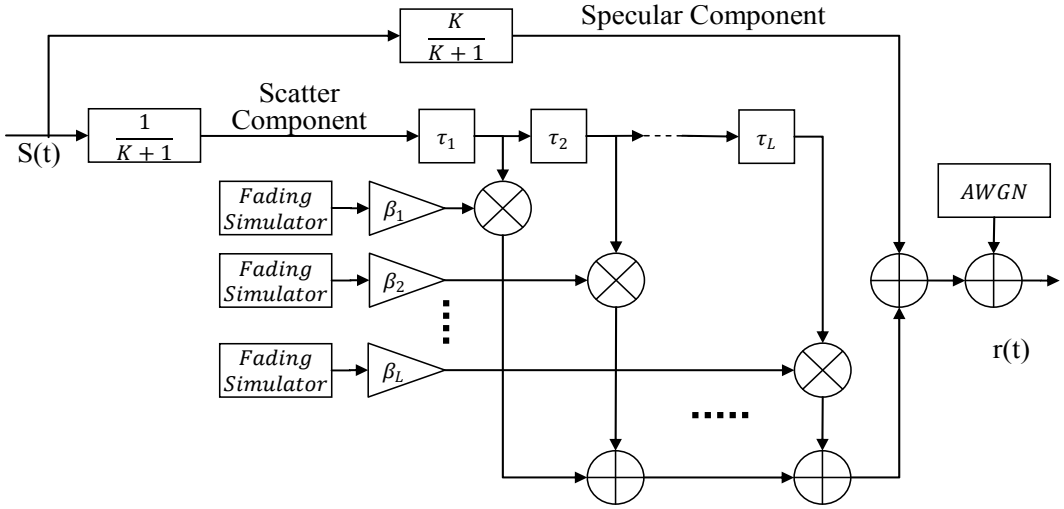

Figure 5.2 Channel model with multipath scattering, specular (LOS), and Rayleigh (no-LOS) portions and AWGN.

OFDM systems are able to mitigate ISI. However, the orthogonality principle is no longer valid in time-varying channels [38], [43], [44] and [45], which leads to the presence of ICI. The ICI factor increases with increased vehicular speed. ISI and ICI exist due to two physical phenomena known as the multipath fading and the Doppler shift, respectively. Multipath refers to both line-of-sight (LOS) and non-line-of-sight (non-LOS) components, due to the reflections of the transmitted signals by the surrounding objects. Multipath may cause what is known as “frequency selective” fading, which induces ISI when the

symbol duration or symbol period (T_s) is less than approximately 10 times the multipath root-mean-square delay (RMS) spread (σ_τ), ($T_s \leq 10\sigma_\tau$) [28]. The channel may be considered flat if the range of the channel frequencies or coherence bandwidth (B_c) satisfies the following condition [42],

$$B_c \approx \frac{1}{50\sigma_\tau}, \tag{5-5}$$

In time-varying channels, a nonzero relative velocity is produced, because both antennas may be moving towards each other or in the same direction but at different speeds. The resulting maximum Doppler shift (f_D) is related to the relative velocity via the equation ($f_D = V \cdot f_c/c$), where V is the relative velocity in meters per second ($^m/_s$), f_c is the carrier frequency in Hertz (Hz), and c is the speed of light in ($^m/_s$) [42]. Also, the channel may be characterized as a "fast fading" channel if $T_s \cdot N_s \gg T_c$, where T_c is the coherence time [42],

$$T_c = \frac{0.423}{f_D} = \frac{0.423}{V \cdot f_c/c} = \frac{0.423\ c}{V \cdot f_c}\,\mu s, \tag{5-6}$$

In other words, the channel impulse response is changing within the duration of a packet if $T_s \cdot N_s \ll T_c$ is not satisfied. Since c and f_c remain constant throughout a particular system, the rate of fading is proportional to one of the parameters T_s, N_s or V while the others remain constant. Rician fading channel (with K factor not equal to zero) [46] could be used if a strong LOS component exists, while Rayleigh fading could be considered when time-varying channels exist with No-LOS. The time-varying Rayleigh fading channel can be produced using the Jakes' fading channel simulator with no-LOS [47]. Jake's method works by simulating the physical model of 2D isotropic scattering with non-LOS. It assumes that there are -X equi-spaced or uniformly distributed scatters around the moving transmitter or receiver. The phase angle $\left(\theta_i = \frac{2\pi i}{X}, i = 1,2,\dots,X\right)$ associated with each scatter is chosen at random. The received complex envelope is treated as wide-sense stationary Gaussian random process with zero mean, when Rayleigh channel is concerned. In order to produce a zero mean Gaussian envelope, the following relation is used as in [48, 47],

$$\begin{aligned} g(t) &= g_I(t) + j\, g_Q(t) \\ &= \sqrt{2}\left[2\sum_{n=1}^{M}\cos\beta_n \cos 2\pi f_n t + \sqrt{2}\cos\alpha\cos 2\pi f_m t\right] \\ &+ j\left[2\sum_{n=1}^{M}\sin\beta_n \cos 2\pi f_n t + \sqrt{2}\sin\alpha\cos 2\pi f_m t\right], \end{aligned} \tag{5-7}$$

where $\beta_n = \pi n/M$. We need M number of oscillators with frequencies,

$$f_n = f_m \cos\frac{2\pi n}{X}, n = 1,2,\dots,M. \tag{5-8}$$

According to [46], M greater than 6 should suffice. In addition, $M = \frac{1}{2}\left(\frac{X}{2} - \frac{1}{2}\right)$ and $\frac{X}{2}$ must be an odd integer. In order to visually demonstrate the effect of the channel on the message bits, scatter plots in Figure 5.3 are produced for an OFDM system over a single packet message of duration of 0.64 ms, using

QPSK modulation scheme. Different Rayleigh fading envelopes are simulated using different velocities. As illustrated in Figure 5.3, as the velocity is increased there exist a greater shift in both amplitude and phase, which result in the deviation of the received symbols from their constellation points. Figure 5.4 on the other hand, shows an example of how AWGN increases the chance of erroneously interpreting the symbols.

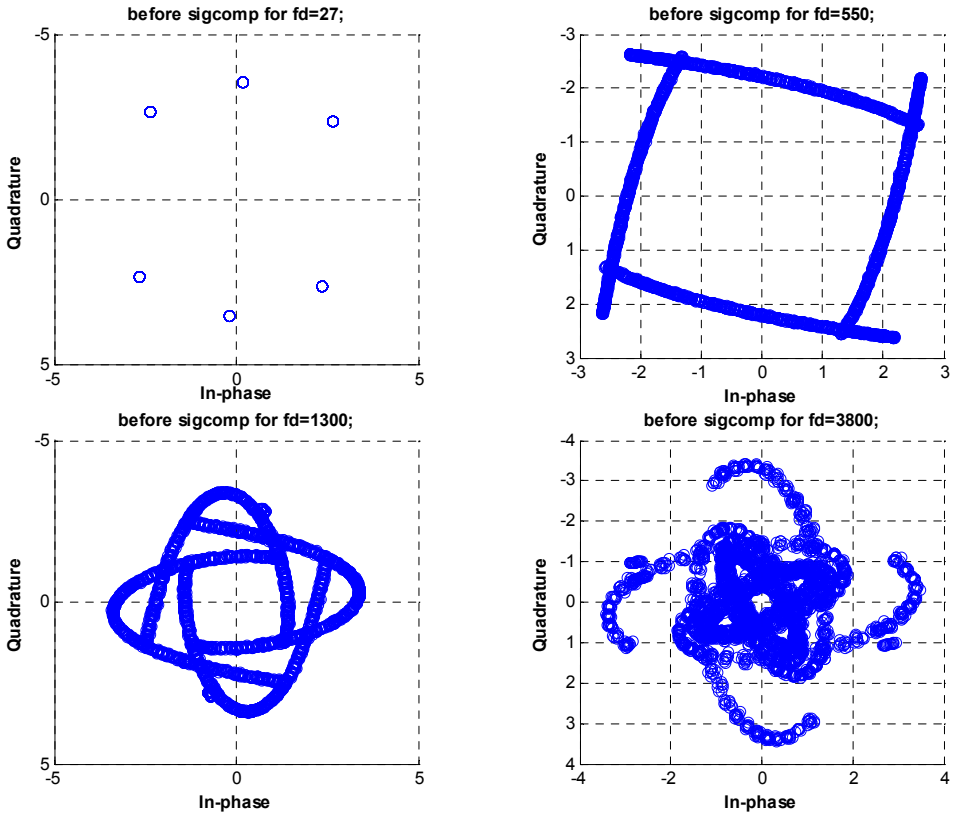

Figure 5.3. Scatter plots showing distortions caused by Doppler shift.

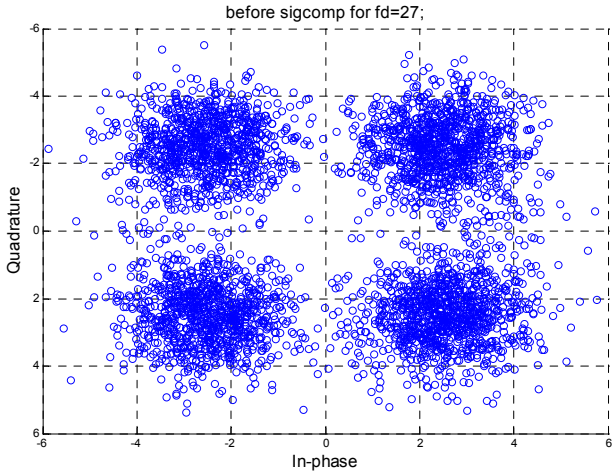

Figure 5.4. Scatter plots showing distortions caused by AWGN shift.

5.3 Performance Enhancement of DSRC PHY Using Improved Demapper

As mentioned in Chapter 1, the conventional DSRC system uses digital Viterbi decoding for forward error correction (FEC) [7]. Digital Viterbi decoders are extensively used in communication systems. It is well known that soft-decision decoders achieve coding gain over the hard-decision. Four types of analog-input decoders are discussed in [49] including the hard-decision, soft-decision, ideal analog and non-ideal analog decoders [49]. The non-linear demapping scheme we focus on, namely the S and Π-decision demapper [50], was shown to outperform hard-decision, 4-level and 8-level soft-decision decoders. Performance evaluations of DSRC such as [51] do not address higher order *M*-ary modulations that exist in current standard [7].

Our previous study [28,38], investigated performance limitation on DSRC receivers, using conventional channel estimation and static channel. In this work, we present a study on 5.9 GHz DSRC PHY performance limitations when using linear vs. non-linear demappers with different decoder designs. The linear demapping scheme designed in this dissertation and non-linear demapping scheme presented in [50] are tested with both digital and non-ideal analog decoders presented in [49] with varying signal to noise ratios (SNR), velocities, packet length, channels, modulations, and code rates.

5.3.1 Demapping and Decoding Schemes for the DSRC PHY Systems

Analog Viterbi decoders have been presented previously in [51]. They consist of analog add-compare-select (ACS), where the analog path metric calculations are performed and digital path metric (PM) modules, where the bits are decoded using the trellis structure and survivor path. Analog decoders have potential coding gain over digital Viterbi decoders because of the ability to process unquantized data symbols. However, this coding gain is reduced because of internal circuit noise in the non-ideal analog circuitry [51]. Hard decision Viterbi decoders quantize the input data to two levels {0, 1}. It uses the hamming distance of the received bits to possible outputs obtained from the trellis of the convolutional encoder to determine the most likely path. Alternatively, the soft Viterbi decoders use Euclidean distance to determine the best choice of path for the decoding. Both the analog and soft Viterbi decoders process soft information, where the analog Viterbi decoder receives real valued analog data, while the soft Viterbi decoder receives level data in the range from 0 to $2^{n_{soft}} - 1$ levels (where n_{soft} is the number of bits used to represent the digital input to the decoder). This soft information is created by quantizing the demodulator soft decision demapping output.

5.3.1.1 Linear decision demapper

The linear demapper attempts to give a linear estimate of the received in-phase and quadrature-phase component ranges given to the DSRC PHY demodulator. QPSK and QAM modulation schemes have in-phase and quadrature phase components which are mapped according to Gray-coded constellation mappings. According to the IEEE 802.11p standard [7], the same average power should be achieved for all created modulated symbol. Therefore, the relative energy of each modulated symbol is normalized

according to the K_{MOD} factor, which is equal to $1/\sqrt{2}$, $1/\sqrt{10}$ and $1/\sqrt{42}$ for QPSK, 16-QAM and 64-QAM, respectively. The main relationship between these modulation schemes is found in Table 5-3.

Table 5-3: Modulation relationship according to DSRC standard

Modulation type	Bits per symbol	K_{MOD}	Denormalized Range	Data points	Bit pattern
QPSK	2	$1/\sqrt{2}$	[-1, 1]	4	I_0Q_0
16-QAM	4	$1/\sqrt{10}$	[-3 -1, 1 3]	16	$I_0I_1Q_0Q_1$
64-QAM	6	$1/\sqrt{42}$	[-7 -5 -3 -1, 1, 3, 5, 7]	64	$I_0I_1I_2Q_0Q_1Q_2$

During demodulation the mapped data ranges are proportional to the inverse of K_{MOD}, where each constellation data point is mapped to values in the de-normalized constellation points. The variable I_0 represents the first received in-phase contributed bit and Q_0 represents the first received quadrature-phase contributed bit, which come into the demodulator after signal compensation in the form of $Y_m = (I + jQ) \cdot K_{MOD}$. The linear decision demapper implementation of each respective demodulation schemes needs to estimate the bit pattern of the in-phase and quadrature phase components, to the bit pattern from Table 5-3. The bit pattern is composed of I_b and Q_b, where b is the b^{th} bit pair of the demodulated symbol Y_m.

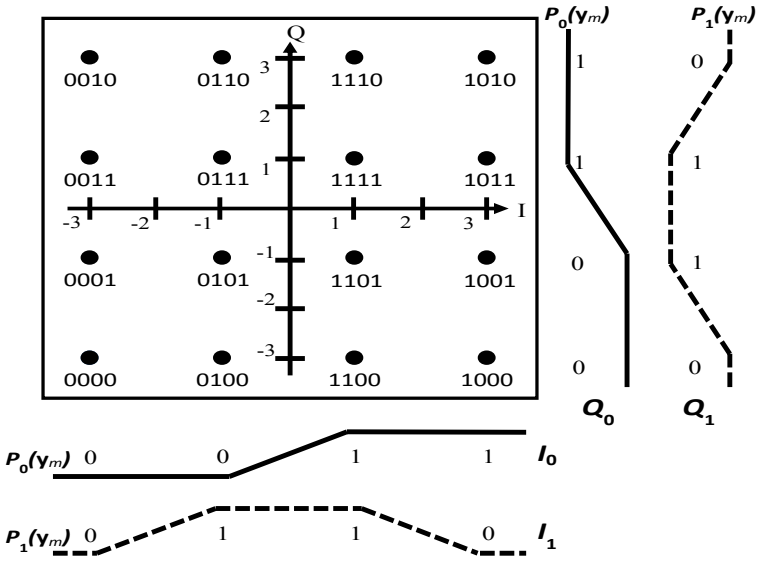

Figure 5.5 QAM modulation with associated linear decision mapping.

For example, for 16-QAM modulated symbols, the input to the demodulator is de-normalized using $1/K_{MOD} = \sqrt{10}$ resulting in data which is then compared to the constellation points intersecting at {-3, -1, 1, 3} of the I and Q axes. The linear decision demapper attempts to give a linearly proportional estimate to the received data based on the constellation point regions. This serves as a probabilistic representation which is useful in soft decision decoding, and is done using a combination of linear mapping and cutoff patterns. Figure 5.5 shows the linear mapping and cutoff patterns for each 16-QAM I and Q bits, as well as 16-QAM modulation constellation points.

5.3.1.2 Equations for the linear decision mapping

In linear decision demapping, the demapper maps each input signal Y_m onto I_b and Q_b output bits using pattern functions derived according to the pattern and position of the constellations points. Since the difference between one adjacent constellation point and its closest neighboring constellation point is 1 bit difference. The individual bit difference can be modeled as a line between those individual bits of the constellation points. For the case of bit difference, the line is modeled linearly in the range of either {0 to 1} or {1 to 0}. For the case of no bit difference, the line is modeled as either a 0 or a 1. It can be seen from Figure 5.5, for 16-QAM modulation, that the I_b and Q_b bits in the constellations follow a pattern of $\{I_0I_1\,||Q_0Q_1 \in [00, 01, 11, 10]\}$, which are broken down into $\{I_0||Q_0 \in [0, 0, 1, 1]\}$ and $\{I_1||Q_1 \in [0, 1, 1, 0]\}$ bottom to top for Q_n and left to right for I_n. These mapping functions are shown as $P_0(Y_m)$ and $P_1(Y_m)$, in Equations (5-9) and (5-10), respectively. Similar approach is applied to the 64-QAM modulation, where the I_b and Q_b bits in the constellations follow a pattern of$\{I_0I_1I_2\,||Q_0Q_1Q_2 \in [000, 001, 011, 010, 110, 111, 101, 100]\}$, which are broken down into$\{I_0||Q_0 \in [0, 0, 0, 0, 1, 1, 1, 1]\}$, $\{I_1||Q_1 \in [0, 0, 1, 1, 1, 1, 0, 0]$, and finally $\{I_2||Q_2 \in [0, 1, 1, 0, 0\ 1, 1, 0]\}$.

In what follows we present the linear soft decision mapping transfer functions for QPSK, 16-QAM, and 64-QAM demodulators. Equation (5-9) $P_0(Y_m)$ is used for both I_0 and Q_0 of the QPSK demodulator for input data Y_m.

$$P_0(Y_m) = \begin{cases} 0 & \text{if } Y_m \le -1 \\ (Y_m - 1)/2 & \text{if } -1 < Y_m \le 1. \\ 1 & \text{if } Y_m > 1 \end{cases} \tag{5-9}$$

For 16-QAM, $P_0(Y_m)$ from Equation (5-9) is used for I_0 and Q_0 bit pattern matching, while Equation (5-10) generates the output soft values for the bit pairs I_1 and Q_1.

$$P_1(Y_m) = \begin{cases} 0 & \text{if } Y_m \le -3 \\ (Y_m + 3)/2 & \text{if } -3 < Y_m \le -1 \\ 1 & \text{if } -1 < Y_m \le 1 \\ (-Y_m + 3)/2 & \text{if } 1 < Y_m \le 3 \\ 0 & \text{if } Y_m > 3 \end{cases}. \tag{5-10}$$

64-QAM also uses the same $P_0(Y_m)$ transfer function to realize the linear pattern for bits I_0 and Q_0, and a modified version of $P_1(Y_m)$ to represent I_1 and Q_1, shown as Equation (5-11), which has extended range over the 16-QAM version.

$$P_1'(Y_m) = \begin{cases} 0 & \text{if } Y_m \le -5 \\ (Y_m - 3)/2 & \text{if } -5 < Y_m \le -3 \\ 1 & \text{if } -3 < Y_m \le 3 \\ (-Y_m + 5)/2 & \text{if } 3 < Y_m \le 5 \\ 0 & \text{if } Y_m > 5 \end{cases}. \tag{5-11}$$

In addition, 64-QAM also has a third linear decision mapping for I_2 and Q_2, namely $P_2'(Y_m)$ in Equation (5-12).

$$P_2'(Y_m) = \begin{cases} 0 & \text{if } Y_m \le -7 \\ (Y_m + 7)/2 & \text{if } -7 < Y_m \le -5 \\ 1 & \text{if } -5 < Y_m \le -3 \\ (-Y_m - 1)/2 & \text{if } -3 < Y_m \le -1 \\ 0 & \text{if } -1 < Y_m \le 1 \\ (Y_m - 1)/2 & \text{if } 1 < Y_m \le 3 \\ 1 & \text{if } 3 < Y_m \le 5 \\ (-Y_m + 7)/2 & \text{if } 5 < Y_m \le 7 \\ 0 & \text{if } Y_m > 7 \end{cases} . \quad (5\text{-}12)$$

where $P_2'(Y_m)$ can be visualized as two $P_1(Y_m)$ functions of Equation (5-10), concatenated over the range from -7 to 7.

5.3.2 Simulation Results

DSRC PHY has been simulated to compare its performance among a recently proposed non-linear demapper and our derived linear demapper, as well as non-ideal analog and conventional DSRC. To show realistic decoding, the add-compare-select noise, comparator offset, and nonlinear branch metric are chosen to be 0.07, 20% and 10%, respectively. The digital Viterbi decoder model includes the effect of 3-bit quantization at its input.

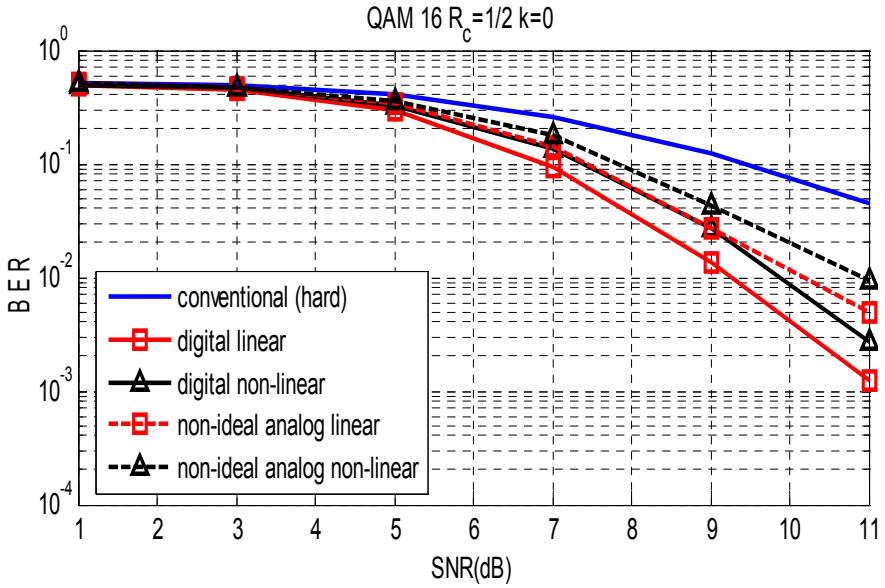

Figure 5.6 BER comparison for QAM16 DSRC with varying SNR at v = 238 km/h, R_c =1⁄2, at 12Mb/s in Rayleigh channel.

The simulations parameters were carefully considered to ensure that all possible situations are tested in WAVE. Both under the worst case scenario, namely no line of sight (NLOS) Rayleigh fading channel, and less severe channel, namely LOS Rician fading channel with Rice factor (K=1) is also considered. Hence, the DSRC PHY systems were tested with varying SNR, packet length, velocity, AWGN, Rayleigh and Rician fading channels, 960 data symbols, different modulation schemes, and different FEC code rates (R_C) for convolutional code. Puncturing was used to achieve the higher code rates as per standard [7]. The legal

maximum relative speed in highways was assumed to be 238 km/h. Exhaustive simulations were produced, and without loss of generality, only few plots are presented as examples.

Figures 5.6-5.10 show the performance of DSRC PHY with varying SNR, relative velocity, and packet length for the tested modulations and decoders. Figure 5.6 shows that both the linear and non-linear demappers yield an improved performance at 16-QAM with $R_C = 1/2$ over the hard Viterbi decoder used in the conventional DSRC; however our proposed digital linear demapper outperforms the non-linear demapper.

From Figure 5.7, a substantial improvement is noticed for both linear and non-linear demappers used with digital and analog decoders at the highest code rate and modulation (64-QAM and at $R_C = 3/4$) used in DSRC while our linear demapper performs better than the non-linear demapper. The linear demapper with digital decoder has reduced bit-error-rate (BER) by approximately a factor of 5.

In addition, at lower relative velocity ($v = 100$ km/h) and with the existence of LOS component, Figure 5.8 shows that our proposed scheme performs better than the non-linear demapper scheme. Figure 5.9 shows that our proposed scheme provides an improved performance in both kind of decoders and at lower Doppler shifts or velocities (around the legal relative speed in a city).

Figure 5.10 confirms that our proposed scheme can offer performance advantage of around a couple of orders of magnitude over both the conventional and non-linear demapper designs.

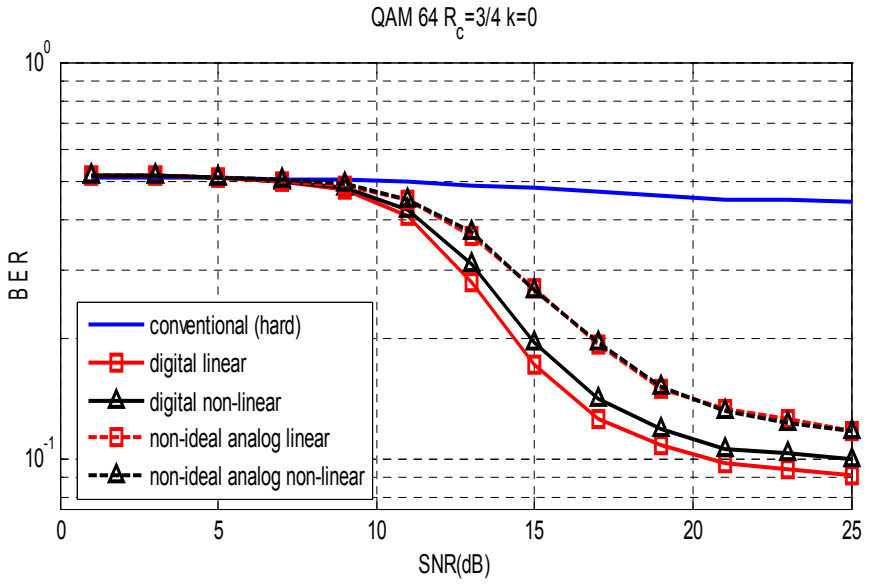

Figure 5.7 BER comparison for QAM64 DSRC with varying SNR at v = 238 km/h, R_c =3⁄4, at 27 Mb/s in Rayleigh channel.

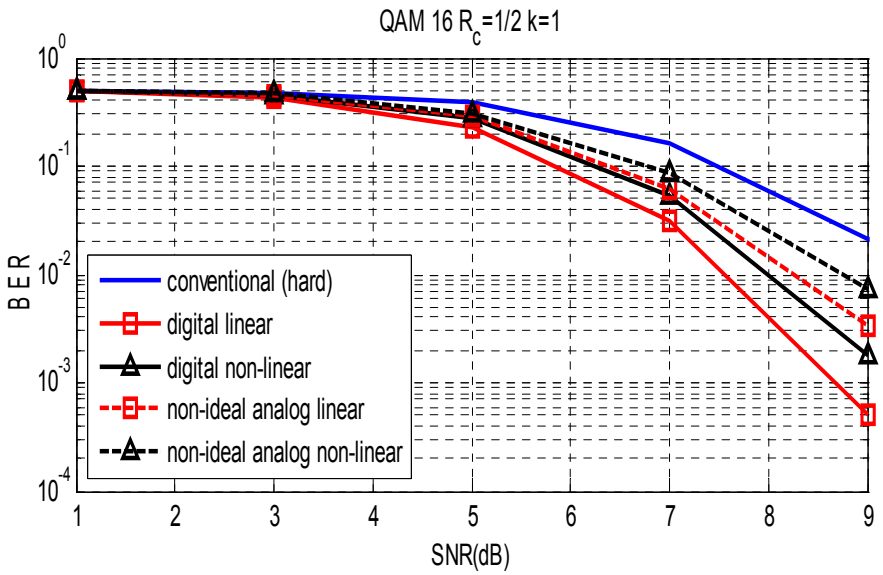

Figure 5.8 BER comparison for QAM16 DSRC with varying SNR at v = 100 km/h, R_c =1⁄2, at 12 Mb/s in Ricean channel.

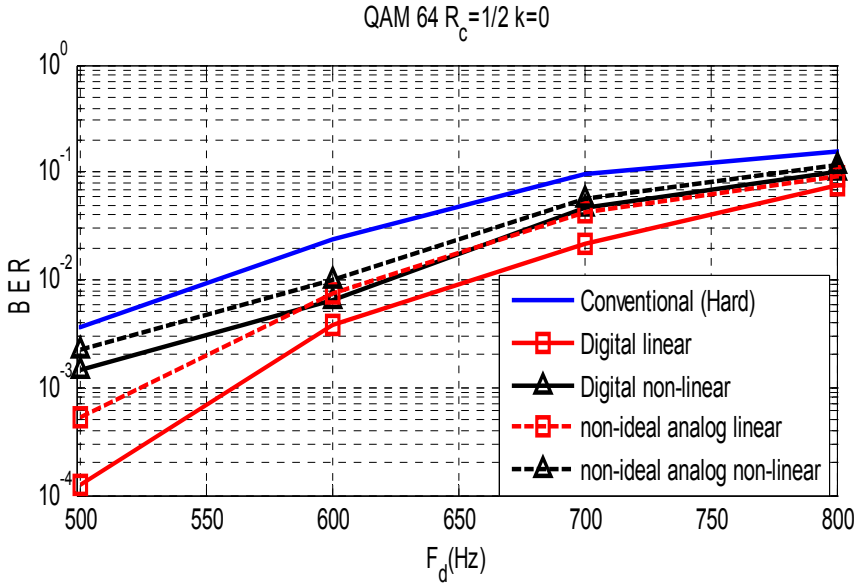

Figure 5.9 BER comparison for QAM64 DSRC with varying velocity at SNR = 30 dB, R_c =1⁄2, at 18Mb/s Rayleigh channel.

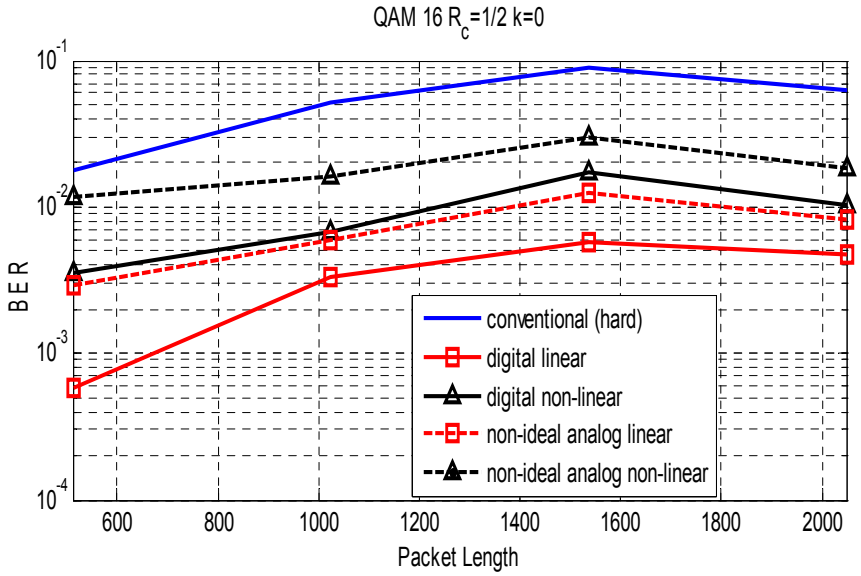

Figure 5.10 BER comparison for QAM16 DSRC with varying packet length at SNR = 10 dB, v = 238 km/h, at 12Mb/s Rayleigh channel.

5.4 Performance Enhancement of DSRC PHY Using Improved Equalization

The physical layer (PHY) of DSRC is currently being developed by work group of IEEE 802.11p [52]. DSRC PHY is originally based on the IEEE 802.11a standard with increased symbol duration [7], [38,28]. It uses orthogonal frequency division multiplexing (OFDM). OFDM systems are able to mitigate ISI, through the use of sufficient guard intervals inserted in front of each OFDM symbol. Therefore, a 1-tap equalizer is sufficient to equalize the OFDM systems in time-invariant channels [53]. Orthogonal subcarriers carry the modulated data symbols that compromise the OFDM symbols. The orthogonality principle is no longer valid in time-variant channels, which leads to the presence of inter-carrier interference (ICI) [54,55]. The ICI factor increases with increased vehicular speed. Pilot, demapper and Viterbi-aided receiver design schemes were discussed for channel tracking for DSRC systems [27]. It was shown that the Viterbi-aided channel tracking technique improved the overall performance of DSRC systems in higher constellation modulations compared to the other two schemes [27,40]. In [30], a second-order iterative tracking scheme, which runs the feedback loop twice was proposed to make use of the additional information obtained from the decision-directed channel estimation schemes of [40], [56], which resulted in a slight performance improvement for higher order quadrature amplitude modulation (QAM) schemes, however, no improvement was reported for quadrature phase shift keying (QPSK) and binary phase shift keying (BPSK) modulated schemes compared to the corresponding first-order-scheme [56].

These channel tracking schemes did not consider the individual ICI coefficients in their calculations. In addition, channel tracking schemes rely heavily on the integrity of the decoding scheme for additional information. For example, the decoder is more likely to produce unreliable data back through the feedback loop at the occurrences of deep fades.

This dissertation proposes applying a receiver design for the 5.9 GHz DSRC system that can make use of ICI information caused by the time-varying channels. The proposed receiver uses a maximum a posteriori (MAP)-based equalization concept in frequency-domain to combat ICI instead of ISI in DSRC systems without the need of feedback loops. The proposed system is tested for QPSK and BPSK modulation schemes, and is compared to the conventional system and the schemes in [40], [56]. The improvements are achieved through a worst-case scenario at relatively high and low speed limit studies, i.e. by using Rayleigh fading channel at high and low legal limits of relative vehicular velocity.

This chapter starts with a discussion on the baseband model of the current conventional DSRC PHY system. Then we describe and present the proposed receiver design that uses frequency domain equalization to combat ICI. Later in this chapter we present simulation results for all three DSRC receiver designs, namely the conventional, Viterbi-aided, and proposed receiver designs, which illustrate the substantial performance improvement achieved by the proposed receiver design.

5.4.1 Frequency-domain equalizer

A thorough study of the effectiveness of different demapping and decoding schemes for the DSRC system were included in [38]. It was shown that both BER and PER performances of the DSRC system with different soft decoding (MAP-based or Viterbi) schemes relative to that of the conventional DSRC system, resulted in a slight improvement in the case of the higher constellation modulations, while almost no improvement in the case of the lower constellation modulations.

For clarity, Figure 5.11 illustrates an example of such findings. It can be seen that the DSRC system with different demapping precision outputs (hard output and soft output demappers) and decoding (MAP [46] and Viterbi) schemes have similar BER performances [38].

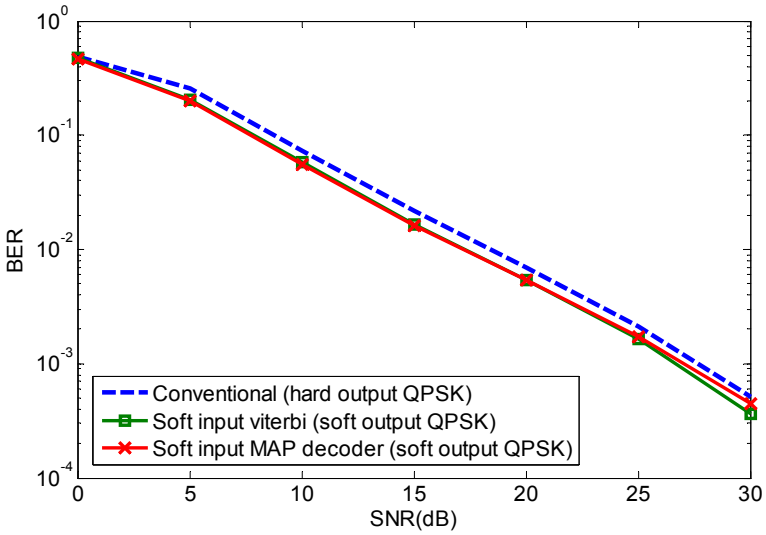

Figure 5.11 BER vs. SNR at 238 km/hr for different demappers and decoders.

The fact is that the conventional IEEE 802.11a systems assume static channel characteristics [28], which means that the conventional signal compensator provides a poor equalized representation of the symbols to the remaining of the system. In practical mobile communication applications, the Doppler spread associated with time-varying channels cause error floor, hence it should be taken into account [57]. Various techniques for reducing ICI caused by the time-varying channels are defined, presented, and referenced in [57]. An example of time-varying Rayleigh fading envelopes produced by the channel simulator is shown in Figure 5.12. It can be seen that at around the legal maximum relative velocity of vehicles (238 km/hr), deep fades exist across one DSRC packet with duration of 1.0 ms, with 125 DSRC/OFDM symbols per packet. However, the change is relatively slow within one DSRC symbol with duration of 8.0 μs.

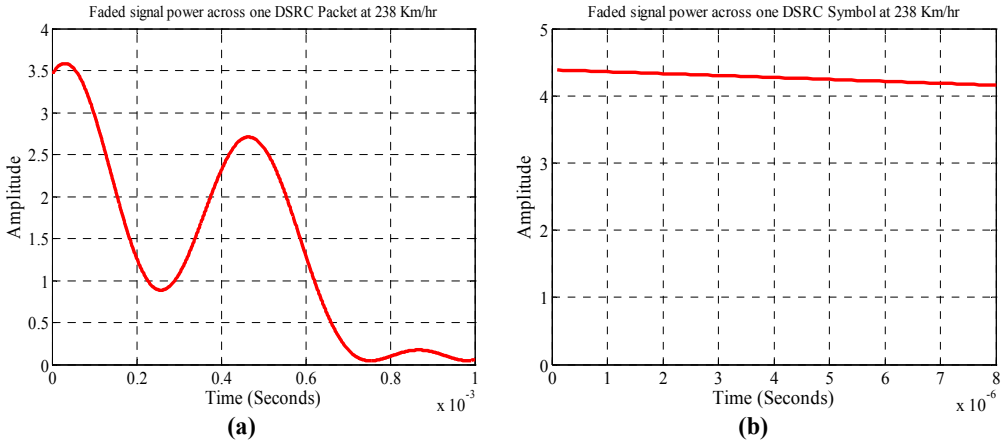

Figure 5.12 Rayleigh fading envelope examples for DSRC (a) over one packet with duration of 1.0 ms with 125 DSRC/OFDM symbols, and (b) over one DSRC symbol with duration of 8.0 μs.

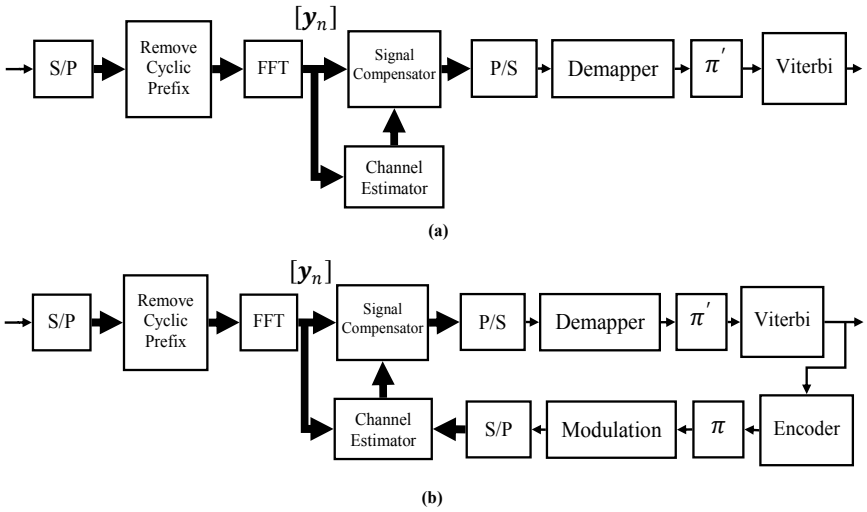

Figure 5.13 DSRC Receiver Designs with: (a) Viterbi-aided channel tracking, (b) Frequency-domain equalization.

The DSRC conventional and the DSRC receiver with the Viterbi-aided schemes are shown in Figures 5.13(a) and 5.13(b). The figure illustrates that the output of the Viterbi decoder is fed back to the channel estimator. The serial output of the decoder is first encoded, interleaved, and then modulated to obtain the "desired signal" which is used to obtain an error estimate, which is in turn used to update the channel coefficients symbol-by-symbol [40].

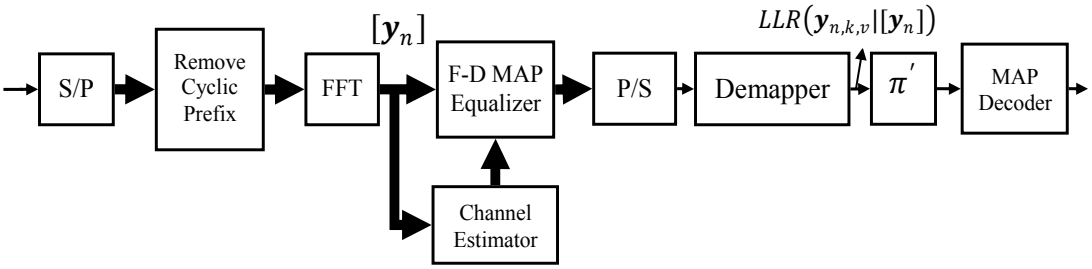

Figure 5.14 DSRC receiver design with frequency-domain equalization.

Figure 5.14 shows the frequency-domain (F-D) MAP equalizer block. The MAP equalizer is based on the BCJR algorithm [46]. In order to obtain the channel coefficients in frequency-domain, it is necessary to have an equivalent channel coefficient model in frequency-domain. Under the approximation of linear variation in a DSRC/OFDM symbol, the frequency-domain $N_{sc} \times N_{sc}$ channel coefficients matrix $\boldsymbol{H}$ is given as [58]:

$$\boldsymbol{H}_{i,j} = \frac{1}{N_{sc}} \sum_{n=0}^{N_{sc}-1} \boldsymbol{h}_{n,k} \cdot e^{-j2\pi(i-j)n/N_{sc}}. \tag{5-13}$$

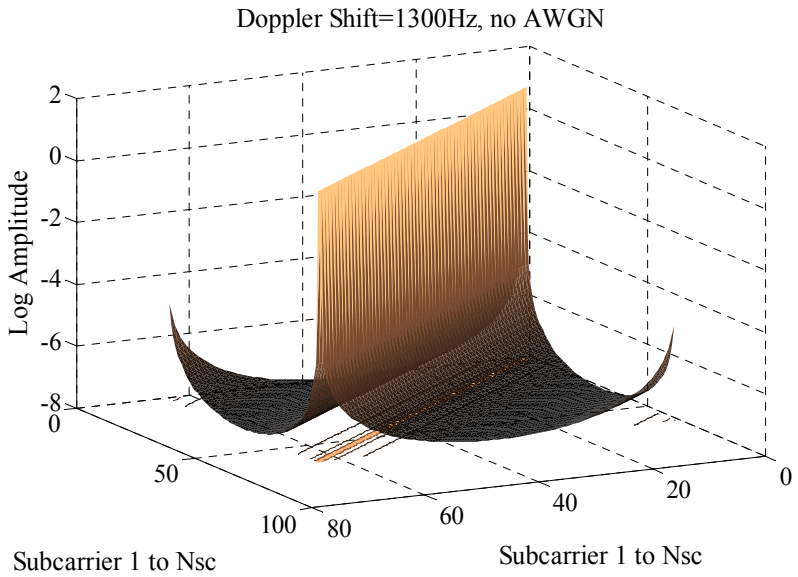

Figure 5.15 Subcarrier to subcarrier ICI contributions.

The off-diagonal elements represent the ICI coefficients (due to the time-varying channel). It should be noted that the elements around the main diagonal of $\boldsymbol{H}$ contain the most concentration of ICI power. The channel frequency response $\boldsymbol{h}_{n,k}$ can also be expressed as the *FFT* of the complex channel impulse response (CIR) for the subcarrier k at time n, i.e., $\boldsymbol{h}_{n,k} = \sum_{l=0}^{L-1} h_{n,l}.\, e^{-j2\pi lk/N_{sc}}$, where $h_{n,l}$ is the CIR for the l^{th} path at time n. It is important that an OFDM-based DSRC system with time-variant channels be able to exploit the ICI elements in its receiver design. Figure 5.15 illustrates the ICI power in log form of the $\boldsymbol{H}$ matrix of one OFDM symbol under Rayleigh fading with Doppler frequency of 1300 Hz. The output of the frequency-domain MAP equalizer including the demapping operation is given by the relation:

$$LLR\left(\boldsymbol{y}_{n,k,v}|[\boldsymbol{y}_n]\right) = \; log\frac{p\left(\boldsymbol{y}_{n,k,v} = +\boldsymbol{1}|[\boldsymbol{y}_n]\right)}{p\left(\boldsymbol{y}_{n,k,v} = -\boldsymbol{1}|[\boldsymbol{y}_n]\right)} = \frac{\sum_{\boldsymbol{y}_{n,k,v}=+1,\; s,s'\in\boldsymbol{S}} \alpha_k(s').\beta_{k+1}(s).\gamma_k(s',s)}{\sum_{\boldsymbol{y}_{n,k,v}=-1,\; s,s'\in\boldsymbol{S}} \alpha_k(s').\beta_{k+1}(s).\gamma_k(s',s)}, \tag{5-14}$$

where $LLR\left(\boldsymbol{y}_{n,k,v}|[\boldsymbol{y}_n]\right)$ is the log-likelihood ratio of the conditional probability of the received coded bit $\boldsymbol{y}_{n,k,v}$, i.e., the received symbol at the k^{th} subcarrier and the n^{th} time and the v^{th} bit (there are 2 bits for QPSK and 1 bit for BPSK). The terms $\alpha_k(s)$ and $\beta_k(s)$ are the forward and backward probability recursions [46]. The term $\gamma_k(s,s')$ is given by [58]:

$$\gamma_k(s,s') = \; p(s'|s).p(\boldsymbol{y}_k|s,s') = \begin{cases} e^{\left\{-\frac{1}{2\sigma^2}\left|\boldsymbol{y}_k - \sum_{l=-f}^{f} \boldsymbol{h}_{k,<k-l>_{N_{sc}}}.\, \boldsymbol{x}_{<k-l>_{N_{sc}}}\right|^2\right\}}, & (s,s')\in\boldsymbol{S} \\ 0, & \text{Otherwise} \end{cases} \tag{5-15}$$

where $<.>_{N_{sc}}$ is the modular N_{sc} operation, and is used together with the non-zero positive integer f to specify which interfering subcarriers or ICI elements in the matrix $\boldsymbol{H}$ are used in the $\gamma_k(s,s')$ calculation; σ^2 is the complex AWGN noise variance, while s and s' are the present state and the next state, respectively, in all possible states $\boldsymbol{S}$ of the channel trellis.

5.5 Performance Simulations

Since the IEEE 802.11p or the DSRC PHY standard is still under development, and the conventional system fails in Wireless access vehicular environments (WAVE), this study is carried out to propose modifications to the receiver that enable the system to take ICI into account to achieve improved PER and BER performances. The DSRC systems are simulated using MATLAB. For a fair comparison, the DSRC receivers receive the same distorted data from the channel. In DSRC systems, a strong specular component is usually present, but sometimes strong specular components don't exist [27]. The DSRC systems are tested in time-varying channels. Therefore, the BER and PER vs. the signal-to-noise ratio (SNR) per bit performances are simulated under the worst case scenario, i.e. No-line of sight (No-LOS) 1-path Rayleigh fading channel. The SNR per bit refers to the non-dimensional ratio E_b/N_0 measure, or the ratio of the energy per information bit (E_b) to the noise spectral density (N_0). The DSRC systems with the channel tracking receiver and the conventional receiver are designed according to the specifications in [40] and [7],

respectively. The relative velocities of 238 km/hr, and 74 km/hr (or Doppler frequencies of around 1300 Hz and 400 Hz, respectively) are selected, which are around the legal maximum and low relative speed limits of vehicles. All the simulations are carried out with 60 OFDM symbols for each packet for 1200 packets. Due to the fact that the elements around the main diagonal of $\boldsymbol{H}$ contain the most concentration of ICI power, we select the diagonal elements of matrix $\boldsymbol{H}$ and its 2 neighboring subcarriers (the previous and the next subcarriers to the subcarrier of interest), by choosing the value $f = 1$ in Equation (5-15).

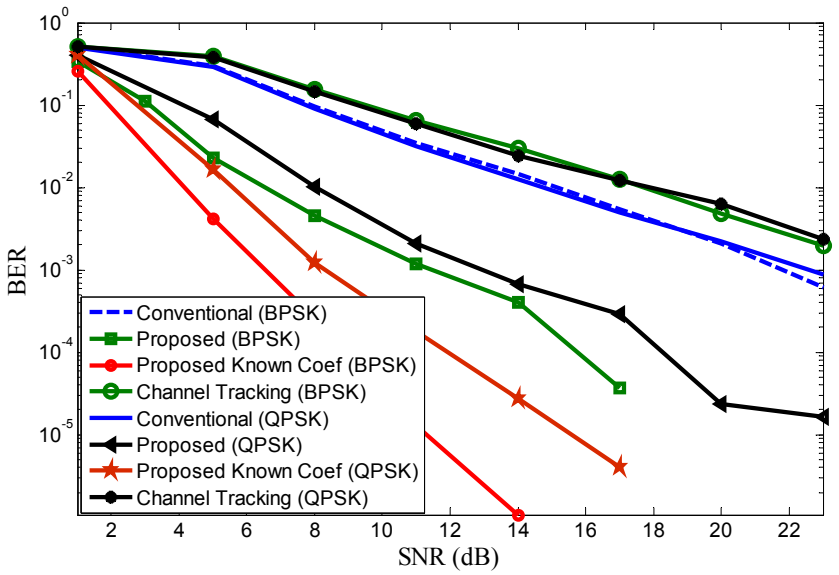

(a)

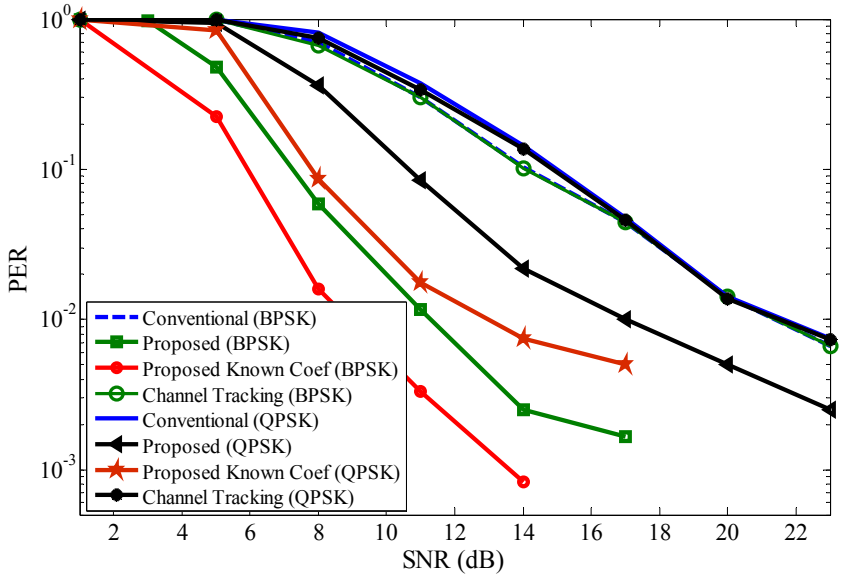

(b)

Figure 5.16 BER and PER vs. SNR at 238 km/hr and 60 OFDM symbols under Rayleigh fading.

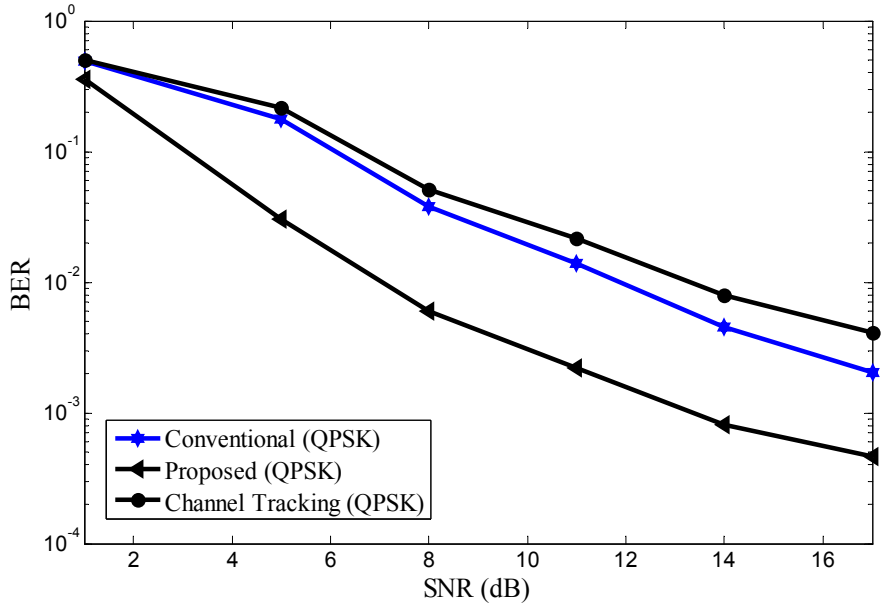

(a)

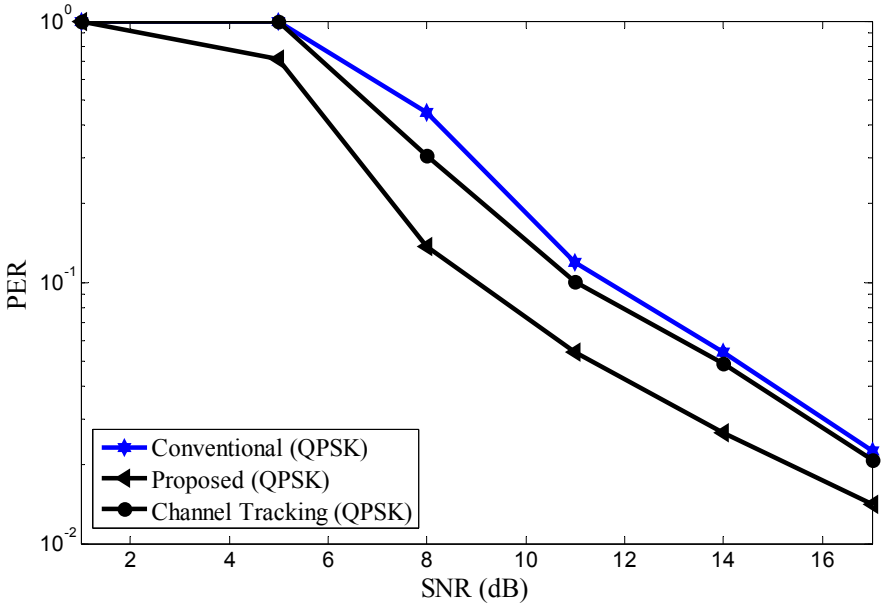

(b)

Figure 5.17 BER and PER vs. SNR at 74 km/hr and 60 OFDM symbols under Rayleigh fading.

Figures 5.16 and 5.17 show the BER and PER performances at both high and low velocities versus SNR per bit, respectively. In the following, the observed SNR per bit for Figure 5.16 are those of the BER and PER levels of 10^{-2}. For Figure 5.17, the observed SNR per bit are those of the BER and PER levels of 10^{-2} and 10^{-1}, respectively. Without loss of generality, and since the systems with BPSK modulation

outperform the systems with the QPSK modulation, we use QPSK modulation in this study to provide the performance comparisons at the relatively low velocity. The proposed system is also simulated using perfectly known coefficients for the system with the velocity of 238 km/hr, to identify the performance trend that can be used as a benchmark. Figure 5.16 shows that the proposed system with the high velocity and the QPSK scheme has performance gains of about 9.8 dB and 6.75 dB for BER, and about 4.5 dB for PER over the DSRC system with the channel tracking scheme and the conventional system, respectively; while the proposed system with the BPSK scheme has performance gains of around 11.25 dB and 9 dB for BER, and about 10 dB for PER over the DSRC system with the channel tracking scheme and the conventional system, respectively.

It is shown in Figure 5.17 that a substantial performance improvement in both BER and PER performances is achieved in QPSK modulation scheme over both the DSRC conventional and the DSRC channel tracking schemes. It is at the lower velocity that the channel tracking scheme slightly outperforms the conventional system for PER. It is also noted that the system with the channel tracking scheme resulted in a very poor BER performance in all cases.

Chapter 6

Reconfigurable Simulator Using Graphical User Interface and Object Oriented Design for DSRC PHY

6.1 Introduction

In the development of any new communication technology, either a full prototype or a simulation must be modelled and developed alongside analytical/theoretical models. Prototyping is time consuming and costly, especially during the research and development stage where simulation is more attractive.

Object-oriented simulation environments have modularity, abstraction, reusability and encapsulation features [48]. These features can for example, allow for a fair comparison for multiple receiver designs in a communication system to be tested under the same transmission conditions. In object-oriented simulation environments, the objects interact with each other at different states of the simulation. This makes object-oriented simulation more useful for getting reliable estimates of performance once all simulation components have been verified.

Orthogonal frequency division multiplexing (OFDM) systems were first proposed by Chang and Gibby for digital communications [59]. It has been used in wireless local area network (WLAN) standards (IEEE 802.11a/g and HIPERLAN/2), digital video broadcasting (DVB), digital audio broadcasting (DAB), new broadband wireless access standard WiMax (IEEE 802.16e), and now dedicated short range communication systems (DSRC) [38, 60]. OFDM wireless communication physical layer (PHY) is a versatile communication model [59, 38]. This is due to the OFDM PHY having multistage components that share dependent symmetrical parameters/settings on each side of the communication channel [7], which is capable of being used in many different configurations within one or more technologies, such as in [61], [3], [62], and [63]. Testing various OFDM receiver designs under various levels of strain is important because it gives a more objective analysis of a particular implementation. In other words, OFDM PHY receivers have to be optimized and compared to one another in different environments, and hence is a useful candidate for object-oriented simulation analysis.

OFDM communication systems have different configurations depending on different applications, and can also have different performance characteristics. Hence, the OFDM communication systems are

required to operate in different operating modes, and having a simulator with a modular structure, capable of reconfiguring on demand is desirable as it gives the ability to test full system performance. Object-oriented simulators can be made compatible with other object-oriented simulators, and hence can be deployed as subsystems [64] when simulating other aspects/layers of a communication system. An example would be for use in cross-layer analysis at different levels such as network layer or medium access control (MAC) layer [7].

The majority of the simulation designs focus on simulation of higher layers of the open systems interconnection (OSI) communication stack, such as the ones shown in [65]. It is shown that changes in the physical layer or the channel of a communication system can have great repercussions in the higher layers [66]. In addition, other layers require information from the PHY to perform optimally. For example, a more realistic PHY implementation is important when it comes to a dynamic MAC layer design [37]. Due to this fact, and with the PHY being the lowest part of the OSI Model in a communication system, it is very important to have a well optimized and accurate PHY model for simulations.

Other works discuss OFDM simulators from different aspects, as heterogeneous simulation improvement, Network Simulator 2 (NS2) PHY accuracy improvement, model abstraction and approximation, Matlab and/or Simulink detailed modeling, and hardware accelerated simulation.

Authors in [67] study the effects of detailed modeling of OFDM PHY and focus on the integration between a Matlab/Simulink OFDM PHY simulator and a Qualnet Medium Access Control (MAC) layer simulator. The authors emphasize the importance of detailed modeling of the OFDM PHY and perform heterogeneous runtime performance study which resulted in improved simulation time. In [67], Network Simulator 2 (NS2) is used in conjunction with Qualnet with its proposed model, and studies the effects of accurate PHY modeling on higher layers, and shows upwards of six fold TCP/UDP throughput difference. Studies [68] and [69] investigate the use of hardware assisted OFDM simulation, showing that using field programmable gate arrays (FPGAs) programmed using Hardware Description Language (HDL) can improve simulation runtime performance over pure software simulation.

Some OFDM simulators use PHY abstraction to make approximations for parts of the OFDM PHY to improve simulator performance runtime and resource usage. For example, authors in [70] focused on OFDM channel realization in the frequency domain for reducing complexity of simulation to increase simulation runtime performance. There are advantages to OFDM PHY abstraction, but this may not be accurate in all OFDM PHY scenarios.

In our OFDM PHY simulator model description, we use Unified Modeling Language (UML) diagrams to allow for understanding and implementation of the concepts we present regardless of platform choice or familiarity. The UML diagrams express and emphasise the building of our high level objects that are inherently modular, flexible, and interactive. Consequently, the flexibility and interaction of our simulator's objects improve usability by introducing automatic reconfiguration, and parallel processing capabilities are improved through modularity of these objects. Although, the initial development time investment in a high level simulator designs, such as ours, is arguably higher than that of a purely

functional implementation of a specific problem. This fact is mitigated by the re-usability of the object-oriented generic design, code modularity, and potential for rapid reconfiguration. We choose to illustrate the benefit of using an object-oriented design to improve parallel processing, and a graphical user interface (GUI) to control simulation parameters of a versatile/reconfigurable and complex OFDM PHY communication simulation system. Our object-oriented OFDM simulator allows for ideas to be expressed to others working in the same field through analysis of the simulation results.

High-level object-oriented design is a technique that is used to create flexible simulation objects. Parallel processing and distributed computing reduces overall time to complete a simulation by transferring process load in a simulation. Our work is based on the underlying complexity of designing OFDM PHY communication systems that need to be studied under various dynamic situations. The creation of a platform for rapid design and preliminary evaluation is studied and developed, building on existing software development techniques to apply them to OFDM PHY communication engineering problems. In addition, for explaining the development of our high level OFDM simulator, we are not focusing on any particular platform/programming language, such as Matlab, Simulink, IT++, Scilab, C++, Java.

6.2 Modelling

As stated by Bratley et al [71]: "a model is a description of some system intended to predict what happens if certain actions are taken," which is an essential definition of a model of a real system. For a communication simulation, the model would be based on the communication protocol with rules and algorithms used to emulate environmental reactions, that is, emulating the behaviour of both the engineered communication elements and the natural elements.

Using generic simulations of the components of the OFDM system allow for testing and optimization of the PHY under unusual stress conditions or for specific applications such as for high mobility or high data rate conditions. There are other components that can be added depending on what the designer wishes to include as a component such as coherent detection enhancement, alternate piloting schemes, ISI or inter-carrier interference (ICI) cancelation compensation, or multi-input/multi-output features. The diversity of OFDM communication systems both for application, medium, and technological improvements make it worthy of further study.

OFDM PHY offers flexibility in the number of subcarriers used in transmission, modulation level, coding type, code rate, channel estimation technique, zero padding, interleaving type, and many other features which significantly affect the performance, as can be seen in [40], [41], and [7]. Table 6-1 presents the value parameters used for running IEEE 802.11p OFDM PHY system scenarios, which are used for the models that produced the simulated results in the Figures 6.1, 6.2, and 6.3.

Table 6-1: General IEEE 802.11p OFDM PHY parameter value combinations used in simulated examples.

Name	**Symbol**	**Unit**	**Values**
Signal-to-Noise Ratio	SNR	dB	[1, 2, 3, 6, 10, 15, 20, 25, 30]
Channels			Rayleigh and Rician (1-path, 2-path), AWGN
Rice Factor	K		[0, 1]
Pilot			48
Interleaver			Block
FFT			64-point
Maximum Doppler Frequency (velocity)	f_d (v)	Hz (km/h)	[137,273,546,819, 1043,1300,1311] ([25,50,100,150,200,238,240])
Symbol Duration	T_s	μs	[8,4]
Packet Length	N_s	Symbols/ packet	[60]
Number of Packets			5000
Modulation	M		[BPSK, QPSK, 16QAM, 64QAM]
Demapping			[hard and soft (linear quantization) decisions]
Decoding			[hard, soft, BCJR, Viterbi]

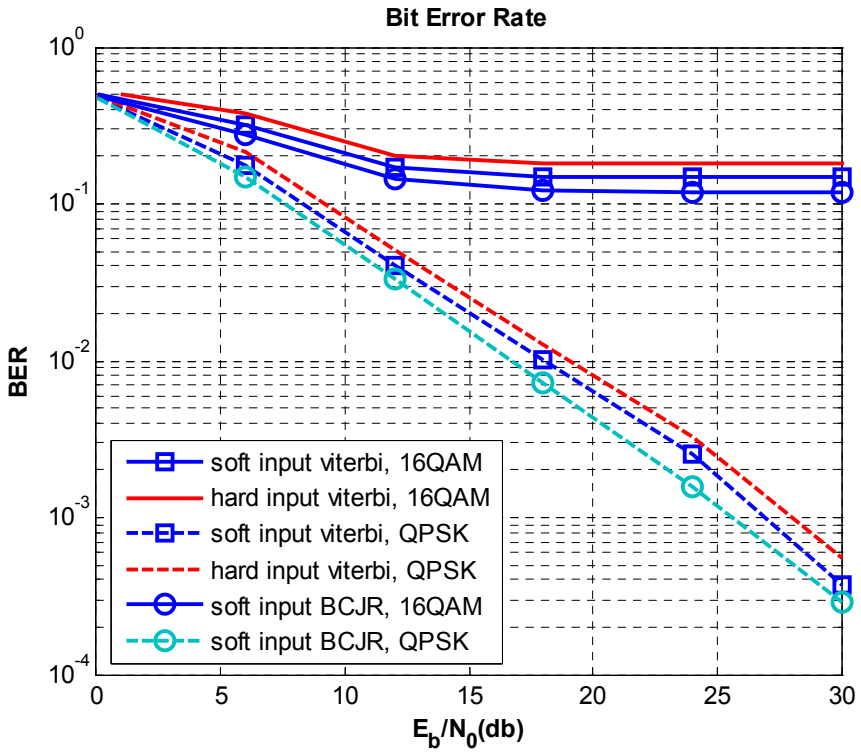

Figure 6.1 BER vs. signal to noise ratio for different channel, transmitter and receiver scenarios.

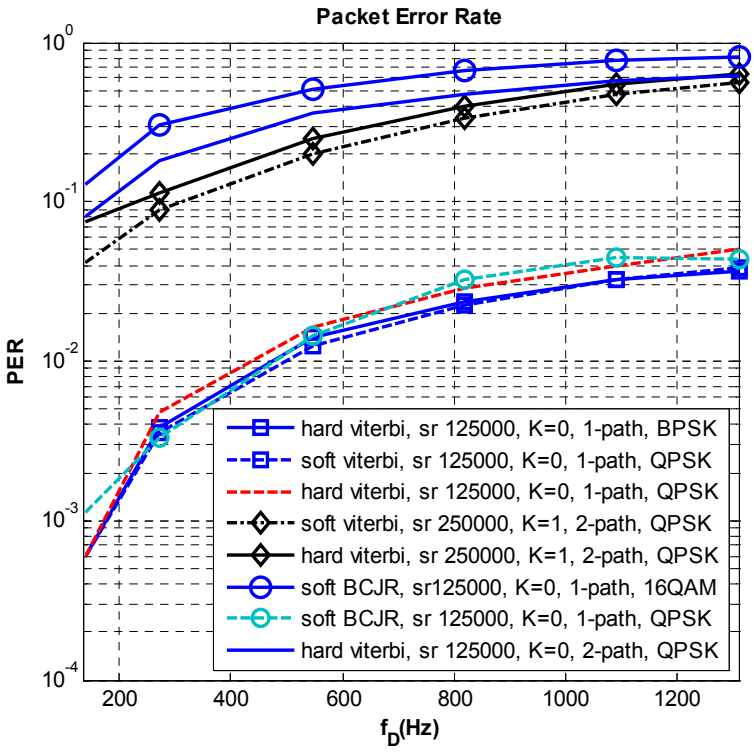

Figure 6.2 PER vs. Doppler shift for different channel, transmitter and receiver with different symbol durations.

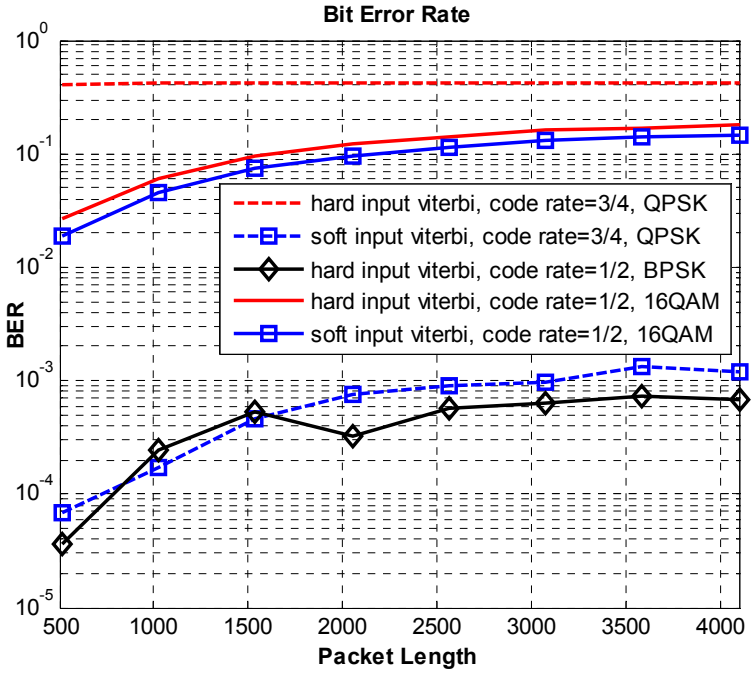

Figure 6.3 BER vs. packet length for different channel, transmitter and receiver scenarios.

Figures 6.1, 6.2 and 6.3, are sample result plots based on the system configurations and components presented in Table 6-1. It is from these plot results, that the designer may be able to draw conclusions on the performance of his/her design compared to the conventional or other OFDM PHY designs. For example, it can be concluded from Figure 6.1 that the OFDM system designs with the higher modulation scheme (16-QAM) suffers error floor. On the other hand, the OFDM systems with the lower modulation scheme (QPSK) outperform the systems with 16-QAM modulation, but at the expense of a lower data rate, calculated from Equation (1). Another important observation from the figure would be that the OFDM receiver designs with soft decision capabilities outperform their relative receiver designs with hard decision capabilities. Figure 6.2 will later be used as a specific example of how the simulator can be used to compare different system designs and configurations, and later on in this chapter as the case study for the proposed packet partitioning technique.

6.3 GUI Considerations

An outline of some considerations to create a GUI for an object-oriented simulation system is presented in this section. This will facilitate in the understanding related to the simulation design. The GUI is the primary interface between the computer simulation and the user. The GUI for the proposed simulation environment is built as a separate entity from the simulator, and is used to define configuration of the simulator. The simulator is composed of classes that are configured to define the simulation environment metrics that change and select different components from the OFDM PHY to be simulated, as will be discussed. It is important that a feedback relationship exists between the GUI and the simulator so that as the simulator is modified to feature new functionality, the GUI during simulation setup can query the components for what features are available. For example, if new modulation types are added to a modulator class at the simulation level, the GUI will reflect those additions in its platform for the user to see. Components such as these needs to be designed so that they can give appropriate update information to the GUI as part of their development. Section 6.4 will illustrate this feedback relationship.

Use of a GUI is recommended because it allows for fast reconfiguration of the components in the simulation. Each component can have compatibility with each other based on the underlying programmatic relationships between the objects, but the actual control of the parameters should be controlled by the GUI. Additionally, if the designer wants to reconfigure an OFDM PHY design, many variables and parameters may be changed at the GUI level. Coding these changes by hand can lead to errors. By using a GUI with our proposed simulation environment, all of the parameters are in one place with constraints on the user input. Therefore, when changing scenarios in our object-oriented simulator with GUI, the user does not have to worry about those errors because of the inherent flexibility of the system.

6.3.1 Simulation control

The functionality of adding new components to the simulation is very useful when testing different versions of a design. From the new component design point of view, once the input/output of the designed

components have been made compatible with the existing OFDM system, it is with relative ease that the new design can be fully integrated with the existing object-oriented simulator. Configuring the individual components using a GUI is straight forward, while individual parameters are constrained based on the existing simulation objects. Constraints on the components are stored as bounded limits, and are communicated back to the GUI so that simulator does not exceed these limits.

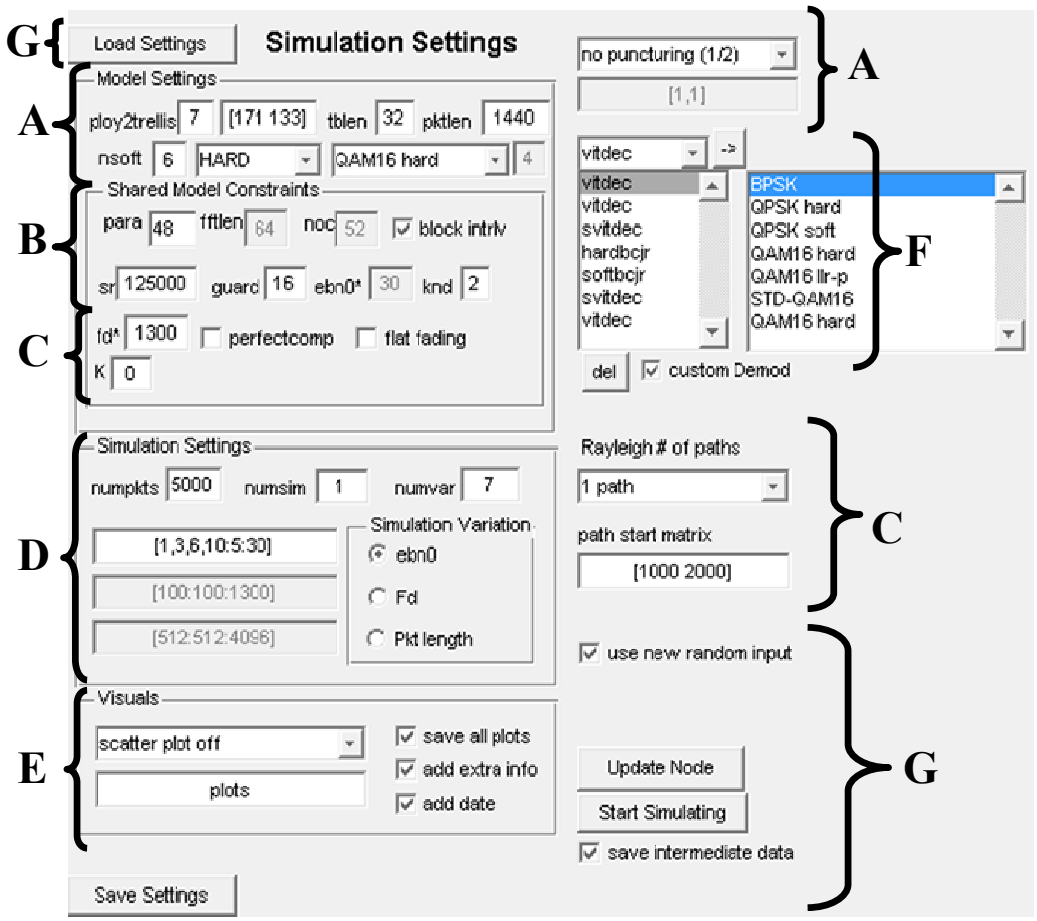

A: Main Model Settings
B: Transmitter/Receiver Settings
C: Channel Settings
D: Simulation Controller Settings
E: Output/Visual Settings
F: Modulation/Decoding Settings
G: Simulation Initialization, and State Settings

Figure 6.4 Example GUI parameter setup for the OFDM PHY model.

Figure 6.4 shows example parameters that may be used in a GUI for a versatile OFDM communication system scenario simulator. Our implementation is achieved using the Matlab platform. However, the theory behind our simulation environment can be used in many other object-oriented capable platforms. The layout of the GUI is divided into different sections with each section having different configuration settings, namely: main model settings, transmission/receiver settings, channel settings, simulation controller settings, output/visual settings, decoding settings, and simulation initialization and state settings, which is used for current state saving/loading configuration (for multi-stage simulations). For clarity, basic

descriptions of some of the main configuration settings found in our example GUI platform of Figure 6.4 are presented in Table 6-2. In general, the GUI has settings linked to all of the configurable OFDM System parameters, found in [41], [7] and [38].

Table 6-2: Main user configurable GUI platform parameters

Name	Symbol/Variable	Descriptions
Convolutional Encoder	poly2trellis	Encoder generator used for FEC purposes
Puncturing		Different encoders with different code rates require different puncturing levels to ensure relatively higher throughput
Number of soft values	nsoft	The number of information bits needed (granularity of the information)
Packet length	pktlen	Number of packets in an OFDM system
Traceback length	tblen	Needed for proper storage of path decisions made by the decoder
Modulation type		[BPSK, QPSK, 16QAM, 64QAM]
Parallel carriers	para	Number of parallel data subcarriers in an OFDM symbol
Fast Fourier Transform length	fftlen	Total number of subcarriers, which include para, zero padding and pilots subcarriers in an OFDM symbol
Number of carriers	noc	Number of para, and pilot subcarriers combined in one OFDM symbol
Intearleaver	block intrlv	Block interleaving is adopted if selected, or else random interleaving will be used as the interleaver
Symbol duration	sr	The symbol duration of an OFDM symbol
Guard interval	guard	Length of guard intervals in one OFDM symbol
Signal to noise ratio	ebn0	Ratio of energy per information bit to the noise spectral density
Maximum Doppler Frequency	f_d	This phenomenon exists when the relative velocity between 2 antennas is greater than zero

It is at the simulation controller settings (part D in Figure 6.4) that the user would specify a range of values that reflect how the user wishes to compare different OFDM designs. Specifically, the user could compare the designs in varying signal-to-noise ratio, Doppler shift, and packet length values. If needed, the user can save current plot results for later retrieval by selecting the save all plots option at the output/visual settings section (part E in Figure 6.4).

The following is a specific example of how the simulator can be used for a fair comparison of different system designs and configurations in a step-by-step format (refer to Table 6-2 for definitions of OFDM PHY GUI settings, and Figure 6.4 for the simulator GUI layout).

1. Initialize

    a. Start the GUI on the client computer.

    b. If previous settings have been saved, the user can use the "Load Settings" button to load previously saved settings if desired (Figure 6.4 part G).

2. Specify Simulation Settings and Visualizations

    a. Specify "Simulation Settings" including: number of OFDM packets to simulate; control variable (i.e. signal to noise ratio, Doppler shift, and packet length); number of times to run simulation ("*numsim*" in Figure 6.4 part D); and number of variations in the chosen control variable ("*numvar*" in Figure 6.4 part D). Note that selecting the "Simulation Variation" (i.e. ebn0, f_d, pktlen) control variable will disable some blocks in the Model

Settings/Constraints because it is overriding the fixed variable settings (ebn0, f_d, pktlen in Figure 6.4 parts A, B and C).

b. Chose visualizations to include in simulation output using the drop down menu (for example scatter plots as depicted in Figure 5.4 from previous chapter). The location to save files defaults in the plots folder, which can be changed by the user by typing the folder and subfolder names if applicable (Figure 6.4 part E). For example, the user can specify the simulation output save folder location as "home\OFDM\testX".

3. Specify OFDM PHY design configuration

a. The user then specifies "Model Settings" such as convolutional trellis for the convolutional encoder, modulation level/scheme, puncturing, packet length, system quantization level etc. (Figure 6.4 part A). Note that drop down boxes contain all detected settings in the OFDM Simulator that can be chosen by the user.

b. Afterwards "Shared Model Constraints" are specified which includes: number of parallel transmissions, symbol rate (sr), *FFT* length, guard interval length, number of training symbols, noise level (disabled if ebn0 is the control variable selected in "Simulation Variation" in Figure 6.4 part D).

c. The user specifies decoder by selecting the decoder type from the drop down box (Figure 6.4 part F).

d. Then the user repeats steps 3a – 3c for each OFDM system configuration or design as applicable for comparison requirements.

e. Time-varying channel conditions are then specified (Figure 6.4 part C).

4. Simulate and Analyze

a. The user then runs the simulation and waits for results by pressing the "Start Simulating" button (Figure 6.4 part G).

b. BER and PER performance results are plotted by default for immediate comparison between the different system designs and configurations the user specified.

Note that only compatible options are made available to the user because of the high level object interactions in our simulator. This is due to the automatic simultaneous class object inspections of source and user settings. This prevents simulation setting mistakes, which could otherwise cost time in debugging or simulation of incorrect systems.

For a specific numeric example of the steps above for specifying an OFDM system configuration refer to system 1 of the total 8 systems in Figure 6.2. That is, to specify an OFDM system that uses symbol rate of 125000 symbols per second, pure 1-path Rayleigh fading channel operating under BPSK modulation with hard decision Viterbi decoding, under varying f_d at constant ebn0 of 30dB, do the following: 1) Start the simulator GUI; 2) set the control variable to f_d, and specify the desired range interval for the Doppler shift; 3) set the modulation level to BPSK from the drop down list, initialize sr to be 125000, set rice factor K to 0 for pure Rayleigh fading, set ebn0 to 30dB, and chose 1-path Rayleigh fading; add another similar

system for comparison in the same way; 4) press the "Start Simulating" button and results will be displayed and saved by default after simulation completion.

In order to make good comparisons between different configurations, various saved states of the simulation can be continued and reused at different parts along the transmission and reception processing. A similar implementation of the concept is presented in [72]. The authors in [72] have shown that in scenarios with multiple runs that shared a lot of similarities among them acheived a significant reduction in simulation time when a technique called updateable simulations is used. Rather than re-executing an entire simulation in scenarios where variations in the simulation model need to be taken into account, the technique reuses prior simulations run and updates them to accomodate these variations. In our proposed simulator, loading and saving of previously run or paused simulations from the GUI is beneficial because saved state information can be analysed, compared, or even modified for evaluation. The loading, saving and initialization process are controlled in part G of Figure 6.4.

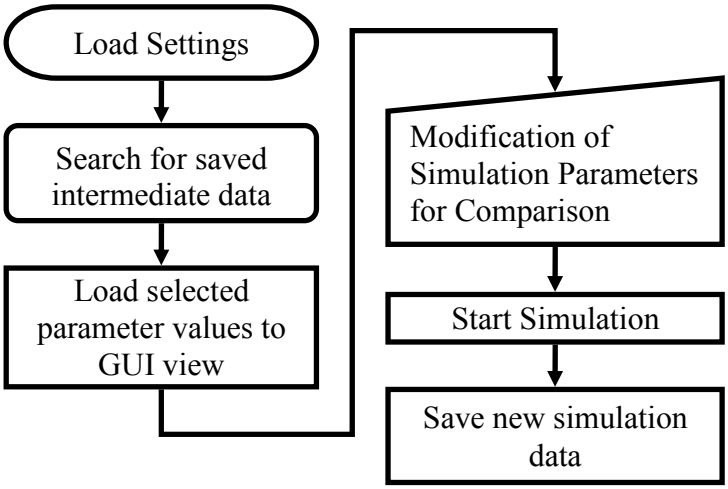

Figure 6.5 Example of GUI level state loading method.

Figure 6.5 shows a method of how the settings could be loaded for simulation. The figure demonstrates that after the load settings operation is initiated, the GUI level will search for saved intermediate data, and loads the selected parameter values that were used for the generation of those intermediate data. The user may wish to change these parameters for a more meaningful comparison. Using this method, any simulation created by the model can be continued from another simulation and/or can be branched off from the current or previously saved simulation for comparison. The saved intermediate data are saved in buffers and can be at such locations as the transmission input, transmission output, channel output and decoder input. From the saved data information, other simulation scenarios can be manually simulated in parallel using the GUI to load an intermediate data point, and then combined post simulation for comparison.

6.4 Simulation Design

This section presents the connection between high level object-oriented design and usability for a flexible OFDM communication simulator. Example flow charts, UML and sequence diagrams are presented with descriptions in order to assist in the understanding of the material.

In order to create reconfiguration, information must be exchanged to configure the components to interact with each other. It is important to understand some of the key parameters being used in the simulator in order to be able to control it appropriately, and so we present common parameters in Section 6.4.2 along with relationship models coinciding with the parameters in the GUI previously presented. The generic OFDM PHY parameters for the simulator including packet size, symbol size, modulation type, and code rate are updated from the configuration information to ensure interoperability of the components between each other. The configuration information for each object consists of user input from the GUI, and some automatically extrapolated information based on overall system parameters as well.

The tendency when creating an environment for testing OFDM PHY is to follow a pattern/standard, or to use pre-existing tools, such as [41], that limit the amount of flexibility of the simulator. This limits the creativity of the person using the simulator to rigid design constraints, when a more flexible environment is preferable. To build an effective object-oriented simulator for OFDM PHY, the components available for simulation must have their own information transfer such that each component of the OFDM system that is capable of changing must be able to convey the input/output constraints to the rest of the system. The configuration settings can be stored in a database or in a data structure. For example, in the case of a modulator at the transmitter, there must also exist an appropriate de-modulation technology at the receiver that will be performed, hence the demodulator will be chosen and set sharing information from the current modulation scheme.

6.4.1 Simulation Environment Overview

The simulation environment of the flexible simulator is designed to allow for many changes to be made to the system being simulated without having to change the code defining the simulator. Figure 6.6 illustrates the simulation environment, which shows the flow of information between GUI level specifications and the simulation level specifications and the implementation of the reconfigurable OFDM PHY. The GUI level contains the simulation parameters, such as varying E_b/N_0 (or ebn0 as seen if Figure 6.4, and is defined as the ratio of the energy per information bit to the noise spectral density), and the system parameters (such as symbol rate (sr)). Both the simulation and the system parameters come from the GUI platform. The simulation parameters define varying parameters in a simulation that the OFDM system is being tested on, while the system parameters are the fixed parameters that define the specific OFDM system that is being tested. For example, to test a transmitter/receiver through a channel with varying E_b/N_0, one would set a vector of simulation parameters with changing E_b/N_0 (ebn0). As can be seen from the figure, the simulation parameters and system parameters are passed to the simulation setup level, which in-turn passes these system parameters as variables for various components composing the simulation level requiring the

information. As the information for the various components update, each OFDM PHY component receives the respective updated parameters, and hence the system changes state.

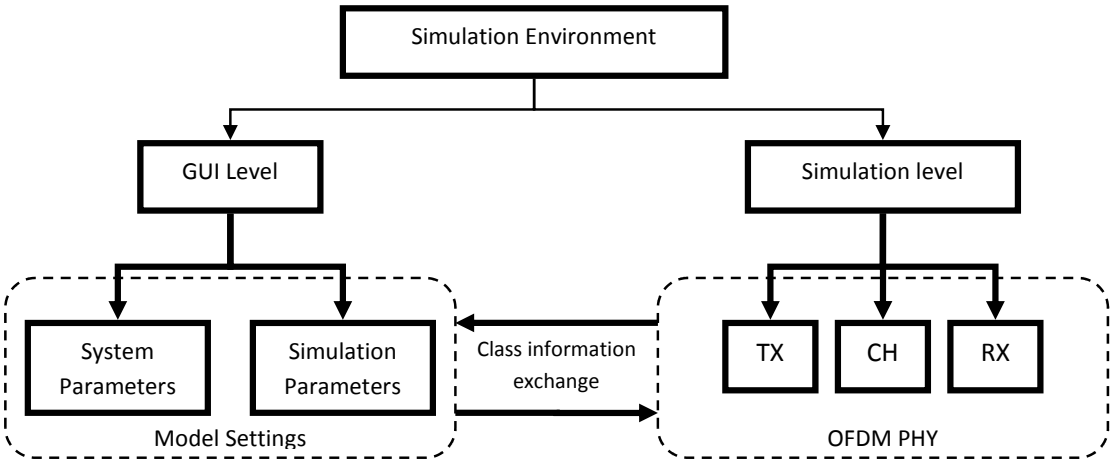

Figure 6.6 Simulation environment overview.

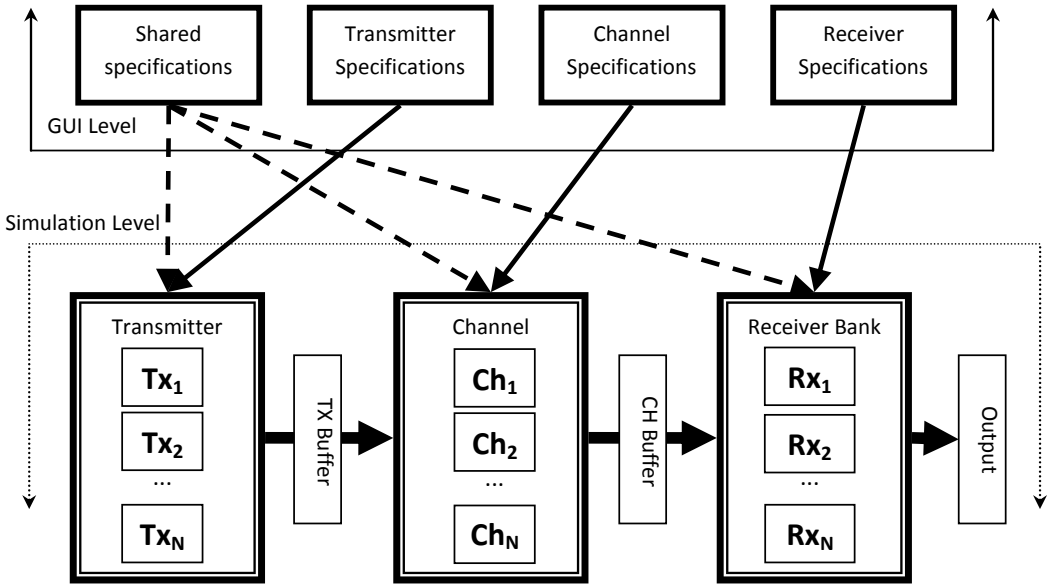

Figure 6.7 Illustration of information exchange between GUI and simulator levels.

From Figures 6.6 and 6.7, the simulation level contains a transmitter bank (Tx_1 to Tx_N), a channel bank (Ch_1 to Ch_N), and a receiver bank (Rx_1 to Rx_N). In addition, it contains components that buffer information such as transmitter buffer (*TX Buffer)* and channel buffer (*CH Buffer)*, which save simulated results of their respective stages for re-use later, as introduced previously. It should be noted that the simulation and system parameters at the GUI level affect component banks at the simulation level differently, i.e. some of

them should affect specific component banks, while others share or affect all or multiple, as seen in Figure 6.7. For example, 'para' is shared by all the banks, while 'ebn0' is only used in the channel bank. Therefore, different OFDM system models can be created with flexibility. This flexibility is accomplished because the simulation environment is defined entirely using object-oriented programming with class information exchanging between the GUI level and the simulation level.

6.4.2 Simulation Configuration Considerations

Simulation configuration represents all the parameters and the settings that affect the behaviour of the simulator. Simulation configuration is important to be considered for ensuring accuracy in the simulator. The flexible parameters, which are part of the simulation configuration, and consist of the simulation and system parameters, are completely defined in the GUI from earlier section. For an OFDM PHY system, the transmitter, channel and receiver must be compatible with the simulation configuration. Component configuration incompatibilities are eliminated by the sharing of configuration information between components. In addition, sharing simulation configuration information for compatible simulations becomes a viable option for facilitating fair comparisons. For example, the performance of the OFDM system is sensitive to variations in the channel [37], and hence each OFDM design has to go through the same channel for reliable comparison results.

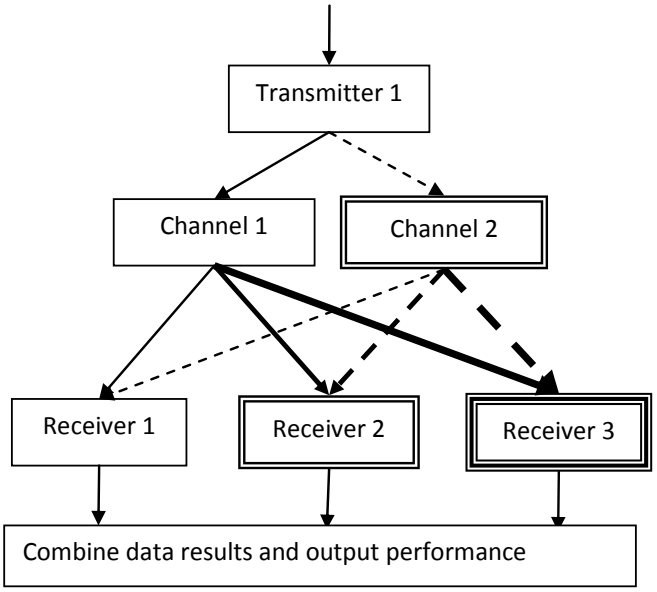

Figure 6.8 Tiered simulation with each path resulting in dataset for output.

Figure 6.8 shows a general tiered simulation scenario that uses sharing of simulation configuration and processed intermediate data sharing. It has two channels and three receiver combinations, with the data from each simulation run processed for comparison. Output data from transmitter 1 is run through both channels 1 and 2, and afterwards, the output data from channels 1 and 2 are processed individually by receivers 1, 2, and 3.

6.4.2.1 The High Level Design of the GUI and Simulation Layers

Figure 6.9 shows the sequence diagram showing the interaction between the GUI level or layer and the simulation level. The interaction occurs with the user starting the GUI; from there the GUI level polls the simulation level for what features are available in each module of the simulator. This information is defined by each class in the simulator so that the GUI level needs to poll a functionality method which returns a list of variables that can be modified for each mode of operation. The GUI level combines this information into a useful grouping of controls for the user to be able to modify as desired. The user starts the simulation after making desired changes to the simulation and system parameters which triggers the GUI level to store the modified parameters into the *Model_Settings* class (seen in Figure 6.10). The GUI layer passes the information to the simulation layer or level, which interprets the *Model_Settings* class information to reconfigure the OFDM PHY simulator (seen in Figure 6.11), potentially multiple times depending on what scenarios and systems the user has selected for testing. As a summary, the GUI is linked with the simulator (at the simulation level) to both receive and provide simulator system parameters. In addition, it is also used to initialize configuration classes, and hence serves as the blueprint for the objects used by the rest of the simulator.

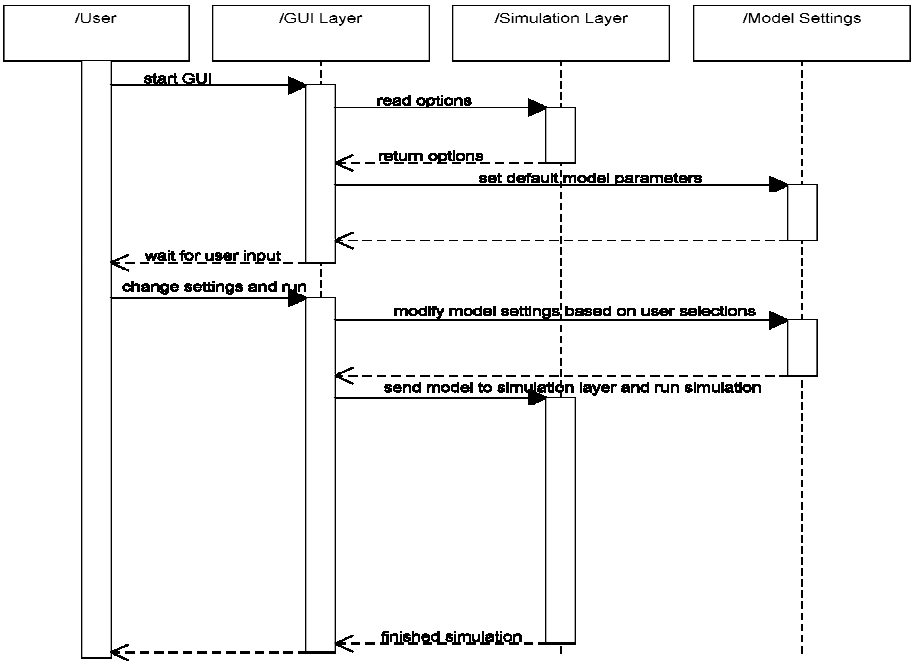

Figure 6.9 Sequence diagram showing information exchange between the GUI and simulation levels.

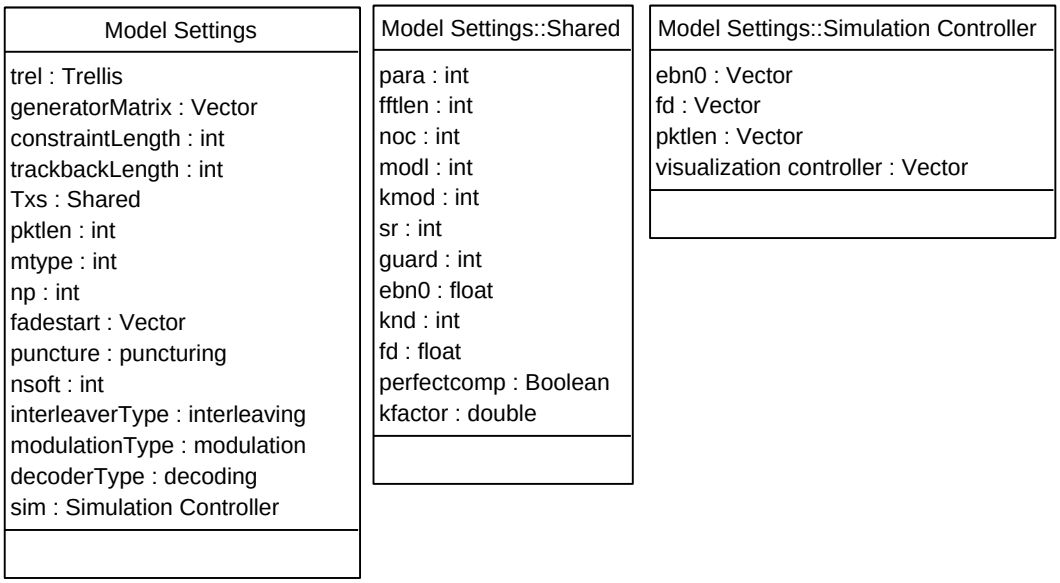

Figure 6.10 The GUI level main simulation model control classes (*Model_Settings*).

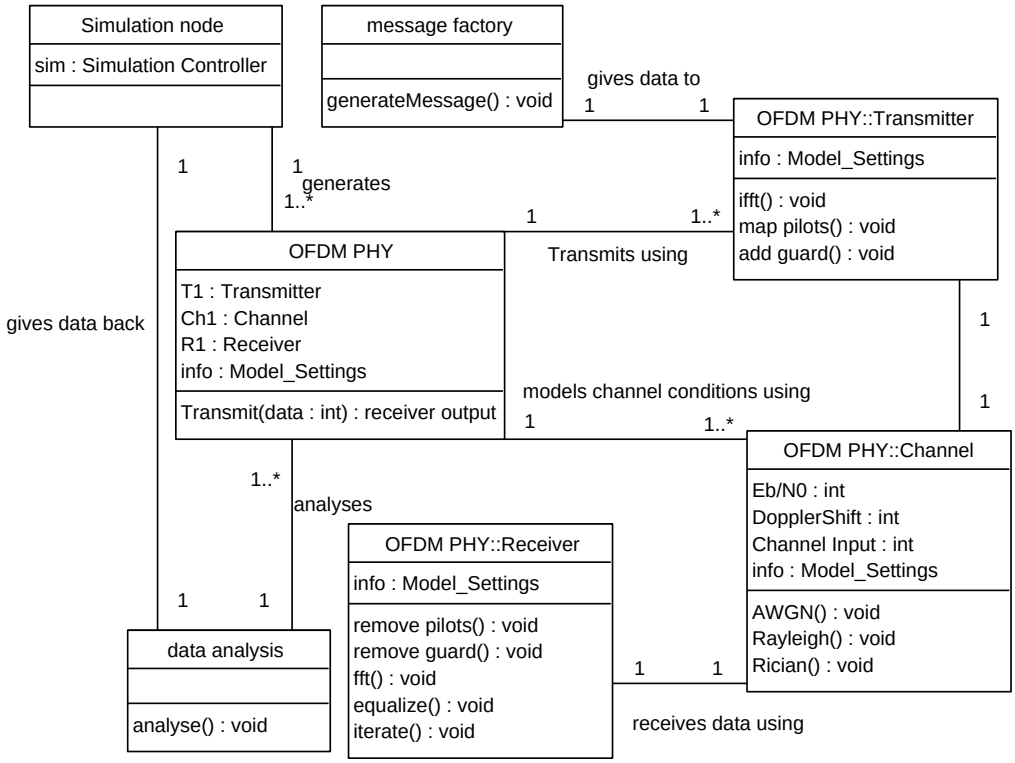

Figure 6.11 Overview of main classes for simulation level showing relationship between its classes.

An example usage scenario with associated UML class diagrams of the proposed OFDM PHY simulator will follow. A discussion of some of the main features and functions of the important configuration classes and how they relate to configuring the simulation will also be presented. The user will start the GUI. The GUI level or layer obtains the default features available in the simulator, and then

displays a visual representation of these features by showing the GUI platform dialog presented in Figure 6.4. The user then operates and modifies variables that define the simulation configuration of the system according to requirements. The user than runs the simulator, which in turn will pass the modified variables to a simulation node seen in Figure 6.11. The simulation node then initializes an OFDM PHY instance (where an instance is one class that has been constructed and stored in the simulation memory) based on the parameters stored in the *Model_Settings*, *Shared_Model_Settings* and *Simulation_Controller* classes shown in Figure 6.10, which were defined at the GUI level. Figure 6.11 shows the class diagram showing the high level relationships between the main classes for the simulator, also defined as the high level simulation level. From the figure, the lines between the classes represent the entity relationship between the classes, where '1' to '1..*' means one class instance to many. For example, an OFDM PHY system class can contain multiple transmitter modes for each system design. The individual scenarios inherit their configuration from the *Model_Settings* classes presented in Figure 6.10.

For simplicity, we show the configuration information inheritance as the variable "system info" in Figure 6.11, which defines the system and simulation parameters, and is an instance of class type *Model_Settings*. As mentioned earlier, *Model_Settings* is used to store important information that is used throughout the system to ensure continuity of parameters, and serves as a verification and control check because functions explicitly retrieve parameter values from this structure only. Incompatibilities between different OFDM PHY components can be avoided because each component is sharing its own copy of 'system info'. Also in Figure 6.10, the class *Model_Settings::Shared* stores information related to the reshaping of output data and sharing of that data between various components and ensures end-to-end compatibility of data, and *Model_Settings::Simulation_Controller* is used to control varying attributes of the simulation, which is used for comparisons between model instances after final output processing (for example, it is key in comparing a OFDM PHY design with itself at different E_b/N_0 (ebn0) or Doppler shift (f_D) levels). From previous section, the simulation parameters define varying parameters in a simulation; hence the *Model_Settings::Simulation_Controller* class contains these parameters. A description of the variables from the *Simulation_Settings* classes in Figure 6.10 is presented in Table 6-3 for reference. Most of these variables receive initialization from the GUI platform in Figure 6.4, and can also be found in Table 6-3.

The OFDM PHY class in our simulator, synonymous to the actual implementation, is composed of a transmitter class, a channel class, and a receiver class. The transmitter class in Figure 6.12 contains components such as the encoder, interleaver, and modulator, with each of these capable of being designed with significant variation. In order to perform flexibly and to perform the various tasks required by the OFDM PHY, the major classes such as the transmitter and the receiver must have internal classes of their own constructed to handle the operations and configurations, as shown in Figures 6.12 and 6.13 respectively. Each of these classes can be extended to behave in a different manner in order to react differently. For example, with the modulator, it can be extended to perform additional modulation schemes with compatible input/output, as well as symmetrical demodulation schemes at the demodulator. In order

to link objects together, even during reconfiguration, it is beneficial to use the same data addressing and dimensions of array elements being passed from one block to another. This can be done by using either dynamic object types or pointers. Exchange between components such as the signal compensator and decoder requires this for the option to have a flexible choice of demodulator designs because array indexing would lose consistency when using two-dimensional array or pointer indexing.

Table 6-3: Attributes used in the classes defining the parameters used by the GUI and simulation levels

Variables	Description
trel	Convolutional encoder trellis structure
generatorMatrix	Convolutional encoder generator matrix
constraintLength	Convolutional code constraint length
trackbackLength	Convolutional code trackback length
Txs	Instance of class type Shared, used for the shared variables between different OFDM designs
pktlen	Integer packet length for the system
mtype	Number of bits per constellation point, decided by the modulation type (modulationType)
np	Number of paths for the Rayleigh fade
fadestart	The initial point or the delay of the fade signal
puncture	Puncture level for the convolutional encoder
nsoft	Number of soft bits for defining the number of quantization level purposes
interleaverType	For choosing between Block or symbol interleaving type
modulationType	Modulation type = [BPSK, QPSK, 16QAM, 64QAM]
decoderType	Decoder type selection
sim	Instance of class type Simulation Controller, used for the simulation parameters
Para	Number of parallel data transmission lines
fftlen	FFT/IFFT length of one OFDM symbol, includes para, zero paddings and pilot subcarriers
noc	Number of carrier lines (para +pilot subcarriers)
modl	Shared modulation level information
kmod	Modulation normalization factor
sr	OFDM Symbol rate
Perfectcomp	Enable perfect compensation tracking
Kfactor	Rice factor, used in fading
Guard	Guard interval
ebn0	Signal to noise ratio
fd	Doppler frequency
pktlen	Vector or varying packet length
Visualization Controller	Used for saving and displaying result plots

The channel class contains channel related information and methods for creating various channel conditions, including a mixture between multipath, AWGN and LOS components along with interference modelling, introduced earlier in this chapter. With the receiver classes shown in Figure 6.13, channel estimation and equalization classes collectively correct for detected channel distortions. For a more detailed look at channel estimation and equalization, the reader may refer to [38, 73]. Additionally, the demodulator and decoder classes are able to transform data for interpretation. As mentioned earlier, each class can be extended to include alternate methods for performing their main operation according to preference of the designer and the implementation language. These alternate methods are added to the class, and can be accessed when creating a new implementation of an OFDM system for simulation. Hence, this facilitates comparison and collaboration between researchers who want to benchmark their designs in a common environment.

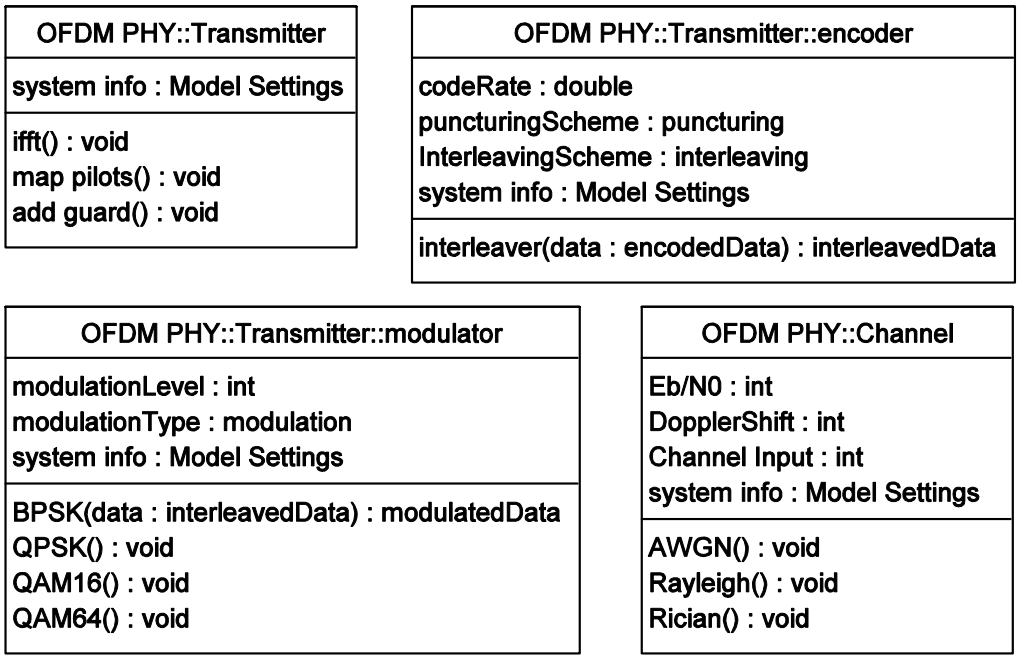

Figure 6.12 OFDM PHY and its transmitter and channel subclasses.

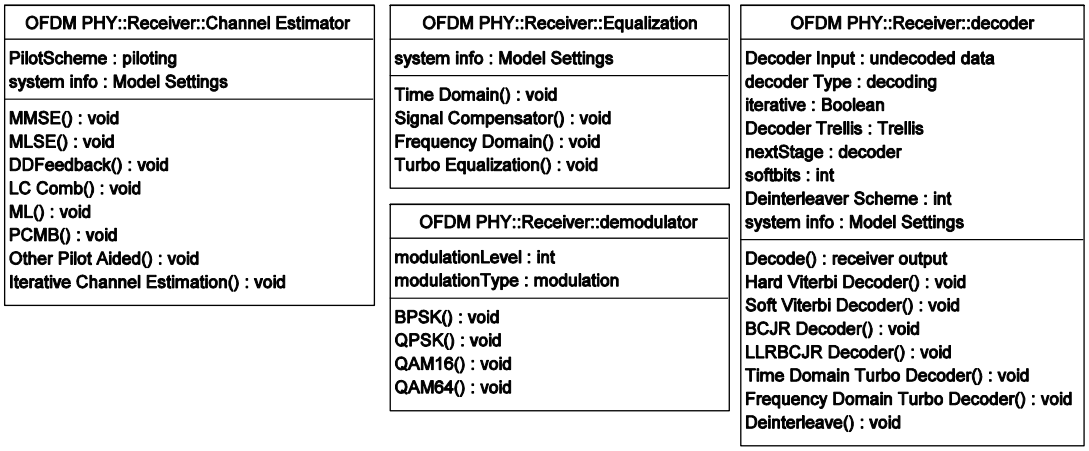

Figure 6.13 OFDM PHY and its receiver subclasses.

6.4.2.2 Iterative Case

The reduced granularity of feedback information is becoming increasingly important for turbo receivers, such as [74], and the amount of granularity required can be tested using our simulator, as shown in part A of Figure 6.4. The rest of this section contains some relevant information for creating simulations that include iterative processing in the receiver portion of the physical layer. It is assumed that the goal of the receiver is to reproduce the original transmission information in its original format, and hence the receiver should output in the same format as the transmitter's input for comparison.

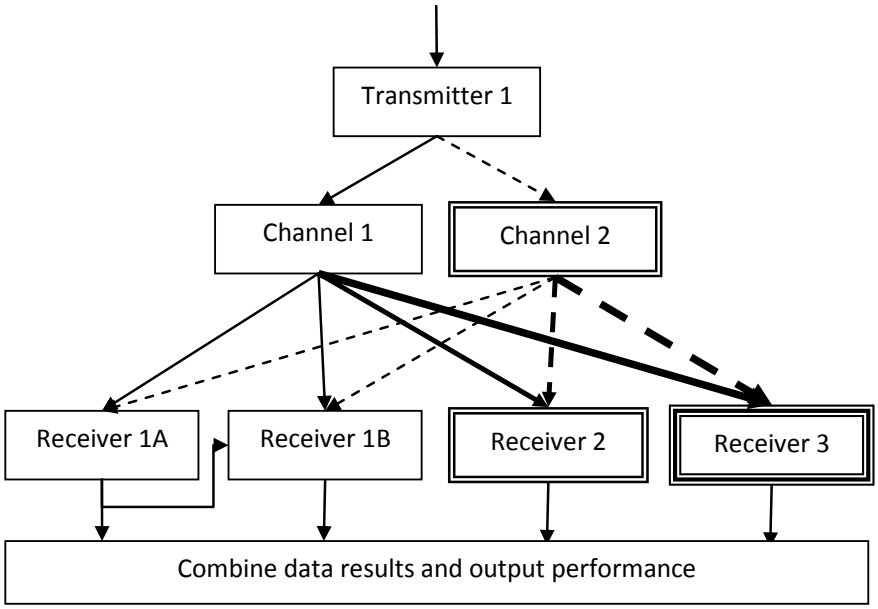

Figure 6.14 Modified tiered simulation to include iteration.

As seen in Figure 6.14, the simulation data feeds back when an iterative receiver is added for comparison against other receiver versions. To achieve this, the iterative receiver needs to have a feedback component and save the feedback information for the next iteration. *Receiver 1A* and *Receiver 1B* in Figure 6.14 denote the first iteration and the second iteration in an iterative receiver, respectively, while *Receiver 2* and *Receiver 3* are alternate receiver designs. The decoding portion of the transmitter can decode an entire packet or decode an OFDM symbol (symbol-by–symbol), and feedback information can be transferred to have the receiver behave as an adaptive receiver. When implementing this change in decoding OFDM Symbol size, one must be careful that the chosen decoder does not lose too much information during the decoding process, that is, for the case of the Viterbi decoder [75], a trackback length delay occurs between the encoded and decoded streams. One way that could be done to overcome this is to store trellis state transition information for recursive reuse for subsequent decoding runs. In order to simulate this type of shared information exchange, the receiver class would be iterated using a call to the iterate method (a recursive call), which treats the receiver class as if it is recursively being called, but instead of a full recursion where extra memory copies would be saved. Hence, the receiver alternatively updates current instance of the receiver class based on the previous values, and processes it as a standard receiver. Examples of OFDM PHY receivers that use iterative techniques in their receiver designs include [40, 64].

6.5 Distributed and Parallel Computing

As is evident in [76, 77], using processing components to define the simulation objects inherently creates a natural separation of memory space that can be duplicated for separate processing threads and hence

parallel processing and distributed computing techniques can be used [78]. The general architecture of a distributed computing environment is shown in Figure 6.15 with a mix between sequential and parallel processing and reuse of processing cores. This architecture allows for flexibility and information sharing because of the inter-communication between parallel and sequential processing units. For example, a copy of *Model_Settings* discussed earlier, can be stored in each thread's memory. This will allow each component in these processing threads running in parallel to access the required parameters to allow a fair comparison among variations of the OFDM PHY designs.

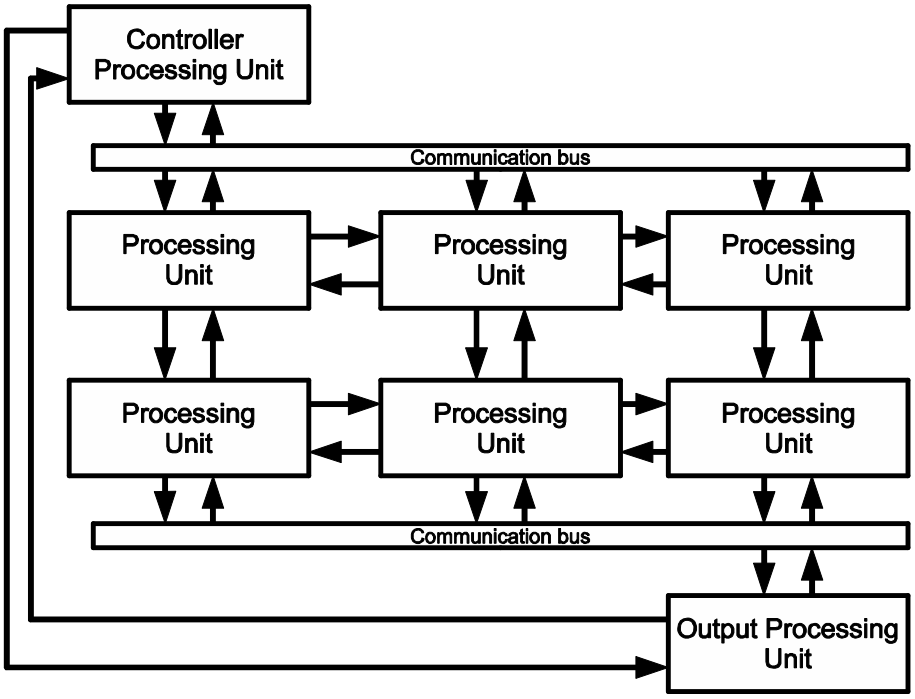

Figure 6.15 Processing units with inter-process communication showing the high level simulator layout.

High level design also lends itself well to usability and control of components because of how attributes can be set in the objects. That is why we have the controller processing unit, in Figure 6.15, taking input from a GUI and submits control instructions to lower processing units, including an output control processing unit for displaying information to the end user of the simulation. The output processing unit collects information from the other processing units and computes useful relationships from the output. The general form of Figure 6.15 can be applied to the application specific form in Figure 6.7 presented earlier. This allows for high throughput simulations for rapid testing of theoretical parameters, with the amount of processing time depending on factors such as packet processing time, iterations, number of processors available, and speed of processors used in the simulation, etc.

In the next section, we propose that for testing multiple physical layer designs, packet partitioning across different scenarios be used instead of the commonly used scenario processing, to maximize the utilization of available processing units.

6.5.1 Simulation Partitioning

A general approach to parallel and distributed computing concepts for object-oriented communication simulators was discussed in the previous section. This section will now highlight some benefits of simulation partitioning for the enhancement of such parallel processing. The simulation partitioning is a method of separating a simulation into smaller parts so as to run with lower memory requirements or for parallel processing. It can be applied to any object-oriented simulator that has parallel components. In order to make use of the multi-core processors that are abundant in computer labs, we suggest finding the right mixture between scenario and packet partitioning. When partitioning packets only, each thread uses different parts of the messages and can perform all scenarios. When partitioning by scenario only, each thread uses identical transmitted messages for different scenarios. Figure 6.16 shows 4 scenarios with equal messages with lines drawn representing packet partitioning (vertical dashed lines intersecting the packet array) and scenario partitioning (horizontal dashed lines).

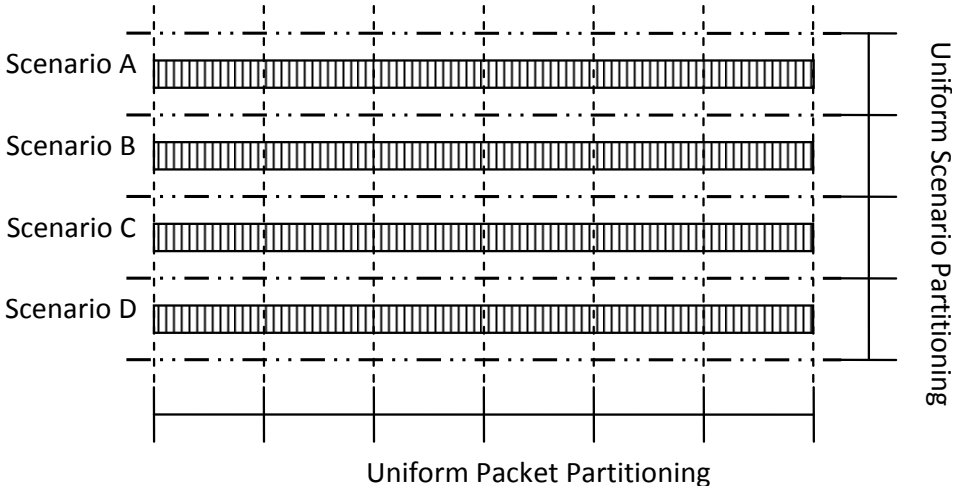

Figure 6.16 General and uniformly distributed packet and scenario partitioning for four OFDM PHY design simulations.

Uniform scenario partitioning can be processed without object-oriented simulators because each scenario can be programmed for the specific task. On the other hand, packet partitioning requires the reconfiguration of the simulator during runtime. This reconfiguration is suited for the object-oriented simulator because of the capability of updating the object attributes, which change the states of the simulator. Spreading out the processing load equally across all processing threads, while minimizing data exchanges between processing units, is an optimal partitioning. For example, using 3 processors to process 3 jobs of different difficulty will be optimum if each processor spends an equal amount of time on the processing. That is, the processor should simulate both packet and scenario partitioned data. If more processors become available during the main simulation, the load can be redistributed to include them.

Hence the job will finish faster because each module is capable of acting as an independent reconfigurable simulation.

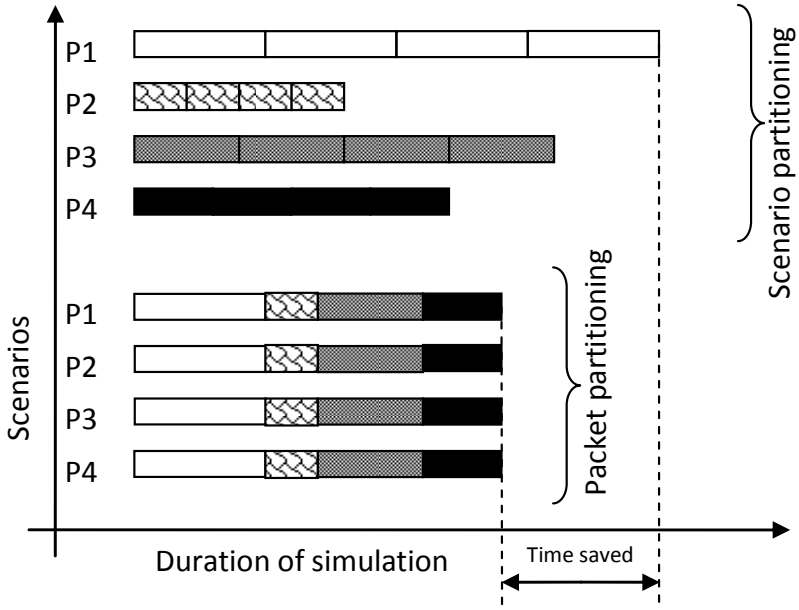

Figure 6.17 Timing diagram showing both packet and scenario partitioning methods used for parallel processing.

The simulation of an OFDM system can be broken down into parts that can be run in parallel, i.e. packet groups can be run through a separate simulator, as seen in Figure 6.17. The general example of Figure 6.17, illustrates 4 processors and 4 different OFDM PHY designs. For the scenario partitioning example, each of these OFDM PHY designs run on separate processors. In the case of the packet partitioning example, each OFDM PHY design will have its packet numbers separated into smaller groups and each of these packet groups will run in separate processors (shown as different shaded blocks). The same procedure applies to each OFDM PHY design. Processing elements of the simulator are represented by P1 through P4, and can be on the same machine or separate machines. For a limited amount of parallel processors, a combination of both parallel and sequential simulation can be joined at the end of a simulation. Besides the packet separation, additionally, the transmitter, channel, and receiver can each be simulated in a hierarchy manner, as in Figure 6.15 presented in an earlier section.

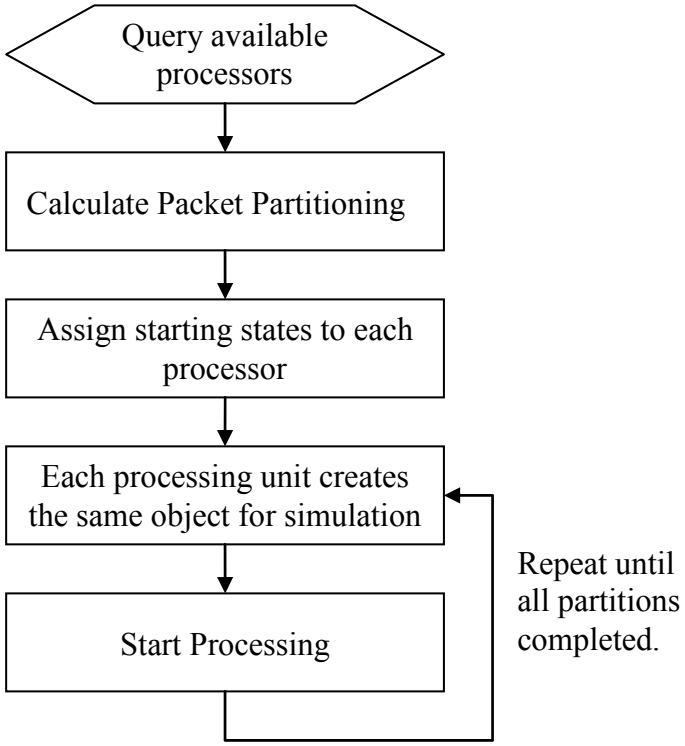

Figure 6.18 Flow chart showing steps for scheduling the objects in the simulation.

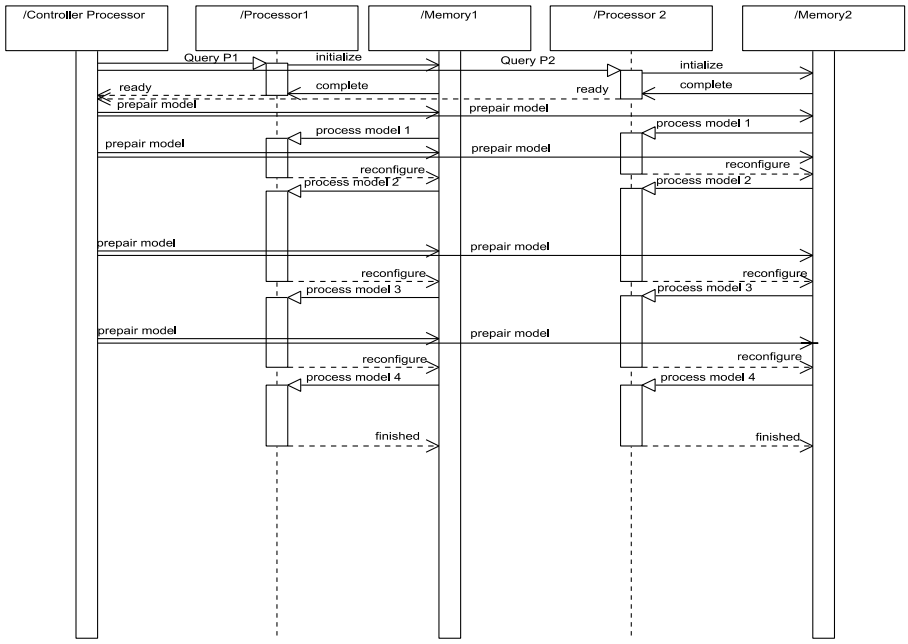

Figure 6.19 Sequence diagram showing an example packet partitioning setup with four scenarios being processed by 2 main processing units and a controller unit.

In order to calculate the scheduling packet partitioning for the object-oriented simulator, several steps must be taken in order for the simulation to be partitioned according to available resources. These steps are outlined by the flow chart in Figure 6.18, which includes a processor availability query for estimating resources. The packet partitioning step allocates the amount of packets to be run on each processing unit for each scenario, and steps for assigning the starting and ending states for each identical object in each partition in order to simulate straight time of the conditions of the OFDM PHY. Rudimentary steps such as these may be calculated by the controller unit (see Figure 6.15) rather than the individual processing units to reduce overhead on those units. Packet partitioning is setup before output, but must be recombined again and processed by the output processing unit. The processing units each repeat the process for each OFDM PHY scenario until all scenarios have been simulated.

The processing units do not have to wait because a controller unit would be processing the design concurrently, as more clearly shown in the example sequence diagram in Figure 6.19. The reconfiguration overhead of the controller unit depends on the number of designs and not the number of processors used. Hence, for a low number of receiver designs being tested at once, which is usually the case, the reconfiguration overhead time is negligible. The flow of the sequence diagram of Figure 6.19 outlines an example for 4 different packet groupings and 3 processors, a controller processor and 2 main processors interacting to produce 2 simulations using packet partitioning. The sequence is as follows: first the controller processor checks to see the processor's availability; the processors units respond with load availability information; from there the controller processor creates a schedule for the simulation task and initializes copies of the *Model_Settings* in the simulator layer of each simulation scenario; the controller processor assists with making sure the other processor units have the next model available in memory so that they can alternate jobs so that the load is evenly distributed. After the simulations have finished, the data can be combined and output results can be analysed using the output processing unit as normal.

Referring back to Figure 6.17, the relative speed increase of this processing arrangement can represent a considerable improvement over a scenario partitioning. The greatest benefit being obtained is due to information exchange between simulator elements. The difference in simulation time between dissimilar OFDM PHY models is due to the differences in design of the elements being simulated. The difference in time between packet partitioning and scenario partitioning is the $Time_{saved}$ defined as the difference between the longest scenario simulation time and the packet partition simulation time. The average or mean of all the scenario partition simulation time happens to be approximately equal to the packet partition simulation time, as can be observed from Figure 6.17. Similarly, it can be expressed as,

$$Time_{saved} \cong \max(t_i) - \mu_s, \tag{6-1}$$

where t_i is the time taken for the i^{th} OFDM PHY model design, and μ_s is the average of all scenario partition simulation times. The resulting time to complete each scenario for all system designs using packet partitioning can be estimated by the following equation:

$$T_S \cong \sum_{i=1}^{\text{Count(Designs)}} \frac{t_{Si} P_{Total}}{n}, \tag{6-2}$$

where T_S is the total time to complete scenario S for all designs i assuming packet partitioning, t_{Si} is the time for 1 packet in scenario S for design i, n is the number of processors available, and P_{Total} is the total number of packets for the scenario.

We choose Figure 6.2 as a case study, which shows simulation results from 8 different OFDM PHY system design scenarios with 1600 simulated packets for each design for varying Doppler shifts (f_D). The purpose of this plot would usually be used by researchers to compare the PER performance of 8 different OFDM PHY designs exposed to time-varying channels with varying f_D. Eight 2.0 GHz processors were used for generating the simulation. We define a 'pass' to mean a scenario or each OFDM PHY system design. The partitioning of the simulation is as follows: pass A of the simulation is the simulation corresponding to hard Viterbi binary phase shift keying (BPSK), and for optimum timing would like equal partitions, and for the scenario with $f_D = 150Hz$ with 1600 packets, the simulation is broken into 8 elements, in this case 200 packets per processor. Doing the same for each pass similarly will then yield the 48 data points for the full plot comparison. We define one data point to mean one f_D instance for a particular OFDM PHY simulated system design. Hence, Figure 6.2 shows a total of 48 data points for all 8 scenarios and 6 f_D variations. Figure 6.20 shows the timing of 8 data points; one for each OFDM simulated system design at a particular f_D scenario. Figure 6.20, and for the case of the scenario partitioning scheme, shows that each OFDM design uses up a whole processor, while in the case of the packet partitioning scheme all 8 processors work in parallel to simulate each OFMD system design. In Figure 6.20, the speed of the simulation for the case study clearly shows an improvement by using packet partitioning in simulation over scenario partitioning. This simple example emphasises elimination of delay incurred in scenario processing time, while optimizing processing resource usage.

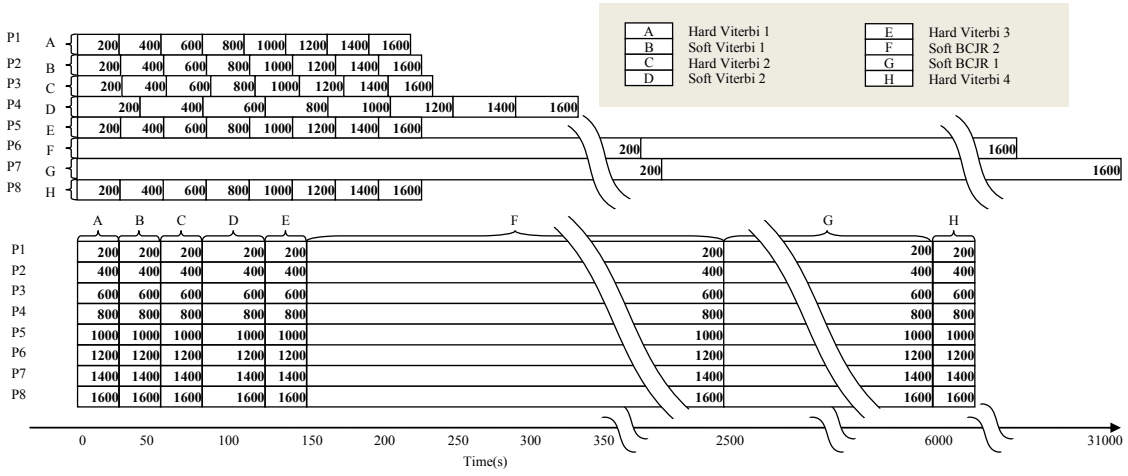

Figure 6.20 Timing diagram for the example case study showing disproportionate simulation time favouring packet partitioning.

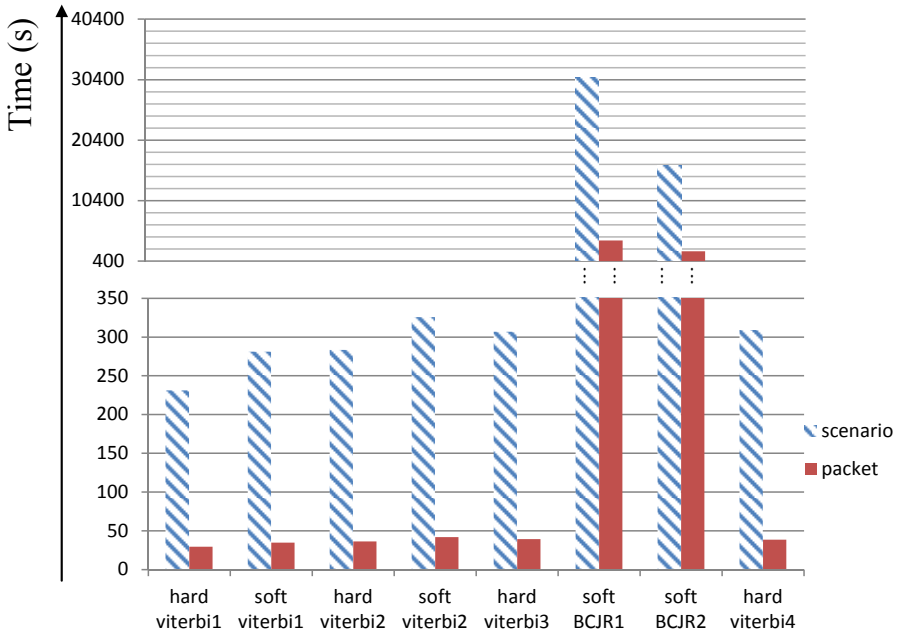

Figure 6.21 Bar plot showing the relative time for simulating different scenarios for the case study with both scenario and packet partitioning (top half scaled differently from bottom to fit).

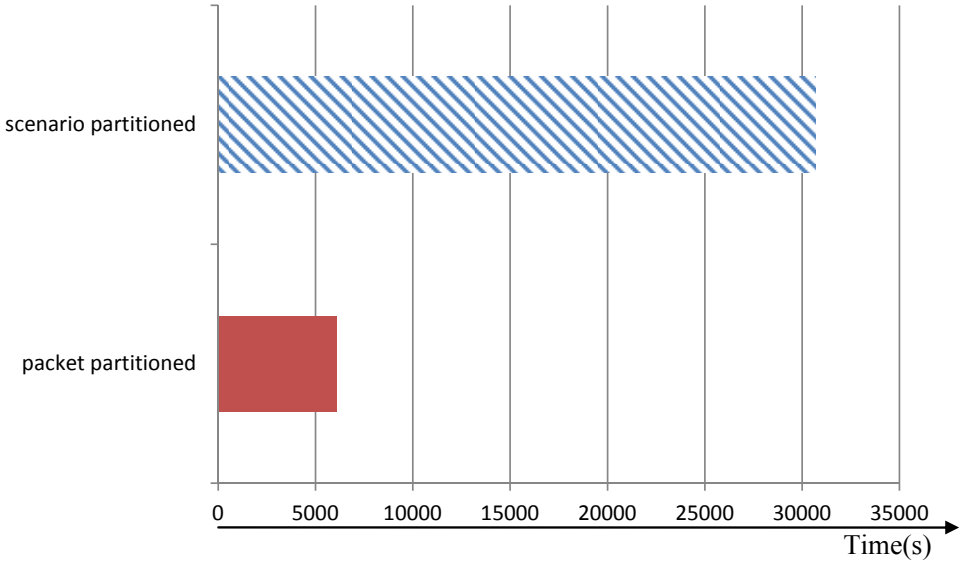

Figure 6.22 Bar plot showing the overall time duration for simulating both scenario and packet partitioning.

Figure 6.21 is the plot of the simulation time for each OFDM PHY simulation scenario for this case study. Notice the difference in time delay for the Bahl Cocke Jelinek Raviv (BCJR) algorithm [46] vs. Viterbi [75]. This difference is also shown in Figure 6.20, as passes F and G for the designs with BCJR algorithms. This is a case of the cost saving as the simulator in this case is using an un-optimized BCJR

algorithm to show the long-time delay that can occur when dealing with new algorithms for OFDM PHY improvement. The timing of each scenario is different because each design has different channels, modulation levels, and decoding, hence perform differently. The final result for the case study gives a final improvement in simulation time of over 5 times faster in favour of the packet partitioning scheme compared to that of the scenario partitioning scheme due to improved utilization of the processing units.

Figure 6.22 graphically shows the time saved using packet partitioning vs. scenario partitioning for the case study from Figure 6.2, which is the $Time\_saved$ and is approximately 30687 - 6075 = 24612 s. When this method is extended to the other 40 of the remaining 48 data points in Figure 6.2, the cost savings is significant. Since this can be extended to even more processors the time saving improves even more.

One particularly useful thing about packet partitioning of the information is that the simulator does not have to know the relative speed of each simulation as it is a simple split of work across all available processors. If each simulation scenario takes the same amount of simulation time, then the same utilization is obtained for packet partitioning, but as long as the number of processors exceeds the number of scenarios being processed, substantial improvement can be obtained through packet partitioning.

6.6 Distinctiveness of Proposed Design

Let us now reflect back on dissertations [36], [67], [68] and [69] introduced earlier for discussion and to emphasize the distinctiveness of our Object Oriented OFDM PHY simulator design. Simulink OFDM simulators have the advantage that the model can be placed entirely using graphical structure blocks that are visually appealing and look like flow charts/block diagrams. While this approach is appealing, many blocks/features of the Simulink platform are proprietary and the user cannot access the source code of the block, which can prevent researchers from implementing their ideas freely. The authors in [67] show improved TCP/UDP throughput performance using NS2 and Qualnet. Network Simulator 2 (NS2) event driven simulator is more commonly used in research projects that involve higher network layers besides the PHY layer due to its inaccurate PHY and channel modeling. However, some modeled PHY flexibility and improved accuracy is made available in [79], [80], and a further improved modelling of 802.11 OFDM PHY through a complete redesign in [81]. Modifications of this sort for the most part are platform specific and do not encourage code modularity, interoperability, and reusability.

Dissertations [68] and [69] show improved simulation runtime performance over pure software simulation using FPGA assisted OFDM simulation programmed using HDL. In general, HDLs used for designing hardware for FPGAs can be adapted from class-based high level design, and also can be adapted to use our OFDM PHY simulation architecture described in our study. Simulators with hardware acceleration can be the most difficult to make reconfigurable if they do not have a sufficiently high level object-oriented code base for which they were designed.

Matlab can implement mathematical models of the OFDM PHY, and can also perform analytical/statistical models for performance comparisons. Matlab is rich in built-in libraries and toolboxes useful for analytical modeling. Basic function-based and inflexible Matlab models for OFDM PHY

simulation design are presented in [41], and allow a novice researcher to investigate a specific OFDM communication scenario. Modern and future mobile/cellular communication environments are complex, inevitably requiring ever growing complexities within OFDM PHY communication systems for optimization and mitigation of diverse channel effects. Hence, we opted to expand upon basic models from [41] for our object-oriented OFDM PHY simulator design to allow for greater flexibility in usage and application.

These works are different from our work in that we concentrate on improving flexibility, simulation time and reconfigurability of the OFDM PHY simulator platform, and making the physical parameters of OFDM easier to set up via GUI interface and high level design. This allows the researcher to understand and implement OFDM systems faster, and facilitates focus on design optimization and creativity. Hence, our work is unique in that our study focuses on three important aspects of designing simulators for creating object-oriented simulation environments for communication systems namely, usability, high-level design, and parallelism. This type of structure is very helpful for independent long-term research in this topic. It is also helpful that the simulator can be used by a research team collaboratively, including shared usage in a simulation laboratory. Additionally, novice researchers can easily use and learn OFDM systems behaviour using our implemented simulator.

Chapter 7

Conclusions

In this dissertation, we proposed a quantitative model to evaluate the problem of hidden terminals in DSRC systems using repetition-based protocols. Repetition-based protocols provide highly reliable probability of success when no hidden terminals are taken into account. However, at high loads and regardless of common vehicle densities, our model performance study has shown a very detrimental outcome due to hidden terminals. On the other hand, the reliability requirements were met at lower loads, but only at relatively low vehicle density and at the expense of increased repetitions. The delay requirements were met in all cases, however, as repetitions increase, unbounded delay results at highest load and vehicle density. Our model can serve as a benchmark for comparing QoS requirements in DSRC safety applications, and for fast evaluation to further improve the system. Future work includes extending current repetition-based DSRC safety MAC protocols to have hidden terminals robustness for better QoS in their design.

Passive Cooperative Collision Warning (PCCW) is passive because it does not introduce additional message packets into the channel like other schemes such as CSMA/CA. The proposed protocol introduces a modification to the 802.11p DSRC MAC protocol for processing received packet headers, and improving reliability of small packet safety messages. The investigation in this dissertation illustrated the performance of our PCCW protocol design through a breakdown of protocol design methodology including comparisons with existing repetition protocols including. In order for the vehicles to cooperatively warn each other of potential collisions, a small header payload is introduced for communicating node intentions. Because of this intention communications, storage of past transmissions by each node, and processing by the PCCW protocol, the nodes collectively act as a distributed memory for use in producing optimized probabilities of transmissions for potential colliding transmissions. Extending PCCW by controlling the physical data rate determined by mutually warned slot. This temporary data rate change is coordinated by PCCW to offer additional probability of successes through creating subslots for which packets can be transmitted into. This is essentially a form of Time Division Multiple Access (TDMA) at very small scale.

In order to communicate the PCCW protocol's functionality, UML diagrams are used to represent the per node processing behaviour. State-machine with conditional slots is presented for the purpose of allowing for easy implementation behaviour of PCCW in hardware or software state-machine. In order to gauge performance of our PCCW protocol, an analytical model is provided that can be used in conjunction with other analytical models, and can be adapted to include various different models for comparison. This

can be beneficial in finding intuitive benefit of using PCCW under particular loading scenarios with varying requirements on reliability and delay. Comparison of probability of success and average delay are the main comparisons because these important metrics in QoS for future safety applications. Model parameters used during simulation are ones in agreement with conditions that theoretically would be present post DSRC safety system deployment. Results show gains up to 40% at optimum repetitions, and 80% improvement at higher repetitions for the repetition protocols tested, with average delay ranging from a slight increase for PCCW, to a much improved average delay performance over non-PCCW repetition protocols. We provided multiple views of our protocol performance against the other leading repetition protocols.

Although DSRC in its current state can only support 3 times data rate increase, that is, we can increase up to 9Mbps data rate to a 27 Mbps, we show simulated results for even higher results to show future potential gains. It is interesting to note that while EPCCW increases throughput by increasing, for example a 9Mbps data rate scheme to a 27Mbps, it also significantly increases the probability of a successful transmission.

Combining existing repetition protocols into our PCCW design allowed for adaptations of PCCW with varying levels of improvement. An important part of this dissertation is the development methodology that we used for comparing analytical performance of the PCCW protocol with existing protocols. This is mainly because the PCCW protocol introduces improved success and delay performance related to past transmission warning success probabilities. Resultantly, our full probability analysis presented takes into account causal effects of warnings produced by PCCW. Additionally, the analytical validation through simulation was discussed and has shown to be an effective indicator of performance when incorporating other analytical models for comparison. Through simulation comparison it is shown that the recursive probability calculations presented is effective at giving correctly correlated PCCW analytical results. Detailed simulation development was presented including accurate PHY correspondence with the mobility model, leading to a simulation design that effectively takes into account PHY and mobility model effects that exist to influence the MAC protocol performances. Each MAC broadcast is transmitted to many vehicles, with each vehicle having a different relative velocity to each other, which is dealt with in our simulator through the integration between the mobility model and the PHY and MAC simulation. The methods for which we achieved an effective model of vehicular transmissions as controlled through PCCW with accurate PHY and mobility models was presented using deployment, activity, and sequence diagrams, showing simulation coordination and how/when information was exchanged between the models. Full simulation modelling was presented so that our simulation methods can be effectively communicated, duplicated, critiqued, and adapted easily.

We also introduced ePCCW for the purpose of improving safety emergency vehicles (EVs) messaging reliability. The ePCCW protocol is a modification of PCCW that gives selective priority to EVs during the conditional transmission stage. The protocol is passive and not greedy because it only broadcasts warning messages in the headers of pre-determined repetition slots, and only if the node has attempted a past

warning informing of that repetition. Because ePCCW operates as a layer above the repetition selection process, it can be added to existing repetition protocols. Both analytic and performance results show scenarios that can be used for benchmarking and quality of service (QoS) considerations for reliability and delay for both MAC and PHY protocols. Performance improvements of 46% relative to the PCCW are observed. This improvement is observed under high load, representing high probability of transmission and vehicular density near jammed. This is important because a jammed scenario is one that would be hardest for EVs to coordinate efficient travel through an area. Additionally up to 77% improvement for ePCCW is recognized for this same scenario versus SFR. Interestingly, although the packet size is slightly increased, due to the header containing warnings of upcoming repetitions, the increased reliability decreases the average delay of first successful packet reception. Using SUMO and an OFDM PHY simulator combined with the ePCCW MAC layer allowed us to show realistic performance, that is still comparable to analytic models.

We have compared our previously proposed linear demapping scheme for the DSRC PHY system to that of a non-linear demapping scheme using different decoders. Both linear and non-linear demappers have equivalent complexities when implemented using look up tables ($\log_2 M$ look-ups for M-ary modulation). Simulation results show that the derived linear demapper improved the BER performance when compared to both the conventional and the non-linear demapper designs in all scenarios (with varying velocity, packet length, and at higher data rates). Substantial performance improvements were noted for higher constellation modulations and at higher code rates, where the conventional DSRC PHY system is found to be infeasible. It is important to note that many different types of OFDM systems may employ such a demapping scheme. The simulation results can also serve as a benchmark for future DSRC modulation schemes or for improving the performance of the DSRC receiver under development.

MAP-based frequency-domain equalization for a 5.9 GHz DSRC receiver has been previously proposed to improve both the BER and PER performance of the receiver. The designed frequency-domain equalizer has been compared with both channel tracking and signal compensator based conventional designs by simulation under Rayleigh fading channels. Simulation results have shown that the receiver with the frequency-domain equalizer improved both BER and PER performances considerably in both BPSK and QPSK modulation schemes, and at both high and low relative vehicular speeds. Hence the DSRC conventional and the DSRC channel tracking schemes considered in this study are relatively inferior in performance to a receiver design that takes ICI into consideration for Rayleigh fading channels

Finally, a new reconfigurable simulator approach for use with the application OFDM PHY for communication systems was covered. Advances in reconfigurable hardware could drive PHY adaptability further, but these optimum situations need to be studied in a highly dynamic way yielding the need for simulators. It can be challenging to model OFDM PHY for changing environments such as urban mobile wireless environments. Creating optimum designs in these environments requires reconfigurable simulation to model performance.

GUI interface can serve as a tool for a student or advanced professionals alike as a means for investigating particular OFDM PHY designs. We showed the information exchange between GUI and simulation levels, including the loading state information from GUI, which is important for fair comparisons between the various OFDM PHY design scenarios. High level design diagrams were presented including UML diagrams to visually specify the structure for the flexible simulator architecture for OFDM PHY. Finally, a particular parallel processing partitioning technique of packet partitioning was proposed. Additionally, a technique for using packet partitioning in reconfigurable object-oriented OFDM simulators for increased parallel performance was introduced. It was shown that packet partitioning is beneficial for simulations that are testing multiple scenarios simultaneously, while minimizing inter-processor communication because the packet processing is separated into isolated blocks of packets. In addition, the packet partitioning technique was shown that it is most useful for providing non-preferential processing of reconfigurable OFDM PHY simulations. These benefits were shown through a provided case study and considerable simulation time improvement was achieved.

As for future works cross layer design is one way to approach reducing the effects of packet collisions. The cross layer design is more feasible using the PCCW protocol presented in this dissertation, because the MAC information that is inherently introduced in the system due to PCCW can also be used at the PHY layer for collisions correction purposes.

Although, this novel research work serves as an assistance/enhancement to research on emerging reconfigurable OFDM systems, it can also be applied to other communication systems that require relative performance studies. The descriptive UML diagrams convey functional information regarding the simulation process of OFDM PHY systems that is platform independent. In addition, even though our implementation of this design was created using the Matlab platform, it is important to note that the concepts involved in our generic OFDM simulator can be applied using other high-level platforms and programming languages such as C++, Java, IT++, NS2, or Scilab.

References

[1] D. Jiang, and L. Delgrossi, "IEEE 802.11p: Towards an International Standard for Wireless Access in Vehicular Environments," IEEE Vehicular Technology Conference, Singapore, pp. 2036-40, May 2008.

[2] N. Jaber, K.E. Tepe, and E. Abdel-Raheem, "Performance enhancement of the DSRC system using frequency-domain equalization for 5.9 GHz DSRC applications," AEU – International Journal of Electronics and Communications, pp. 1434-8411, April 2011.

[3] L. Zhang, C. Zhao, J. Wu, W. Wang, "WLCp1-12: MAP based Equalizer for OFDM Systems in Time-Varying Multipath Channels," in Proceedings of IEEE Global Telecommunications Conference (GLOBECOM), pp.1-5, 2006.

[4] W. Cassidy, N. Jaber, S. Ruppert, J. Toimoor, K. Tepe, E. Abdel-Raheem "Interference Modelling and SNR Threshold Study for Use in Vehicular Safety Messaging Simulation," submitted to *25th Queen's University Biennial Symposium on Communications (QBSC)*, 2012.

[5] Q. Xu, T. Mak, and J. Ko, R. Sengupta, "Medium Access Control Protocol Design for Vehicle–Vehicle Safety Messages," IEEE Transactions on Vehicular Technology, vol. 56, issue 2, pp.499-518, March 2007.

[6] F. Farnoud, S. Valaee, "Reliable Broadcast of Safety Messages in Vehicular Ad Hoc Networks," IEEE INFOCOM 2009, pp. 226-234, April 2009.

[7] IEEE Standard for Information technology--Telecommunications and information exchange between systems--Local and metropolitan area networks--Specific requirements Part 11: Wireless LAN Medium Access Control (MAC) and Physical Layer (PHY) Specifications Amendment 6: Wireless Access in Vehicular Environments, IEEE Standard 802.11p-2010, July 2010.

[8] © [2011] IEEE. Reprinted, with permission, from [N. Jaber, K.A. Rahman, E. Abdel-Raheem, and K.E. Tepe,, A quantitative analysis of improved DSRC system using repetition based broadcast safety messaging with hidden terminal, 7th International Conference on Communications and Mobile Computing Conference (IWCMC), pp.1772-1777, 2011]

[9] J. Zhu, and S. Roy, "MAC for Dedicated Short Range Communications in Intelligent Transport System," IEEE Communications Magazine, vol.41, issue 12, pp. 60- 67, 2003.

[10] R. Mangharam, A. Rowe, R. Rajkumar, "FireFly: a cross-layer platform for real-time embedded wireless networks," Springer Journal on Real-Time Systems, vol. 37, issue 3, pp. 183-231, 2007.

[11] N. Jaber, K.E. Tepe, E. Abdel-Raheem, "Reconfigurable simulator using graphical user interface (GUI) and object-oriented design for OFDM systems," Simulation Modelling Practice and Theory (SIMPAT), vol.19, issue 5, 2011.

[12] The CAMP Vehicle Safety Communications Consortium, "Vehicle Safety Communications Project, Task 3 Final Report, Identify Intelligent Vehicle Safety Applications Enabled by DSRC," NHTSA U.S. Department of

Transportation, DOT HS 809 859, 2005.

[13] M. Sun, L Huang, A. Arora, T Lai, "Reliable MAC layer multicast in IEEE 802.11 wireless networks," in Proceedings of International Conference Parallel Processing, pp. 527- 536, August 2002.

[14] X. Ma, X. Chen, and H. Refai, "Performance and reliability of DSRC vehicular safety communication: a formal analysis," EURASIP Journal on Wireless Communications and Networking, 2009.

[15] X. Chen, H. Refair, X. Ma, "A Quantitative approach to evaluate DSRC highway inter-vehicle safety communication," in Proceedings of IEEE Global Telecommunications Conference (GLOBECOM), pp. 151-155, Nov. 2007.

[16] Q. Xu, T. Mak, J. Ko. R. Sengupt, "Layer-2 protocol design for vehicle safety communications in dedicated short range communications spectrum," in Proceedings of the 7th Int. IEEE Conf. on Intelligent Transportation Systems, pp. 1092- 1097, October 2004.

[17] Q. Xu, T. Mak, J. Ko, R. Sengupta. "Vehicle-to-vehicle safety messaging in DSRC," in Proceedings of the 1st ACM international workshop on Vehicular ad hoc networks (VANET '04), 2004.

[18] C. Foh, G. Liu, B. Lee, B. Seet, K. Wong, C. Fu, "Network connectivity of one-dimensional MANETs with random waypoint movement," IEEE Communications Letters, vol.9, issue 1, pp. 31- 33, Jan. 2005.

[19] Q. Xu, K. Hedrick, R. Sengupta, J. VanderWerf, "Effects of vehicle-vehicle/roadside-vehicle communication on adaptive cruise controlled highway systems," in Proceedings of IEEE 56th Vehicular Technology Conference VTC 2002-Fall, vol. 2, pp. 1249-1253, 2002.

[20] X. Lin, N.B. Shroff, R. Srikant, "A tutorial on cross-layer optimization in wireless networks," IEEE Journal on Selected Areas in Communications, vol.24, issue 8, pp.1452-1463, Aug. 2006.

[21] M. Green, "How Long Does It Take to Stop? Methodological Analysis of Driver Perception- Brake Times," Transportation Human Factors, vol. 2, issue 3, pp. 195–216, 2000.

[22] F. Tosato1, and P. Bisaglia, "Simplified Soft-Output Demapper for Binary Interleaved COFDM with Application to HIPERLAN/2," Imaging Systems Laboratory, 2001.

[23] 802.11e-2005 IEEE Standard for Information Technology - Telecommunications and Information Exchange Between Systems - Local and Metropolitan Area Networks - Specific Requirements Part 11: Wireless LAN Medium Access Control (MAC) and Physical Layer (PHY) Specifications Amendment 8: Medium Access Control (MAC) Quality of Service Enhancements.

[24] J. Yin, et. al. "Performance evaluation of safety applications over DSRC vehicular ad hoc networks," in Proceedings of the 1st ACM international workshop on Vehicular ad hoc networks ACM, 2004.

[25] W. Lewandowski, G. Petit, C. Thomas, "Precision and Accuracy of GPS Time Transfer," IEEE Transactions on Instrumentation and Measurement, vol. 42, issue 2, April 1993.

[26] G. Holland, N. Vaidya, P. Bahl, "A rate-adaptive MAC protocol for multi-Hop wireless networks," in Proceedings of the 7th annual international conference on Mobile computing and networking (MobiCom), 2001.

[27] H. Abdulhamid, E. Abdel-Raheem, and K. E. Tepe, "Channel Tracking Techniques for OFDM Systems in Wireless Access Vehicular Environment," in Proceedings of the 9th International Symposium on Signal Processing and It's Applications (ISSPA), pp. 12-15 February 2007.

[28] H. Abdulhamid, E. Abdel-Raheem and K. E. Tepe, "Performance of DSRC Systems using Conventional Channel Estimation at High Velocities," AEU - International Journal of Electronics and Communications, Volume 61, Issue 8, Pages 556-561, 3 September 2007.

[29] H. Abdulhamid, E. Abdel-Raheem, and K. E. Tepe, "5.9 GHz DSRC Receiver for Wireless Access Vehicular

Environments," IET Communications Journal, February 1st, 2007.

[30] H. Abdulhamid, K. Tepe, and E. Abdel-Raheem, "Iterative Channel Tracking Techniques for 5.9GHz DSRC Applications," Research Letters in Communications, vol. 2008, Article ID 485013, 5 pages, 2008

[31] © [2011] IEEE. Reprinted, with permission, from [N. Jaber, K. E. Tepe, and E. Abdel-Raheem, Improved Performance at Higher Data Rates of DSRC Systems Using a Linear Demapper, CCECE'11, 2011]

[32] Paper on Simulation of Urban Mobility (SUMO), http://sumo.sourceforge.net, Accessed 2011.

[33] N. Jaber, W. G. Cassidy, K. E. Tepe, and E. Abdel-Raheem "Passive cooperative collision warning for repetition based vehicular safety messaging medium access control protocols," submitted to IEEE Journal on Selected Areas in Communications (JSAC on Emerging Technologies in Communications), 2012.

[34] J. Harri, F. Filali, C. Bonnet, "Mobility Models for Vehicular Ad Hoc Networks: A Survey and Taxonomy," IEEE Comm. Surveys and Tutorials, vol. 11, no. 4, 2009.

[35] G. Yeung, M. Takai, R. Bagrodia, A. Mehrnia, B. Daneshrad, "Detailed OFDM modeling in network simulation of mobile ad hoc networks," in Proceedings of the 18th Workshop on Parallel and Distributed Simulation, pp. 26–34, 2004.

[36] G. Yeung, M. Takai, R. Bagrodia, "Effects of detailed OFDM modeling in network simulation," Simulation 81, pp. 241–253, 2005.

[37] L. Zhang, Y. Cheng, X. Zhou, "Rate avalanche: effects on the performance of multi-rate 802.11 wireless networks," Simulation Modelling Practice and Theory (SIMPAT), pp. 487–503, 2009.

[38] N. Jaber, "Performance Enhancement of the OFDM-Based DSRC System Using Frequency-Domain MAP Equalization and Soft-Output Demappers," MASc. Thesis, Department of Electrical and Computer Engineering, University of Windsor, Ontario, 2009.

[39] R. Prasad, "OFDM for Wireless Communication Systems," Artech House, Inc., USA, 2004.

[40] H. Abdulhamid, "Channel estimation for 5.9 GHz dedicated short-range communications (DSRC) Applications," MASc. Thesis, Department of Electrical and Computer Engineering, University of Windsor, Ontario, December 2006.

[41] H. Harada, R. Prasad, S"imulation and Software Radio for Mobile Communications," Artech House, USA, 2002.

[42] T.S. Rappaport, "Wireless Communications Principles and Practice, Prentice Hall," Saddle River, NJ, 1999.

[43] W. G. Jeon, K. H. Chang, Y. S. Cho, "An equalization technique for orthogonal frequency-division multiplexing systems in time-variant multipath channels," IEEE Transactions on Communications, pp. 27–32, 1999.

[44] P. Robertson, S. Kaiser, "The effects of doppler spreads on OFDM(A) mobile radio systems," in Proceedings of IEEE Vehicular Technology Conference, pp. 329–333, 1999.

[45] M. Russel, G.L. Stüber, "Interchannel interference analysis of OFDM in a mobile environment," in Proceedings of IEEE Vehicular Technology Conference, pp. 820–824, 1995.

[46] L. R. Bahl, J. Cocke, F. Jelinek, J. Raviv, "Optimal decoding of linear codes for minimizing symbol error rate, IEEE Transactions on Information Theory," pp. 284–287, 1974.

[47] W. C. Jakes, "Microwave Mobile Communications," Wiley, New York, USA, 1974.

[48] R. G. Fichman, C. F. Kemerer, "Object-oriented and conventional analysis and design methodologies," Computer, vol. 25, issue 10, pp. 22–39, 1992.

[49] K. He, and G. Cauwenberghs, "Performance of analog Viterbi decoding," in Proceedings of the 42nd Midwest

Symposium on Circuits and Systems, vol.1, pp.2-5, 1999.

[50] J. Mar, and C. Kuo, "Performance Improvement of the DSRC System Using a Novel S and PI-Decision Demapper," ICC Workshops IEEE International Conference on Communications, pp.405-409, May 2008.

[51] B. Lee, C. S. Yim, D. H. Ahn, and D. G. Oh, "Performance Evaluation of the Physical Layer of the DSRC Operating in 5.8 GHz Frequency Band," ETRI Journal, vol.23, pp.121-128, 2001.

[52] ASTM E2213-03. Standard Specification for Telecommunications and Information Exchange Roadside and Vehicle Systems—5GHz Band Dedicated Short Range Communications (DSRC) Medium Access Control (MAC) and Physical Layer (PHY) Specifications. September 2003.

[53] Z. Wang, G. B. Giannakis, "Wireless multicarrier communications: where Fourier meets Shannon," IEEE Signal Processing Mag., vol. 17, pp. 29-48, May 2000.

[54] P. Robertson, s. Kaiser, "The effects of Doppler spreads on OFDM(A) mobile radio systems," in Proceedings of IEEE Vehicular Technology Conference, pp. 329-33, September 1999.

[55] M. Russel, G. L. Stüber, "Interchannel interference analysis of OFDM in a mobile environment," in Proceedings of IEEE Vehicular Technology Conference, Chicago, IL, pp. 820-4, July 1995.

[56] Z. S. Lin, T. L. Hong, D. C. Chang, "Design of an OFDM system with long frame by the decision-aided channel tracking technique," in Proceedings of IEEE Sixth Electro/Information Technology Conference, Lansing, MI, USA, May 2006.

[57] L. Rugini, P. Banelli, G. Leus, "Simple Equalization of Time-Varying Channels for OFDM," IEEE Communication Letter, vol 9, no. 7, pp.619-21, July 2005.

[58] L. Zhang, Z. Chunming, J. Wu, W. Wang, "WLCp1-12: MAP based Equalizer for OFDM Systems in Time-Varying Multipath Channels," in Proceedings of IEEE Global Telecommunications Conference, pp.1-5, November 27 2006 - Dec. 1 2006.

[59] R. Chang, R. Gibby, "A theoretical study of performance of an orthogonal multiplexing data," IEEE Transactions on Communication Technology, vol. 16, issue 4, pp. 529–540, 1968.

[60] Standard Specification for Telecommunications and Information Exchange Roadside and VehicleSystems-5GHz Band Dedicated Short Range Communications (DSRC) Medium Access Control (MAC) and Physical Layer (PHY) Specifications, ASTM E2213-03, 2003.

[61] H. Bogucka, "Bit and power loading game of the flexible OFDM transceiver in a wireless environment," IEEE 10th International Symposium on Spread Spectrum Techniques and Applications, ISSSTA'08, pp. 682–687, 2008.

[62] J. Heiskala, J. Terry, "OFDM Wireless LANs: A Theoretical and Practical Guide, second ed." Sams Publishing, USA, 2002.

[63] H. Rohling, R. Gruneid, "Performance comparison of different multiple access schemes for the downlink of an OFDM communication system," in Proceedings of IEEE Vehicular Technology Conference, pp. 1365–1369, 1997.

[64] S. Narayanan et al, "Research in object-oriented manufacturing simulations: an assessment of the state of the art," IIE Transactions, vol. 30, issue 9, pp. 795–810, 1998.

[65] M. A. Rahman, A. Pakštas, F. Z. Wang, "Network modelling and simulation tools," Simulation Modelling Practice and Theory (SIMPAT), vol. 17, issue 6, pp. 1011–1031, 2009.

[66] G. Yeung, M. Takai, R. Bagrodia, A. Mehrnia, B. Daneshrad, "Detailed OFDM modeling in network simulation of mobile ad hoc networks," in Proceedings of the 18th Workshop on Parallel and Distributed Simulation, pp.

26–34, 2004.

[67] J. Lee, J. Ryu, Sung-Ju Lee, T. Kwon, "Improved modeling of IEEE 802.11a PHY through fine-grained measurements," Computer Networks, Advances in Wireless and Mobile Networks, vol. 54, issue 4, pp. 641–657, March 2010.

[68] A. Veiverys, "A generic hardware-accelerated OFDM system simulator," in Proceedings of Norchip Conference, pp. 62 – 65, November 2005.

[69] A. Maltsev, A. Khoryaev, A. Lomayev, R. Maslennikov, M. Shilov, V. Pestretsov, "Hardware link level emulator for system level simulations of WiMAX-like systems," in Proceedings ICT-Mobile Summit, Stockholm, Sweden, 2008.

[70] W. Liao, H. Su, "Simulation method for realizing correlated OFDM channel in frequency domain," in Proceedings of the 20th IEEE International Symposium on Personal, Indoor and Mobile Radio Communications, pp. 2002–2006, September 2009.

[71] P. Bratley, L.E. Schrage, B.L. Fox, "A Guide to Simulation," second edition, Springer, 1987.

[72] S.L. Ferenci, R.M. Fujimoto, M.H. Ammar, K. Perumalla, "Updateable simulation of communication networks," in Proceedings of the 16th Workshop on Parallel and Distributed Simulation, pp. 107–114, 2002.

[73] Y. Shen, E.F. Martine, "Channel Estimation in OFDM Systems," Application Note AN3059, Freescale Semiconductor, Inc., 2006.

[74] R. Otnes, M. Tuchler, "Iterative channel estimation for turbo equalization of time-varying frequency-selective channels," IEEE Transactions on Wireless Communications, vol. 3, issue 6, pp. 1918–1923, 2004.

[75] A. J. Viterbi, "Error bounds for convolutional codes and an asymptotically optimum decoding algorithm," IEEE Transactions on Information Theory 13 (2) (1967) 260–269.

[76] C. Kiddle, R. Simmonds, B. Unger, "Performance of a mixed shared/distributed memory parallel network simulator," in Proceedings of the 18th Workshop on Parallel and Distributed Simulation, pp. 17–25, 2004.

[77] A. Verbraeck, "Component-based distributed simulations. The way forward?," in Proceedings of the 18th Workshop on Parallel and Distributed Simulation, pp. 141–148, 2004.

[78] J. Banks, "Handbook of Simulation: Principles, Methodology, Advances, Applications, and Practice," Wiley, New York, USA, 1998.

[79] L. Betancur, R. Hincapié, R. Bustamante, "WiMAX Channel: PHY Model in Network Simulator 2," in Proceedings of the 2006 workshop on ns-2: the IP network simulator, ACM, New York, USA, 2006.

[80] Dei80211mr Library: Multirate 802.11 Implementation for the Network Simulator, Version 2. <http://www.dei.unipd.it/ricerca/signet/tools/dei80211mr>.

[81] Q. Chen, F. Schmidt-Eisenlohr, D. Jiang, M. Torrent-Moreno, L. Delgrossi, H. Hartenstein, "Overhaul of IEEE 802.11 modeling and simulation in ns-2," in Proceedings of the 10th ACM Symposium on Modeling, Analysis, and Simulation of Wireless and Mobile Systems, pp. 159–168, 2007.

Appendix A

Elsevier and IEEE Reprint Permissions

From AEÜ International Journal of Electronics and Communications, and Int. Journal of Simulation Modelling Practice and Theory (SIMPAT), Elsevier, 2011. doi: 10.1016/j.aeue.2011.03.001.

ELSEVIER LICENSE
TERMS AND CONDITIONS

Nov 06, 2011

This is a License Agreement between Nabih Jaber ("You") and Elsevier ("Elsevier") provided by Copyright Clearance Center ("CCC"). The license consists of your order details, the terms and conditions provided by Elsevier, and the payment terms and conditions.

All payments must be made in full to CCC. For payment instructions, please see information listed at the bottom of this form.

Supplier	Elsevier Limited The Boulevard,Langford Lane Kidlington,Oxford,OX5 1GB,UK
Registered Company Number	1982084
Customer name	Nabih Jaber
Customer address	104-980 St. Luke Road Windsor, ON N8Y4Y8
License number	2783240069598
License date	Nov 06, 2011
Licensed content publisher	Elsevier
Licensed content publication	AEU - International Journal of Electronics and Communications
Licensed content title	Performance enhancement of the DSRC system using frequency-domain equalization for 5.9GHz DSRC applications
Licensed content author	Nabih Jaber,Kemal E. Tepe,Esam Abdel-Raheem
Licensed content date	November 2011
Licensed content volume number	65
Licensed content issue number	11
Number of pages	5
Start Page	924
End Page	928
Type of Use	reuse in a thesis/dissertation
Intended publisher of new work	other
Portion	full article
Format	both print and electronic
Are you the author of this Elsevier article?	Yes
Will you be translating?	No

Order reference number	
Title of your thesis/dissertation	Towards More Reliable MAC and PHY Layer Designs for High QoS Achievements for Safety Messaging in DSRC Systems
Expected completion date	Dec 2011
Estimated size (number of pages)	120
Elsevier VAT number	GB 494 6272 12
Permissions price	0.00 USD
VAT/Local Sales Tax	0.0 USD / 0.0 GBP
Total	0.00 USD
Terms and Conditions	

ELSEVIER LICENSE
TERMS AND CONDITIONS

Nov 06, 2011

This is a License Agreement between Nabih Jaber ("You") and Elsevier ("Elsevier") provided by Copyright Clearance Center ("CCC"). The license consists of your order details, the terms and conditions provided by Elsevier, and the payment terms and conditions.

All payments must be made in full to CCC. For payment instructions, please see information listed at the bottom of this form.

Supplier	Elsevier Limited The Boulevard,Langford Lane Kidlington,Oxford,OX5 1GB,UK
Registered Company Number	1982084
Customer name	Nabih Jaber
Customer address	104-980 St. Luke Road Windsor, ON N8Y4Y8
License number	2783231360869
License date	Nov 06, 2011
Licensed content publisher	Elsevier
Licensed content publication	Simulation Modelling Practice and Theory
Licensed content title	Reconfigurable simulator using graphical user interface (GUI) and object-oriented design for OFDM systems
Licensed content author	Nabih Jaber,Kemal E. Tepe,Esam Abdel-Raheem
Licensed content date	May 2011
Licensed content volume number	19
Licensed content issue number	5
Number of pages	24
Start Page	1294
End Page	1317
Type of Use	reuse in a thesis/dissertation
Portion	full article
Format	both print and electronic
Are you the author of this Elsevier article?	Yes
Will you be translating?	No
Order reference number	
Title of your	Towards More Reliable MAC and PHY Layer Designs for High QoS

thesis/dissertation	Achievements for Safety Messaging in DSRC Systems
Expected completion date	Dec 2011
Estimated size (number of pages)	120
Elsevier VAT number	GB 494 6272 12
Permissions price	0.00 USD
VAT/Local Sales Tax	0.0 USD / 0.0 GBP
Total	0.00 USD
Terms and Conditions	

INTRODUCTION

1. The publisher for this copyrighted material is Elsevier. By clicking "accept" in connection with completing this licensing transaction, you agree that the following terms and conditions apply to this transaction (along with the Billing and Payment terms and conditions established by Copyright Clearance Center, Inc. ("CCC"), at the time that you opened your Rightslink account and that are available at any time at http://myaccount.copyright.com).

GENERAL TERMS

2. Elsevier hereby grants you permission to reproduce the aforementioned material subject to the terms and conditions indicated.

3. Acknowledgement: If any part of the material to be used (for example, figures) has appeared in our publication with credit or acknowledgement to another source, permission must also be sought from that source. If such permission is not obtained then that material may not be included in your publication/copies. Suitable acknowledgement to the source must be made, either as a footnote or in a reference list at the end of your publication, as follows:

"Reprinted from Publication title, Vol /edition number, Author(s), Title of article / title of chapter, Pages No., Copyright (Year), with permission from Elsevier [OR APPLICABLE SOCIETY COPYRIGHT OWNER]." Also Lancet special credit - "Reprinted from The Lancet, Vol. number, Author(s), Title of article, Pages No., Copyright (Year), with permission from Elsevier."

4. Reproduction of this material is confined to the purpose and/or media for which permission is hereby given.

5. Altering/Modifying Material: Not Permitted. However figures and illustrations may be altered/adapted minimally to serve your work. Any other abbreviations, additions, deletions and/or any other alterations shall be made only with prior written authorization of Elsevier Ltd. (Please contact Elsevier at permissions@elsevier.com)

6. If the permission fee for the requested use of our material is waived in this instance, please be advised that your future requests for Elsevier materials may attract a fee.

7. Reservation of Rights: Publisher reserves all rights not specifically granted in the combination of (i) the license details provided by you and accepted in the course of this licensing transaction, (ii)

these terms and conditions and (iii) CCC's Billing and Payment terms and conditions.

8. License Contingent Upon Payment: While you may exercise the rights licensed immediately upon issuance of the license at the end of the licensing process for the transaction, provided that you have disclosed complete and accurate details of your proposed use, no license is finally effective unless and until full payment is received from you (either by publisher or by CCC) as provided in CCC's Billing and Payment terms and conditions. If full payment is not received on a timely basis, then any license preliminarily granted shall be deemed automatically revoked and shall be void as if never granted. Further, in the event that you breach any of these terms and conditions or any of CCC's Billing and Payment terms and conditions, the license is automatically revoked and shall be void as if never granted. Use of materials as described in a revoked license, as well as any use of the materials beyond the scope of an unrevoked license, may constitute copyright infringement and publisher reserves the right to take any and all action to protect its copyright in the materials.

9. Warranties: Publisher makes no representations or warranties with respect to the licensed material.

10. Indemnity: You hereby indemnify and agree to hold harmless publisher and CCC, and their respective officers, directors, employees and agents, from and against any and all claims arising out of your use of the licensed material other than as specifically authorized pursuant to this license.

11. No Transfer of License: This license is personal to you and may not be sublicensed, assigned, or transferred by you to any other person without publisher's written permission.

12. No Amendment Except in Writing: This license may not be amended except in a writing signed by both parties (or, in the case of publisher, by CCC on publisher's behalf).

13. Objection to Contrary Terms: Publisher hereby objects to any terms contained in any purchase order, acknowledgment, check endorsement or other writing prepared by you, which terms are inconsistent with these terms and conditions or CCC's Billing and Payment terms and conditions. These terms and conditions, together with CCC's Billing and Payment terms and conditions (which are incorporated herein), comprise the entire agreement between you and publisher (and CCC) concerning this licensing transaction. In the event of any conflict between your obligations established by these terms and conditions and those established by CCC's Billing and Payment terms and conditions, these terms and conditions shall control.

14. Revocation: Elsevier or Copyright Clearance Center may deny the permissions described in this License at their sole discretion, for any reason or no reason, with a full refund payable to you. Notice of such denial will be made using the contact information provided by you. Failure to receive such notice will not alter or invalidate the denial. In no event will Elsevier or Copyright Clearance Center be responsible or liable for any costs, expenses or damage incurred by you as a result of a denial of your permission request, other than a refund of the amount(s) paid by you to Elsevier and/or Copyright Clearance Center for denied permissions.

LIMITED LICENSE

The following terms and conditions apply only to specific license types:

15. **Translation**: This permission is granted for non-exclusive world **English** rights only unless your license was granted for translation rights. If you licensed translation rights you may only translate this content into the languages you requested. A professional translator must perform all translations and reproduce the content word for word preserving the integrity of the article. If this license is to re-use 1 or 2 figures then permission is granted for non-exclusive world rights in all languages.

16. **Website**: The following terms and conditions apply to electronic reserve and author websites:
Electronic reserve: If licensed material is to be posted to website, the web site is to be password-protected and made available only to bona fide students registered on a relevant course if:
This license was made in connection with a course,
This permission is granted for 1 year only. You may obtain a license for future website posting,
All content posted to the web site must maintain the copyright information line on the bottom of each image,
A hyper-text must be included to the Homepage of the journal from which you are licensing at http://www.sciencedirect.com/science/journal/xxxxx or the Elsevier homepage for books at http://www.elsevier.com , and
Central Storage: This license does not include permission for a scanned version of the material to be stored in a central repository such as that provided by Heron/XanEdu.

17. **Author website** for journals with the following additional clauses:

All content posted to the web site must maintain the copyright information line on the bottom of each image, and
he permission granted is limited to the personal version of your paper. You are not allowed to download and post the published electronic version of your article (whether PDF or HTML, proof or final version), nor may you scan the printed edition to create an electronic version,
A hyper-text must be included to the Homepage of the journal from which you are licensing at http://www.sciencedirect.com/science/journal/xxxxx , As part of our normal production process, you will receive an e-mail notice when your article appears on Elsevier's online service ScienceDirect (www.sciencedirect.com). That e-mail will include the article's Digital Object Identifier (DOI). This number provides the electronic link to the published article and should be included in the posting of your personal version. We ask that you wait until you receive this e-mail and have the DOI to do any posting.
Central Storage: This license does not include permission for a scanned version of the material to be stored in a central repository such as that provided by Heron/XanEdu.

18. **Author website** for books with the following additional clauses:
Authors are permitted to place a brief summary of their work online only.
A hyper-text must be included to the Elsevier homepage at http://www.elsevier.com

All content posted to the web site must maintain the copyright information line on the bottom of each image
You are not allowed to download and post the published electronic version of your chapter, nor may you scan the printed edition to create an electronic version.

Central Storage: This license does not include permission for a scanned version of the material to be stored in a central repository such as that provided by Heron/XanEdu.

19. **Website** (regular and for author): A hyper-text must be included to the Homepage of the journal from which you are licensing at http://www.sciencedirect.com/science/journal/xxxxx. or for books to the Elsevier homepage at http://www.elsevier.com

20. **Thesis/Dissertation**: If your license is for use in a thesis/dissertation your thesis may be submitted to your institution in either print or electronic form. Should your thesis be published commercially, please reapply for permission. These requirements include permission for the Library and Archives of Canada to supply single copies, on demand, of the complete thesis and include permission for UMI to supply single copies, on demand, of the complete thesis. Should your thesis be published commercially, please reapply for permission.

21. **Other Conditions**:

v1.6

If you would like to pay for this license now, please remit this license along with your payment made payable to "COPYRIGHT CLEARANCE CENTER" otherwise you will be invoiced within 48 hours of the license date. Payment should be in the form of a check or money order referencing your account number and this invoice number RLNK500659226. Once you receive your invoice for this order, you may pay your invoice by credit card. Please follow instructions provided at that time.

Make Payment To:
Copyright Clearance Center
Dept 001
P.O. Box 843006
Boston, MA 02284-3006

For suggestions or comments regarding this order, contact RightsLink Customer Support: customercare@copyright.com or +1-877-622-5543 (toll free in the US) or +1-978-646-2777.

Gratis licenses (referencing $0 in the Total field) are free. Please retain this printable license for your reference. No payment is required.

IEEE Reprint Permission

Dear Nabih Jaber:

The IEEE does not require individuals working on a thesis to obtain a formal reuse license, however, you may print out this statement to be used as a permission grant:

Requirements to be followed when using any portion (e.g., figure, graph, table, or textual material) of an IEEE copyrighted paper in a thesis:

1) In the case of textual material (e.g., using short quotes or referring to the work within these papers) users must give full credit to the original source (author, paper, publication) followed by the IEEE copyright line © 2011 IEEE.

2) In the case of illustrations or tabular material, we require that the copyright line © [Year of original publication] IEEE appear prominently with each reprinted figure and/or table

3) If you expect to use a substantial portion of the original paper, and if you are not the senior author, please obtain the senior author's approval.

Requirements to be followed when using an entire IEEE copyrighted paper in a thesis:

1) The following IEEE copyright/ credit notice should be placed prominently in the references: © [year of original publication] IEEE. Reprinted, with permission, from [author names, paper title, IEEE publication title, and month/year of publication]

2) Only the accepted version of an IEEE copyrighted paper can be used when posting the paper or your thesis on-line.

3) In placing the thesis on the author's university website, please display the following message in a prominent place on the website: In reference to IEEE copyrighted material which is used with permission in this thesis, the IEEE does not endorse any of [university/educational entity's name goes here]'s products or services. Internal or personal use of this material is permitted. If interested in reprinting/republishing IEEE copyrighted material for advertising or promotional purposes or for creating new collective works for resale or redistribution, please go to http://www.ieee.org/publications_standards/publications/rights/rights_link.html to learn how to obtain a License from RightsLink.

If applicable, the Archives of Canada may supply single copies of the dissertation.

Sincerely,

Jacqueline Hansson, Coordinator
IEEE Intellectual Property Rights Office
445 Hoes Lane
Piscataway, NJ 08855-1331 USA
+1 732 562 3828 (phone)
+1 732 562 1746(fax)
e-mail: j.hansson@ieee.org
IEEE Fostering technological innovation
and excellence for the benefit of humanity.

©©©©©©©©©©©©©©©©©©©©©©©©©©©©©©©©

From: William Hagen/PUBS/STAFF/US/IEEE

To: Jacqueline Hansson/PUBS/STAFF/US/IEEE@IEEE
Date: 11/07/2011 08:34 AM
Subject: Fw: IEEE Publications

----- Forwarded by William Hagen/PUBS/STAFF/US/IEEE on 11/07/2011 08:33 AM -----
From: Nabih Jaber <jaber@uwindsor.ca>
To: w.hagen@ieee.org
Cc: jaber <jaber@uwindsor.ca>
Date: 11/06/2011 03:42 AM
Subject: IEEE Publications

Dear Mr. Hagen,

I would appreciate it if you reply to me by November 11, 2011 concerning the following matter:

I have published the following papers in IEEE and would like to use the material as part of my dissertation:

1 - Nabih Jaber, Kazi Rahman, Esam Abdel-Raheem, Kemal Tepe, "A Quantitative Analysis of Improved DSRC System using Repetition Based Broadcast Safety Messaging with Hidden Terminals," IEEE IWCMC - Wireless Communications and Mobile Computing Conference 7th International Symposium on Vehicular Communications, pp. 1772 - 1777, August 2011.

2 - Nabih Jaber, Kemal Tepe, Esam Abdel-Raheem, "Improved Performance at High Code Rates of DSRC PHY Systems using a Linear Demapper," 24th IEEE CCECE International Symposium on Vehicular Communications, pp.000370-000374, September 2011.

I have submitted the following paper to IEEE and also would like to use the material as part of my dissertation:

3 - Nabih Jaber, William Cassidy, Esam Abdel-Raheem, Kemal Tepe, " New Vehicular Broadcast Messaging Reliability Enhancement Protocol for Emergency Vehicle Communication," IEEE Wireless Communications and Networking Conference (IEEE WCNC).

Additionally, I will soon be submitting the following paper to IEEE and also would like to use the material as part of my dissertation:

4 - Nabih Jaber, William Cassidy, Kemal Tepe, Esam Abdel-Raheem, " New Passive Cooperative Collision Warning (PCCW) MAC Protocol Designs for Reliability Enhancement of Vehicular Safety Messaging," IEEE International Journal Transactions on Vehicular Technology.

I would appreciate it if you reply to me by November 11, 2011.

Thank you.

Nabih Jaber.

Appendix B

List of Publications

PUBLICATIONS IN REFEREED JOURNALS [J] AND CONFERENCES [C] (PUBLISHED AND ACCEPTED)

1 - [J] **Nabih Jaber**, Kemal Tepe, Esam Abdel-Raheem, "Reconfigurable simulator using graphical user interface (GUI) and object-oriented design for OFDM systems," *International Journal of Simulation Modelling Practice and Theory (SIMPAT), Elsevier*, 2011. doi: 10.1016/j.aeue.2011.03.001.

2 - [J] **Nabih Jaber**, Nicholas Doyle, Kemal Tepe, "New Combined WiMAX-DSRC Infrastructure Design for Efficient Vehicular Networking," *International Journal on Wireless Communications and Networking (EURASIP)* (resubmitted with revision), 2011.

3 - [J] **Nabih Jaber**, Kemal Tepe, Esam Abdel-Raheem, "Performance Enhancement of the DSRC System Using Frequency-Domain MAP Equalization," *AEÜ International Journal of Electronics and Communications, Elsevier*, vol. 19, no. 5, pp. 1294-1317, 2011.

4 - [J] Nicholas Doyle, **Nabih Jaber**, Kemal Tepe, "Complete Architecture and Demonstration Design for a New Combined WiMAXDSRC System with Improved Vehicular Networking Efficiency," Ad *Hoc Networks International Journal (Elsevier)*, 2012.

5 - [J] **Nabih Jaber**, William Cassidy, Kemal Tepe, "Towards 5.9 GHz DSRC Receiver Design Improvement Using a Systolic Array of Multi-Rate FIR Filters," *International Journal of Research and Reviews in Computer Science (IJRRCS),* vol. 2, no. 3, 2011.

6 - [C] **Nabih Jaber**, Kazi Rahman, Esam Abdel-Raheem, Kemal Tepe, "A Quantitative Analysis of Improved DSRC System using Repetition Based Broadcast Safety Messaging with Hidden Terminals," *IEEE IWCMC - Wireless Communications and Mobile Computing Conference 7th International Symposium on Vehicular Communications, pp. 1772 - 1777, August* 2011.

7 - [C] **Nabih Jaber**, Kemal Tepe, Esam Abdel-Raheem, "Improved Performance at High Code Rates of DSRC PHY Systems using a Linear Demapper," *24th IEEE CCECE International Symposium on Vehicular Communications,* 2011.

8 - [C] Kazi Rahman, **Nabih Jaber**, Kemal Tepe, " Markov analysis of the mobile hidden station problem in MANET," *7th International Symposium on Vehicular Networking Wireless Communications and Mobile Computing Conference (IWCMC), pp 2186 - 2191,* 2011.

9 - [C] Patrick Casey, **Nabih Jaber**, Kemal Tepe, "Design and Implementation of a Cross-Platform Sensor Network for Smart Grid Transmission Line Monitoring," *IEEE SmartGridComm International Symposium on Communication networks for Smart Grid*, 2011.

10 - [C] Nicholas Doyle, **Nabih Jaber**, Kemal Tepe, "Improvement in Vehicular Networking Efficiency Using a New Combined WiMAX and DSRC System Design," *IEEE Pacific Rim International Conference on Communications, Computers and Signal Processing (IEEE PacRim)*, 2011.

PUBLICATIONS IN REFEREED JOURNALS [J] AND CONFERENCES [C] (SUBMITTED)

11 - [J] **Nabih Jaber**, William Cassidy, Kemal Tepe, Esam Abdel-Raheem, " New Passive Cooperative Collision Warning MAC Protocol Designs for Reliability Enhancement of Vehicular Safety Messaging," *IEEE Journal on Selected Areas in Communications (JSAC on Emerging Technologies in Communications), 2012*.

12 - [C] William Cassidy, **Nabih Jaber,** Shawn Ruppert, Jahangir Toimoor, Kemal Tepe, Esam Abdel-Raheem "Study of SNR Thresholds for Precise MAC and PHY Layer Vehicular Network Designs," *25th Queen's University Biennial Symposium on Communications (QBSC), 2012*.

13 - [C] William Cassidy, **Nabih Jaber**, Kemal Tepe, "MAC/PHY Cross Layer Design for Reliability Improvement of Vehicular Safety Messaging," *IEEE/IFIP International Conference on New Technologies, Mobility and Security (NTMS), 2012*.

14 - [C] William Cassidy, **Nabih Jaber**, Kemal Tepe, "Cross Layer Consideration for DSRC Safety Messaging," *25th Queen's University Biennial Symposium on Communications (QBSC), 2012*.

15 - [C] **Nabih Jaber**, William Cassidy, Esam Abdel-Raheem, Kemal Tepe, "Vehicular Broadcast Messaging Reliability Enhancement Protocol for Emergency Vehicle Communication," *IEEE/IFIP International Conference on New Technologies, Mobility and Security (NTMS), 2012.*

16 - [C] A. El Baba, S. A. Ruppert, **Nabih Jaber**, Kemal Tepe, "Vehicular Broadcast Messaging Reliability Enhancement Protocol for Emergency Vehicle Communication," International Conference on Smart Grid Engineering (SGE'12) (abstract submitted), August, 2012.

17 - [C] K. M. Shazzad, W. G. Cassidy, S. M. Sami, K. E. Tepe, **N. Jaber**, K. A. Rahman, A. El Baba, S. Ruppert, and I. Ahmed, "Improved Electric Vehicle Usage and Driver Experience for Smart Grid Through Enabling Smart Device Information Profiling," International Conference on Smart Grid Engineering (SGE'12) (abstract submitted), August, 2012.

Appendix C

Pseudo Codes for PCCW, EPCCW and ePCCW Analytical Equations

For Passive Cooperative Collision Warning (PCCW) and Enhanced-PCCW (EPCCW)

function sfrPCCWs

Initialize the number of users in the system N
Initialize frame length L (frame length) //L = τ /t_{slot} where t_{slot} is the
//duration of one time slot, and τ is the lifetime of a message, or the
//duration of a frame.
Initialize communication load l
for $r \leftarrow 1$ to r_{max} //loop through each repetition scenario
Initialize probability of success for SFR at repetition r :
prS_SFR(r) ← 0
Initialize probability of success for SFR //using PCCW at
//repetition r : prS_PCCW(r) ← 0
for $m \leftarrow 0$ to m_{max} //loop through all possible interferers
//Store the probability of the number of interferers being m: $Pr_{l,M,N}(m = m)$ (Eq. 7)
pmm ← PrMgivenM(l,m,N)
//Find the probability of success for SFR as $Pr_{r,L,m}(S_{SFR})$ (Eq. 2):
prS1 ← PrSFR(r,L,m)
Store success into
prS_SFR(r) ← prS_SFR(r) + prS1 × pmm;
Set the probability of slot transmission p ← r/L
//Initialize PCCW windows success to SFR success
Set initial recursion probability of success
PrPCCW(0) ← prS1
for $R \leftarrow 1$ to R_{max} //loop through R recursions for
//subsequent window successes
PrPCCW (R) ← Pr_PCCW(p,w,M,N,L,t PrPCCW(R-1))
// PCCW window success
end
//Find the probability of success for PCCW $Pr_m(S_{PCCW})$
//(Eq. 4) as :

prS2 ← Pr_PCCW(p,w,M,N,L, PrPCCW (R))
Store success into
prS_PCCW(r) ← prS_PCCW(r) + prS2 × pmm

end

end

Display the success vs. repetition of prS_SFR and prS_PCCW

end function

---

function PrSFR(r, L, m)

// PrSFR calculates the probability of success of SFR

$$\text{prSFR} \leftarrow \Pr_{r,L,m}(S_{SFR}) = \sum_{k=1}^{r}(-1)^{k+1}\binom{r}{k}\left(\frac{\binom{\frac{L-k}{r}}{}}{\binom{L}{r}}\right)^{m}$$

return prSFR

end function

---

function PrMgivenM(l,m,N) //binomial distributed data traffic

// PrMgivenM implements equation $\Pr_{l,m,N}(m = m)$ (Eq. 7) as

$$\text{prMgivenM} \leftarrow \Pr_{l,m,N}(m = m) = \binom{N-1}{m} l^{m}(1-l)^{N-m-1}$$

return prMgivenM

end function

---

function PrMgivenM(l,m,N) //Poisson distributed data traffic

// PrMgivenM implements equation $\Pr_{l,m,N}(m = m)$ (Eq. 8) as

$$\Pr_{l,m,N}(m = m) = e^{-m\lambda\tau}\frac{(m\lambda\tau)^{n}}{n!}$$

//n is the number of messages generated by all transmitters

//λ is the rate of message generation

end function

---

function Pr_PCCW(p,r,m,N,L,SW)

// Pr_PCCW implements the probability of success for PCCW

Initialize PCCW probability of success prPCCW← 0
Set the probability of a node being a γ user to be $p_g = (1 - l)$
for γ ← 0 to m// loop through all combinations of gamma
Initialize prS_CW0 ← 0 for calculating the probability of success

---

```
  //(for given α, β, and γ)
  for α ← 0 to m − γ
      Set β ← (m − γ − α)
      //to set the users that did not warn successfully
      //Calculate prStateCW0 as Pr_{α,β,γ}(S_{state=CW0}) as (Eq. 13):
      prStateCW0 ← PrStateCW0(r,L,m,γ,α,SW)
      prS_CW0 ← prS_CW0 + prStateCW0;
  end
  //calculate probability of success due to backing-off users Pr_{m,γ}(S_{state=CP0}) as (Eq. 11):
  prS_CP0 ← C(m, γ) × (p_g^γ) × ((1 − p_g)^{m−γ})
  prPCCW ← prPCCW + prS_CP0 × prS_CW0;
end
return prPCCW
end function
```

```
function PrStateCW0(r,L,m,γ,β,α,SW)

  // Calculate the probability of having alpha users Pr_{m,α,γ}(α = α)
  prA← C(m−γ, α) × (l × SW)^α × (1 − (l × SW))^{m−γ−α}
  // r_i is the i^th repetition out of r total repetitions. Used only
  //when calculating the delay equations.
  Set r_i ← r for success of r repetitions
  // use j as a control variable, j = 0, 1, 2 when desired user is an α, β, γ user respectively.
  if decision mode enhancement is enabled
    Set the data rate factor R_factor according the EPCCW
    prScw0a ← PrScw0_EPCCW(m,r,r_i,L,γ,α,β,j = 0,SW, R_factor)
    prScw0b ← PrScw0_EPCCW (m,r,r_i,L,γ,α,β,j = 1,SW, R_factor)
    prScw0g ← PrScw0_EPCCW (m,r,r_i,L,γ,α,β,j = 2,SW, R_factor)
      else //regular decision mode
      prScw0a ← PrScw0(m, r, r_i, L, γ, α, β, j = 0,SW)
      prScw0b ← PrScw0(m,r,r_i,L,γ,α,β,j = 1,SW)
      prScw0g ← PrScw0(m,r,r_i,L,γ,α,β,j = 2,SW)
  end
  //find the probability of the desired user being an α, β, and γ user:
  pr_{d=a} ← l × SW
  pr_{d=b} ← l × (1 − SW)
  pr_{d=g} ← 1 − l
  prStateCW0 ← PrA × ((pr_{d=a} × prScw0a) + (pr_{d=b} × prScw0b) + (pr_{d=g} × prScw0g))
  return prStateCW0
end function
```

```
function PrScw0 (m,r,r_i,L,γ,α,β,j,SW)

  Set the probability of transmission into a particular slot p ← r/L
```

//Initialize the probability of success during CW0 state to zero:

$\text{prScw0} \leftarrow 0;$

Initialize the summation of g possible transmitting out of γ users: $\text{sum}_\text{g} \leftarrow 0$

// loop through all g users out of γ users transmitting in the time slot

for $\text{g} \leftarrow 0$ to γ

//Calculate the probability of having specific g transmitting out of the γ users $\text{Pr}_\gamma(\text{g})$ as in (Eq. 16):

$\text{pr}_\text{g} \leftarrow Prg = \text{Pr}_\gamma(\text{g}) = \binom{\gamma}{\text{g}} p^\text{g} \times (1-p)^{\gamma-\text{g}}$

Initialize summation for all combinations of a transmitting users out of alpha α: $\text{sum}_\text{a} \leftarrow 0$

for $\text{a} \leftarrow 0$ to α // loop through all a users out of α users transmitting

//in the time slot

//Similarly calculate $\text{Pr}_\alpha(\text{a})$ for a transmitting out of α users

//as in (Eq. 16):

$\text{pr}_\text{a} \leftarrow Pra = \text{Pr}_\alpha(\text{a}) = \binom{\alpha}{\text{a}} p^\text{a} \times (1-p)^{\alpha-\text{a}}$

Initialize $\text{sum}_\text{b} \leftarrow 0$

for $\text{b} \leftarrow 0$ to β // loop through all b users out of β users

//transmitting in the time slot

//Calculate $\text{Pr}_\beta(\text{b})$ for b transmitting out of β users

//as in (Eq. 16):

$\text{pr}_\text{b} \leftarrow Prb = \text{Pr}_\beta(\text{b}) = \binom{\beta}{\text{b}} p^\text{b} \times (1-p)^{\beta-\text{b}}$

//Calculate desired user's transmission under cw0 probability $s_{D,j}$ as in (Eq. 17)

$$\text{sd} \leftarrow s_{D,j} = \begin{cases} \frac{1}{\alpha+1}, & \text{when } j < 2 \\ 1, & \text{when } j \text{ is 2 and a} = 0 \\ 0, & \text{when } j \text{ is 2 and a} \geq 1 \end{cases}$$

//Calculate the a users' transmission under cw0 probability $s_{\text{a},j}$ out of α users as in (Eq. 18)

$\text{sa} \leftarrow s_{\text{a},j} = \frac{1}{\alpha + \frac{1}{2}j^2 - \frac{3}{2}j + 1}$

// Calculate b users' transmission under cw0 probability $s_{\text{b},j}$ out of β users as in (Eq. 19)

$\text{sb} \leftarrow s_{\text{b},j} = \frac{1}{\alpha + \frac{1}{2}j^2 - \frac{3}{2}j + 2}$

//Calculate g users' transmission under cw0 probability $s_{\text{g},j}$ out of γ users as in (Eq. 20)

$$\text{sg} \leftarrow s_{\text{g},j} = \begin{cases} 0, & \text{when } j = 0, \text{or a} \geq 1, \text{or g} = 0 \\ 1, & \text{otherwise} \end{cases}$$

//Calculate the probability of success of transmission for the desired user

//given a, b, and g users $\text{Pr}_{\text{a,b,g}}(S_D)$

$\text{pr}_\text{D} \leftarrow \text{Pr}_{\text{a,b,g}}(S_D)$

$= \text{sd} \times (1-\text{sa})^\text{a} \times (1-\text{sb})^\text{b} \times (1-\text{sg})^\text{g}$

//Sum for all b combinations knowing the desired user's success

$\text{sum}_\text{b} \leftarrow \text{sum}_\text{b} + \text{pr}_\text{b} \times \text{pr}_\text{D}$

end

//Sum for all a user combinations, knowing b user combinations

//given desired user's success.

$\text{sum}_\text{a} \leftarrow \text{sum}_\text{a} + \text{pr}_\text{a} \times \text{sum}_\text{b}$

end

//Sum for all g user combinations, knowing a and b user

//combinations given desired user's success.

$\text{sum}_\text{g} \leftarrow \text{sum}_\text{g} + \text{pr}_\text{g} \times \text{sum}_\text{a}$

end

//Save final sum_g as the probability of success of transmission for the
//desired user
//given all combinations of α, β and γ users into $\Pr_{\alpha,\beta,\gamma}(S_D) \leftarrow \text{sum}_\text{g}$
//Calculate the last step in calculating probability of the desired user's
//frame success for all r //repetitions in the frame, $\Pr_{r,\alpha,\beta,\gamma}(S_{state=CW0})$ as
//in (Eq. 14) (note r_i repetitions for delay calculations)
$\text{prScw0} \leftarrow \Pr_{r,\alpha,\beta,\gamma}(S_{state=CW0}) = 1 - \left(1 - \Pr_{\alpha,\beta,\gamma}(S_D)\right)^r$
return prScw0

end function

---

function PrScw0_EPCCW(m,r,r_i,L,γ,α,β,j,SW)

Set the probability of transmission into a particular slot $p \leftarrow r/L$
//Initialize the probability of success during CW0 state to zero:
$\text{prScw0} \leftarrow 0$;
Initialize the summation of g possible transmitting out of γ users: $\text{sum}_\text{g} \leftarrow 0$
for g ← 0 to γ // loop through all g users out of γ users transmitting
//in the time slot
//Calculate the probability of having specific g transmitting out of the γ users $\Pr_\gamma(\text{g})$ as in (Eq. 16):
$\text{pr}_\text{g} \leftarrow \Pr_\gamma(\text{g}) = \binom{\gamma}{\text{g}} p^\text{g} \times (1-p)^{\gamma-\text{g}}$
Initialize summation for all combinations of a transmitting users out of alpha α: $\text{sum}_\text{a} \leftarrow 0$
for a ← 0 to α // loop through all a users out of α users transmitting in the time slot
//Similarly calculate $\Pr_\alpha(\text{a})$ for a transmitting out of α users as in (Eq. 16):
$\text{pr}_\text{a} \leftarrow \Pr_\alpha(\text{a}) = \binom{\alpha}{\text{a}} p^\text{a} \times (1-p)^{\alpha-\text{a}}$
Initialize $\text{sum}_\text{b} \leftarrow 0$
for b ← 0 to β // loop through all b users out of β users transmitting
//in the time slot
//Calculate $\Pr_\beta(\text{b})$ for b transmitting out of β users
//as in (Eq. 16):
$\text{pr}_\text{b} \leftarrow \Pr_\beta(\text{b}) = \binom{\beta}{\text{b}} p^\text{b} \times (1-p)^{\beta-\text{b}}$
Initialize the sum of enhanced a_E users: $\text{sum}_{\text{a}_\text{E}} \leftarrow 0$
for a_E ← 0 to a //loop through a users that are transmitting in same sub slot as desired user.
//Calculate the probability of having a_E of the a users
//transmitting in the same sub slot $\Pr_\text{a}(\text{a}_\text{E})$ as in (Eq. 16).
$\text{pr}_{\text{a}_\text{E}} \leftarrow \Pr_\text{a}(\text{a}_\text{E}) = \binom{\text{a}}{\text{a}_\text{E}} \left(\frac{1}{R_{factor}}\right)^{\text{a}_\text{E}} \times \left(1 - \left(\frac{1}{R_{factor}}\right)\right)^{\text{a}-\text{a}_\text{E}}$
Initialize the sum of enhanced b_E users: $\text{sum}_{\text{b}_\text{E}} \leftarrow 0$
for b_E ← 0 to b //loop through b users that transmitting in same sub slot as desired user.
//Calculate the probability of having b_E of the b users
// transmitting in the same sub slot $\Pr_\text{b}(\text{b}_\text{E})$ in (Eq. 28).
$\text{pr}_{\text{b}_\text{E}} \leftarrow \Pr_\text{b}(\text{b}_\text{E}) = \binom{\text{b}}{\text{b}_\text{E}} \left(\frac{1}{R_{factor}}\right)^{\text{b}_\text{E}} \times \left(1 - \left(\frac{1}{R_{factor}}\right)\right)^{\text{b}-\text{b}_\text{E}}$
//Calculate desired user's transmission under cw0 probability $s_{D,j}$ as in (Eq. 17).

$\text{sd} \leftarrow s_{D,j} = \begin{cases} \frac{1}{\alpha+1}, & \text{when } j < 2 \\ 1, & \text{when } j \text{ is 2 and a} = 0 \\ 0, & \text{when } j \text{ is 2 and a} \geq 1 \end{cases}$

//Calculate the a users' transmission under cw0

//probability $s_{\text{a},j}$ out of α users as in (Eq.).

$\text{sa} \leftarrow s_{\text{a},j} = \frac{1}{\alpha+\frac{1}{2}j^2-\frac{3}{2}j+1}$

//Calculate b users' transmission under cw0 probability $s_{\text{b},j}$ out of β users as in (Eq. 18).

$\text{sb} \leftarrow s_{\text{b},j} = \frac{1}{\alpha+\frac{1}{2}j^2-\frac{3}{2}j+2}$

//Calculate g users' transmission under cw0 probability $s_{\text{g},j}$ out of γ users as in (Eq. 19).

$\text{sg} \leftarrow s_{\text{g},j} = \begin{cases} 0, & \text{when } j = 0, \text{or a} \geq 1, \text{or g} = 0 \\ 1, & \text{otherwise} \end{cases}$

//Calculate the probability of success of transmission for the desired user

//given a, b, and g users $\text{Pr}_{\text{a,b,g}}(S_D)$ as in (Eq. 20).

$\text{pr}_\text{D} \leftarrow \text{Pr}_{\text{a,b,g}}(S_D) = \text{sd} \times (1-\text{sa})^{\text{a}_\text{E}} \times (1-\text{sb})^{\text{b}_\text{E}} \times (1-\text{sg})^{\text{g}}$

//Sum for all b_E combinations knowing the desired user's success

$\text{sum}_{\text{b}_\text{E}} \leftarrow \text{sum}_{\text{b}_\text{E}} + \text{pr}_{\text{b}_\text{E}} \times \text{pr}_\text{D}$

end

//Sum for all a_E combinations, knowing b_E user combinations

//given desired user's success.

$\text{sum}_{\text{a}_\text{E}} \leftarrow \text{sum}_{\text{a}_\text{E}} + \text{pr}_{\text{a}_\text{E}} \times \text{sum}_{\text{b}_\text{E}}$

end

//Sum for all b user combinations, knowing a_E and b_E combinations

//given desired user's success.

$\text{sum}_\text{b} \leftarrow \text{sum}_\text{b} + \text{pr}_\text{b} \times \text{sum}_{\text{a}_\text{E}}$

end

//Sum for all a user combinations, knowing b, a_E, and b_E user combinations

//given desired user's success.

$\text{sum}_\text{a} \leftarrow \text{sum}_\text{a} + \text{pr}_\text{a} \times \text{sum}_\text{b}$

end

//Sum for all g user combinations, knowing a, b, a_E, and b_E user combinations

//given desired user's success.

$\text{sum}_\text{g} \leftarrow \text{sum}_\text{g} + \text{pr}_\text{g} \times \text{sum}_\text{a}$

end

//Save final sum_g as the probability of success of transmission for the desired user

//given all combinations of α, β and γ users into $\text{Pr}_{\alpha,\beta,\gamma}(S_D) \leftarrow \text{sum}_\text{g}$

//Calculate the last step in calculating probability of the desired user's frame success for all r

//repetitions in the frame, $\text{Pr}_{r,\alpha,\beta,\gamma}(S_{state=CW0})$ as in (Eq. 14) (note r_i repetitions for delay calculations)

$\text{prScw0} \leftarrow \text{Pr}_{r,\alpha,\beta,\gamma}\left(S_{D,j}\right)_{Frame} = 1 - \left(1 - \text{Pr}_{\alpha,\beta,\gamma}(S_D)\right)^r$

return prScw0

end function

For emergency-PCCW (ePCCW)

function PrScw0_ePCCW (m,r,r_i,L,γ,α,β,j,tmpPrS)

Set the probability of transmission into a particular slot $p \leftarrow r/L$ // r repetition and L slots
//Initialize the probability of success during CW0 state to zero: $\text{prScw0} \leftarrow 0$;
Initialize the summation of g possible transmitting out of γ users: $\text{sum}_\text{g} \leftarrow 0$
for g ← 0 to γ // loop through all g users out of γ users transmitting in the time slot
//Calculate the probability of having specific g transmitting out of the γ users $\text{Pr}_\gamma(\text{g})$:
$\text{pr}_\text{g} \leftarrow \text{Pr}_\gamma(\text{g}) = \binom{\gamma}{\text{g}} p^\text{g} \times (1-p)^{\gamma-\text{g}}$
Initialize summation for all combinations of a transmitting users out of alpha α: $\text{sum}_\text{a} \leftarrow 0$
for a ← 0 to α // loop through all a users out of α users transmitting in the time slot
//Similarly calculate $\text{Pr}_\alpha(\text{a})$ for a transmitting out of α users:
$\text{pr}_\text{a} \leftarrow \text{Pr}_\alpha(\text{a}) = \binom{\alpha}{\text{a}} p^\text{a} \times (1-p)^{\alpha-\text{a}}$
Initialize $\text{sum}_\text{b} \leftarrow 0$
for b ← 0 to β // loop through all b users out of β users transmitting in the time slot
//Calculate $\text{Pr}_\beta(\text{b})$ for b transmitting out of β users:
$\text{pr}_\text{b} \leftarrow \text{Pr}_\beta(\text{b}) = \binom{\beta}{\text{b}} p^\text{b} \times (1-p)^{\beta-\text{b}}$
//Calculate desired user's transmission under CW0 probability $s_{D,j}$ as in (Eq. 7)

$$\text{sd} \leftarrow s_{D,j} = \begin{cases} \frac{1}{e+1}, & \text{when } j < 2 \\ 1, & \text{when } j \text{ is 2 and a} = 0 \\ 0, & \text{when } j \text{ is 2 and a} \geq 1 \end{cases}$$

//Calculate the a users' transmission under CW0 probability $s_{\text{a},j}$ out of α users as in (Eq. 8)

$$\text{sa} \leftarrow s_{\text{a},j} = \frac{1}{\alpha}\left(\frac{3}{2}j - \frac{1}{2}j^2\right)$$

// Calculate b users' transmission under CW0 probability $s_{\text{b},j}$ out of β users as in (Eq. 9)

$$\text{sb} \leftarrow s_{\text{b},j} = \frac{1}{\alpha+1}\left(\frac{3}{2}j - \frac{1}{2}j^2\right)$$

//Calculate g users' transmission under CW0 probability $s_{\text{g},j}$ out of γ users as in (Eq. 10)

$$\text{sg} \leftarrow s_{\text{g},j} = \begin{cases} 0, & \text{when } j = 0, \text{or a} \geq 1, \text{or g} = 0 \\ 1, & \text{otherwise} \end{cases}$$

//Calculate the probability of success of transmission for the desired user D
//given a, b, and g users $\text{Pr}_{\text{a,b,g}}(S_D)$ as in (Eq.11)
$\text{pr}_\text{D} \leftarrow \text{Pr}_{\text{a,b,g}}(S_D) = \text{sd} \times (1-\text{sa})^\text{a} \times (1-\text{sb})^\text{b} \times (1-\text{sg})^\text{g}$
//Sum for all b combinations knowing the desired user's success
$\text{sum}_\text{b} \leftarrow \text{sum}_\text{b} + \text{pr}_\text{b} \times \text{pr}_\text{D}$
end
//Sum for all a user combinations, knowing b user combinations given desired user's success.
$\text{sum}_\text{a} \leftarrow \text{sum}_\text{a} + \text{pr}_\text{a} \times \text{sum}_\text{b}$
end
//Sum for all g user combinations, knowing a and b user combinations given desired user's success.
$\text{sum}_\text{g} \leftarrow \text{sum}_\text{g} + \text{pr}_\text{g} \times \text{sum}_\text{a}$
end
//Save final sum_g as the probability of success of transmission for the desired user
//given all combinations of α, β and γ users into $\text{Pr}_{\alpha,\beta,\gamma}(S_D) \leftarrow \text{sum}_\text{g}$
//Calculate the last step in calculating probability of the desired user's frame success for all r
//repetitions in the frame, $\text{Pr}_{r,\alpha,\beta,\gamma}(S_{state=CW0})$ as in (Eq. 13) (note r_i repetitions for delay calculations)

prScw0 $\leftarrow \Pr_{r,\alpha,\beta,\gamma}(S_{state=CW0}) = 1 - \left(1 - \Pr_{\alpha,\beta,\gamma}(S_D)\right)^r$

return prScw0

end function

Vita Auctoris

Nabih Jaber was born in London, England. He received his B.A.Sc. and M.ASc degrees in electrical engineering/communications option in 2006 and 2009 respectively from the University of Windsor. He is currently pursuing his PhD degree in the electrical and computer engineering. He also served as a lab manager at WiCIP laboratory. His research interests include Intelligent Transportation Systems (ITS), wireless communications, coding and information theory, Dedicated Short Range Communications (DSRC) vehicular systems, smart grid power line communications, and sensor networks. He also has hands on experience and is very much interested in test-bed implementations, and innovative simulation system designs.